

Final Report

NASA CR-179503

Fabrication of Cooled Radial Turbine Rotor

(NASA-CR-179503) FABRICATION OF COOLED
RADIAL TURBINE ROTOR Final Report (Solar
Turbines International) 258 p CSCL 21E

N87-11789

G3/07 44795
Unclas



Final Report

NASA CR-179503

Fabrication of Cooled Radial Turbine Rotor

By:

A. N. Hammer
G. G. Aigret
T. P. Psychogios
C. Rodgers

For:

NASA-Lewis Research Center
21000 Brookpark Road
Cleveland, OH 44135

Under Contract NAS3-22513
SR86-R-4938-39
June 1986



**SOLAR
TURBINES
INCORPORATED**

SUBSIDIARY OF CATERPILLAR TRACTOR CO.
P.O. Box 85376, San Diego, CA 92138-5376

1. Report No. NASA CR-179503		2. Government Accession No.		3. Recipient's Catalog No.	
4. Title and Subtitle Fabrication of Cooled Radial Turbine Rotor				5. Report Date June 1986	
				6. Performing Organization Code	
7. Author(s) Alvin N. Hammer				8. Performing Organization Report No. SR86-R-4938-39	
				10. Work Unit No.	
9. Performing Organization Name and Address Solar Turbines, Inc. P.O. Box 85376 San Diego, CA 92138-5376				11. Contract or Grant No. NAS3-22513	
				13. Type of Report and Period Covered Contractor Report	
12. Sponsoring Agency Name and Address National Aeronautics and Space Administration Washington, DC 20546 U.S. Army Aviation R&T Activity (AVSCOM) Propulsion Directorate, Cleveland, OH 44135				14. Sponsoring Agency Code 535-05-01 1L1612209AH76	
				15. Supplementary Notes Project Manager, Jeffrey E. Haas NASA Lewis Research Center Cleveland, OH 44135	
16. Abstract <p>A design and fabrication program was conducted to evaluate a unique concept for constructing a cooled, high-temperature radial turbine rotor. This concept, called "split blade fabrication" was developed as an alternative to internal ceramic coring. In this technique, the internal cooling cavity is created without flow dividers or any other detail by a solid (and therefore stronger) ceramic plate which can be more firmly anchored within the casting shell mold than can conventional detailed ceramic cores. Casting is conducted in the conventional manner, except that the finished product, instead of having finished internal cooling passages, is now a "split blade." The internal details of the blade are created separately together with a carrier sheet. The inserts are superalloy. Both are produced by essentially the same software such that they are a net fit. The carrier assemblies are loaded into the split blade and the edges sealed by welding. The entire wheel is Hot Isostatic Pressed (HIPed), braze bonding the internal details to the inside of the blades. Subsequently, the weld bead is removed, exposing the steel carrier which is leached away in an acid bath, leaving the superalloy details.</p> <p>During this program, two wheels were successfully produced by the split blade fabrication technique. One of these wheels was successfully thermal shock, spin, and flow tested, and conformed to all dimensional and design requirements.</p>					
17. Key Words (Suggested by Author(s)) Air-cooled, Radial turbine, Split blade, HIPing, Composite Fabrication			18. Distribution Statement General Release STAR Category 07		
19. Security Classif. (of this report) Unclassified		20. Security Classif. (of this page) Unclassified		21. No. of pages	22. Price*

TABLE OF CONTENTS

<u>Section</u>		<u>Page</u>
	EXECUTIVE SUMMARY	1
1	INTRODUCTION	3
2	DETERMINATION OF PROGRAM DIRECTION	5
	2.1 Design Considerations - Castings	5
	2.2 Economic Considerations	8
3	DETAIL DEVELOPMENT	11
	3.1 Carrier Assembly	11
	3.2 Braze-Bonding Development	14
4	DESIGN	21
5	PROTOTYPE PRODUCTION	23
	5.1 Application of Principles	23
	5.2 Casting Procurement	23
	5.3 Assembly	30
	5.4 Thermal Treatment	33
	5.5 Leaching	33
	5.6 Machining, Assembly, and Aging	34
6	INSPECTION	35
	6.1 Visual and Dimensional	35
	6.2 Non-Destructive Inspection	35
	6.3 Flow Test	35
	6.4 Spin Test	36
	APPENDIX A - Mechanical Design Summary	39
	APPENDIX B - Engineering Report	143
	DISTRIBUTION LIST	339

LIST OF FIGURES

<u>Figure</u>		<u>Page</u>
1	Air-Cooled Radial Turbine (Full Size)	7
2	Carrier, Initial Design	12
3	Partially Leached Composite Structure	12
4	Photomicrograph of IN-792 Casting Surface Cross-Section Showing Negligible Effect of Removal of Molybdenum Carrier by Kolene DGS Fused Descaling Salt	12
5	Trip Strip Formed by Sintered Superalloy/Braze Powder Mixture	13
6	Flow Divider Formed by Sintered Superalloy/Braze Powder Mixture	13
7	HIP Bonded Specimens	15
8	HIP Bonded Specimens	16
9A	Sectioned Blade Produced With Detail Core P/N 131454	24
9B	Sectioned (Split) Blade Produced With Solid Core P/N 131103	25
10	Total Casting Procurement	26
11	Leading Faces of Conventionally Cored Star Wheel, Split Blade Star Wheel, and Exducer	26
12	Trailing Faces of the Wheels	27
13	Modified Weibull Analysis	28
14	Radiographic Positive Enlargement Showing Core Shift in Star Wheel Blade	29
15	Radiographic Positive Enlargement Showing Cracked and Metal Infiltrated Core in a Star Wheel Blade	29
16	Milling Split Blade Cavities	31

PRECEDING PAGE BLANK NOT FILMED

v

PAGE IV INTENTIONALLY BLANK

LIST OF FIGURES (Continued)

<u>Figure</u>		<u>Page</u>
17	Machined Wheel and Carrier Assemblies	31
18	EDM Wire Sawed Carriers and Inserts	32
19	Mis-machined Blade Tip	34
20	Completed Wheel	36
21	Spin Testing	36

LIST OF TABLES

<u>Table</u>		<u>Page</u>
1	High-Temperature Cooled Radial Turbines	6
2	Radial Air-Cooled Turbine Wheel Estimate	9
3	Braze Alloy Strength, Room Temperature	17
4	Tensile Properties, IN 792, As-HIPed	17
5	871°C (1600°F) Tensile Data, Ni Flex 77 Braze Alloy	18
6	Braze Alloy Shear Strength, 870°C (1600°F), IN 792	18
7	HIP Bonded Joining Specimens	19
8	Occurrence of Defects in Wheels	27
9	Flow Test Data	37
10	Spin Test Results	38

EXECUTIVE SUMMARY

This program was concerned with the evaluation of a new concept for manufacturing air cooled blades called "split blade fabrication"*. The split blade manufacturing procedure was developed as an alternative to internal ceramic coring. In this system the internal cooling cavity is created without flow dividers or any other detail by a solid (and therefore stronger) ceramic plate which can be more firmly anchored within the casting shell mold than can conventional detailed ceramic cores.

Casting is conducted in the conventional manner, except that the finished product, instead of having finished internal cooling passages, is now a "Split Blade". The internal details of the blade are created separately together with a carrier sheet. The parts were created on a CAD/CAM wire EDM saw. The carrier is a low carbon steel. The inserts are superalloy. Both are produced by essentially the same software such that they are a net fit. The carrier assemblies are loaded into the split blade and the edges sealed by welding. The entire wheel is Hot Isostatic Pressed (HIPed), braze bonding the internal details to the inside of the blades. Subsequently, the weld bead is removed, exposing the steel carrier which is leached away in an acid bath, leaving the superalloy details.

Two wheels were successfully produced by the split blade fabrication technique. The main detriment to the process in the majority of other attempts was unsatisfactory welding closure of the blade edges (and a lack of reliable pressure testing method) resulting in leakage and unsound bonding in the HIPing operation. Of these wheels, one was successfully thermal shock, spin, and flow tested, and conformed to all dimensional and design requirements.

The rationale for the split blade approach is avoidance of excessive casting rejections in a multi-blade wheel. If the acceptance of a single cast blade is A percent, combining N blades within a single monolithic wheel generates a condition wherein acceptance of the wheel becomes $0.A^N$, often a prohibitively small number, unless A is unrealistically high. A number of conventionally cored bladed wheels procured (together with the split blade wheels) yielded no perfect castings and a projection of only about 5% in further production. The split bladed castings were 100 percent acceptable.

The second advantage of the evaluated manufacturing technique is the ease with which the design of the cooling passages can be modified, requiring only changes in the software which creates the flow dividers and carriers. Changes,

*Patent application in process.

in conventional coring require, in most cases, alteration of hard tooling required to create the detailed ceramics.

In summary, production of multi-bladed wheel casting by the split blade technique proved to hold a significant advantage over conventionally cored wheel castings. The techniques for creating internal details within the split blade were shown to be sound in concept but suffering from reliable welding (and weld testing) procedures.

1

INTRODUCTION

The objectives of this program were to design, fabricate, and test an advanced air-cooled radial turbine wheel. Design constraints included the following as specified by NASA:

- 2.25 kg/sec (5 lb/sec) primary flow
- 190 newtons/cm² (280 psia) turbine inlet and coolant inlet pressure
- 745 kW (1000 hp) shaft power
- 780°K (950°F) cooling air temperature
- 0.45 kg/sec (1 lb/sec) maximum cooling air flow for stator and rotor
- 1500 hour life
- Rotor inlet temperature as close as possible to 1900°K (2960°F) with a minimum of 1600°K (2420°F)
- Convective cooling with the majority of ejection from the blade trailing edges

Five fabrication methods all involving casting were analyzed as to ease and cost of fabrication, and structural integrity. The five methods included three configurations suggested by NASA and two by Solar:

1. NASA Configuration 1 - Pie Slices. Cast identical rotor segments, equal in number to the number of blades, each of which includes the suction side of one blade, the hub segment, and the pressure side of the adjacent blade. The internal blade cooling passage would be integral with either or both sides of the blade. The joining surface between adjacent segments would lie within the blade and would approximate a mean camber surface with radial or near-radial elements.
2. NASA Configuration 2 - Cover Plates. Cast a monolithic rotor that includes all but one side of each blade. The mating blade sides would be cast separately and bonded to the rotor. The internal blade cooling passages would be cast into either or both surfaces.
3. NASA Configuration 3 - Radial Plane Sections. Cast the rotor in two or three parts, one including the radial-flow portions, and the other(s) the axial-flow portion.

4. Solar Configuration 4 - Split Blades and Inserts. Cast a monolithic rotor but one in which each blade is divided into two sections, pressure and suction sides, by a relatively thick, plain, ceramic core which can be anchored in the investment; (1) within the hub, at the (2) leading and (3) trailing edges, and (4) on the outer periphery of the blades, i.e., virtually entirely around. Subsequent to casting and removal of the core, a steel matrix fitted with superalloy insert pin fins, trip strips, and flow directors would be slipped into the split blade, welded gas tight around the periphery, and HIPed at the appropriate times, temperature and pressures to effect a liquid interface bond of the various inserts to the blade surfaces. Final leaching of the casting in appropriate acids would remove the steel matrix, opening the cooling passages, while leaving the inserts bonded in place.
5. Solar Configuration 5 - Segmented Blade Sections. Cast individual segmented sections, each comprised of a radial blade, an endwall platform, and a shank ending in a dovetail type of attachment to a central forged hub.

The initial tasks were the selection of method by design and analysis together with generation of enough fabrication data to perform the essential trade-offs with design. Principal considerations were:

- . determination of velocity diagrams
- . aerodynamic design of the rotor
- . selection of the rotor material
- . selection of the cooling configuration
- . mechanical and thermal analysis of the rotor
- . detailed mechanical design of the rotor
- . joint strength

Subsequent work included casting and fabrication by the selected methods. Prototype wheels were produced and tested for cooling air flow, structural integrity, and by cold and hot spin tests.

Solar personnel involved in the program included: Dr. Arthur Metcalfe, Program Director; Alvin Hammer, Program Manager; George Aigret, Thermal Analysis; Tom Psychogios, Stress Analysis; and Colin Rodgers, Aerodynamic Design.

2

DETERMINATION OF PROGRAM DIRECTION

2.1 DESIGN CONSIDERATIONS - CASTING

A preliminary design was formulated for the aerodynamic shape and cooling passages applicable to the design constraints. The wheel has 10 blades, is 16.5 cm (6.5 in.) in diameter, and has a speed of 65,000 rpm. Table 1 presents preliminary data as to this design in comparison to other recent air-cooled rotors. Figure 1 shows a schematic representation of the wheel.

A meeting was held with technical and sales representatives of the foundry to discuss the five manufacturing approaches under consideration. The foundry reaffirmed the difficulty of attempting to cast a 10-bladed, monolithic rotor with cooling passages generated by internal ceramic coring. Unless the cores can be securely anchored at most edges the danger that one of the ten will slip creates odds which are prohibitive to economical production. NASA Configuration #3, Radial Plane Sections, more than halves the odds of this happening since the shorter cores can be supported in the investment much more securely.

Similarly, the foundry felt that the split blade approach offered significant advantages in that the core can be very securely anchored in the investment. There is a further advantage in that the positions of strip trips, pin fins, and cooling passages can be revised at will, without recourse to altering ceramic core tooling.

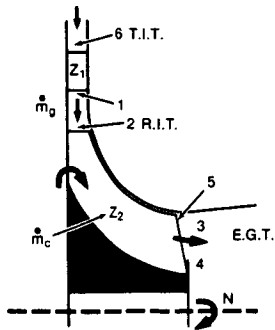
The third approach which the foundry favored was segmented blade sections. The fact that the blades are cast individually eliminates the chance that one bad blade can scrap an entire 10 blade wheel. This approach also has much to recommend it in facilitating cooling of the hub sections.

Of the several NASA- and Solar-suggested configurations there was general agreement that the best approach was the radial plane method, i.e., casting the wheel as separate star wheel and exducer sections. The exducer section can be produced using conventional ceramic cores for the internal cooling passages. The star wheel section is less easily produced by this method and the risk factor was estimated as high as 300%, e.g., casting 40 parts to get 10 good ones. Conventional monolithic, uncored wheels of about the same size, have a risk factor of only about 10% and a price of about \$300 each in quantity production. Although no specific numbers or risk factors were assigned, the consensus of opinion was that fabrication of the star wheel portion by the split blade method would improve the chances of recovery. Conversely, the foundry estimated lower risk in producing the exducer with contoured ceramic cores.

Table 1

High-Temperature Cooled Radial Turbines

	Units	P.W.A.-AVLABS	Allison-AVRADCOM	Solar-NASA-Lewis
Reference	--	Okapuu-Calvert (AGARD 1970)	Monson-Ewing (1980)	Rodgers-Hammer-Aigret-Psichogios Conf 1 10-21-80
T.I.T. - Total temperature T ₀₀	°F	2300	--	--
R.T.T. - Total temperature T ₀₂	°F	2225	2300	2800
EGT	°F	1462	1730	2336
Enthalpy drop Δh	Btu/lb	219.6	171	139.6
Total pressure P ₀₀	psia	257.5	172.0	280.0
Total pressure P ₀₃	psia	50.0	52.14	128.8
Diameter D ₂	in.	7.896	8.71	6.50
Diameter D _{3s}	in.	4.7	5.534	4.25
Diameter D _{3h}	in.	2.0	2.400	2.40
Blade tip height b ₂	in.	0.38	0.438	0.30
Vane number Z ₁	--	20	--	21
Blade number Z ₂	--	12	12	10
Speed N	rpm	67,000	54 862	65,000
Tip speed U ₂	ft/s	2,308	2,085	1,844
U ₂ /c _s spouting, isentr.	--	--	0.67	0.65
U ₂ /√T ₀₂	ft/s R ²	44.5	39.7	32.3
Gas flow rate ṁ _g	lb/s	4.9	5.20	4.933
Flow function ṁ _g √T ₀₂ /P ₀₂	lb R ^{1/2} /s psia	0.986	1.588	1.006
Shaft power	HP	1 522	1,258	974
Blading coolant flow ratio	--	0.03	0.030	0.10
O _g = ṁ _c /ṁ _g	--	--	0.015	0.03
Bore and hub coolant flow ratio O _g = ṁ _c /ṁ _g	--	--	0.015	0.03
Coolant, in temperature	°F	850	800	950
Cooling scheme	--	2 passes, smooth	2 passes, smooth	--
A _{ann} 3N ²	(ft/min) ²	443.10 ⁶	408.10 ⁶	284.10 ⁶
Material	--	cast In-100	. airfoils assy; cast MAR-M247 . hub: PA101 PM	In-792
Design Life	hrs	?	1000 (100%) +6000 cycles	1,500
Results	--	fabrication problems; tested at 2045°F, at reduced rpm - waiting for final report	successful fabrication; 6000 cycles + spin test completed	--
Specific speed N _s	$\left(\frac{\text{ft.lbm}}{\text{lb}_f}\right) \frac{3/4 I}{\text{min.s}^{1/2}}$	<66	65	63
Specific dia. D _s	$\left(\frac{\text{lb}_f}{\text{ft.lbm}}\right)^{1/4} \text{s}^{1/2}$	1.66	1.60	1.61
<u>Casting data</u>				
Tip-L.E. thickness	in.	--	0.090	0.10
T.E. thickness	in.	--	0.052	0.10
Min. wall thickness	in.	--	0.025	0.025
Core thickness	in.	--	0.040 to 0.12	≥0.050



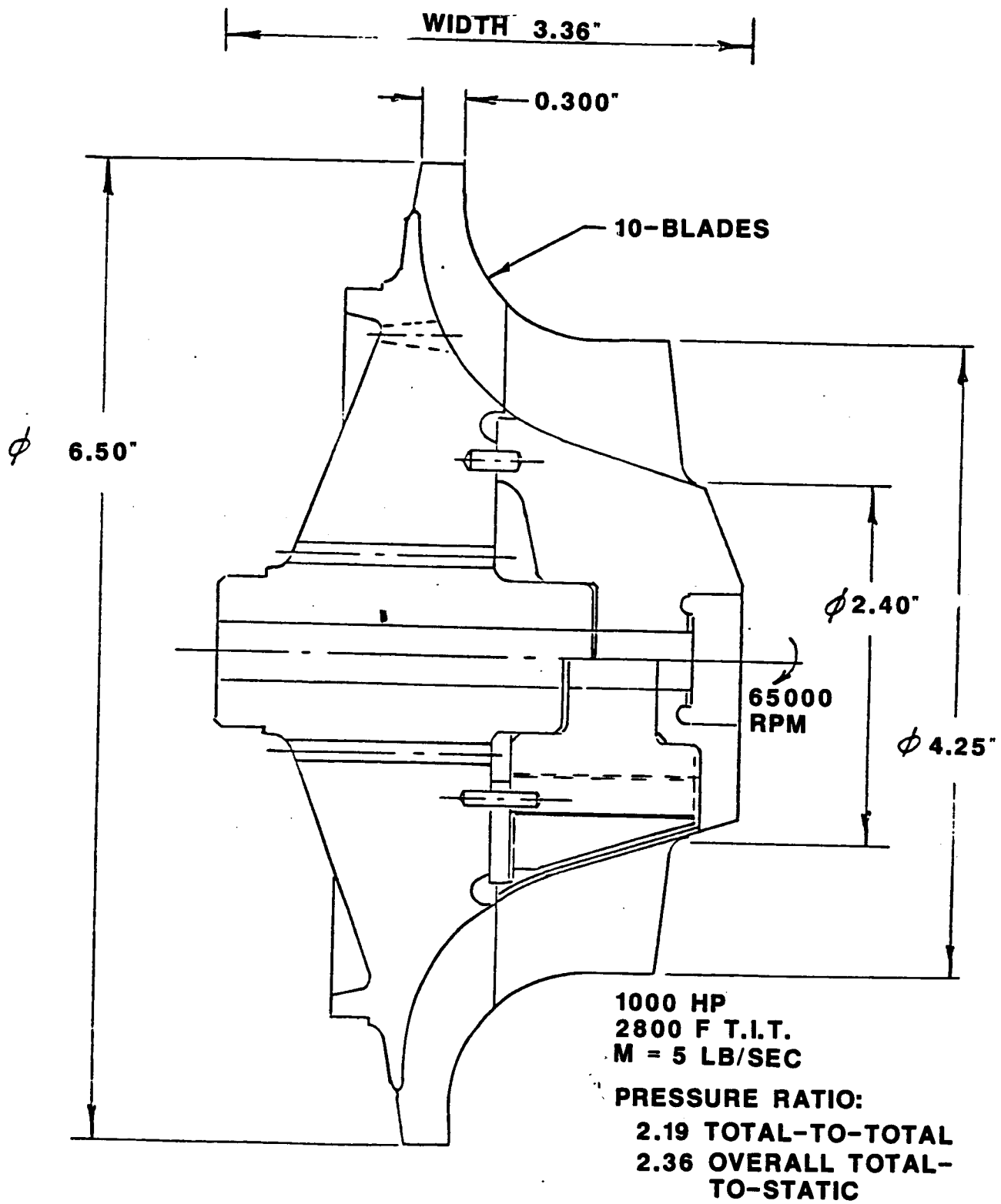


Figure 1. Air-Cooled Radial Turbine (Full Size)

Ceramic coring for the star wheel cooling passages is relatively more fragile than that for the exducer. It was decided, therefore, to proceed with split blade fabrication. The use of solid ceramic cores to produce split blades reduces the risk of rejection to the point where the castings can be made as monolithic units.

2.2 ECONOMIC CONSIDERATIONS

Table 2 is a compilation of costs quoted by several machining and assembly vendors for manufacture of the rotor by any of four methods, i.e., individually bladed exducer versus monolithic, and fabricated star wheel cooling passages versus cast-in-place. Also included are the quotations for ten castings of each of the various types received from the foundry, but no quotes could be obtained for larger quantities. These quotations are for best effort only and it is speculative as to what the costs would be for guaranteed production quality in larger amounts.

Based upon these data (and previously described casting considerations) it was decided to proceed with development of monolithic, rather than separately bladed, dual star wheel and exducer. The internal cooling passage would be cast into the exducer and fabricated in the star wheel. A number of star wheels with cast cooling passages also subsequently were ordered (at Solar expense) to verify casting production yield. ,

Table 2

Radial Air-Cooled Turbine Wheel Estimate

Part No.	Title	Part Cost - Qty 10		Part Cost - Qty 200+		Tooling	
		Material	Machining	Material	Machining	Material	Machining
1	Rotor Assy, Cast Star Wheel - Assy	83	83	83	83	65,920	8,500
	Turbine-Star Wheel	2000	2480	N/Q	397	75,840	4,600
	Exducer	1500	1873	N/Q	294	--	3,500
	Dowel Pin (2)	--	12	--	12	--	79,340
TOTAL		3500	948	4448	786	141,760	16,600
2	Rotor Assy, Cast Star Wheel, Exducer	83	83	83	83	65,920	8,500
	with Separate Blades - Assy	2000	2480	N/Q	480	63,040	4,600
	Turbine Wheel	2000	2702	--	653	--	61,450
	Blades (10)	12	12	12	--	--	--
	Dowel pin	--	380	--	288	--	15,800
	Hub Exducer	--	206	--	113	--	--
	Ring Exducer	--	145	--	95	--	--
	Retainer, Exducer	--	40	--	40	--	--
	Assy & Balance Exducer	--	--	--	--	--	--
TOTAL		4012	2036	6048	1669	128,960	90,350
3	Rotor Assy, Fabricated Star Wheel,	83	83	83	83	--	8,500
	Cast Exducer - Assy.	1800	2251	--	390	59,200	10,300
	Turbine Wheel	550	550	--	370	--	3,500
	Insert Blade	1500	1873	--	294	75,840	3,500
	Exducer	12	12	--	12	--	79,340
	Dowel Pin (2)	--	--	--	--	--	--
TOTAL		3312	1457	4769	1149	135,040	25,800
TOTAL		3312	1457	4769	1149	135,040	25,800
TOTAL		4012	2036	6048	1669	128,960	90,350
TOTAL		3312	1457	4769	1149	135,040	25,800
TOTAL		3312	1457	4769	1149	135,040	25,800

3

DETAIL DEVELOPMENT

3.1 CARRIER ASSEMBLY

The carrier assembly, i.e., the leachable component and integral superalloy flow passage dividers, flow straighteners, and trip strips, underwent several evolutions of change before development of the final configuration used for the prototype wheels. The initial configuration, seen in Figure 2, was produced by an electrodischarge machining (EDM) numerically controlled wire saw. The carrier (etchable) portion was low carbon, low silicon enameling steel.

Experiments were conducted in forming trip strips and passage partitions by plasma spraying grooved and indented steel carriers. The plasma sprayed alloy employed was a NiCrAlY, with an approximate composition of 75 w/o Ni, 19 w/o Cr, and 6 w/o Al.

A second approach to forming the trip strips and partitions was filling the steel carrier grooves and slots with a superalloy/braze alloy powder blend and partially sintering in vacuum, prior to HIP bonding at higher temperature. Reproduction of details by this technique was excellent. Figure 3 shows an example which has been partially acid leached to remove the steel carrier. No pressure was applied in braze bonding the superalloy details to the simulated blade halves, yet near 100 percent density is achieved.

With the addition of some pressurization, about 10 MPa (1500 psi), with a vacuum bellows fixture, the superalloy additions were converted to full density. The results were virtually porosity free and indicate that the actual HIP cycle will achieve a 100 percent dense structure.

Estimates were also sought for production of the carrier (used to hold superalloy inserts in place) as sintered powder metallurgy compacts. If these parts (which are ultimately etched or leached away) are made from molybdenum they would be strong enough during the HIP exposure to support small diameter wires which would serve as trip strips in the inner cooling passages. As a further advantage of moly, we found that it dissolves very readily in a fused salt bath, much more efficiently than does iron or steel in acid. There is no observable effect of the salt bath on the surface of the superalloy castings, as seen in Figure 4, a photomicrograph of a sample IN-792 casting after removal of the moly. The molybdenum can also be removed by exposure to air at temperatures of 760°C (1400°F) or more, but this method is much slower and tends to become ineffective in penetrating more than a fraction of a millimeter between the superalloy sidewalls where there is limited access to a fresh supply of air.

PRECEDING PAGE BLANK NOT FILMED

ORIGINAL PAGE IS
OF POOR QUALITY

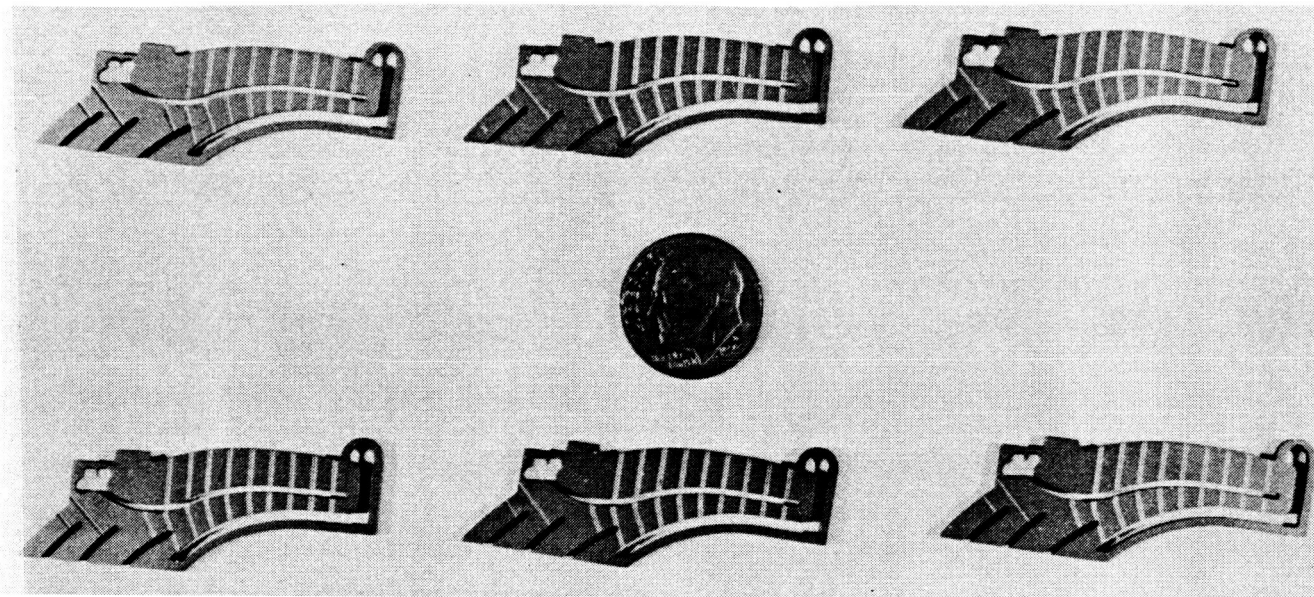


Figure 2. Carrier, Initial Design

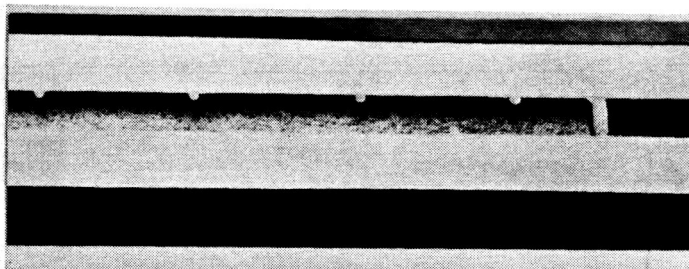


Figure 3. Partially Leached Composite Structure (Mag: 4X)



Figure 4.

Photomicrograph of IN-792
Casting Surface Cross Section
Showing Negligible Effect of
Removal of Molybdenum Carrier
by Kolene DGS Fused Descaling
Salt

Etchant: Kallings
Magnification: 250X

**ORIGINAL PAGE IS
OF POOR QUALITY**

Ultimately a procedure was developed, working with the subcontract wire EDM vendor, DATM of Santa Ana, CA, for producing both the steel carrier and the superalloy inserts used in fabrication of the split blade star wheel. Trip strip grooves in the steel carrier were produced by photo-resist chemical milling. In actual practice we decided to also wire EDM the superalloy flow dividers and edge closure from superalloy sheet, fit them into the machined slots, and fill the trip strip grooves with powder metal/braze mixtures. This was accomplished four parts to a panel which were then double disc sanded, both sides, and EDM wire sawed to final shape prior to insertion within the blade cavity.

At about \$20 per piece, this system is more expensive than high production stamping and coining, but involves less in the way of hard tooling and is more flexible in terms of design change.

Figures 5 and 6 are photomicrographs showing 100 percent dense trip strips and flow divider in the mild steel carrier by sintering a mixture of Hastelloy

Figure 5.

Trip Strip Formed by Sintered
Superalloy/Braze Powder Mixture

(Magnification: 75X)

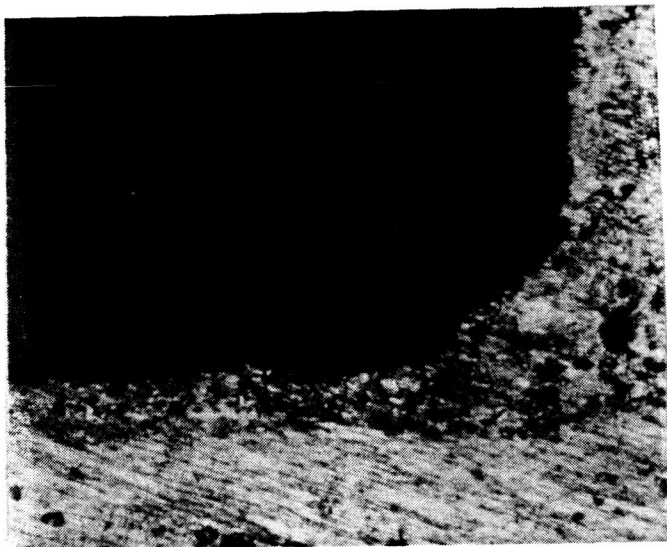
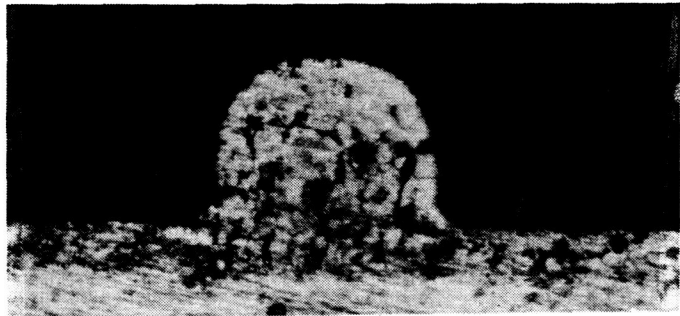


Figure 6.

Flow Divider Formed by Sintered
Superalloy/Braze Powder Mixture

(Magnification: 75X)

X powder, -325 mesh, and nickel braze alloy powder. The resulting composite, including Inco 625 superalloy flow divider strips was subsequently braze-bonded between two samples of IN 792 castings and the steel removed by boiling in a refluxed solution of 50 percent nitric acid in methanol. Complete dissolution of the steel was achieved in less than one hour, and the definition of cooling passage and trip strips conformed to print requirements.

The etching medium selected for most efficient removal of the fabricated split blade steel core after bonding was:

50 v/o Nitric Acid, conc.
50 v/o Alcohol, (ethyl, methyl)*
50-65°C (120-150°F)

3.2 BRAZE-BONDING DEVELOPMENT

Four braze alloys, all in foil form, were selected as candidates for bonding the internal details to the split blades.

AMS 4777	Ni-Flex 77**	0.051 & 0.084 mm (0.002 & 0.0033 in.)
AMS 4778	Ni-Flex 78**	0.051 & 0.084 mm (0.002 & 0.0033 in.)
AMS 4779	Ni-Flex 79**	0.025, 0.051, & 0.10 mm (0.001, 0.002, & 0.004 in.)
	Ni-Flex 95**	0.025, 0.051, & 0.10 mm (0.001, 0.002, & 0.004 in.)

Tests included lap shear bonds, butt joint specimens, and simulated blade sections containing the carrier and HIP bonded inserts. All were prepared with cast samples of the candidate casting alloys, IN 792 and MAR-M-247 obtained from the foundry. Flat plates were used for double lap shear tests; dog bone tensiles, cut apart and subsequently rebonded, as butt joint specimens.

Initial bonding tests were conducted within a vacuum furnace using a fixture through which pressure could be supplied by an expandable bellows. Despite several rebuilds to strengthen the mechanism, joining studies proceeded with great difficulty due to problems in pressurizing the specimens at the high bonding temperatures. The desired cycle is 1150°C/100 MPa/2 hours

*It is important to monitor the reaction and to keep the level of alcohol near the 50 percent level to avoid oxidation by the nitric acid. Equally important, only ethyl or methyl alcohols should be used. Other varieties, e.g., isopropyl, can react violently with nitric acid.

**Materials Development Corporation, Medford, Mass.

(2100°F/15 ksi/2 hours). We were not able to sustain a load above about 35 MPa (5 ksi) for more than a few minutes, however, and the fixture was abandoned. Subsequent bonding tests were conducted within evacuated, hermetically sealed tubes or boxes subjected to an actual HIP environment and cycle.

Figures 7 and 8 are photographs of HIP processed braze joint specimens returned from Pressure Technology, following 1175°C(2150°F), 103 MPa (15,000 psi) HIP processing. All of the double lap joint specimens contained in stainless steel boxes were bonded. One tube of the butt joint specimens apparently leaked due to an undetected crack in the closure weld, and consequently saw no differential pressure in the HIP cycle. The specimens in this tube were only superficially bonded, and could not be tested. Figure 7 also shows the IN 792/steel/IN 792 laminates, edge-welded and HIP bonded to simulate actual split blade fabrication of the wheels. The internal cooling passage dividers, edge closures, and trip strips were filled with pre-sintered powders prior to bonding, as follows:

- a) Hastelloy X powder -- -325 mesh
- b) Hastelloy X powder -- -325 mesh plus 5 wt. % AMI 775 braze alloy
- c) 80-20 Ni-Cr powder -- -325 mesh
- d) 80-20 Ni-Cr powder -- -325 mesh plus 5 wt. % AMI 775 braze alloy

Of the two specimens evaluated metallographically, one was seen to be heavily contaminated and not bonded, due to what we suspect was a cracked weld. The second showed the powder to be fully compacted and bonded to the cast IN 792.

Table 3 is a compilation of tensile and shear strengths of the IN 792 cast specimens bonded with a variety of high temperature braze alloys in the HIP runs. Both the strongest and the most consistent results were demonstrated

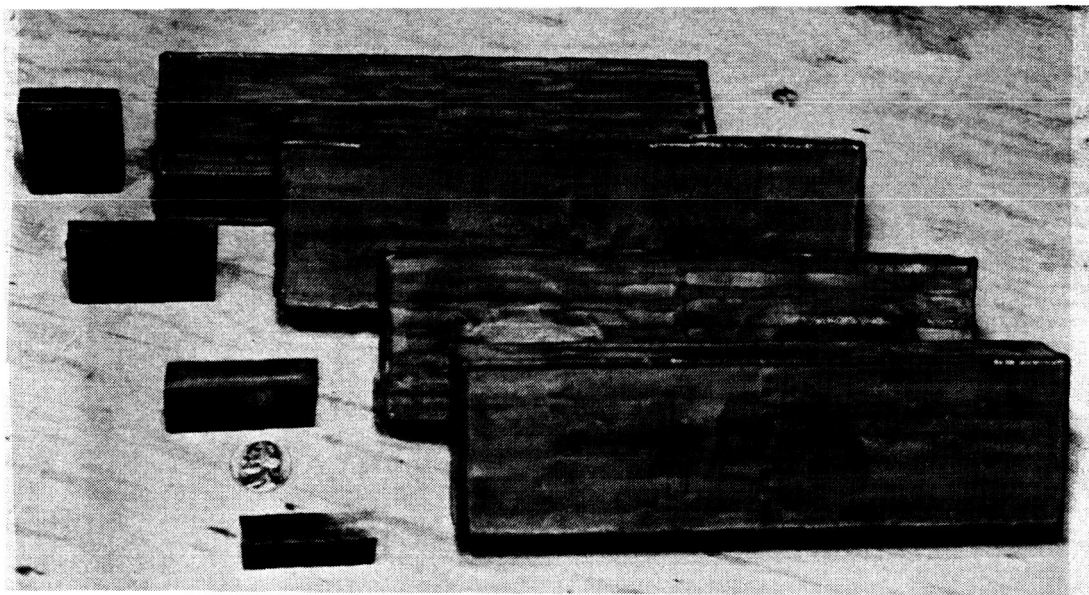


Figure 7. HIP Bonded Specimens

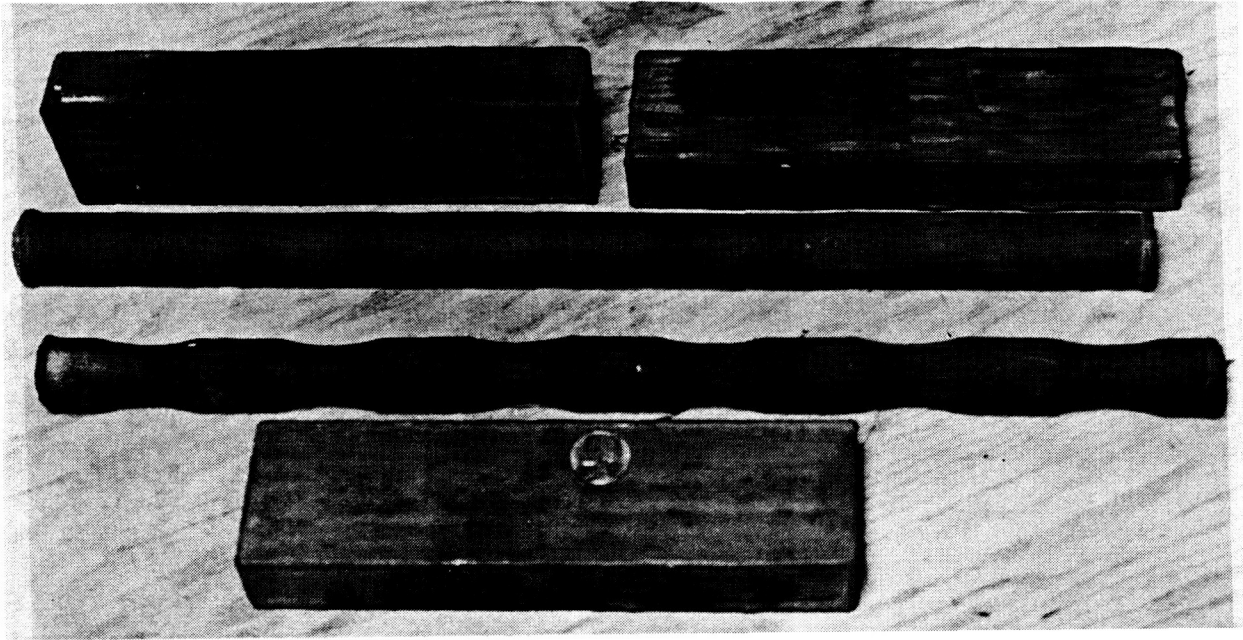


Figure 8. HIP Bonded Specimens

by Ni-Flex Alloy 77, 0.05 mm (0.002 in.) thick. Table 4 shows room temperature tensile data for two specimens of the IN 792 material in the as-HIPed condition. The alloy exhibits good ductility. Yield strength is approximately that of the braze alloy tensile test, Table 3.

Table 5 presents elevated temperature tensile data on five butt joint braze specimens which were given a brazing cycle simulating a HIP-bonding cycle and subsequently heat treated. The alloy is NI-Flex 77. The braze and heat treat cycles were as follows:

Braze	1177°C (2150°F)/Vac./2 hours/furnace cool
Heat Treat	1121°C (2050°F)/Vac./2 hours/fast cool*
Age	843°C (1550°F)/Vac./4 hours/furnace cool
Age	760°C (1400°F)/Vac./16 hours/furnace cool

*10 minutes or less to 538°C (1000°F)

Table 6 is a compilation of three shear strength tests conducted on brazed and heat treated IN 792 lap joints. Two values are noted for the first two specimens since the holes in the double leg of the specimen were mis-aligned, causing the joint to be loaded as a single lap, each side independently. As with previous results, the Ni-Flex 77 alloy provided the strongest and most consistent joint. These specimens were brazed with a simulated HIP cycle and subsequently vacuum heat treated as noted above.

Table 3
Braze Alloy Strength, Room Temperature

Braze Alloy Thickness mm (in.)	Base Material, IN 792 Casting			
	Tensile Strength MPa (ksi)		Shear Strength MPa (ksi)	
Ni-Flex 77 0.05 (0.002)	782.6	(113.5)	348.9	(50.6)
Ni-Flex 77 0.083 (0.0033)			383.3	(55.6)
Ni-Flex 78 0.05 (0.002)	257.0	(37.4)	77.2 313.0	(11.2) (45.4)
Ni-Flex 78 0.083 (0.0033)			388.9	(56.4)
Ni-Flex 79 0.05 (0.002)			436.4 38.6	(63.3) (5.6)
Ni-Flex 95 0.025 (0.001)	594.3	(86.2)	342.7	(49.7)
Ni-Flex 95 0.05 (0.002)	415.8	(60.3)		
Ni-Flex 95 0.10 (0.004)	137.2	(19.9)		

Table 4
Tensile Properties, IN 792, As-HIPed

0.2% Yield Strength MPa (ksi)	Tensile Strength MPa (ksi)	Elongation % in 4D
813.6 (118.0)	1005.3 (145.8)	9.0
808.1 (117.2)	1065.9 (154.6)	9.8

Table 5

871°C (1600°F) Tensile Data, Ni Flex 77 Braze Alloy

Specimens Number	Ultimate Tensile		Fracture
	MPa	(ksi)	
A02-8	826	(119.8)	50% Parent Metal
A01-7	799.1	(115.9)	65% Parent Metal
A06-9	700.5	(101.6)	35% Parent Metal
A02-10	759.8	(110.2)	65% Parent Metal
A06-11	797.0	(115.6)	75% Parent Metal

Table 6

Braze Alloy Shear Strength, 870°C (1600°F), IN 792

Specimen Number	Braze Alloy	Shear Strength		Notes
		(MPa)	(ksi)	
DL-8	Ni-Flex 77 0.084 mm (0.0033 in.)	311.0	45.1	Opposite side of double lap joint broke independently.
		311.6	45.2	
DL-9	Ni-Flex 95 0.025 mm (0.001 in.)	194.4	28.2	Opposite sides of double lap joint broke independently.
		295.1	42.8	
DL-10	Ni-Flex 95 0.10 mm (0.004 in.)	110.3	16.0	

Eight split blade simulation specimens were electron beam (vacuum) welded and processed by HIPing. They are included in Table 7. These simulated split blade specimens were evaluated metallographically. There was no particular advantage or disadvantage noted in the integrity of any of the braze alloy, substrate combinations. In all cases the steel or molybdenum carrier etched away cleanly with no damage to the superalloy inserts or casting. Experience with preparation of these samples demonstrated that the placement of individual trip strip wires is an unworkable system. We therefore went to a method wherein the superalloy addition is made by filling the trip strip grooves

Table 7

HIP Bonded Joining Specimens

Test Bar Sample Number	Material	Braze Alloy	Etching	Insert
2 ₁	MAR-M247	Ni-Flex 95 0.050 mm thick (0.002 in. thick)	Nitric Acid	1010 steel, 1.5 mm (0.058 in.) carrier; 2 round plugs (Hast X) 7 mm (9/32 in.) dia.; 16 0.9 mm (0.035 in.) Hast X pins; 2 trip strips fabricated of Inconel 718 wire.
2 ₂	MAR-M247	Ni-Flex 95 0.05 mm thick (0.002 in. thick)	Nitric Acid	" "
3 ₁	IN-792	Ni-Flex 78 0.05 mm thick (0.002 in. thick)	Nitric Acid	" "
3 ₂	IN-792	Ni-Flex 79 0.05 mm thick (0.002 in. thick)	Nitric Acid	" "
4 _s	IN-792	Ni-Flex 79 0.05 mm thick (0.002 in. thick)	Nitric Acid	6 trip strip wires, grooves at various depths; 1010 steel 1.5 mm (0.0589 in.) carrier
4 _m	IN-792	Ni-Flex 79 0.05 mm thick (0.002 in. thick)	Kolene DGS fused salt	Molybdenum 1.2 mm (0.047 in.) carrier; 6 trip wires
5 _s	MAR-M247	Ni-Flex 77 0.05 mm thick (0.002 in. thick)	Nitric Acid	1010 steel carrier; 6 trip wires at various depth
5 _m	MAR-M247	Ni-Flex 77 0.05 mm thick (0.002 in. thick)	Kolene DGS fused salt	Molybdenum 1.2 mm (0.047 in.) carrier; 6 trip wires

with a powder/braze alloy mixture and sintering. This method results in about ten volume percent porosity, which the subsequent HIP densification corrects.

4 DESIGN

Four assemblies, comprised of two types of star wheel and two types of exducer, were designed. The engineering drawings and specifications of these various components can be made available to qualified parties for examination by application through NASA-Lewis.

Descriptions and drawing numbers are as follows:

- 131100 Proposal - engine assembly, with high temperature turbine wheel (full size to fit T-62)
- 131102 Layout - turbine wheel, air-cooled (two-piece 10X size)
- 131301 Proposal - air-cooled turbine wheel assembly (multi-piece construction 10X size)
- 131454 Wheel, turbine - air cooled (cast star wheel)
- 131103 Wheel, turbine - air cooled (brazed star wheel)
- 131467 Insert, blade - air cooled (brazed star wheel)
- 131455 Exducer, turbine - air cooled (cast one-piece)
- 131599 Blade, exducer - air cooled (cast and machined)
- 954959C1 Hub, exducer - air cooled (machined)
- 954960C1 Ring, exducer - air cooled (machined)
- 131453-100 Wheel assembly, turbine - air cooled (cast wheel and exducer)
- 200 Wheel assembly (brazed wheel and cast exducer)
- 300 Wheel assembly (cast wheel and multi-piece exducer) (includes assembly, balancing and spinning)
- DSK 17073 Material specification

The mechanical and thermal design procedures are covered in Appendices A and B of this report.

5

PROTOTYPE PRODUCTION

5.1 APPLICATION OF PRINCIPLES

Following the definition of design manufacturing techniques, braze bonding cycles, thermal treatment, and sealing and leaching cycles, it was decided to proceed with the production of prototype wheels to demonstrate the practicality of these methods in simulated production. This section describes the course of the various tasks from procurement through final machining.

5.2 CASTING PROCUREMENT

Approval was received from the local DCAS administrator in 1982, to proceed with procurement of the tooling. Purchase orders were let for the exducer, P/N 131455, to be cast with integral ceramic cores; for the star wheel, P/N 131103, with split blade, fabricated passages; and an adaptor to allow fabrication of the star wheel, P/N 131454, with integral ceramic cores. The foundry contracted with a second source for all tooling.

The purchase order was let to cover the casting of the wheels on a best effort basis. The foundry was to make up to 25 pours to produce ten good castings in each of the components, star wheel and exducer. The exducer was cast only with detail ceramic cores. The first attempts at the star wheel were with the split blade type core. If a requisite number of good castings, 10, were attained in the initial attempts, the balance of the 15 pours could be devoted to detail type ceramic cored star wheels.

In casting the first (tool proof) star wheel plunger over-travel (during the wax injection) caused the solid cores to be cracked prior to assembly. The problem was corrected by restricting the stroke during subsequent operations.

Evaluation was conducted during subsequent production of cast star wheels, both the integrally cored and split blade designs, P/N's 131454 and 131103. A photograph of the sectioned blade of each is seen in Figure 9. The only difficulty reported was that some of the cores forming the air entry holes in P/N 131103 were broken in the wax injection process and that these castings needed reworking to reform the holes.

Figures 10, 11 and 12 are photographs of the total casting procurement, the leading faces, and the trailing faces of the wheels, respectively.

PRECEDING PAGE BLANK NOT FILMED

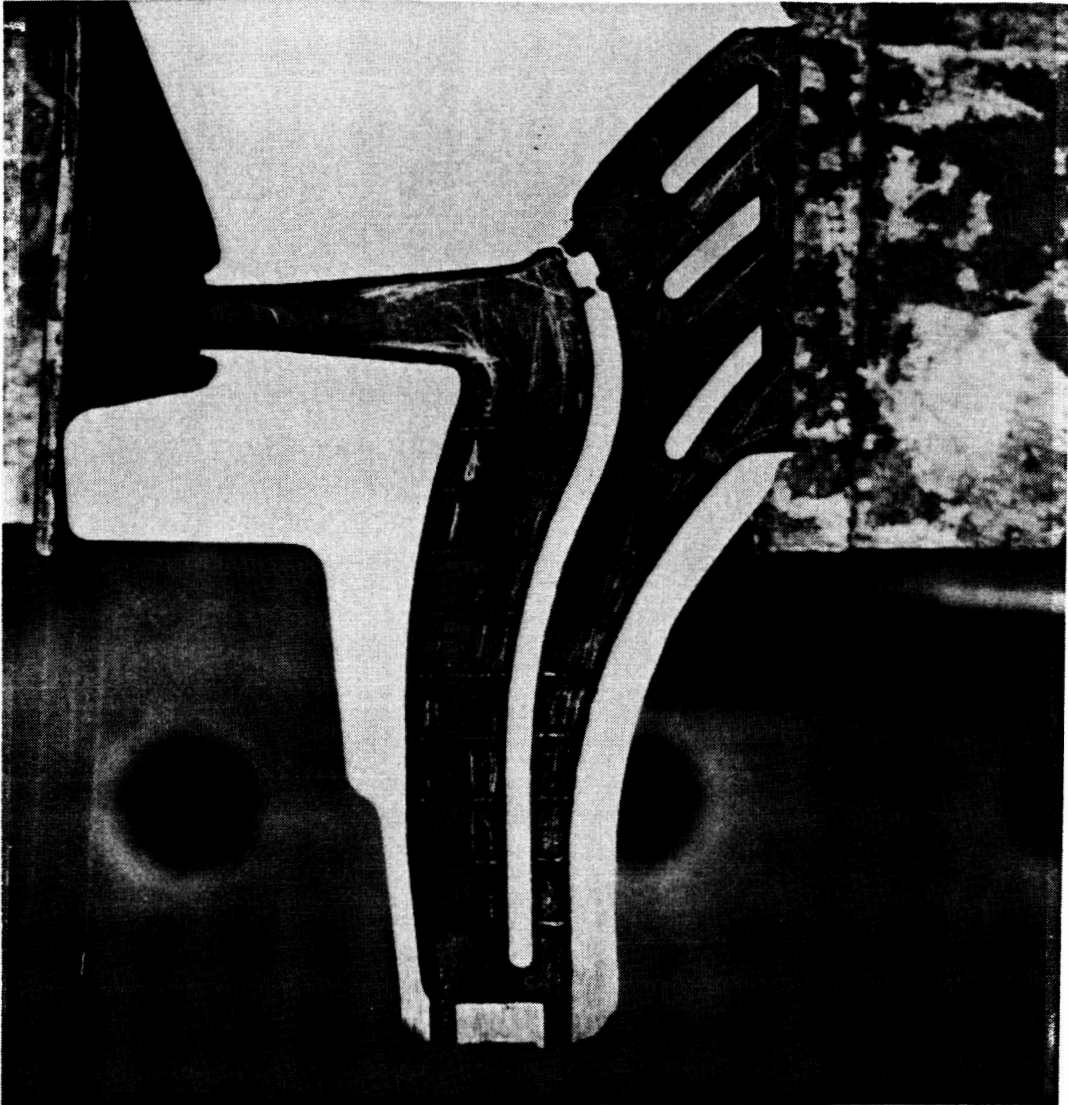


Figure 9A. Sectioned Blade Produced With Detail Core
P/N 131454

Seventeen conventionally cored star wheel were cast by the same foundry with the same cooling passage design as that of the split blade wheels, except that the passage was made 0.075 in. (1.9 mm) wide, rather than the specified 0.050 in. (1.27 mm), due to the need for more rigidity in the detailed core. Of the 17, four were supplied to Solar and the balance scrapped. Table 8 shows the relationship of unacceptable blades per wheel. No specific details are known for the 13 scrapped at the foundry so they are simply assumed to have had at least as many as six bad blades per wheel, one more than the worst of the four we received.



Figure 9B. Sectioned (Split) Blade Produced With Solid Core
P/N 131103

ORIGINAL PAGE IS
OF POOR QUALITY

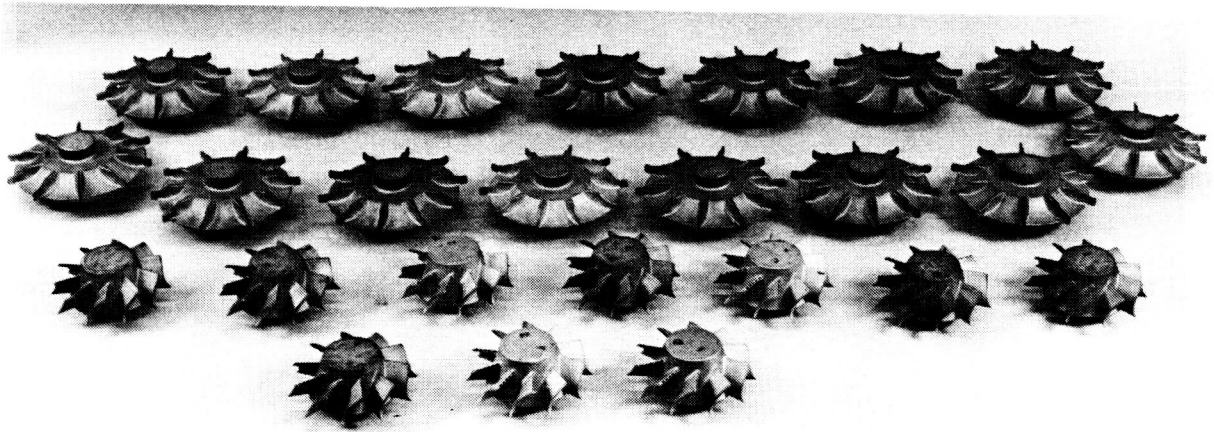


Figure 10. Total Casting Procurement: 4 Conventionally Cored Star Wheels (Solar Procurements); 11 Split Blade Star Wheels; and 10 Exducers

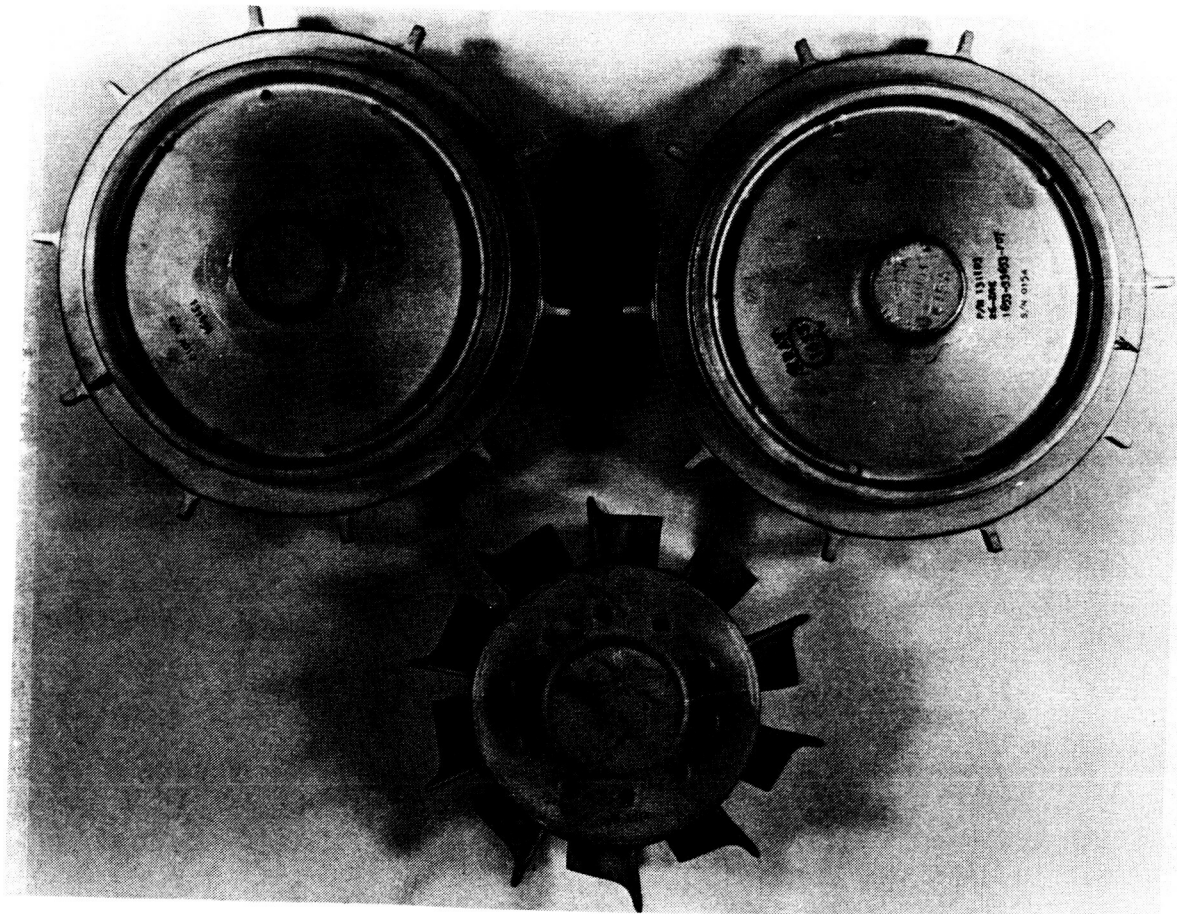


Figure 11. Leading Faces of (Clockwise) Conventionally Cored Star Wheel, Split Blade Star Wheel, and Exducer

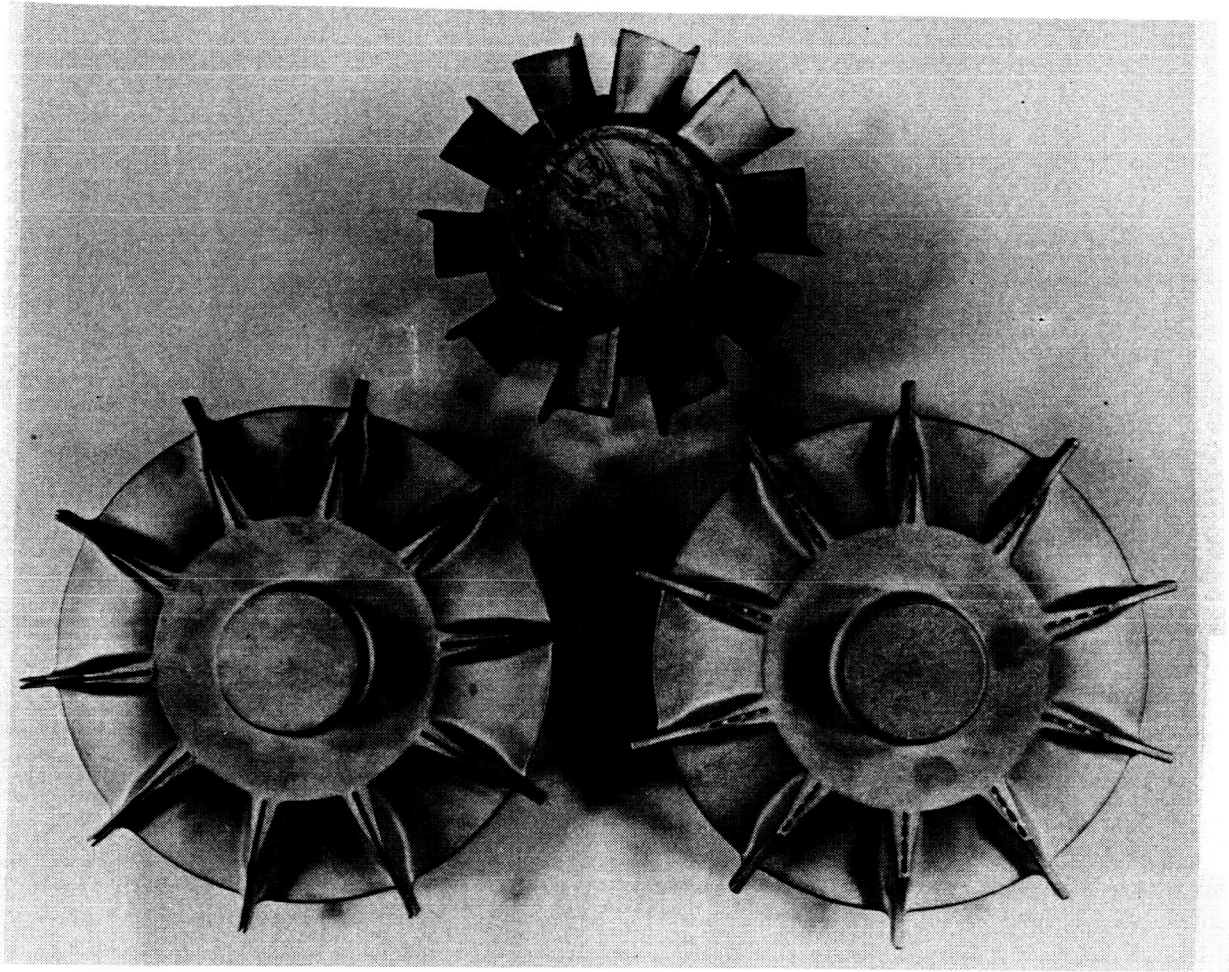


Figure 12. Trailing Faces of the Wheels

Table 8

Occurrence of Defects in Wheels

Number of Castings	Defects Per Wheel
1	1
1	2
1	3
1	5
13	6 or more

ORIGINAL PAGE IS
OF POOR QUALITY

A very approximate Weibull analysis of these data (Fig. 13) show the probable acceptance rate to be less than 3%, corresponding to an acceptance rate, had they been single blades, of about 70%, not an unreasonable figure. Recognizing that this was the first production trial with this design, we will assume that subsequent production will bring some kind of improvement through a learning curve.

Of castings completed and shipped by the foundry, we received 4 pieces of P/N 131454, the conventionally cored star wheel; eleven pieces of 131103, the split blade star wheel; and 10 pieces of 131455, the exducer. The number of trials for the latter two castings were not reported. P/N 131455 and 131454 were HIPed and heat treated, without aging. P/N 131103 was not HIPed or heat treated as this will follow as a part of the fabrication procedure. The foundry supplied a complete record of certification, NDT records, HIP and heat treatment parameters.

Review of radiographs submitted with the castings show generally definable structures in the star wheels, both conventionally cast and those which were to be fabricated by the split blade technique. Several (Table 8) of the former had variations in the blade wall passages, however, examples of which (magnified and shown as a positive print) are shown in Figures 14 and 15.

Definition of the exducer blade detail is very much complicated by overlap of the blades and the central hub. For this reason, a casting was submitted to Aerojet Strategic Propulsion Company, Sacramento, CA, for an assessment of

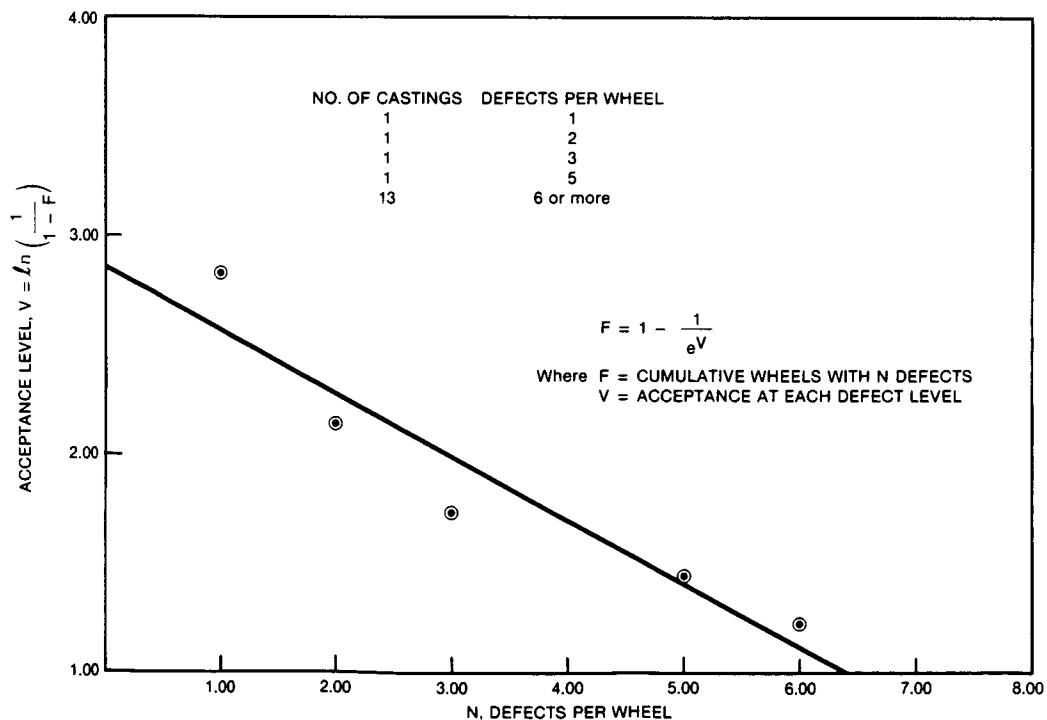


Figure 13. Modified Weibull Analysis

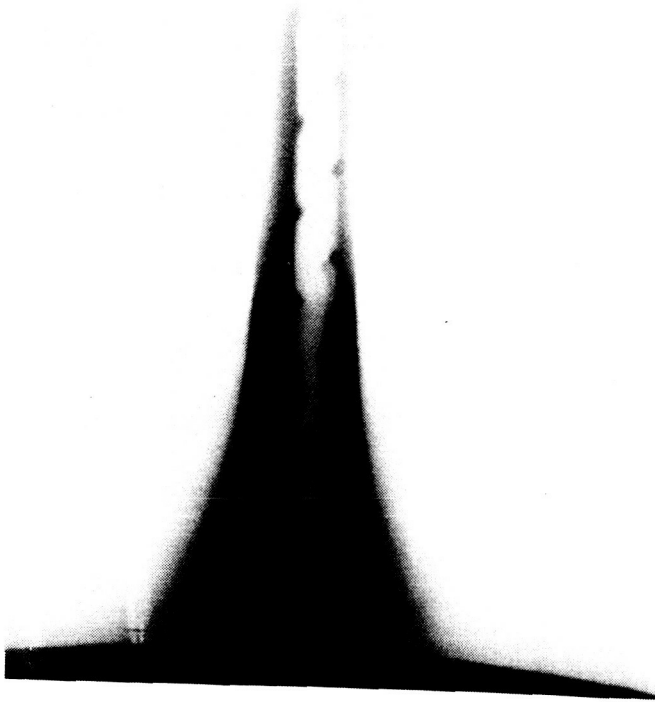


Figure 14.

Radiographic Positive Enlargement
Showing Core Shift in Star
Wheel Blade

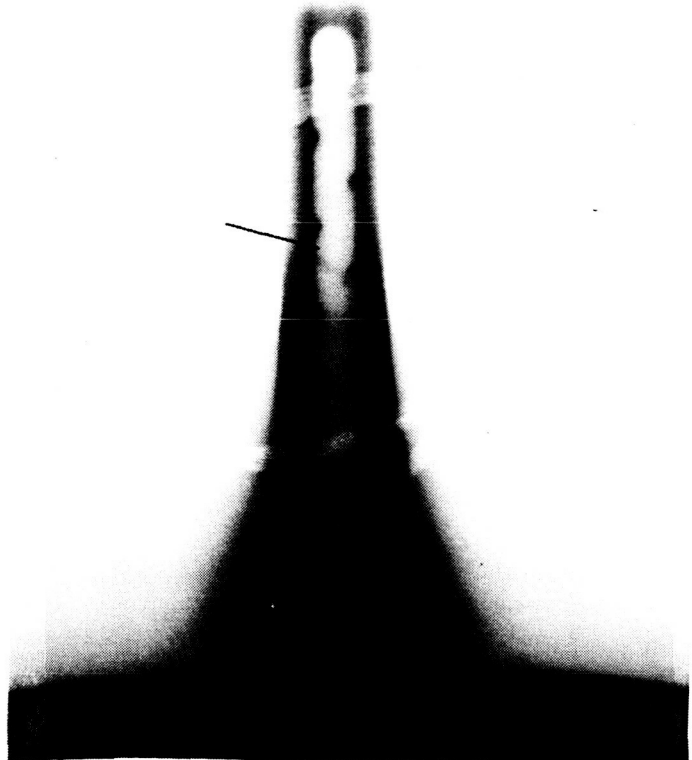


Figure 15.

Radiographic Positive Enlargement
Showing Cracked and Metal
Infiltrated Core in a Star Wheel
Blade

inspection by the Computed Tomography (CT) Process, developed under sponsorship of Materials Laboratory, Air Force Wright Aeronautical Laboratories. This system appears to have great promise in resolution of the complicated inner structures of the blades. A disadvantage was seen in the estimated cost of adapting the system to the exducer, e.g., two blades for \$3,245; in the actual inspection of the first casting, all 10 blades, \$1,849; and in the probable cost of prototype and/or production inspection, probably in excess of \$1,000 each. For this reason further investigation of the process was put on hold, with the hope that further studies will eventually be made.

No surface defects were noted by fluorescent penetrant inspection in any of the castings supplied, nor were defects noted in visual examination.

5.3 ASSEMBLY

All wheels were lathe turned to locate the blade diameters. The star wheel casting split blades were milled internally with a carbide slitting saw to clean out the cavity between the blade halves, Figure 16.

Saw blade thickness was selected such that approximately 0.050 to 0.075 mm (0.002 to 0.003 in.) was removed on either side opening the slots to 1.27 mm (0.050 inch) minimum width. It was also necessary that an electro-discharge machining tool be fabricated to shape and deburr the oval air passage slots at the base of the split blades. The steel carriers, inserts and trip strip assemblies were prebrazed, sanded flat and parallel and cut to shape preparatory to assembly in the split-blade star wheels (Fig. 17). The carrier assemblies were, in this final lot, prepared with EDM wire saw fabricated inserts and a powder/alloy mixture prebrazed in photochemically milled grooves to form trip strips. The total configuration, seen in Figure 18, was comprised of:

- . carrier - enameling steel
- . flow dividers - Hastelloy X inserts
- . trip strips - Hastelloy X powder/AMI 775 braze powder, 95/5 mixture

Two wheels were assembled with the carrier-inserts and welded, preparatory to HIP-bonding.

These wheels, Numbers 1 and 5, were returned from the HIP-bonding operation, lathe machined to define the blade contours, and the blade tip holes (4) and air inlet holes electro-discharge machined to expose the steel core to acid leaching. The leaching operation proceeded satisfactorily, requiring about 10 hours exposure to warm [70°C (160°F)] nitric acid, alcohol 1/1 mixture. Subsequent destructive metallographic analysis revealed all traces of the steel to be gone and no evidence of reaction of the casting, superalloy inserts, or braze alloy with the acid.

The wheels were radiographed in two planes: axially, which did little to reveal the inner structure; and tangentially (after sectioning out the blade segments), which indicated the arrangement of the inner structures. The

ORIGINAL PAGE IS
OF POOR QUALITY

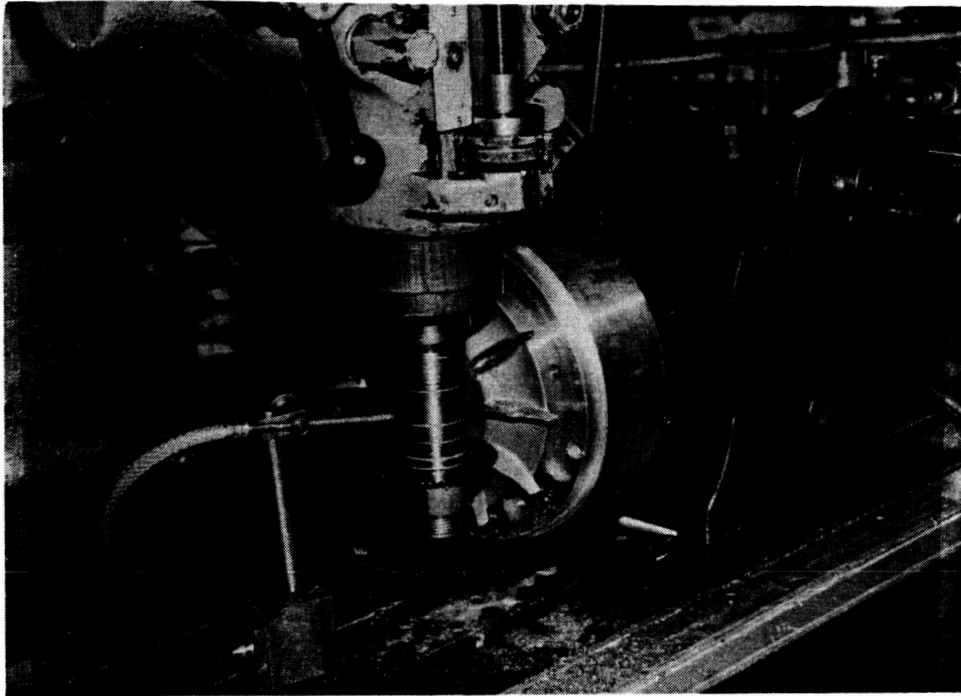


Figure 16. Milling Split Blade Cavities

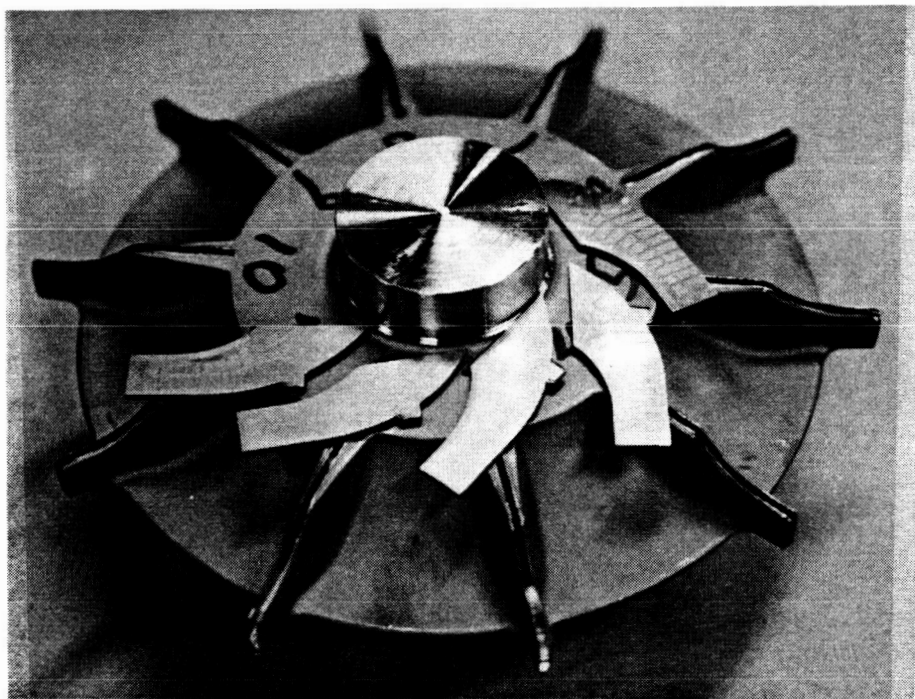


Figure 17. Machined Wheel and Carrier Assemblies

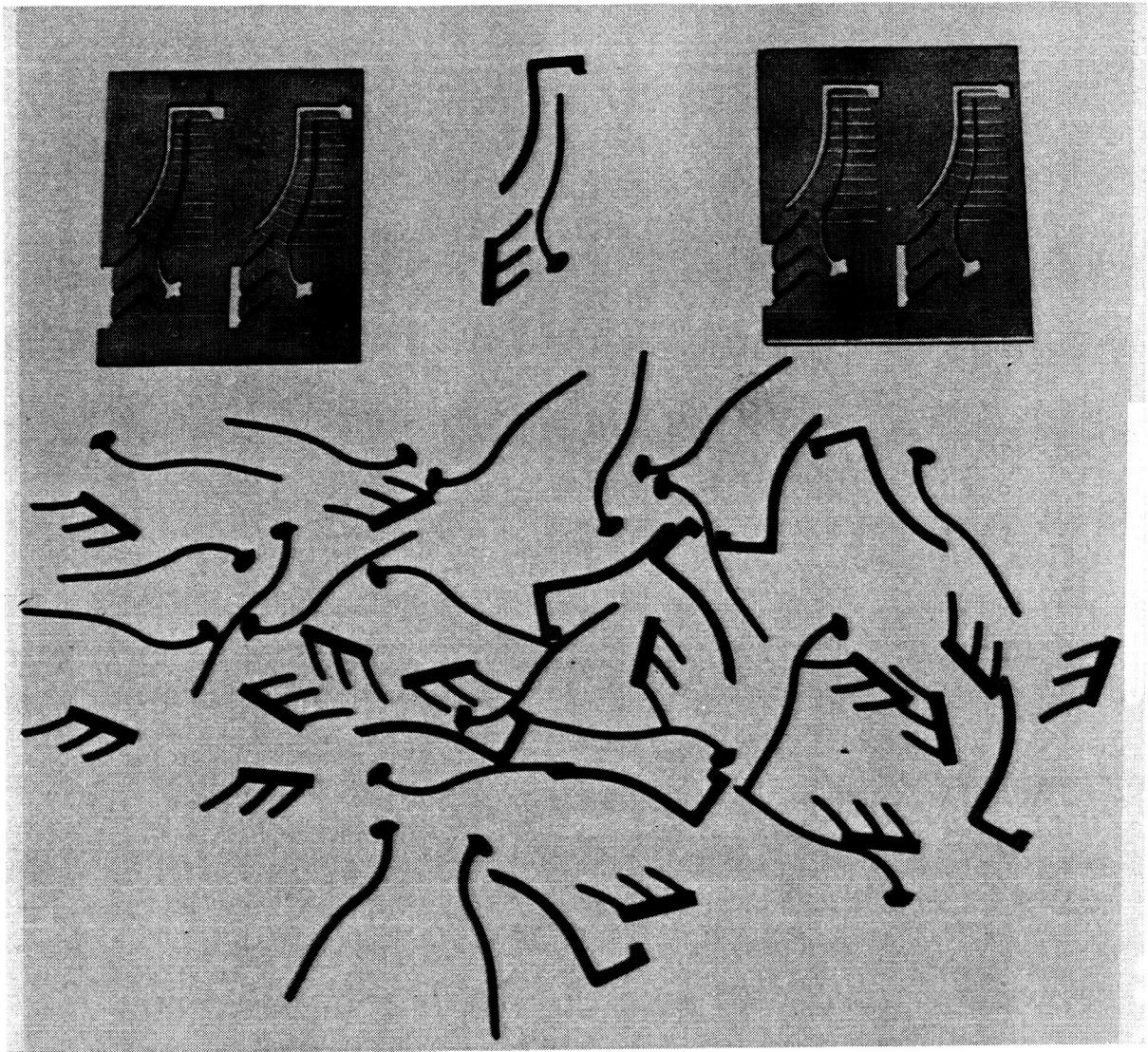


Figure 18. EDM Wire Sawn Carriers and Inserts

blades were subsequently sectioned and metallographically examined. Two discrepancies were noted in the results: firstly, the alignment of the carrier/insert assemblies within the slots was compromised by the inadvertent removal of the tab which should key into the air inlet passage. A shaped, steel tab was substituted to prevent passage collapse during HIPing, but since this was not an integral part of the carrier, the alignment was compromised. This caused four of the assemblies to protrude excessively from either the blade tip or trailing edge. Secondly, it was obvious that several of the closure welds had not been sound, resulting in lack of pressurization of the joints and a contaminated brazing atmosphere. It appears that four of the blades were so affected.

The first discrepancy resulted from misinterpretation of the instruction to "radius the tabs" on the carrier/insert assemblies, and therefore was corrected in subsequent production. The second discrepancy, unsound welding, was partially compensated for in sealing the second lot of wheels by variations in the technique. These included sealing the curved and trailing edges of the blade by conventional TIG welding, proofed by fluorescent penetrant inspection prior to final closure by EB welding of the blade tip. A 12-hour pumpdown of the vacuum chamber was included to compensate for the reduced area of the final sealed joint. The probable more ideal technique would be to core the air inlet hole in the casting directly into the slot and to use it for leak testing after sealing the blade edges. It could then be sealed, in a vacuum, by crimping a welded-in tube, or by a similar, more reliable technique.

The second batch of two wheels was assembled -- this time with the carrier tab intact -- welded, with the improved technique, HIP-bonded as before, and solution heat treated, preparatory to rough machining and acid leaching.

5.4 THERMAL TREATMENT

Bonding of the assembled and weld sealed wheels was conducted by an outside toll HIPing facility according to the schedule established in earlier tests, Section 3.2. Both the first lot, wheels S/N 1 and 15, and second lot, wheels S/N's 9 and 20, were processed identically:

1185°C (2165°F)
103.4 Mpa (15,000 psi) pressure
4 hours at temperature

Both runs were monitored by continuous recordings of temperature, pressure, and gas quality and conformed to requirements in every respect.

Upon receipt of the HIP-bonded wheels at Solar, they were each solution heat treated in vacuum, 1×10^{-5} Torr or better as follows:

1177°C (2150°F) for 2 hours at temperature
Argon fan cool to below 538°C (1000°F)
Reheat to 1121°C (2050°F) for 2 hours at temperature
Argon fan cool to below 538°C (1000°F)

5.5 LEACHING

Preparatory to acid leaching of the blade cores, the diameter and trailing edge contours of the blades were shaped to net dimension (removing the weld beads) by cutting on a numerically controlled EDM wire saw. One wheel, S/N 20, was damaged in the cutting process (Fig. 19) when the sensing mechanism of the wire saw mispositioned the back side of one blade tip and cut about 1.3 mm (0.05 in.) too deeply into the internal cooling cavity. The air inlet

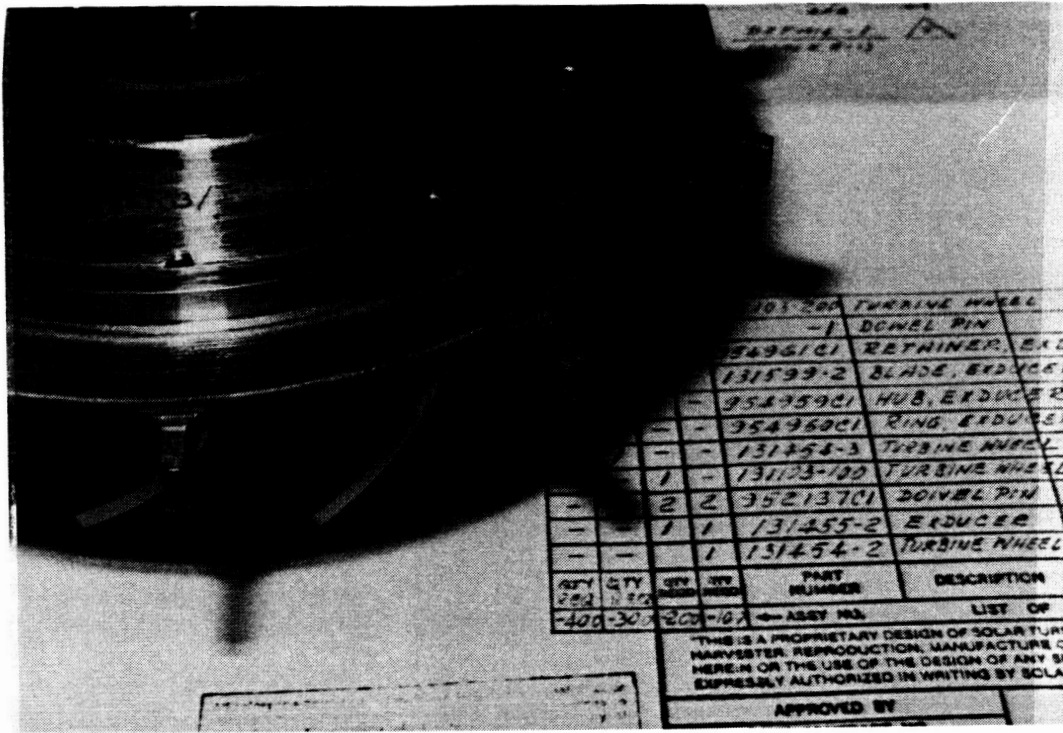


Figure 19. Mis-machined Blade Tip

passages and tip ejection holes also were opened by electro-discharge drilling. The parts were subsequently immersed in a refluxed nitric acid-methanol solution, 50-50 mixture, at approximately 70°C (160°F), for ten hours. Gas evolution was observed to stop after about six hours. For the final four hours of leaching, the obverse side of the wheel was placed uppermost in order to guarantee complete removal of the steel core in all interstices of the blades. At the cessation of etching, the blade were rinsed with pressurized cold water (serving as a flow test); with a dilute sodium bicarbonate solution; and with a final hot water rinse.

5.6 MACHINING, ASSEMBLY, AND AGING

Machining and assembly to final dimensions was conducted by an outside subcontractor. The majority of the effort was in producing the curvic couplings on the "back" face of the star wheel; the "front" face of the exducer; and mating and pinning the two to form the complete wheel. No machining was necessary on the blade contours or diameters.

The completed assemblies were returned to Solar for final aging (both sections being in the HIPed and double solution heat treated condition). Double aging was conducted in vacuum at 843°C (1550°F) for four hours plus 760°C (1400°F) for 16 hours.

6

INSPECTION

6.1 VISUAL AND DIMENSIONAL

Wheels S/N 1 and 5 which, as noted previously, had the internal spacers and details mispositioned through machining error, were exempted from final machining. It was decided, however, to destructively section wheel S/N 1 to survey the internal cavities. This confirmed the earlier suspicions as to poor quality of the closure welds. In several of the blades the internal details had failed to properly braze.

The second lot of HIP-brazed wheels, S/N's 9 and 20 both, after final machining, conformed to complete dimensional requirements. The completed wheel is seen in Figure 20.

6.2 NON-DESTRUCTIVE INSPECTION

The results of radiographic inspection of the blades were generally inconclusive. Except for delineating improper positioning of the internal components (see Section 5.2) no significant data could be obtained. Inadequate braze strength, for instance, could not be detected.

Liquid penetrant inspection of the blades, after removal of the closure welds, was effective in delineating areas of inadequate bonding, at least at the outer periphery of the blade. Inspection of the internal details was not possible by this method, although it was found (by destructive sectioning of wheel S/N 1) that the external bond quality was in all cases indicative of the internal.

6.3 FLOW TEST

Both wheels, S/N's 9 and 20 were flow tested after assembly and final machining. Water flow testing served to demonstrate that all cooling passages were open and free of obstruction.

Subsequently both wheels were subjected to dynamic pressure drop test with air, simulating more accurately actual operation in the engine. Results were as seen in Table 9. There is close similarity in comparison of the two wheels and in comparison of the cast-to-size cooling passages in the exducer section and the fabricated passages in the exducer.

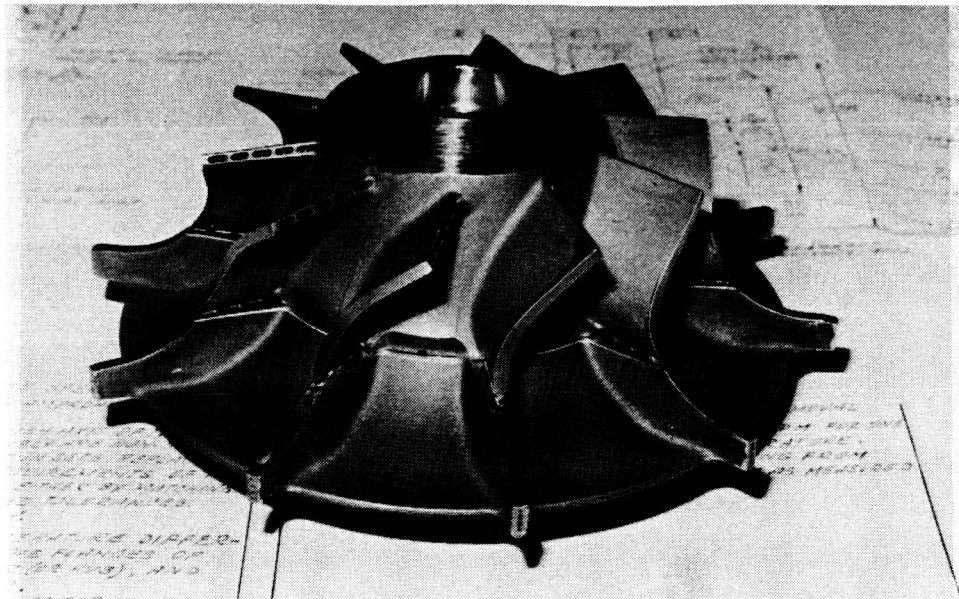


Figure 20. Completed Wheel

6.4 SPIN TEST

Wheel S/N 9 was spin tested (Fig. 21), incrementally at 50, 75, 90, 100, and 110 percent of operating speed, 65,000 rpm, holding one minute at each target speed. Measurements were taken at five diameters of the wheel, across the blade tips. The test was repeated after thermally cycling the wheel from room temperature to 900°C (1650°F) six times. Results, before and after thermal cycling, are seen in Table 10. Neither showed significant growth at any speed.

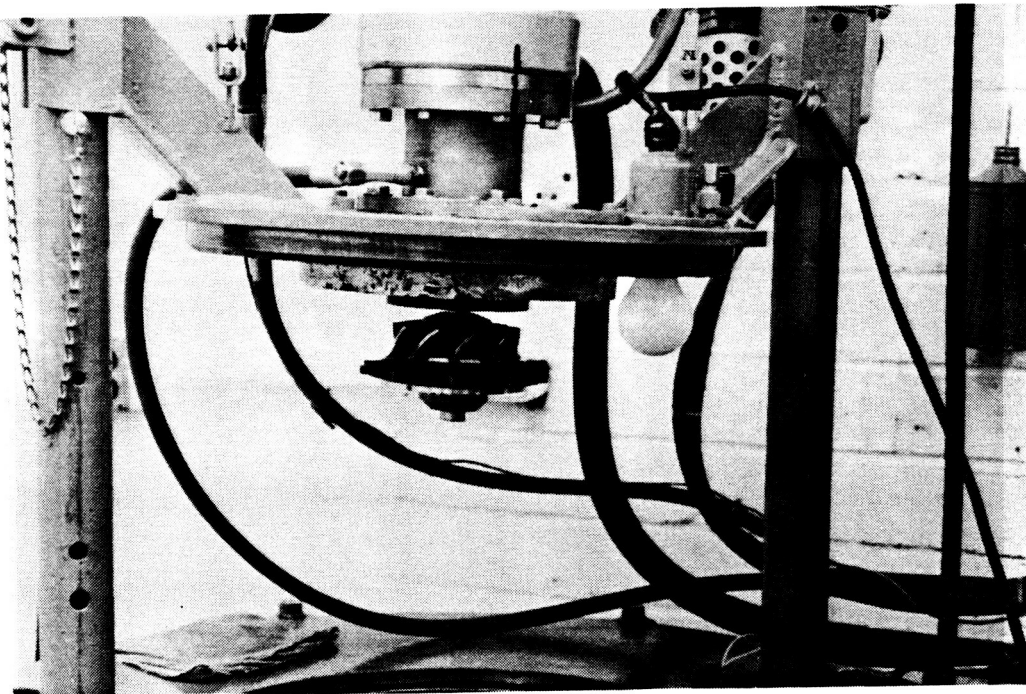


Figure 21. Spin Testing

Table 9
Flow Test Data

	Wheel S/N 9			Wheel S/N 20		
	Total	Exducer	Star Wheel (by difference)	Total	Exducer	Star Wheel (by difference)
Geometric Area, in. ²	1	1		1	1	
Wheel Pressure, in. H ₂ O	25.05	25.15		25.35	25.00	
Nozzle Pressure, in. H ₂ O	1.003	0.62		1.7	0.94	
Ambient Temperature, °F	80	80		80	80	
Ambient Pressure, in. Hg	30	30		30	30	
Number of Nozzles	1	1		1	1	
Effective Area, in. ²	0.0913	0.0718		0.1178	0.0885	
Flow Function	0.0248	0.0196		0.0323	0.0241	
Pressure Drop, %	6.1440	6.1686		6.2177	6.1318	
Wheel Mass Flow, lb/sec	0.0157	0.0214		0.0205	0.0153	
Discharge Coefficient	0.0913	0.0718	0.0195	0.1178	0.0885	0.0293

Table 10
Spin Test Results

Percent of Rated Speed (65,000 rpm)	Temperature		Before After Spin	Diameters, Inches				
	°C	°F		1	2	3	4	5
BEFORE THERMAL CYCLE								
50	24.4	76.0	B.S.	6.4990	6.4950	6.4983	6.4962	6.4951
	24.4	76.0	A.S.	6.4990	6.4951	6.4985	6.4962	6.4953
75	23.9	75.0	B.S.	6.4990	6.4951	6.4985	6.4962	6.4953
	26.1	79.0	A.S.	6.4990	6.4951	6.4985	6.4962	6.4953
90	25.6	78.0	B.S.	6.4990	6.4951	6.4985	6.4962	6.4953
	26.1	79.0	A.S.	6.4990	6.4951	6.4985	6.4962	6.4953
100	26.1	79.0	B.S.	6.4990	6.4951	6.4985	6.4962	6.4953
	27.2	81.0	A.S.	6.4990	6.4951	6.4985	6.4962	6.4953
110	27.2	81.0	B.S.	6.4990	6.4951	6.4985	6.4962	6.4953
	27.8	82.0	A.S.	6.4990	6.4950	6.4990	6.4970	6.4953
AFTER THERMAL CYCLE								
50	26.7	80.0	B.S.	6.4985	6.4945	6.4980	6.4950	6.4946
	26.1	79.0	A.S.	6.4985	6.4945	6.4980	6.4950	6.4946
75	25.6	78.0	B.S.	6.4985	6.4945	6.4980	6.4950	6.4946
	27.2	81.0	A.S.	6.4985	6.4945	6.4980	6.4950	6.4946
90	27.2	81.0	B.S.	6.4985	6.4945	6.4980	6.4950	6.4946
	27.2	81.0	A.S.	6.4985	6.4948	6.4983	6.4955	6.4950
100	26.7	80.0	B.S.	6.4985	6.4948	6.4983	6.4955	6.4950
	26.7	80.0	A.S.	6.4985	6.4948	6.4983	6.4955	6.4950
110	26.7	80.0	B.S.	6.4985	6.4948	6.4983	6.4955	6.4950
	27.2	81.0	A.S.	6.4985	6.4950	6.4983	6.4955	6.4953

APPENDIX A

**MECHANICAL DESIGN SUMMARY
NASA AIR-COOLED RADIAL TURBINE ROTOR**

INTER-OFFICE MEMO

September 21, 1981

To: ~~A. N. Hammer~~

cc: W. A. Compton
A. G. Metcalfe
W. D. Treece
G. L. Padgett
C. Rodgers
G. Aigret
T. P. Psychogios
J. V. Gallagher

From:

A. W. August
A. W. August

Subject: MECHANICAL DESIGN SUMMARY -- NASA AIR-COOLED
RADIAL TURBINE ROTOR

The objective was to design and manufacture a high temperature air-cooled radial inflow turbine rotor per Solar S. O. 6-4938-7.

The following contributors took part in the design of the rotor:

Aero	- C. Rodgers
Heat Transfer	- G. Aigret, N. Anderson
Stress	- T. P. Psychogios, R. P. Barrow
Manufacturing	- A. N. Hammer, Howmet Turbines Corp.
Cost	- J. V. Gallagher
Mechanical Design	- A. W. August, T. P. Psychogios

Based on cooling and manufacturing constraints, two-piece turbine rotor with separate star-wheel and exducer have been selected for design.

Layout Drawings 131101 and 131102 show two main configurations of the turbine rotor considered in the design; Drawing 131103 with one-piece cast star-wheel and one-piece cast exducer; Drawing 131101 with individually bladed star-wheel and exducer.

After final review of the above layouts, the following wheel assembly drawings have been prepared for cost analysis and manufacturing selection:

131453-100	- Rotor Assy, with cast star-wheel & exducer
131453-200	- Rotor Assy, with brazed star-wheel & cast exducer
131453-300	- Rotor Assy, with cast star-wheel & bladed exducer
131453-400	- Rotor Assy, with brazed star-wheel & bladed exducer

SOLAR TURBINES INCORPORATED

September 21, 1981

The following hardware drawings and specifications have been prepared and released to Solar file:

- 131454 - Wheel, Turbine - Air-cooled (cast star-wheel)
 - 131103 - Wheel, Turbine - Air-cooled (brazed star-wheel)
 - 131467 - Insert, Blade - Air-cooled (brazed star-wheel)
 - 131455 - Exducer, Turbine - Air-cooled (one-piece cast)
 - 131599 - Blade, Exducer - Air-cooled (casting & mach.)
 - 954959C1- Hub, Exducer - Air-cooled
 - 954960C1- Ring, Exducer - Air-cooled
 - 954961C1- Retainer, Exducer Blade
- DSK-17073- Material Specifications for Turbine Wheel Castings
131100 - Proposal, T-62 Engine Assy. with Ti-Temp Turbine Wheel

The geometrical description of the turbine wheel was based on C. Rodgers' data and blade coordinates with very slight changes required to optimize wheel cooling.

Cooling of the cast turbine wheel has been described by G. Aigret and N. Anderson in the report T-5500 -- "Heat Transfer and Aerodynamics Design Status." The stress analysis of the turbine wheel assemblies are described in Report T-5537 by T. Psichogios and P. Barrow.

It should be noted that for the individually bladed exducer assembly additional cooling air leakage through the side of blade seals can be expected. The effect of this additional leakage on the wheel cooling has not been reviewed by the heat transfer people.

AWA:gm

Engineering Report

2800°F, R.I.T. NASA COOLED RADIAL TURBINE ROTOR
STRESS ANALYSIS REPORT

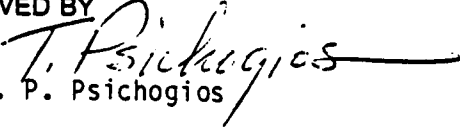
REPORT T-5537

ISSUED October 27, 1981

PREPARED BY


P. Barrow

APPROVED BY


T. P. Psychogios

CUSTOMER REF NAS3-22513

SOLAR REF S.O. 6-4938-7

COPY NO

TABLE OF CONTENTS

<u>Section</u>		<u>Page</u>
1.0	INTRODUCTION	1
2.0	SUMMARY	1
3.0	ANALYTICAL DESIGN	2
3.0.1	Design Analysis	2
3.0.2	Metal Temperatures	3
3.0.3	Rotor Material Properties	3
3.0.4	Rotor Stress Analysis	3
	3.0.4.1 Operating Conditions	3
	3.0.4.2 Star Wheel (One-Piece Casting) Analysis	4
	3.0.4.3 Exducer Wheel (One-Piece Casting) Analysis	4
	3.0.4.4 Inserted (Exducer) Blade Analysis	4
4.0	DESIGN SPECIFICATIONS MARGINS OF SAFETY	5
4.0.1	Star Wheel	5
4.0.2	Cast Exducer Wheel	7
4.0.3	Blade Root Fixing (Exducer)	7
4.0.4	Disc Stub Fixing (Exducer)	8
4.0.5	Forged Disc Hub (Exducer)	8
5.0	CONCLUSION	9
TABLES 1 Thru 6		13-16
FIGURES 1 Thru 41		17-57
ADDENDUM		59-96

PRECEDING PAGE BLANK NOT FILMED

1.0 INTRODUCTION

This report summarizes the stress analyses of the radial inflow cooled turbine rotor designed to NASA RFP 3-188454 of April 22, 1980. Numerous stress and design iterations were completed prior to arriving at the configuration discussed in this report.

The radial turbine wheel design incorporates cast blades with internally cored passages for the flow of cooling air to maintain blade metal temperatures to an acceptable limit consistent with the required creep-rupture life of the metal. Because of the complexity of the blade cored passages and the requirement for multi-path cooling air supply, it was necessary to construct the rotor in two sections as follows:

1. A star wheel section in which the blades lie in axial-radial planes on the disc hub
2. An exducer wheel section in which the blades are axially cambered and disposed radially on the disc hub.

The design/analysis effort included two exducer configurations as follows:

1. A one-piece cast blade-disc design
2. Individually cast blades attached to a (forged) disc hub by conventional dovetail type attachments and shown in Figure 38.

The individual (inserted) blade design was included in case major problems were encountered in the production of sound one-piece blade-disc castings.

Note: The star wheel design has been limited to a one-piece cast blade-disc configuration since no problems are anticipated in the production of sound castings. Fabrication of the star wheel blades can actually be accomplished by an alternate method as shown in Figure 39. This procedure will generate blades similar in design to the one-piece cast configuration and will be investigated along with the cast design.

The blade-disc configurations listed above have all been designed to meet the design and stress criteria listed in para 2.1.4 and para 2.1.5 of Proposal RFP 3-18454, QR 6-4938.

2.0 SUMMARY

The four rotor design configurations (integrally cast star wheel and blades, integrally cast exducer wheel and blades, individually cast exducer blades inserted into a forged hub and fabricated star wheel blades) all conform to the design requirements stipulated in para 2.1.4 and 2.1.5 of RFP 3-188454, QR 6-4938. The one exception to the design requirements is the 1500-hour stress-rupture life of the star blades. In order to meet this requirement, the blade (average) metal temperature must be reduced by 75° to 100°F. This can best be accomplished by reducing the turbine inlet temperature from the present 2800°F value. These rotor designs have been cleared for detailed

PRECEDING PAGE BLANK NOT FILMED 47

PAGE 46 INTENTIONALLY BLANK

design drafting and meet all the requirements of room-temperature spin, stress-rupture life, and gross yield speed.

Finite element analyses have been used in the computation of stress and of local metal temperatures, the respective computer programs for each analysis including all the parametric variables that affect the calculated values. A very high degree of confidence is, therefore, attached to the validity of the design analysis.

The IN-792 alloy (HIPed and heat treated) used in the investment casting of the star and exducer rotors is a proven material extensively used in the production of turbine blades for high-temperature applications in company turbine products. A 6.5 inch diameter uncooled radial turbine rotor integrally cast in IN-792 alloy is also presently used in a production engine. The IN-718 (AMS 5398) wrought alloy selected for the alternate exducer hub design is also extensively used in company turbine disc applications.

A concession was made in the overall design of the star wheel wherein the rear face was contoured radially rather than angled similar to the forward face. This was necessary since it had to be matched with the exducer wheel on assembly and also provide the air supply to the exducer blades. This concession increased the local (radial) stress across the air feed hole at the disc aft face to a value exceeding the material tensile strength. Since the value is, however, higher than what would actually occur in practice and because the high stress is localized on the disc surface, it is not regarded as affecting the wheel integrity for the required 1500-hour (steady-state) operation.

All rotor designs adequately meet the burst and gross yield speed requirements and the rupture life of the star wheel blades will also comply provided the metal temperature is reduced by the margin stipulated.

3.0 ANALYTICAL DESIGN

3.0.1 Design Analysis

The blade and disc designs were completed to comply with the stipulated requirements as stated in RFP 3-188454, QR 6-4938. Design stress analyses were done by use of a two-dimensional finite element program that allowed evaluation of [radial, tangential and axial] stresses in axisymmetric solids and [radial and axial] stress in plate sections. The program permitted evaluation of stresses (mechanical and thermal) in both disc and blade portions of the rotors. Certain hand analyses were also conducted to complete the design analysis. The resulting stress in all rotor components were limited to values that would comply with the requirements as mentioned above. These are:

- (a) Minimum rotor burst speed shall be at least 140 percent of maximum continuous design speed.
- (b) Gross yield speed of the rotor shall be at least 120 percent of maximum continuous design speed.

- (c) Stress-rupture life shall be 1500 hours based on minimum rupture strength data.
- (d) A 1500 start-stop cyclic life is targeted for the rotor and would be met. No component testing will, however, be done to confirm this requirement.

It should be noted that in the evaluation of thermal stress due to temperature gradients, only average (steady-state) temperatures through the blade thickness were used. The two-dimensional computer program does not permit the use of temperature variations in a tangential direction in either the rings or the plates and limited the analysis to the evaluation of average stress to ensure 1500 hours rotor stress-rupture life. For engine (start-stop) use, the analysis would be enlarged to include evaluation of transient metal temperatures and a rotor three-dimensional model to evaluate time-dependent stresses through the blade thickness and in the rotor hub sections.

3.0.2 METAL TEMPERATURES

Metal temperatures used in the overall stress analysis were supplied by the Heat Transfer group. The rotor (disc and blade) metal temperatures were evaluated for a total inlet temperature (T.I.T.) of 2800°F and a cooling flow of 13 percent of total air flow.

The metal temperatures evaluated are shown in Table 1 (disc metal temperatures) and Table 2 (blade metal temperatures). The geometry of the nodes at which temperatures are listed are shown in Figure 1 (disc node geometry) and Figure 2 (blade node geometry). The mid node temperature values through the blade thickness, as shown in Figure 2, were used in the analysis (blade average metal temperature) as explained in para 3.0.1

The above blade and disc metal temperature input into the finite element computer program results in evaluation of thermal stress which adds to the centrifugal stress due to rotation.

3.0.3 ROTOR MATERIAL PROPERTIES

The materials used in the construction of the various blade-disc rotor configurations are listed in Table 3.

Material property data used in the design analysis are listed in Table 4. All material strengths are minimum design values based on -3σ statistical data.

3.0.4 ROTOR STRESS ANALYSIS

3.0.4.1 Operating Conditions

The rotors have been designed to operate at the conditions listed below:

- (a) Maximum rotational speed of 65,000 rpm (1775 ft/sec tip speed)
- (b) Metal temperatures as stipulated in para 3.0.2.

Both the above operating parameters were used as input into the finite element stress analysis program.

3.0.4.2 Star Wheel (One-Piece Casting) Analysis

The results of the stress analysis of the star wheel and blades are shown in Figures 7 through 13 which are computer plots of the input and output data as listed in Table 5.

Note: The numerical value of the Von Mises equivalent stress is

$$e = \frac{1}{\sqrt{2}} \left\{ (\sigma_R - \sigma_Z)^2 + (\sigma_R - \sigma_T)^2 + (\sigma_Z - \sigma_\theta)^2 + 3 \tau_{RZ}^2 \right\}^{1/2}$$

where: σ_R = radial stress
 σ_T = tangential stress
 σ_Z = axial stress
 τ_{RZ} = shear stress in radial-axial plane.

In keeping with the theory of constant energy of distortion for ductile materials, elastic failure occurs when the equivalent stress value approaches the material yield strength (or elastic limit). This value is, therefore, used in computing the gross yield speed of a rotor subjected to multi-axial normal and shear stresses.

It should be noted that in the finite element analysis of the rotor, those elements that are not complete axisymmetric rings are treated as plates with appropriate thickness values. Hence the blades and the metal between the cooling air holes are treated as plates resulting in no tangential stress values being present at these elements (Fig. 11).

Direct (radial) stress on blade (axial) sections at constant radius were minimized by optimizing the blade area taper ratio. From the blade tip (3.25 Rad) down to section B-B (3.00 Rad) the area was held constant allowing the stress at section B-B to rise to 30 ksi. The areas at all other sections down to the disc hub line were increased in a manner to limit the stress at each section to the calculated maximum value of 40 ksi.

3.0.4.3 Exducer Wheel (One-Piece Casting) Analysis

The results of the stress analysis of the exducer wheel and blades are shown in Figures 14 through 20 which are computer plots of the input and output data similar to the values listed in Table 5.

As described in paragraph 3.0.4.2, non-axisymmetric elements (blades and metal between air holes) are treated as plates with appropriate thickness.

3.0.4.4 Inserted (Exducer) Blade Analysis

The stress in the blade (airfoil) section is similar to the values shown in Figures 17 through 19, para. 3.0.4.2. The stress in the blade and disc root fixing and the disc hub are as below.

3.0.4.4.1 Blade Root Fixing Analysis

The blade root fixing (half section) was modeled as a single plate and analyzed using finite element methods. This method allowed the evaluation of the peak fillet stress and was chosen over empirical methods that utilize photo-elastic data.

The centrifugal loading applied to the blade root dovetail fixing and the (hand) calculated average stress across the neck section are shown in Table 6.

The stresses in the blade root are shown in Figures 22 through 26.

Note: Figure 21 is a layout showing the blade and disc dovetail fixing and the location of the above Sections A-A and B-B.

3.0.4.4.2 Disc Stub Fixing Analysis

The disc stub fixing (half section) was modeled as a single plate and analyzed using finite element methods. The external loading applied to the disc stub for stress evaluation was as shown in Table 6. The stresses in the disc stub are shown in Figures 27 through 31.

3.0.4.4.3 Disc Hub Analysis

The results of the stress analysis of the (forged) disc hub are shown in Figures 32 through 37. The value of the load applied to the disc rim is shown in Table 6.

Note: The rim of an inserted blade disc is defined as the surface at the bottom of the blade slot. Material outside this surface is regarded as 'dead' weight contributing to the rim radial load (160,350 lbs).

4.0 DESIGN SPECIFICATIONS MARGINS OF SAFETY

The margin of safety on the design specifications listed in paragraph 3.0.1 are as follows.

4.0.1 Star Wheel

Maximum radial stress in blades	40,000 psi
Blade average temperature	1600°F

From Figure 4 stress rupture life of blade is evaluated as:

$$46 = (1600 + 460) (20 + \text{Log}_{10} t) \times 10^{-3}$$
$$\text{Log } t = 2.33 \quad t = 214 \text{ hours}$$

To achieve the required 1500 hours stress-rupture life the blade (average) metal temperature must be limited to:

$$46 = (T + 460) (20 + \text{Log}_{10} 1500) \times 10^{-3}$$
$$T = 1525^{\circ}\text{F}$$

Since the blade stress cannot be further reduced (by increasing the area taper ratio) the blade average temperature should be reduced by 75° to 100°F to meet the stress-rupture life requirement.

The average tangential stress in the disc is calculated to be 59,370 psi.
Room temperature material tensile strength 150,000 psi.

Assuming a material casting burst factor of .85

$$\text{Disc burst speed} = 65,000 \times \left[\frac{.85 \times 150,000}{59,370} \right]^{1/2} = 65,000 \times 1.47 = 95,250 \text{ rpm.}$$

The required burst margin of 1.40 has hence been met.

The average equivalent stress in the disc is calculated to be 61,270 psi.
Assuming a disc average temperature of 1200°F, material 0.2 percent yield strength is 120,000 psi.

$$\text{Gross yield speed} = 65,000 \times \left[\frac{.85 \times 120,000}{61,270} \right]^{1/2} = 65,000 \times 1.29 = 83,850 \text{ rpm.}$$

The required gross yield speed margin of 1.20 has hence been met.

Examining the values of equivalent stress contours, it is evident that the stress across the wheel cross section and in the blades are all of a progressively increasing and usual pattern, with no local areas of excessively high stress resulting due to the geometric shape of the rotor. Because of this characteristic of the rotor design, it is valid to use the values of average tangential and average equivalent stress of the wheel cross section to estimate the wheel burst speed and gross yield speed (as has been well substantiated in growth and burst spin tests). There is, however, one area of the wheel where the calculated radial stress in the plate section between the lower air holes are higher than desired. This area is toward the wheel aft face (contour J - 200,000 psi). This is due to a compromise in the wheel shape whereby the rear face was made radial to facilitate matching with the exducer wheel that is clamped to it. The high stress is, however, very localized and quickly reduces to 140,000 psi (contour G). This radial stress value is also actually fictitious since in reality tangential stresses will be in evidence in this area (flowing between and over the air hole boundaries) that will result in stiffening of the disc at this section and a consequent reduction in the radial stress. Tangential stress is not included in plate sections in the computer program analysis.

Cyclic fatigue life in the disc bore resulting from a calculated peak 'elastic' stress of 150,000 psi is estimated to be 10^4 cycles, which exceeds the 1500 cyclic start-stop value stipulated. These values are estimated from cyclic strain controlled material test data.

4.0.2 Cast Exducer Wheel

Maximum radial stress in blades 35,000 psi.
Blade temperature 1500°F.

From Figure 4 stress-rupture life of blade is evaluated as:

$$46.75 = (1500 + 460) (20 + \text{Log}_{10} t) \times 10^3$$
$$\text{Log } t = 3.25 \quad t = 7110 \text{ hours}$$

The required 1500 hours stress rupture life has hence been met.

The average tangential stress in the disc is calculated to be 41,250 psi.
Room temperature material tensile strength 150,000 psi.

$$\text{Disc burst speed} = 65,000 \times \left[\frac{.85 \times 150,000}{41,250} \right]^{1/2} = 65,000 \times 1.75 = 114,280 \text{ rpm.}$$

The required burst margin of 1.4 has hence been met.

The average equivalent stress in the disc is calculated to be 38,335 psi.
Assuming a disc average temperature of 1350°F, material 0.2 percent yield strength is 123,000 psi

$$\text{Gross yield speed} = 65,000 \times \left[\frac{.85 \times 123,000}{38,335} \right]^{1/2} = 65,000 \times 1.65 = 107,340 \text{ rpm.}$$

The required gross yield speed margin of 1.20 has hence been met.

Cyclic fatigue life in the disc bore resulting from a calculated peak 'elastic' stress of 130,000 psi is estimated in excess of 10^4 cycles which exceeds the 1500 start-stop value stipulated. The values are again estimated from strain controlled test data.

4.0.3 Blade Root Fixing (Exducer)

Table 6 shows that the average direct (radial) stress on blade fixing stem neck Section A-A is 53,290 psi. Figure 23 shows that the peak radial stress at root fillet is 150,000 psi dropping rapidly to 70,000 psi and to a value of 30,000 psi in the mid-section of the stem neck.

Under steady-state operating conditions, local yielding and time-dependent creep will result in a reduction of the calculated high 'elastic' stress at the fillet surface. For purposes of stress-rupture life evaluation the calculated average stress will be used to obtain a reliable (ball park) value. However, if the rotor is subjected to cyclic (stop-start) conditions, the resulting total strain range at the fillet surface must be evaluated and compared to the material (strain range) fatigue cyclic properties.

In keeping with the above statements the following are estimates of blade neck stress-rupture and cyclic fatigue life:

Average stress across blade neck (Section A-A) 53,290 psi
 Blade neck metal temperature (estimated) 1300°F

Stress-rupture life from Figure 4:

$$44 = (1300 + 460) (20 + \log_{10} t) \times 10^{-3}$$

$$\log_{10} t = 5.00 \quad t = 100,000 \text{ hours}$$

This value far exceeds the required 1500-hour life requirement.

For a peak fillet stress of 150,000 psi the total cyclic strain range generated at each start and stop cycle of the unit would be approximately 0.625 percent. Strain range cyclic data for the material indicates a cyclic life of 10^4 cycles (10,000 cycles) which exceeds the 1500 start-stop requirement.

4.0.4 Disc Stub Fixing (Exducer)

Table 6 shows that the average direct (radial) stress on the disc stub neck Section B-B is 74,000 psi. Figure 28 shows that the peak radial stress at stub neck fillet is 140,000 psi dropping rapidly to a value of 100,000 psi and to a value of 40,000 psi at mid-section. The same reasoning would apply to the reduction of local high 'elastic' stress at the disc stub neck fillet surface (para 4.0.3) under steady-state operating conditions. The resulting stress-rupture and cyclic fatigue life estimates are as follows:

Average stress across disc stub neck (Section B-B) 74,000 psi
 Disc metal temperature (estimated) 1150°F

Stress-rupture life from Figure 7:

$$38 = (1150 + 460) (20 \log_{10} t) \times 10^{-3}$$

$$\log t = 3.60 \quad t = 4000 \text{ hours}$$

This value exceeds the required 1500-hour life requirement.

For a peak fillet stress of 140,000 psi the cyclic strain range would be approximately 0.56 percent which would result in a cyclic life in excess of 10^4 cycles which again exceeds the 1500 start-stop requirement.

4.0.5 Forged Disc Hub (Exducer)

The average tangential stress in the disc is calculated to be 57,490 psi.
 Room temperature material tensile strength 185,000 psi.

$$\text{Disc burst speed} = 65,000 \times \left[\frac{.90 \times 185,000}{57,490} \right]^{1/2} = 65,000 \times 1.70 = 110,630 \text{ rpm}$$

The required burst margin of 1.40 has hence been met.

Note: A forging burst factor of .9 is used (as compared to .85 for the cast disc) because of the large ductility value of the IN-718 alloy (15 percent) as compared to the IN-792 alloy (5 percent).

The average equivalent stress in the disc is calculated to be 52,470 psi. With inserted blades it is estimated that the disc average metal temperature would not exceed 1150°F.

Material 0.2 percent yield strength is 120,000 psi.

$$\text{Gross yield speed} = 65,000 \times \left[\frac{.90 \times 120,000}{52,470} \right]^{1/2} = 65,000 \times 1.43 = 92,950 \text{ rpm.}$$

The required gross yield speed margin of 1.20 has hence been met.

4.0.6 'Ballooning' of Blade Surface

A (hand) calculation has been performed to check on the problem of 'ballooning' of the blade surface due to the cooling air pressure internally being larger than the gas surface pressure externally on the cored blade. The blade surface chosen for the analysis is shown in Figure 40 (largest flat plate area) under the internal and external pressures shown in Figure 41.

The hand calculation included indicates a maximum bending stress in the blade wall of 5000 psi and no possibility of 'ballooning' of the blade wall.

5.0 CONCLUSION

Whereas it is anticipated that some (considerable) difficulty may be experienced in producing sound castings of the star and exducer rotors (because of the complexity of the internally cored passages in the blade sections of the two rotors) the mechanical integrity of the two rotors is assured. No drastic or sudden changes in section have been permitted or included in the design of the two rotors (either blade or disc sections) and excluding the above blade cored passage complexity, the design follows standard, state-of-the-art, company practice.

The spin testing of rotors that will commence at speeds (N) equal to:

$$N = 1.2 \times 65,000 \times \frac{\text{0.2 percent yield strength at room temperature}}{\text{0.2 percent yield strength at operating temperature}}$$

under which condition no measurable growth of the rotor must result will ensure that the gross yield speed requirement of the rotors have been met.

Note: The speed is increased in the above ratio since it is not possible to heat the disc to its operating temperature in the spin pit.

A second test will be conducted at a speed at which the tangential stress in the bore is brought up to the value which results under operating temperature conditions. Following this test no measurable growth must result in the bore.

Following the above tests, rotors will be spun at progressively higher speeds until burst failure results. At each speed disc growth values will be measured and plotted versus speed. Visual and other nondestructive testing (NDT) of the rotors will be conducted to ensure that no localized failures have occurred at either the blade or hub sections of both rotors.

The final bursting of the rotors will confirm the burst speed requirements and the nature of the burst segments will indicate the absence (or presence) of any localized weak elements in the rotor design.

In conclusion it can be stated that the detailed stress and thermal analyses conducted in the rotor design, together with the above testing, will ensure the integrity of the rotors to comply with and meet the operational requirements stipulated.

BLADE WALL BENDING DUE TO INTERNAL PRESSURE

The blade section analyzed is rectangular section shown hatched [.900 x .320] (Fig. 40). Assume plate is uniformly loaded and fixed on all sides.

Plate thickness assumed (constant) \approx .040 inch

Assumed average internal pressure \approx 240 psi (Fig. 41)

Assumed average external pressure \approx 135 psi (Fig. 41)

From Roark "Formulae for Stress and Strain", pg. 203, Case 36.

$$\begin{array}{l} \text{Max } s \text{ (at center)} = \frac{\beta \omega b^2}{t^2} \\ \text{Max } \Delta \text{ (at center)} = \frac{\alpha \omega b^4}{t^3} \end{array} \quad \left| \begin{array}{l} \frac{b}{a} \approx 2.8 \\ \beta = 0.750 \\ \alpha = 0.1422 \end{array} \right.$$

$$s = \frac{0.750 \times 105 \times .320^2}{.040^2} = \underline{5040 \text{ psi}}$$

$$\Delta = \frac{0.1422 \times 105 \times .320^4}{24 \times 10^6 \times .040^3} = \underline{.0001 \text{ inch}}$$

NOTE: The remaining exducer areas have pins joining the two walls and the star portion wall thickness is considerably larger and plate areas smaller than above values. The above values are hence the maximum that can be expected.

TIME HR	MINUTES	COUNT	PREV INC	NEXT INC	MIN RC
1.1212E+02	6.7275E+03	300	3.7500E-01	3.7500E-01	1.5000E+00
PREVIOUS TEMPERATURES					
1.3512E+03	1.3992E+03	3	1.4359E+03	1.3306E+03	1.3655E+03
11	12	13	14	15	16
1.3825E+03	1.2507E+03	1.2820E+03	1.3128E+03	1.3428E+03	1.3720E+03
21	22	23	24	25	26
1.3386E+03	1.3667E+03	1.3944E+03	1.4216E+03	1.0811E+03	1.0925E+03
31	32	33	34	35	36
1.3141E+03	1.3616E+03	1.4102E+03	1.4594E+03	1.0976E+03	1.1129E+03
41	42	43	44	45	46
1.3055E+03	1.3530E+03	1.4021E+03	1.4535E+03	1.1660E+03	1.1959E+03
51	52	53	54	55	56
1.4123E+03	1.4591E+03	1.4928E+03	1.1249E+03	1.1898E+03	1.2624E+03
61	62	63	64	65	66
1.1893E+03	1.2566E+03	1.3282E+03	1.4049E+03	1.4880E+03	1.5789E+03
71	72	73	74	75	76
1.3723E+03	1.4409E+03	1.5130E+03	1.5918E+03	1.0786E+03	1.1234E+03
81	82	83	84	85	86
1.3828E+03	1.4293E+03	1.4647E+03	1.4770E+03	1.0742E+03	1.1159E+03
91	92	93	94	95	96
1.3230E+03	1.3463E+03	1.3481E+03	1.0710E+03	1.1044E+03	1.1450E+03
101	102	103	104	105	106
1.2792E+03	1.2662E+03	1.2013E+03	1.0382E+03	1.0731E+03	1.1301E+03
111	112	113	114	115	116
1.0504E+03	1.0896E+03	1.1198E+03	1.1323E+03	1.1183E+03	1.0867E+03
121	122	123	124	125	126
1.0761E+03	1.0664E+03	1.0421E+03	9.6255E+02	9.7049E+02	9.8105E+02
131	132	133	134	135	136
9.9758E+02	9.6906E+02	9.6900E+02	9.6856E+02	9.7378E+02	9.8184E+02
141	142	143	144	145	146
1.0370E+03	1.0952E+03	1.1531E+03	1.1505E+03	9.6919E+02	9.6927E+02
151	152	153	154	155	156
9.9875E+02	1.0078E+03	1.0210E+03	1.0464E+03	1.0941E+03	1.1383E+03
161	162	163	164	165	166
1.2221E+03	1.2258E+03	1.1860E+03	1.1951E+03	1.2033E+03	1.2145E+03
171	172	173	174	175	176
1.1839E+03	1.1956E+03	1.2612E+03	1.3200E+03	1.3798E+03	1.4203E+03
181	182	183	184	185	186
1.1670E+03	1.1775E+03	1.2405E+03	1.2978E+03	1.3506E+03	1.3961E+03
191	192	193	194	195	196
1.5842E+03	1.1479E+03	1.1627E+03	1.2221E+03	1.2738E+03	1.3250E+03
201	202	203	204	205	206
1.5220E+03	1.5524E+03	1.5727E+03	1.5681E+03	1.1571E+03	1.2053E+03
211	212	213	214	215	216
1.4218E+03	1.4595E+03	1.4829E+03	1.5048E+03	1.5108E+03	1.4910E+03
221	222	223	224	225	226
1.4400E+03	1.4678E+03	1.4464E+03	1.4170E+03	1.1197E+03	1.1611E+03
231	232	233	234	235	236
1.4220E+03	1.4036E+03	1.1085E+03	1.2380E+03	1.3334E+03	1.3910E+03
241	242	243	244	245	246
1.2125E+03	1.3186E+03	1.3746E+03	1.3971E+03	1.3916E+03	1.3815E+03
247	248	249	250	251	252
1.2125E+03	1.3186E+03	1.3746E+03	1.3971E+03	1.3916E+03	1.3815E+03

NASA COOLED RADIAL TURBINE-HALF BLADE-HEAT TRANSFER-G.AIGRET

----- TIME HR MINUTES COUNT PREV INC NEXT INC MIN RC
 2.1825E+02 1.3095E+04 195 1.1250E+00 1.1250E+00 4.5000E+00

CURRENT TEMPERATURES

TIME HR	MINUTES	COUNT	PREV INC	NEXT INC	MIN RC
1.7070E+03	2	3	1.6873E+03	1.5150E+03	6
11	12	13	1.5054E+03	1.3836E+03	16
1.5188E+03	1.3763E+03	1.6191E+03	1.5054E+03	1.3836E+03	16
21	22	23	1.3812E+03	1.5046E+03	26
1.3820E+03	1.5149E+03	1.4800E+03	1.3812E+03	1.5046E+03	26
31	32	33	1.6072E+03	1.5513E+03	36
1.5682E+03	1.5185E+03	1.4670E+03	1.6072E+03	1.5513E+03	36
41	42	43	1.5714E+03	1.5151E+03	46
1.5410E+03	1.4835E+03	1.6266E+03	1.5714E+03	1.5151E+03	46
51	52	53	1.6475E+03	1.7778E+03	56
1.6072E+03	1.7585E+03	1.7029E+03	1.6475E+03	1.7778E+03	56
61	62	63	1.7964E+03	1.7085E+03	66
1.7876E+03	1.7145E+03	1.6409E+03	1.7964E+03	1.7085E+03	66
71	72	73	1.6398E+03	1.5285E+03	76
1.6308E+03	1.4897E+03	1.7733E+03	1.6398E+03	1.5285E+03	76
81	82	83	1.4000E+03	1.4000E+03	86
1.6312E+03	1.4350E+03	1.4050E+03	1.3880E+03	1.4000E+03	86
91	92	93	2.4740E+03	2.5500E+03	96
1.5050E+03	1.5530E+03	1.5700E+03	2.4740E+03	2.5500E+03	96
101	102	103	2.4550E+03	2.4560E+03	106
2.4950E+03	2.4850E+03	2.4740E+03	2.4550E+03	2.4560E+03	106
111	112	113	1.0428E+03	1.0555E+03	116
1.0058E+03	1.0174E+03	1.0299E+03	1.0428E+03	1.0555E+03	116
121	122	123	1.1587E+03	1.1754E+03	126
1.1285E+03	1.1422E+03	1.1587E+03	1.1587E+03	1.1754E+03	126
131	132	133	1.3268E+03	1.3412E+03	136
1.2694E+03	1.2895E+03	1.3086E+03	1.3268E+03	1.3412E+03	136
141	142	143	1.1813E+03	1.1813E+03	146
1.1587E+03	1.1648E+03	1.1723E+03	1.1813E+03	1.1813E+03	146
151	152	153	1.4806E+03	1.4631E+03	156
1.4691E+03	1.3872E+03	1.3020E+03	1.4806E+03	1.4631E+03	156
161	162	163	1.4631E+03	1.4100E+03	166
1.4214E+03	1.3604E+03	1.5135E+03	1.4631E+03	1.4100E+03	166
171	172	173	1.6553E+03	1.6621E+03	176
1.7250E+03	1.7210E+03	1.6881E+03	1.6553E+03	1.6621E+03	176
181	182	183	1.6254E+03	1.5704E+03	186
1.6295E+03	1.5816E+03	1.5321E+03	1.6254E+03	1.5704E+03	186
191	192	193	1.4608E+03	1.3627E+03	196
1.5138E+03	1.4368E+03	1.5538E+03	1.4608E+03	1.3627E+03	196
201	202	203	1.6476E+03	1.7312E+03	206
1.6848E+03	1.7291E+03	1.6892E+03	1.6476E+03	1.7312E+03	206
211	212	213	1.6493E+03	1.5706E+03	216
1.6750E+03	1.6132E+03	1.5490E+03	1.6493E+03	1.5706E+03	216
221	222	223	9.6721E+02	9.7291E+02	226
1.5510E+03	1.4647E+03	9.5500E+02	9.6721E+02	9.7291E+02	226
231	232	233	1.0300E+03	1.0424E+03	236
1.0182E+03	1.0664E+03	1.0763E+03	1.0182E+03	1.0424E+03	236
241	242	243	1.0182E+03	1.0182E+03	246
1.0868E+03	1.1002E+03	1.1126E+03	1.0182E+03	1.0182E+03	246
251	252	253	1.0424E+03	1.0424E+03	256
1.0868E+03	1.1002E+03	1.1126E+03	1.0424E+03	1.0424E+03	256

ORIGINAL PAGE IS
OF POOR QUALITY

Table 3

COMPONENT	MATERIAL
One-piece cast (integral blades and disc) star wheel	IN-792 Mod 5A HIPed and heat treated
One-piece cast (integral blades and disc) exducer wheel	IN-792 Mod 5A HIPed and heat treated
Individually cast exducer blades	IN-792 Mod 5A HIPed and heat treated
Forged exducer hub retaining cast exducer blades	IN-718 (to AMS 5398)

Table 4

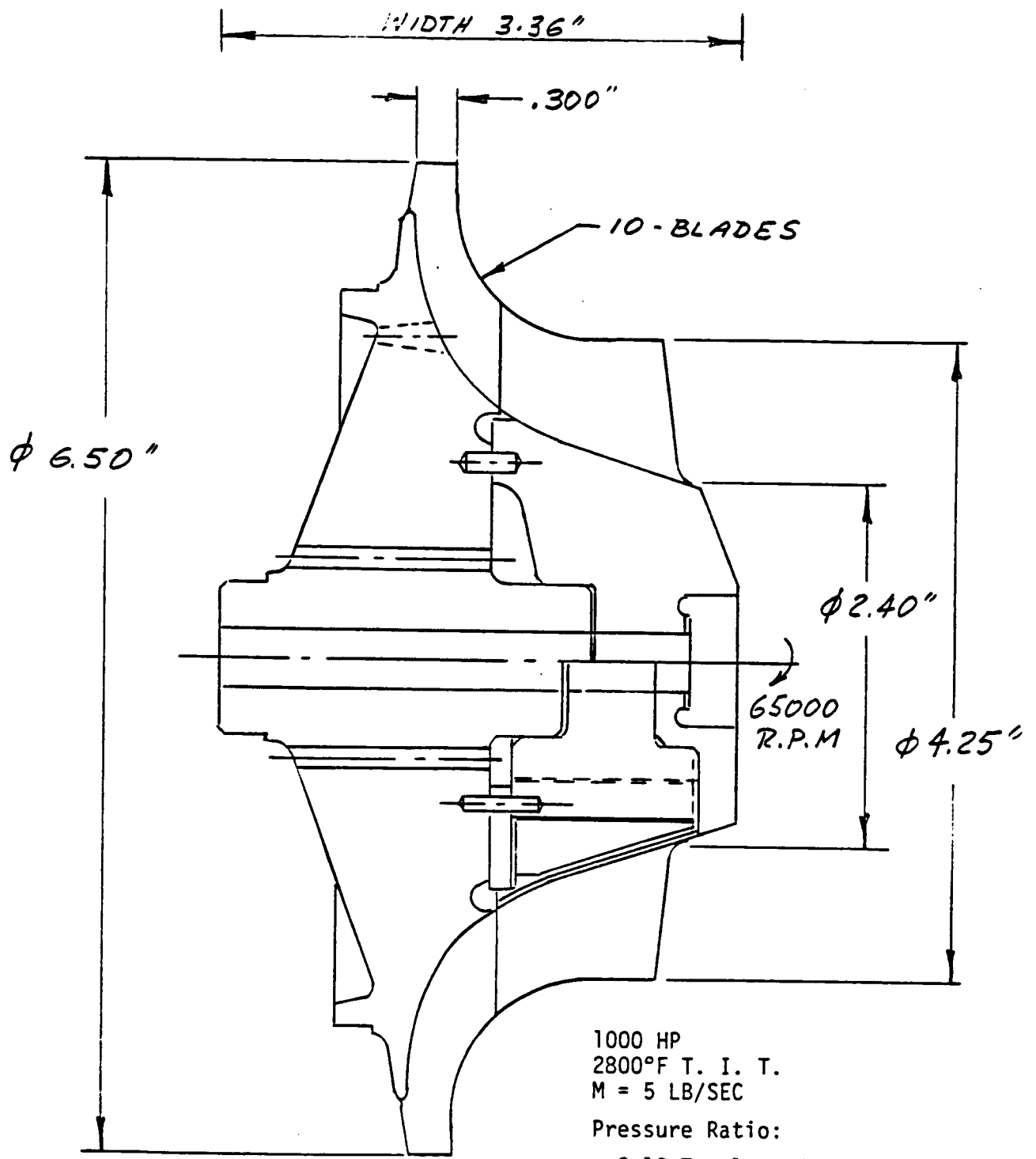
FIGURE NUMBER	PROPERTY
3	IN-792 minimum ultimate tensile strength and 0.2 percent yield strength versus temperature
4	IN-792 Larson-Miller stress rupture data
5	IN-718 minimum ultimate tensile strength and 0.2 percent yield strength versus temperature
6	IN-718 Larson-Miller stress-rupture data

Table 5

FIGURE NUMBER	COMPUTER PLOT DESCRIPTION
7	Finite element geometry node numbers
8	Finite element geometry element numbers
9	Rotor temperature isotherma
10	Rotor radial isostress lines
11	Rotor tangential isostress lines
12	Rotor equivalent isostress lines
13	Rotor operating deflection

Table 6

SECTION	TOTAL LOAD	AVERAGE STRESS
Blade stem neck (Section A-A)	13,480 lbs	53,290 psi
Disc stub neck (Section B-B)	17,575 lbs	74,000 psi
Dovetail fixing bearing surfaces	15,520 lbs	120,725 psi
Disc rim surface	160,350 lbs	



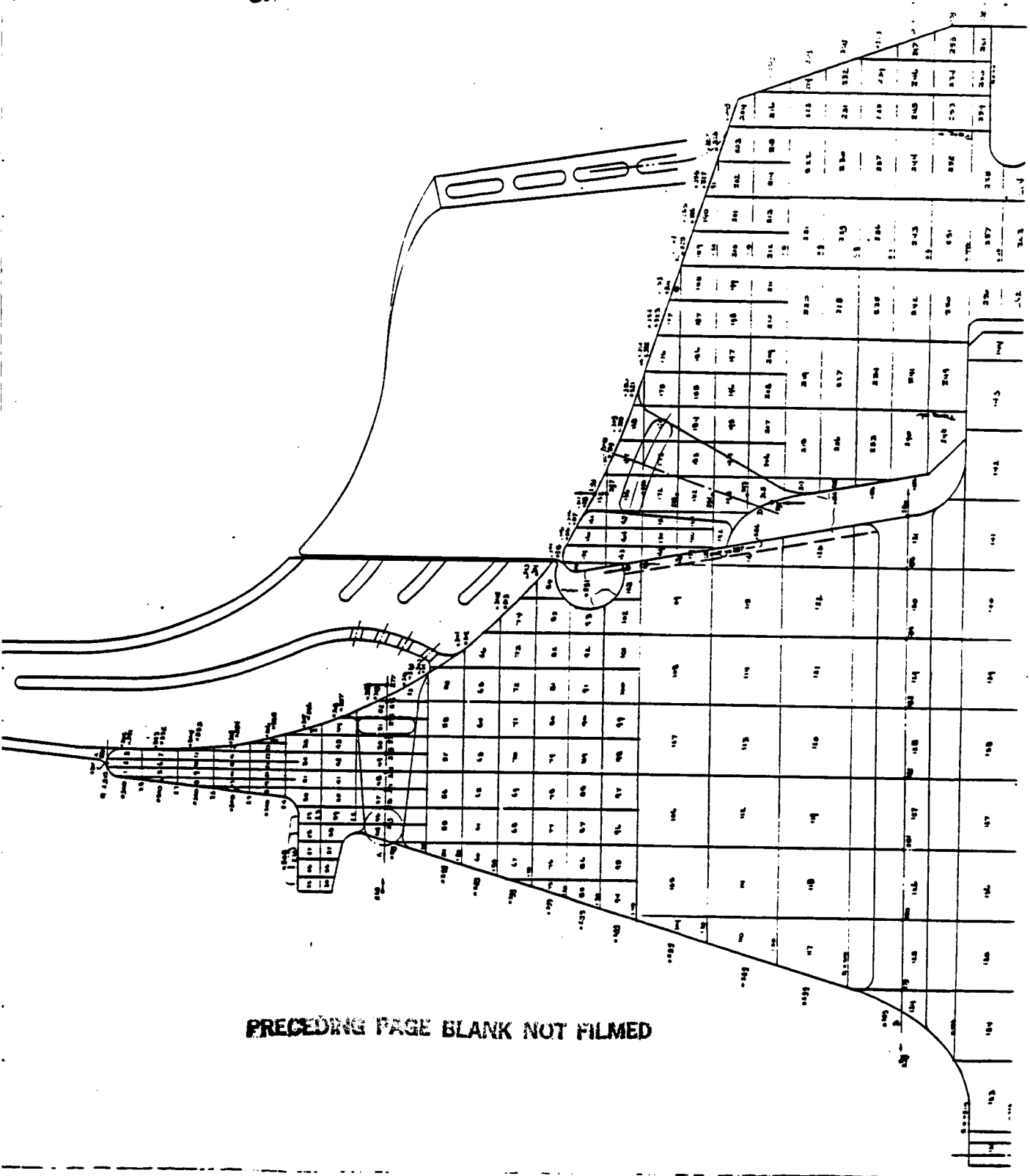
1000 HP
 2800°F T. I. T.
 M = 5 LB/SEC

Pressure Ratio:
 2.19 Total-to-Total
 2.36 Overall Total-To-Static

AIR-COOLED RADIAL TURBINE
 (Full Size)

ORIGINAL PAGE IS
OF POOR QUALITY

FIGURE 1



PRECEDING PAGE BLANK NOT FILMED

ORIGINAL PAGE IS
OF POOR QUALITY

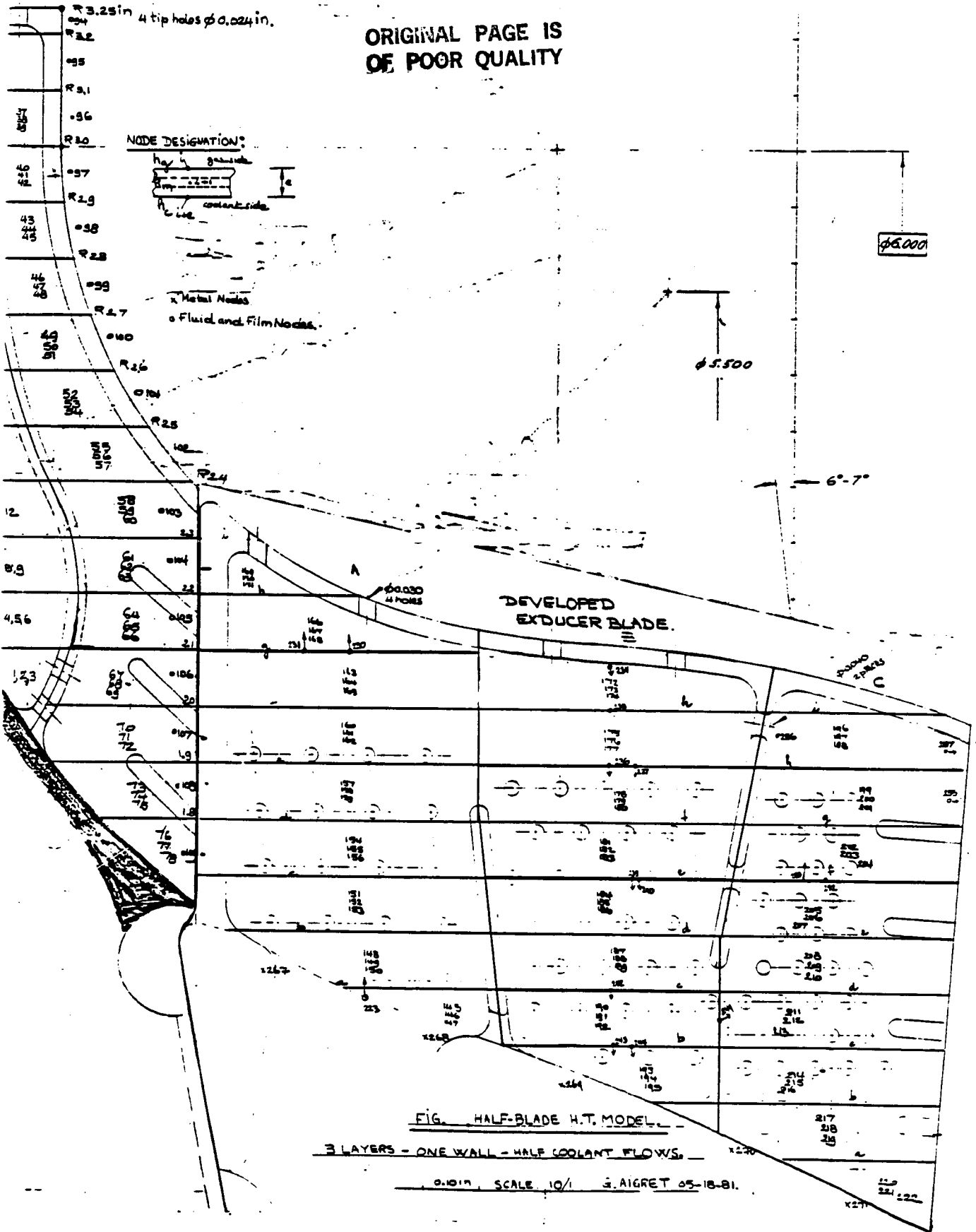


FIG. HALF-BLADE H.T. MODEL

3 LAYERS - ONE WALL - HALF COOLANT FLOWS

0.017 SCALE 10/1 G. AIGRET 05-18-81.

FIGURE 2

FIGURE 3. IN-792 ALLOY (HIPed AND HEAT TREATED)
ULTIMATE TENSILE STRENGTH AND 0.2 PERCENT
YIELD STRENGTH VERSUS METAL TEMPERATURE

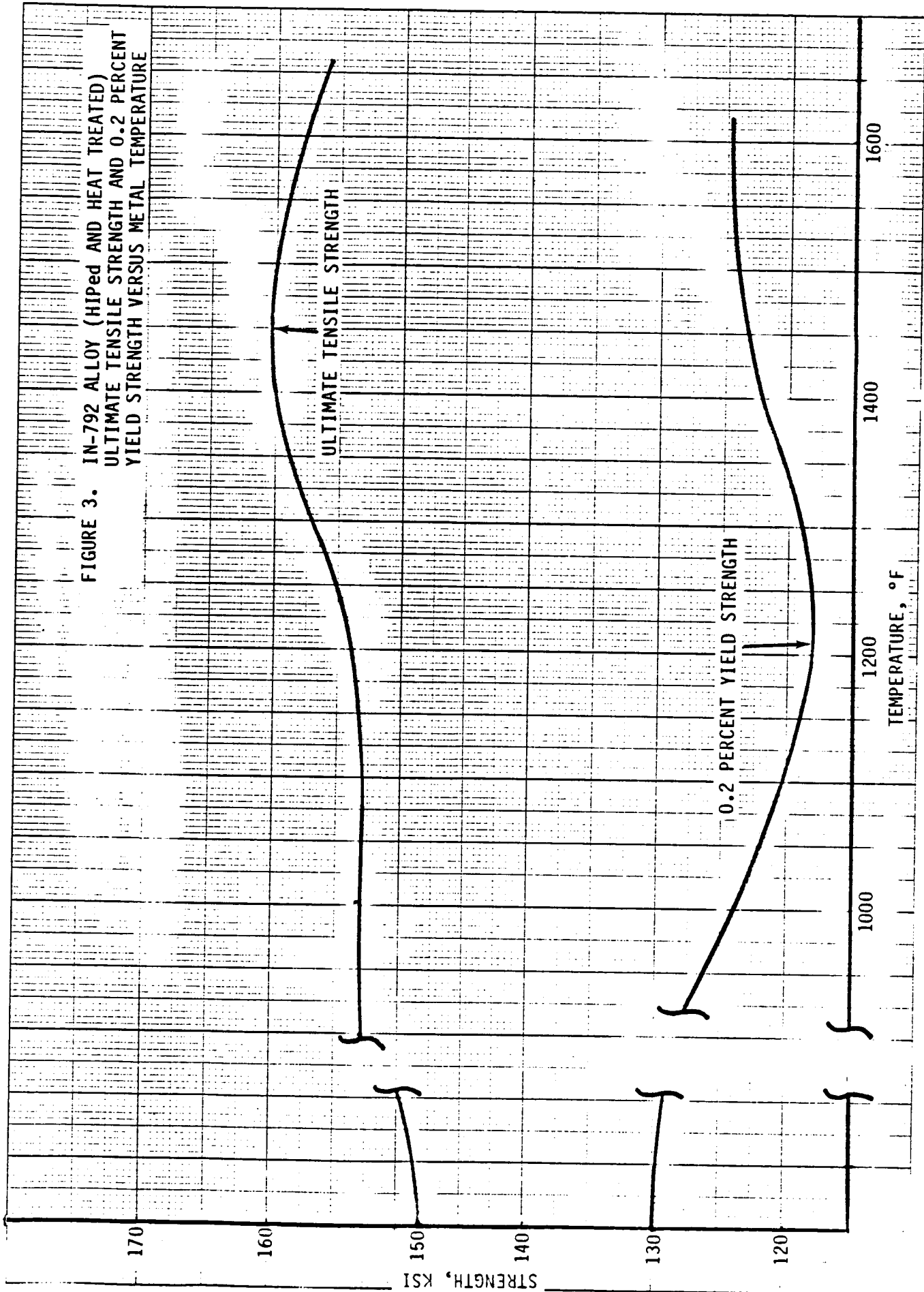
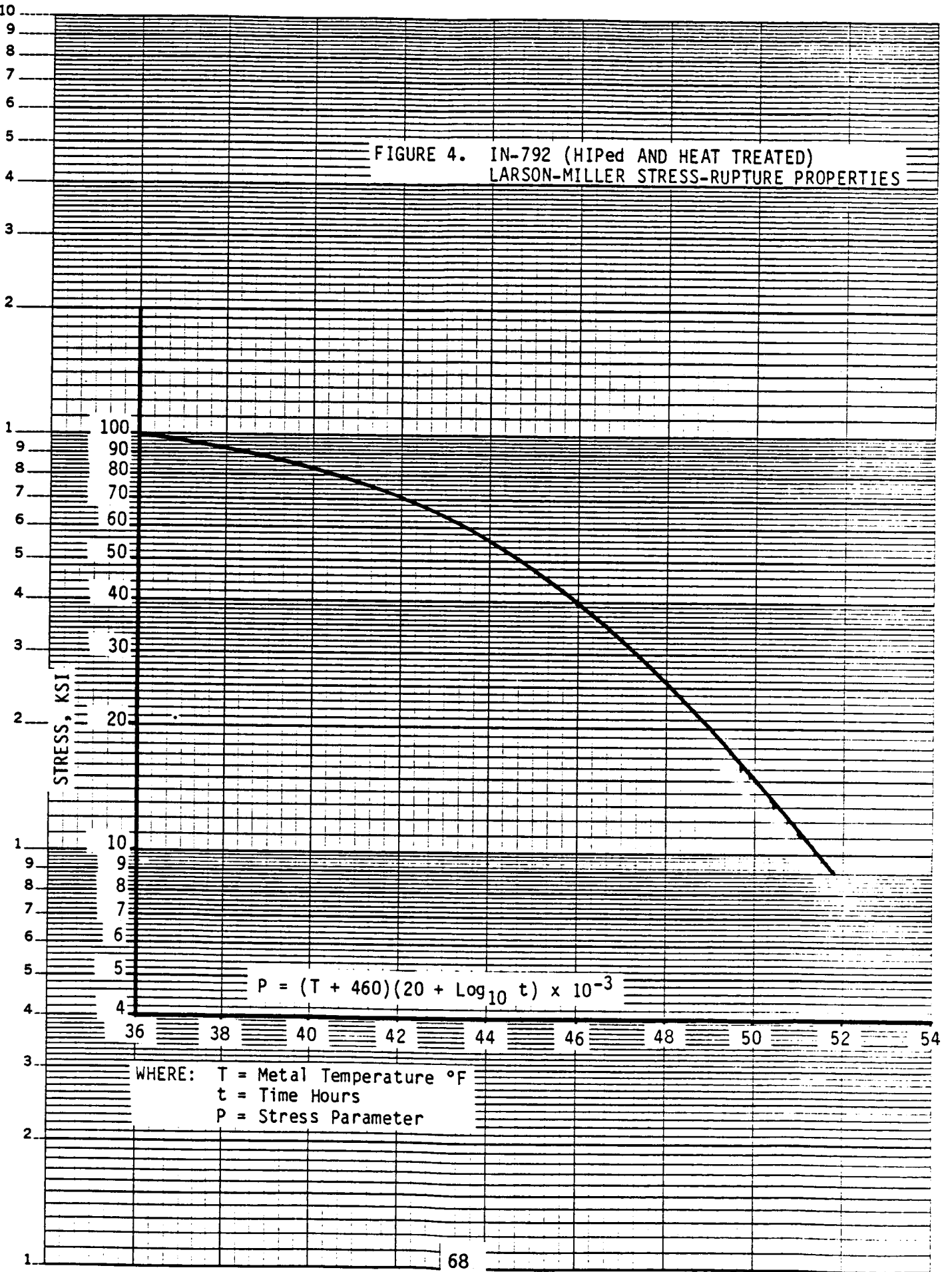


FIGURE 4. IN-792 (HIPed AND HEAT TREATED)
LARSON-MILLER STRESS-RUPTURE PROPERTIES



$$P = (T + 460)(20 + \text{Log}_{10} t) \times 10^{-3}$$

WHERE: T = Metal Temperature °F
t = Time Hours
P = Stress Parameter

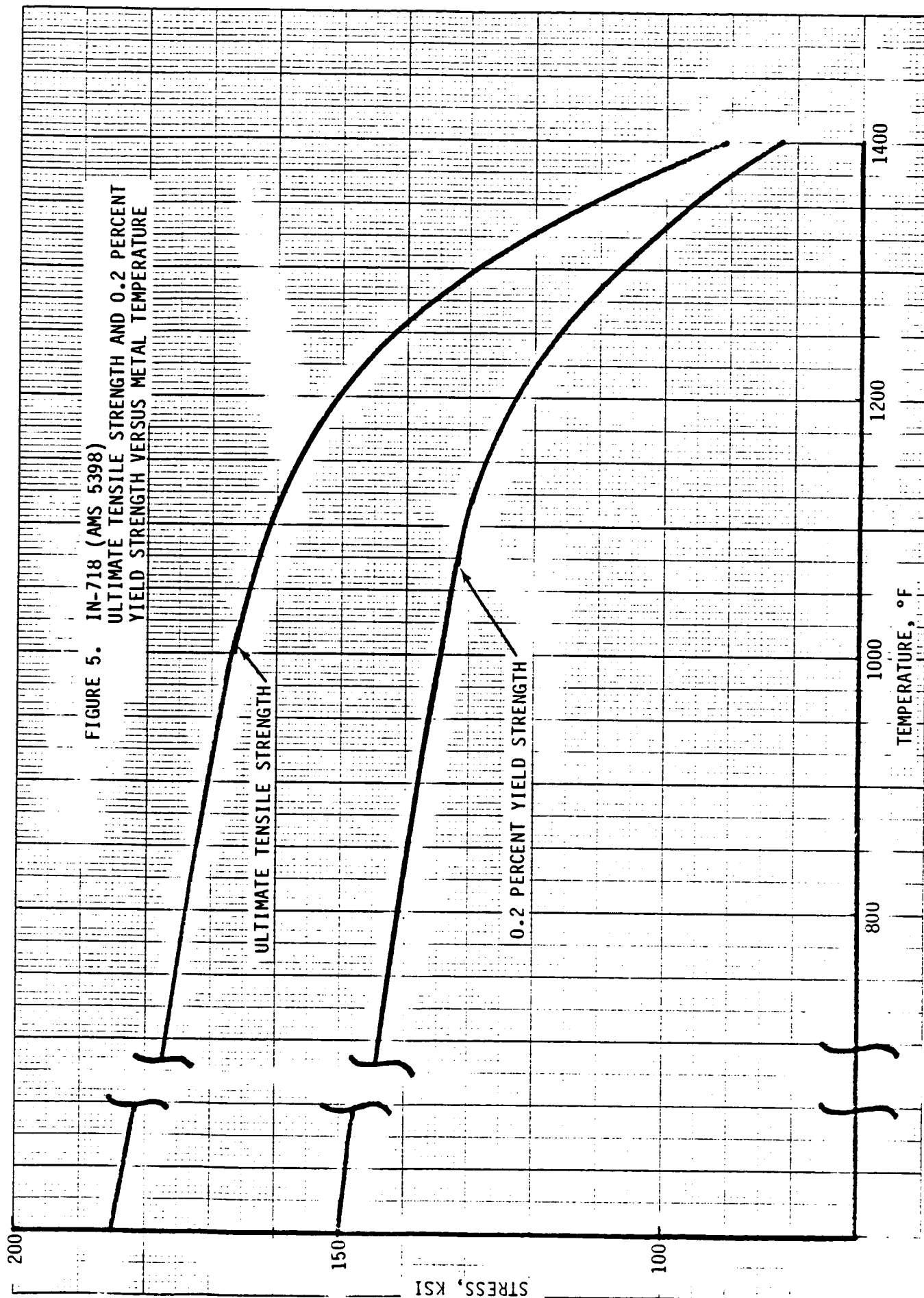


FIGURE 5. IN-718 (AMS 5398)
ULTIMATE TENSILE STRENGTH AND 0.2 PERCENT
YIELD STRENGTH VERSUS METAL TEMPERATURE

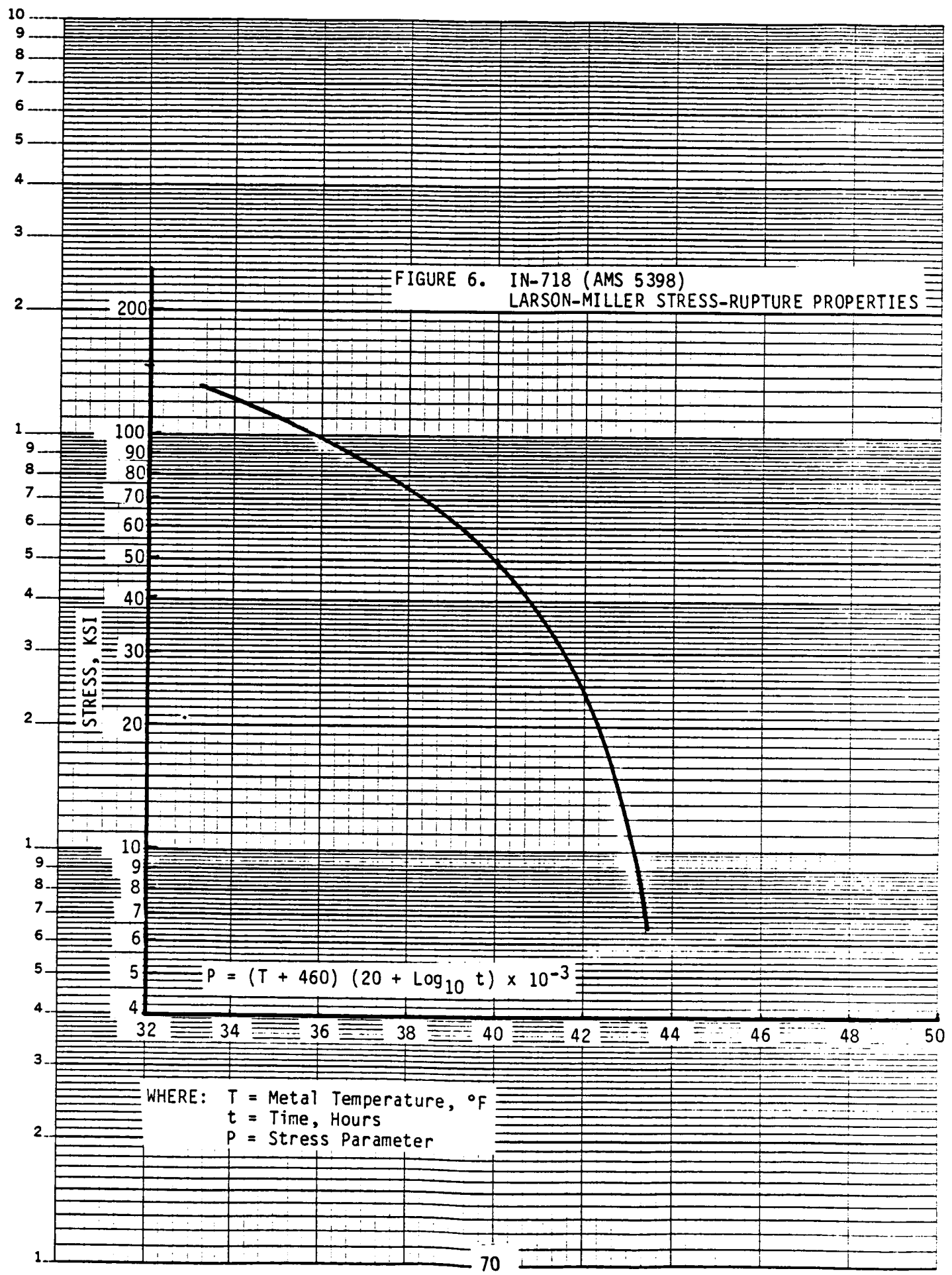
ULTIMATE TENSILE STRENGTH

0.2 PERCENT YIELD STRENGTH

46 5373

KEE SEMI-LOGARITHMIC 3 CYCLES X 60 DIVISIONS
KEUFFEL & ESSER CO. MADE IN U.S.A.

FIGURE 6. IN-718 (AMS 5398)
LARSON-MILLER STRESS-RUPTURE PROPERTIES



PLOT TYPE 1
 SCALF 2.50
 MAX R 3.25
 RPM 65000.
 ORIG. NODE NOS.

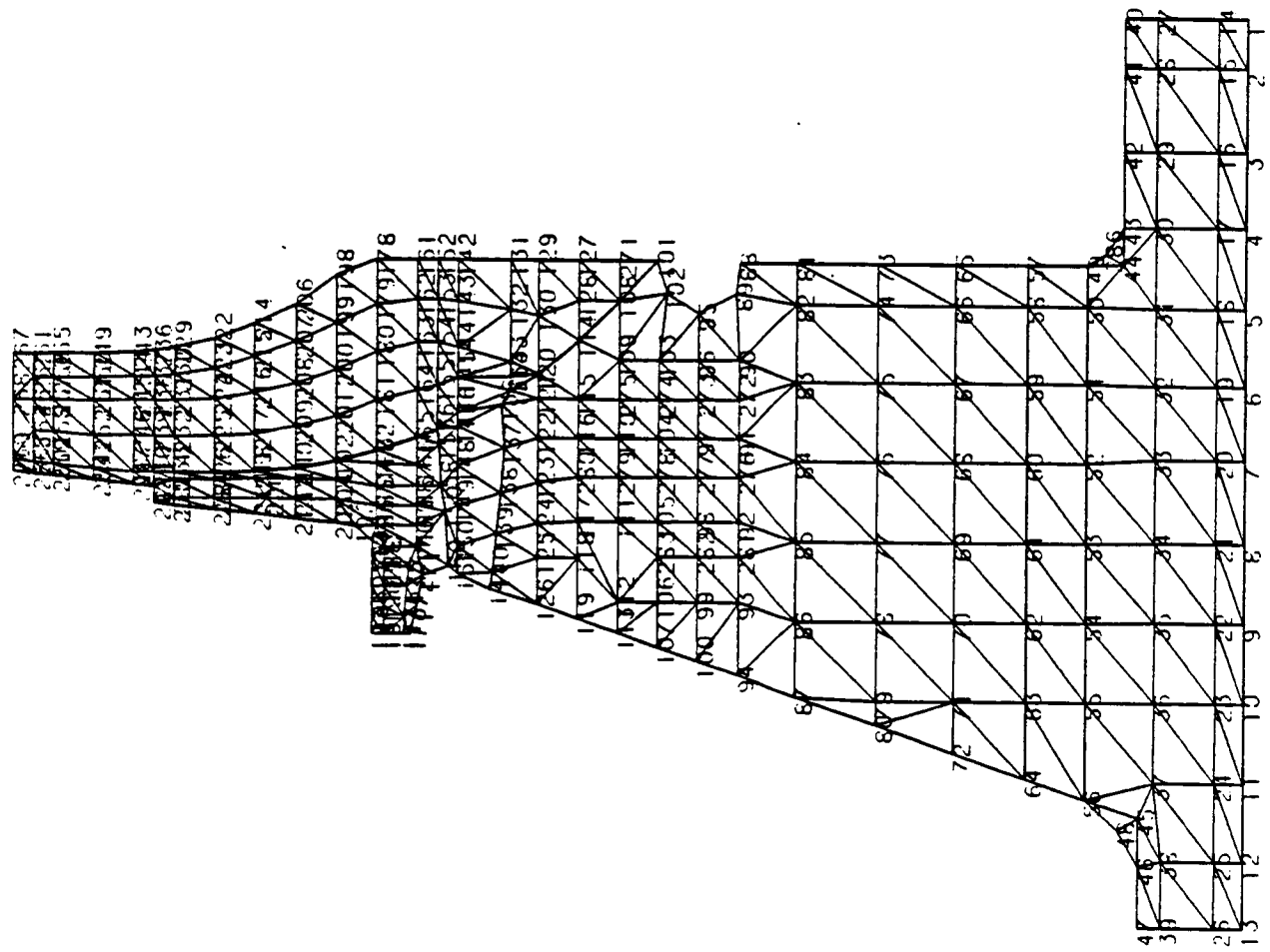
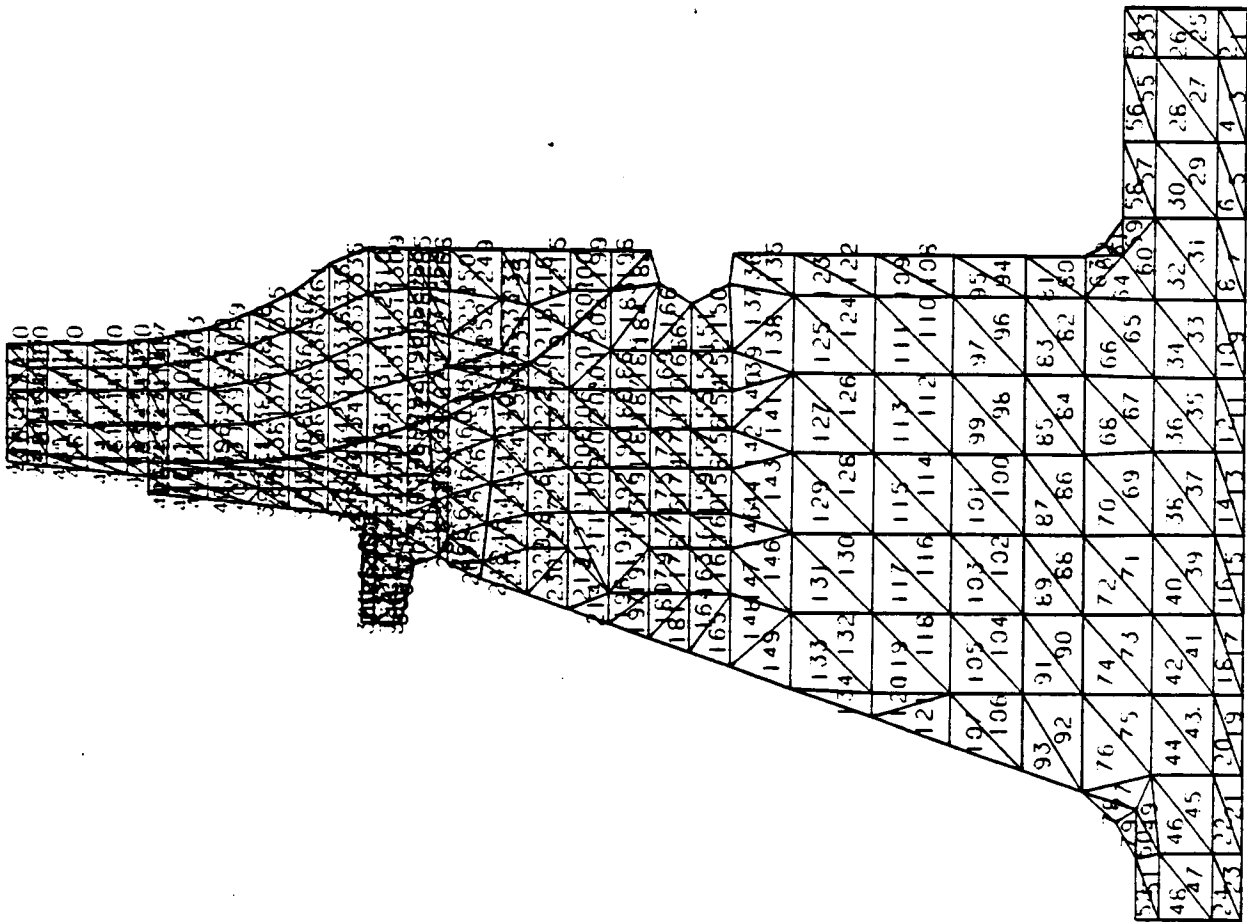


FIGURE 7

2D STRESS PROG.
 PLOT TYPE 2
 SCALF 2.50
 MAX R 3.25
 RPM 65000.
 ELEMENT NOS.



PLOT TYPE 3
SCALE 2.50
MAX R 3.25
RPM 65000.

TEMPERATURE CONTOURS
X 1200. DEGREES
O 1100. DEGREES
□ 1000. DEGREES
+ 900. DEGREES
* 800. DEGREES
Z 700. DEGREES

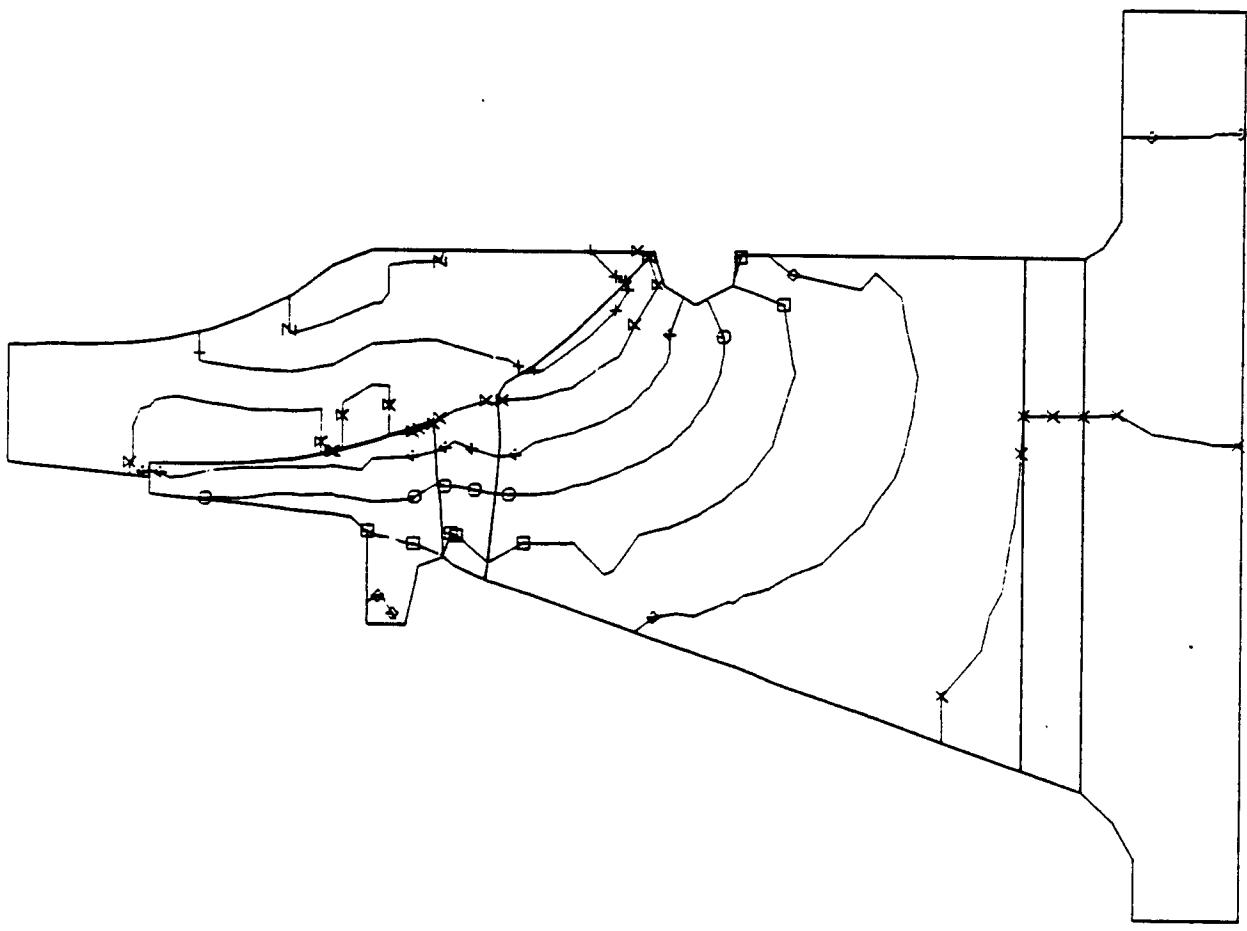
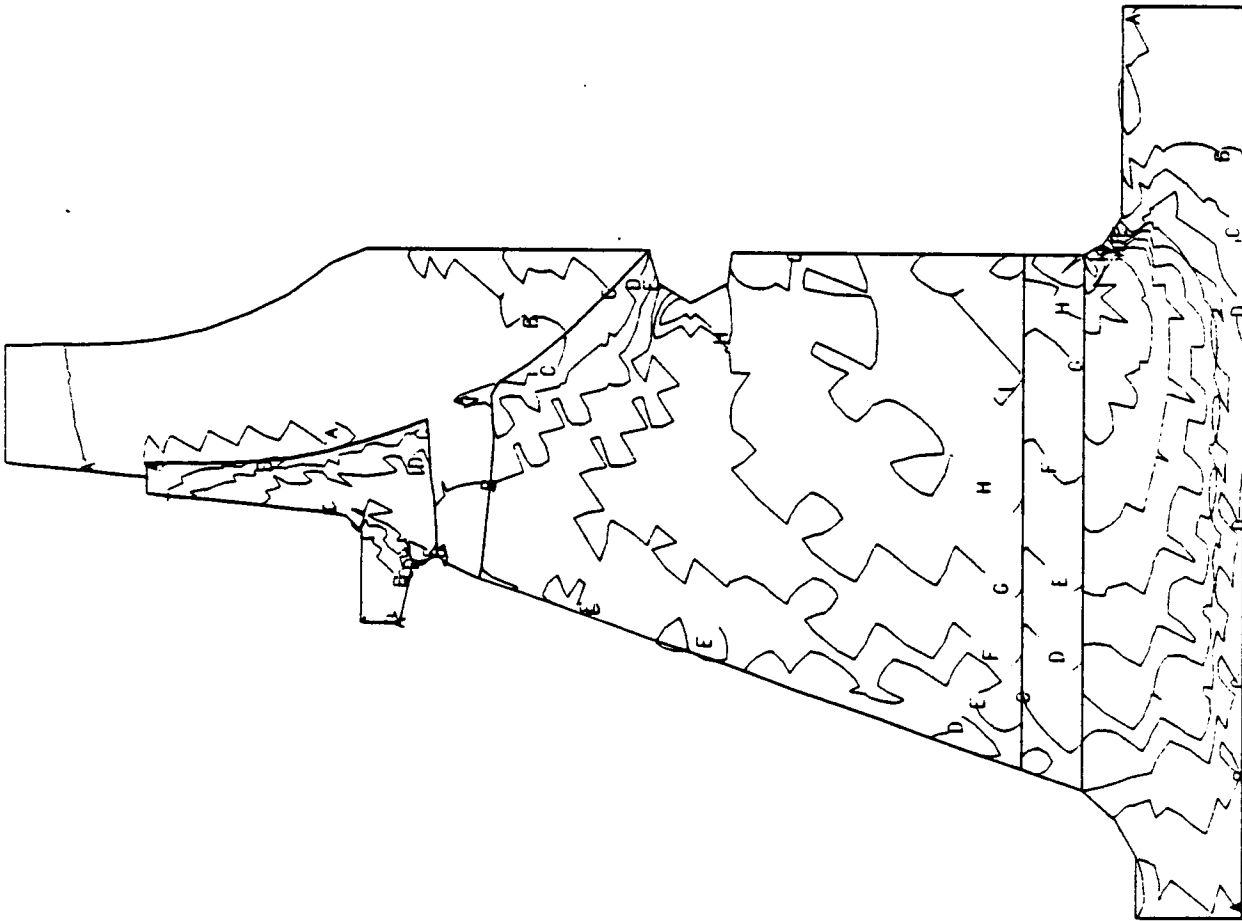


FIGURE 9

2D STRESS PROC.
PLOT TYPE 6
SCALE 2.50
MAX R 3.25
RPM 65000.

RADIAL STRESS RING STRESS
CONTOURS PLATE STRESS
A 20000
B 40000
C 60000
D 80000
E 100000
F 120000
G 140000
H 160000
I 180000
J 200000
K 100000
L 110000



PLOT TYPE 8
 SCALE 2.50
 MAX R 3.25
 RPM 65000.
 TANGENT STRESS CONTOURS
 RING STRESS
 A -30000
 B -20000
 C -10000
 D 0
 E 10000
 F 20000
 G 30000
 H 40000
 I 50000
 J 60000
 K 70000
 L 80000
 M 90000
 N 100000
 O 110000
 P 120000
 Q 130000
 R 140000
 S 150000

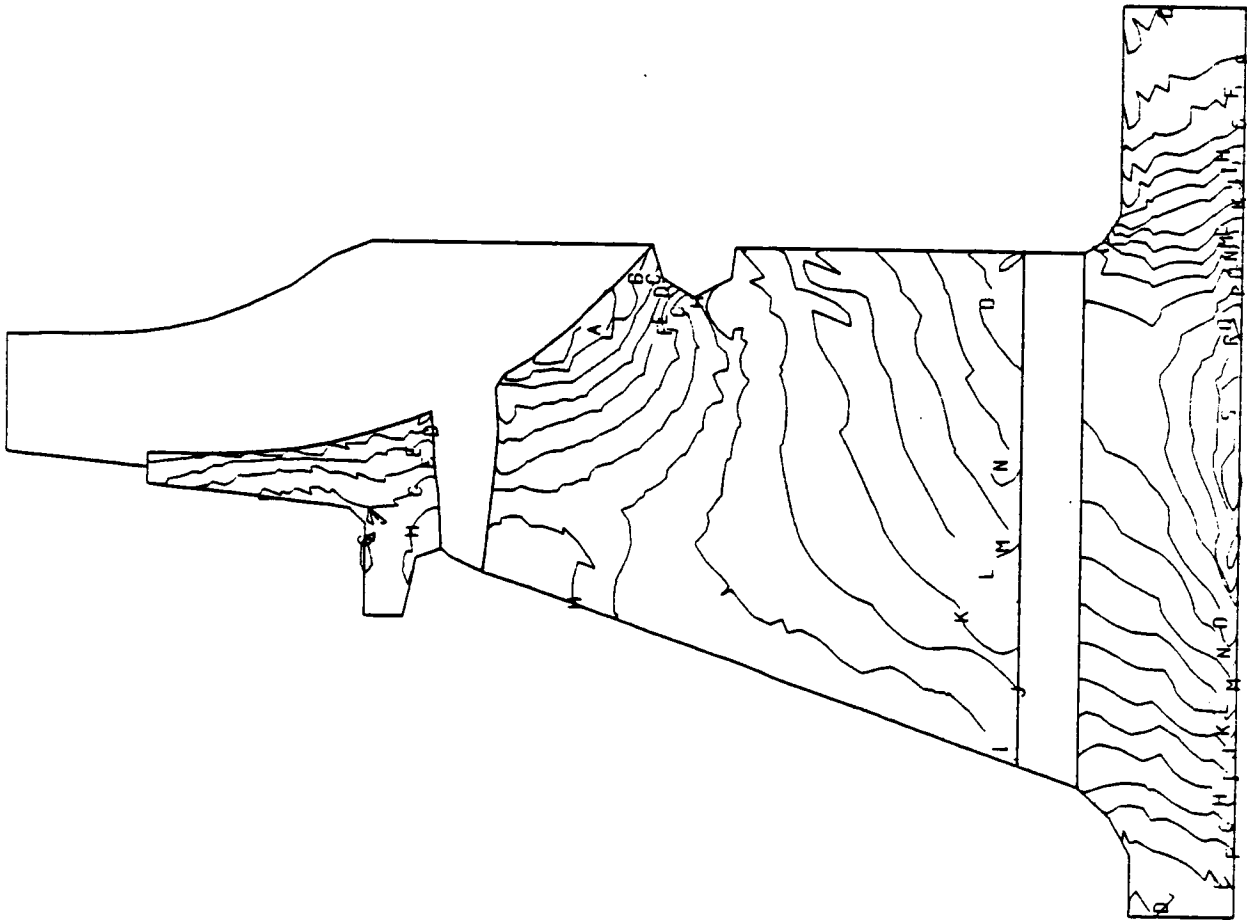
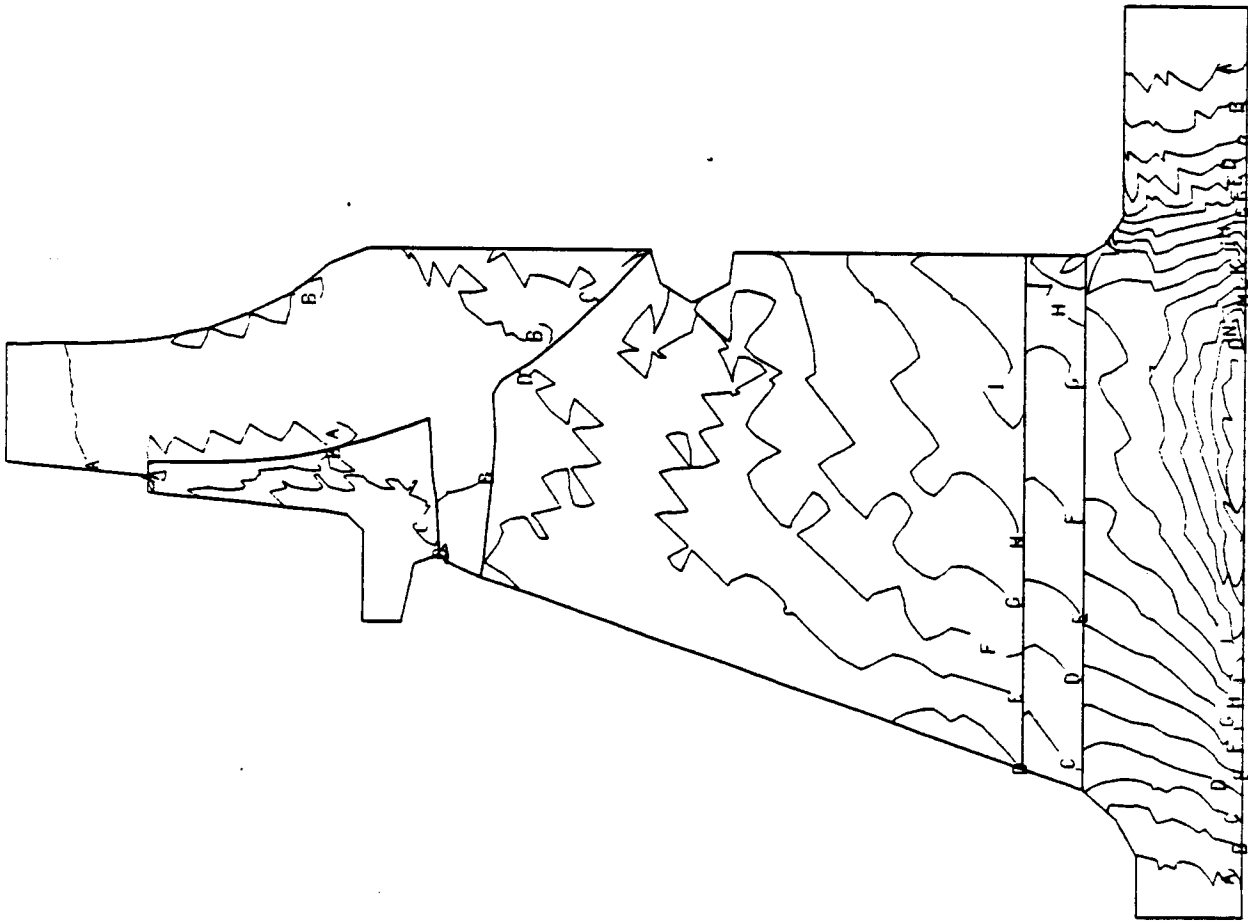


FIGURE 11

2D STRESS PROG.
 PLOT TYPE 10
 SCALE 2.50
 MAX R 3.25
 RPM 65000.

EQUIV. STRESS CONTOUR
 RING STRESS PLATE STRESS
 A 130000 A 20000
 B 200000 B 40000
 C 300000 C 60000
 D 400000 D 80000
 E 500000 E 100000
 F 600000 F 120000
 G 700000 G 140000
 H 800000 H 160000
 I 900000 I 180000
 J 1000000 J 200000



SCALE 2.50
MAX R 3.25
RPM 65000.
DISPLACEMENT MAGNIFICATION
FACTOR = 5.06

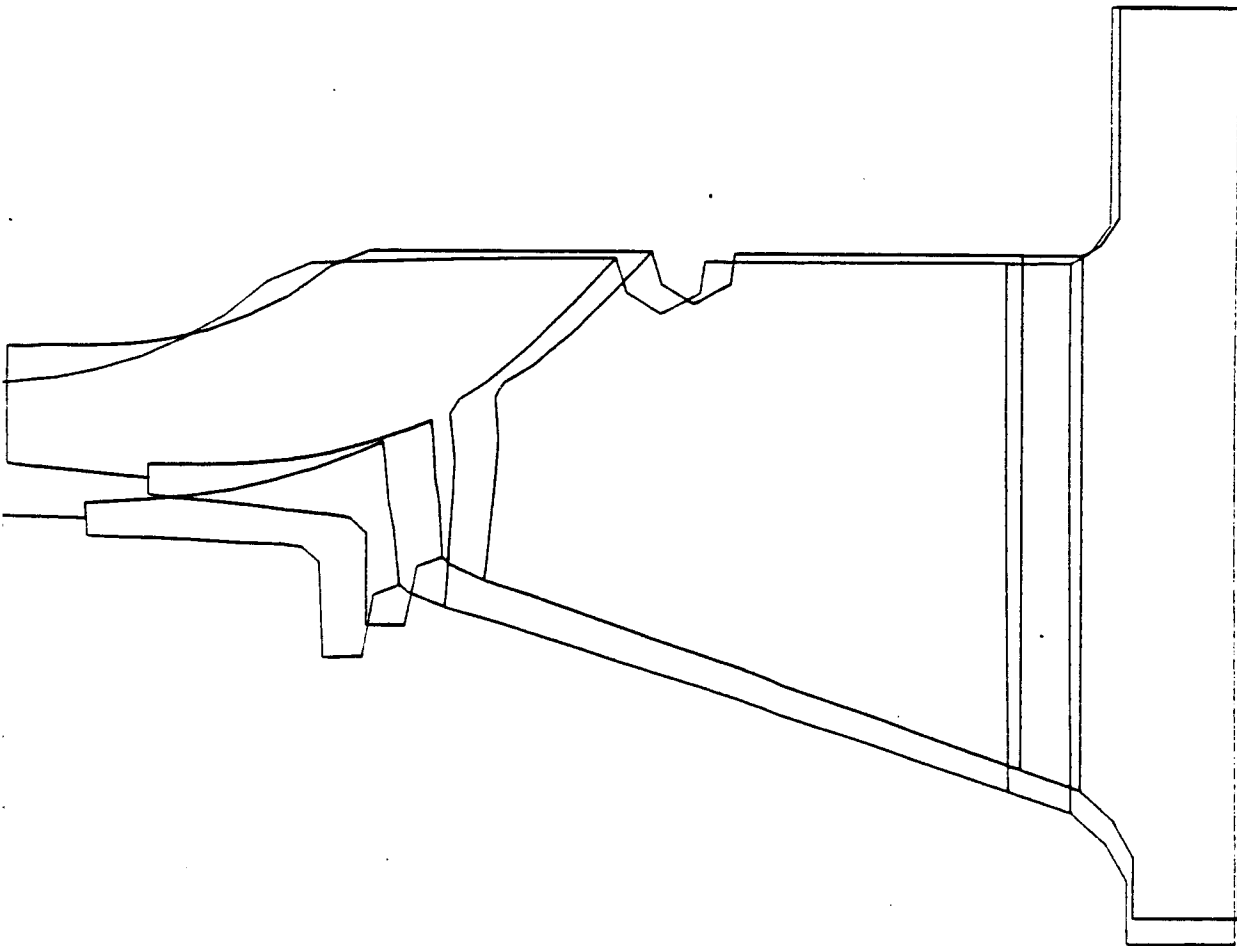
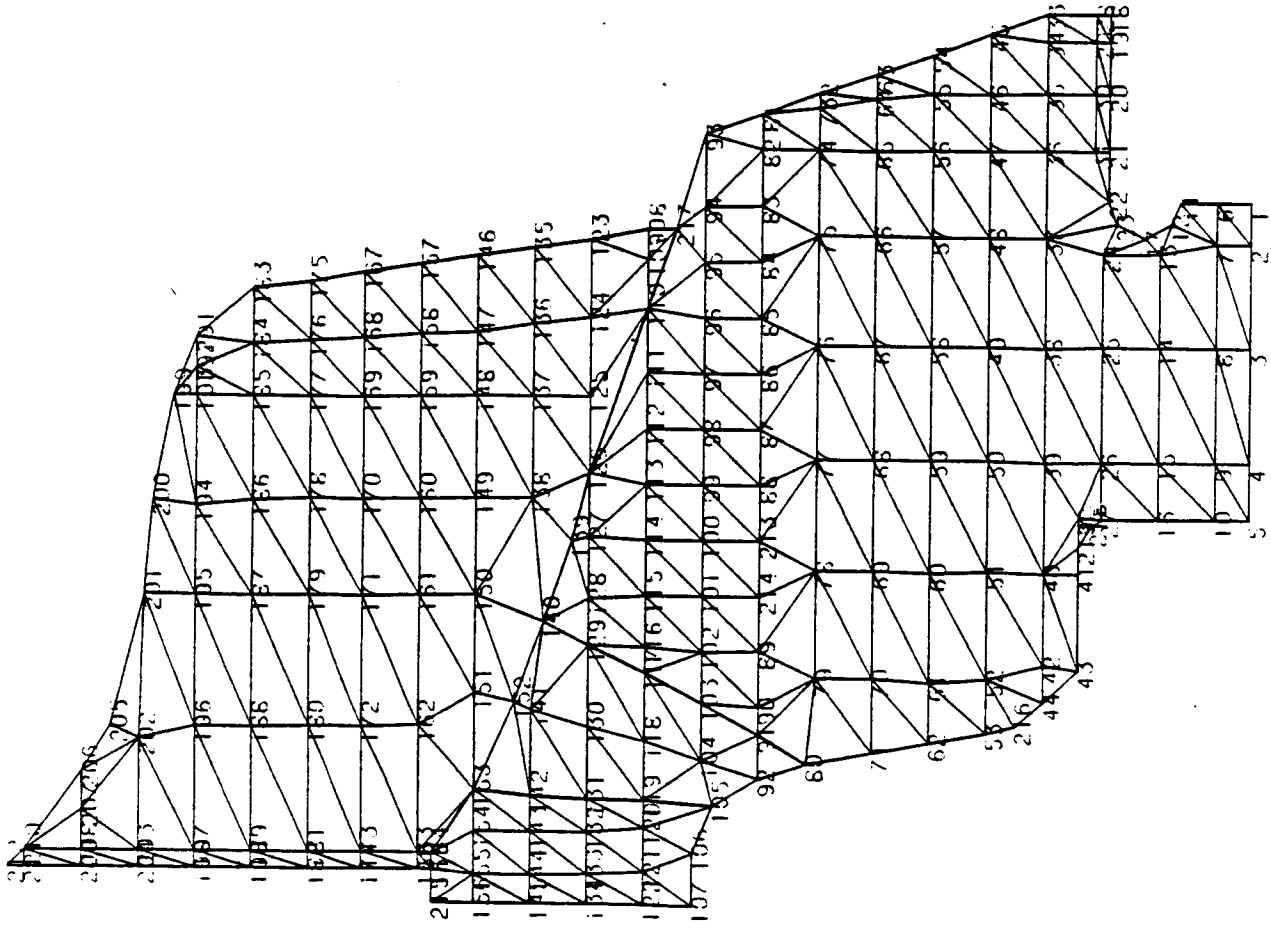


FIGURE 13.

2D STRESS PROG.
 PLOT TYPE 1
 SCALE 3.50
 MAX R 2.38
 RPM 65000.
 ORIG. NODE NOS.



PLOT TYPE: 2
 SCALE: 3.50
 MAX R: 2.38
 RPM: 65000.
 FLAMENT NOS.

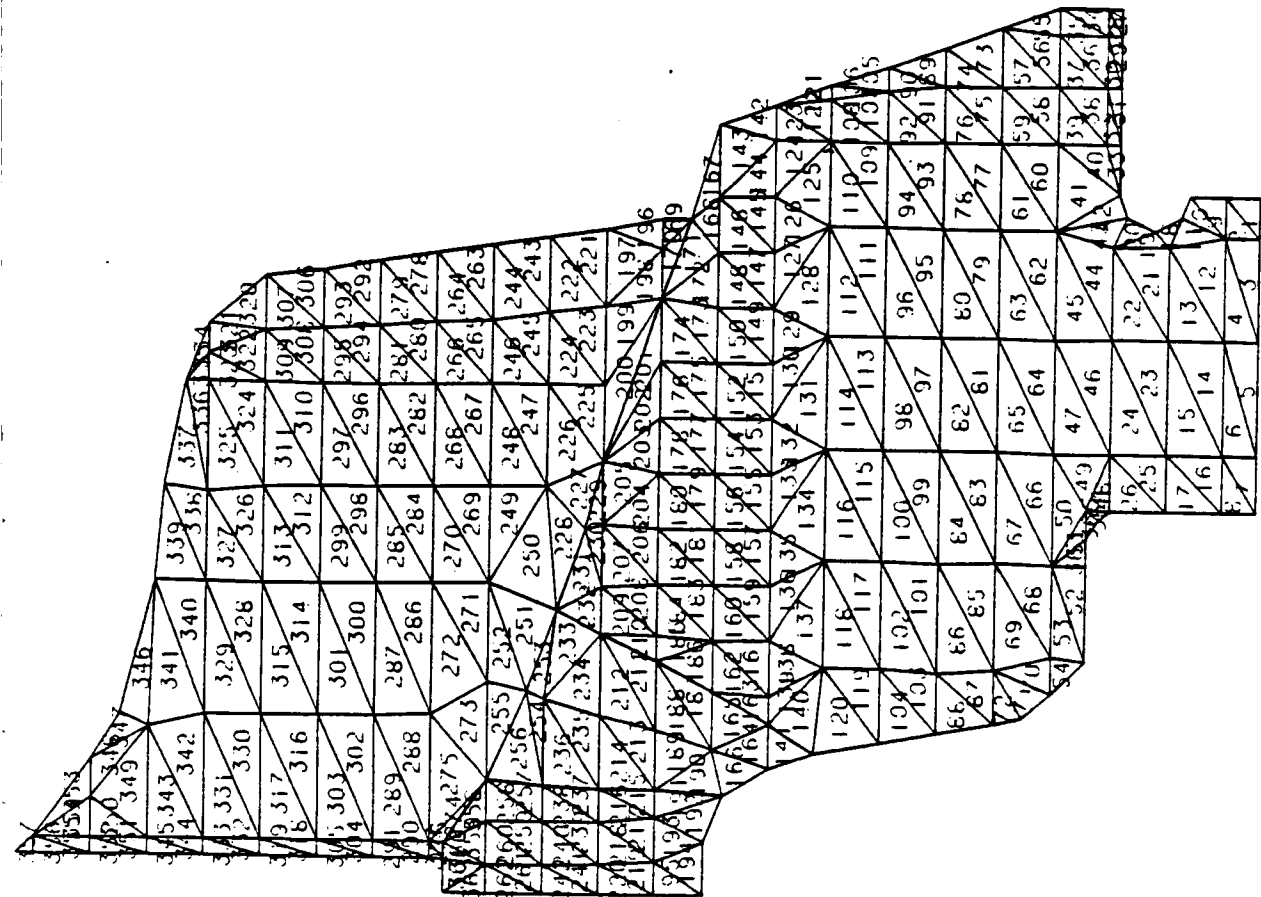


FIGURE 15

2D STRESS PROC.
PLOT TYPE 3
SCALE 3.50
MAX R 2.38
RPM 65000.

TEMPERATURE CONTOURS
X 1100. DEGREES
O 1150. DEGREES
□ 1200. DEGREES
+ 1250. DEGREES
X 1300. DEGREES
+ 1350. DEGREES
+ 1400. DEGREES
Z 1450. DEGREES
Y 1500. DEGREES
X 1550. DEGREES
+ 1600. DEGREES
X 1650. DEGREES
* 1700. DEGREES

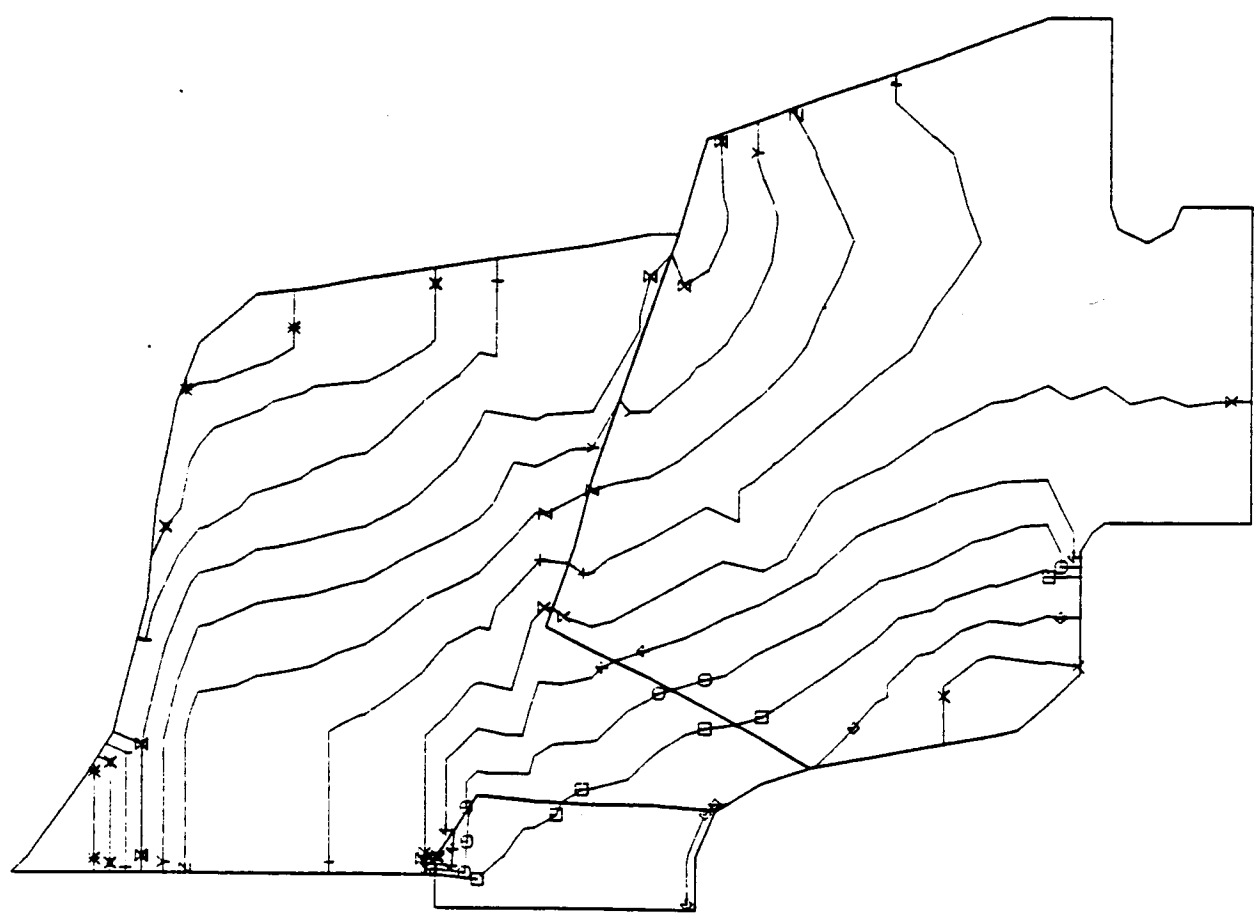


FIGURE 16

PLOT TYPE 6
SCALE 3.50
MAX R 2.38
RPM 65000.

RADIAL STRESS CONTOURS
RING STRESS PLAT STRESS
A 0
B 5000
C 10000
D 15000
E 20000
F 25000
G 30000
H 35000
I 40000
J 45000
K 50000
L 55000
M 60000

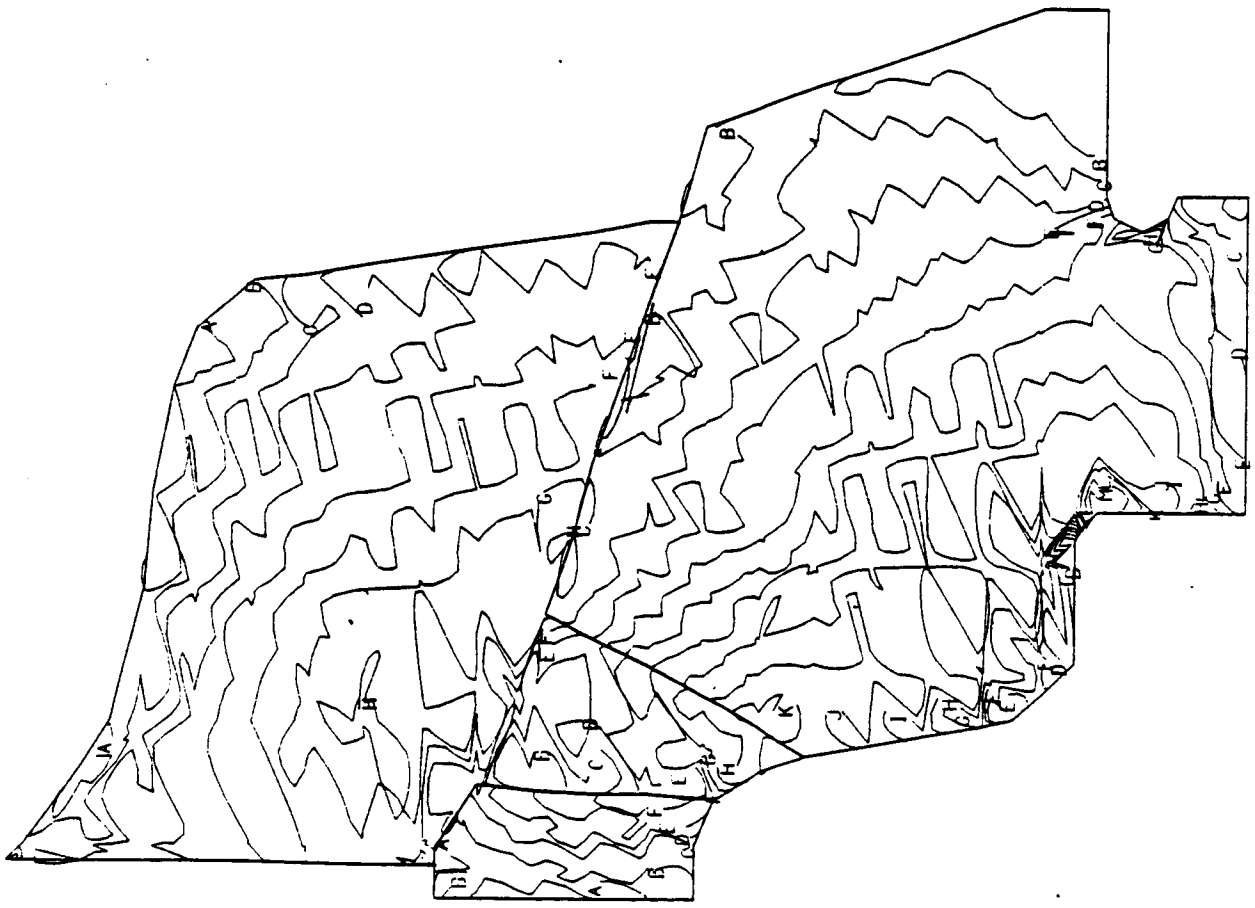


FIGURE 17

PLOT TYPE 8
SCALE 3.50
MAX R 2.38
RPM 65000.

TANGENTIAL STRESS CONTOURS
RING STRESS
A - 10000
B 0
C 10000
D 20000
E 30000
F 40000
G 50000
H 60000
I 70000
J 80000
K 90000
L 100000
M 110000
N 120000
O 130000

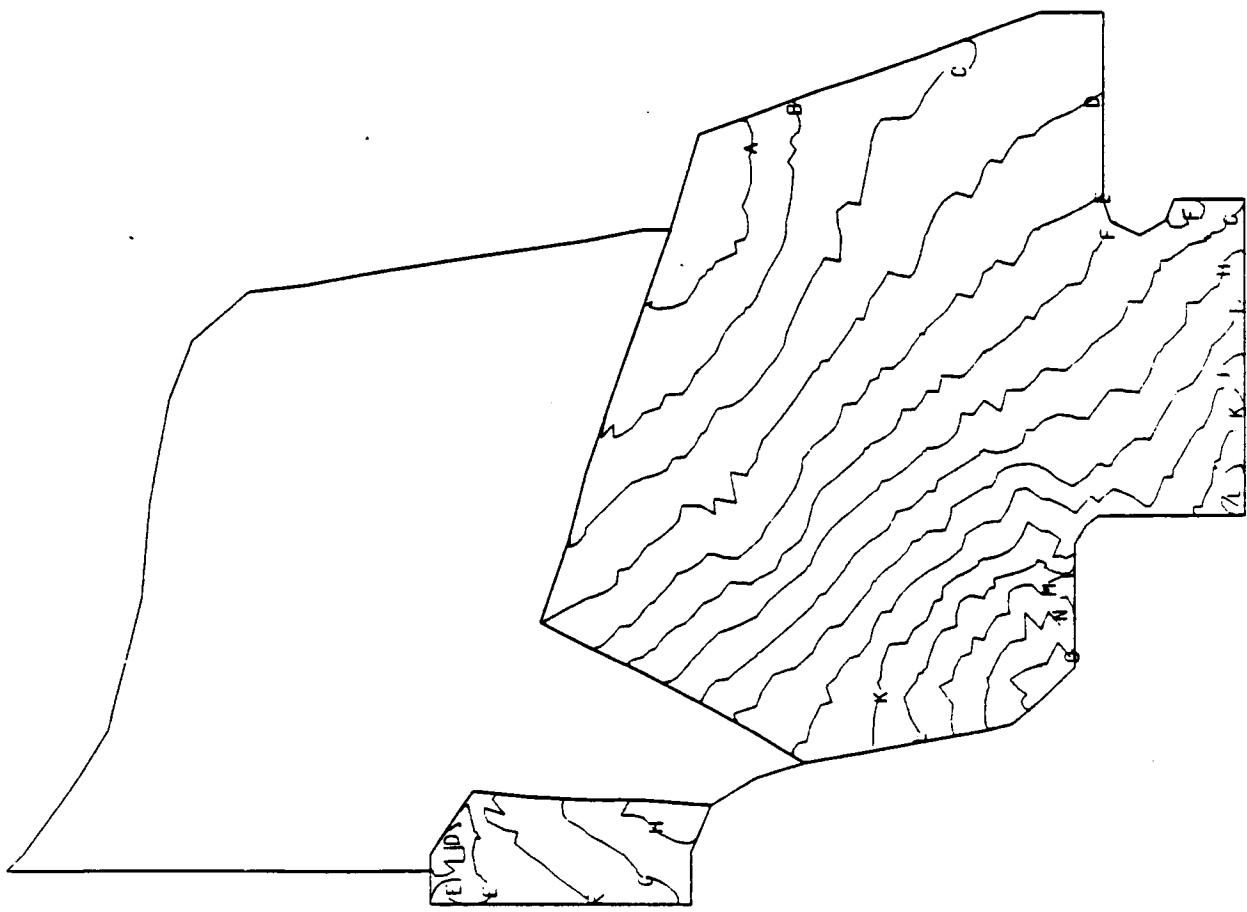


FIGURE 18

PLOT TYPE 10

SCALE 3.50

MAX R 2.38

RPM 65000.

EQUIV. STRESS RING STRESS
A 10000 B 20000 C 30000 D 40000 E 50000 F 60000 G 70000 H 80000 I 90000 J 100000 K 110000 L 120000

CONTOURS PLATE STRESS
A 5000 B 10000 C 15000 D 20000 E 25000 F 30000 G 35000 H 40000 I 45000 J 50000 K 55000

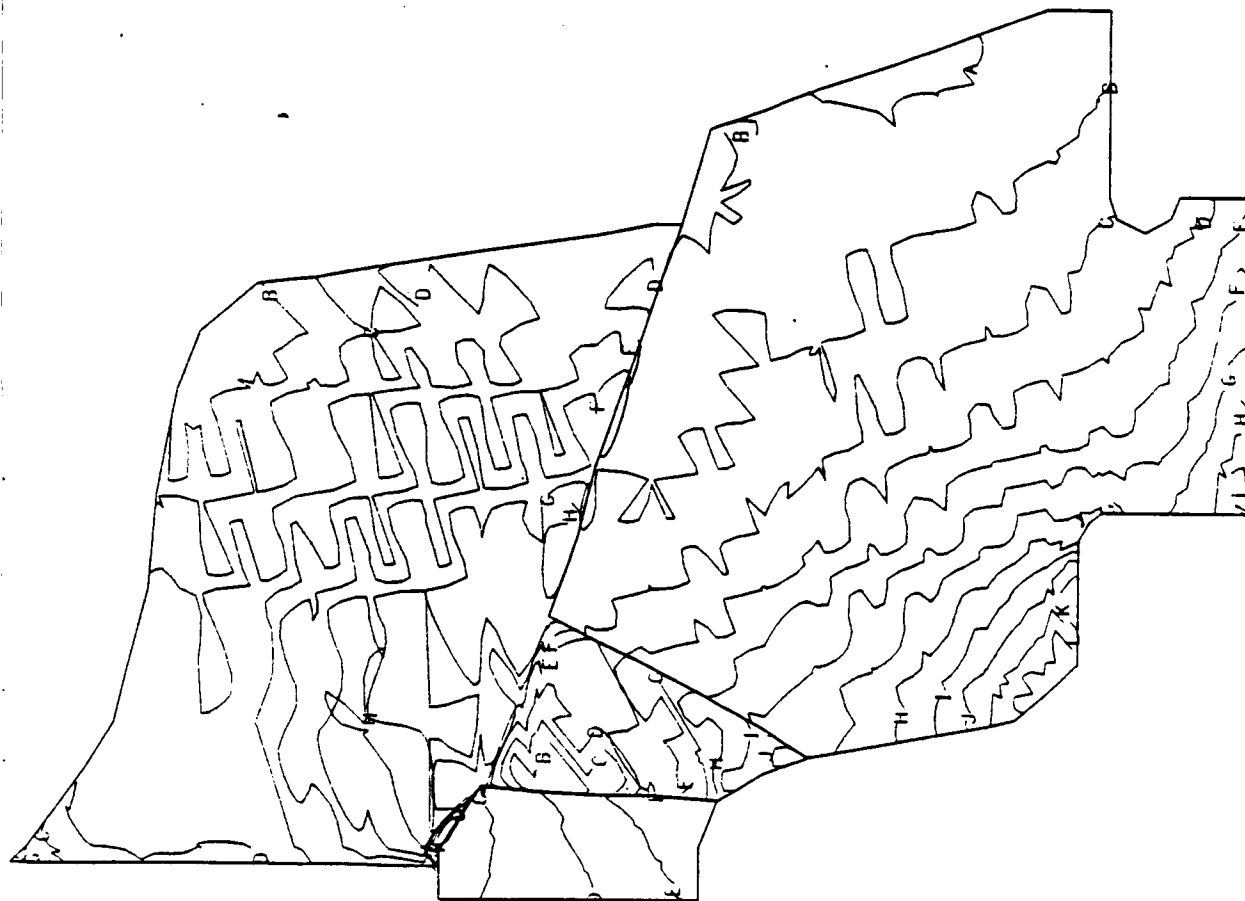


FIGURE 19

2D STRESS PROC.
PLOT TYPE 5
SCALE 3.50
MAX R 2.38
RPM 65000.
DISPLACEMENT MAGNIFICATION
FACTOR - 5.60

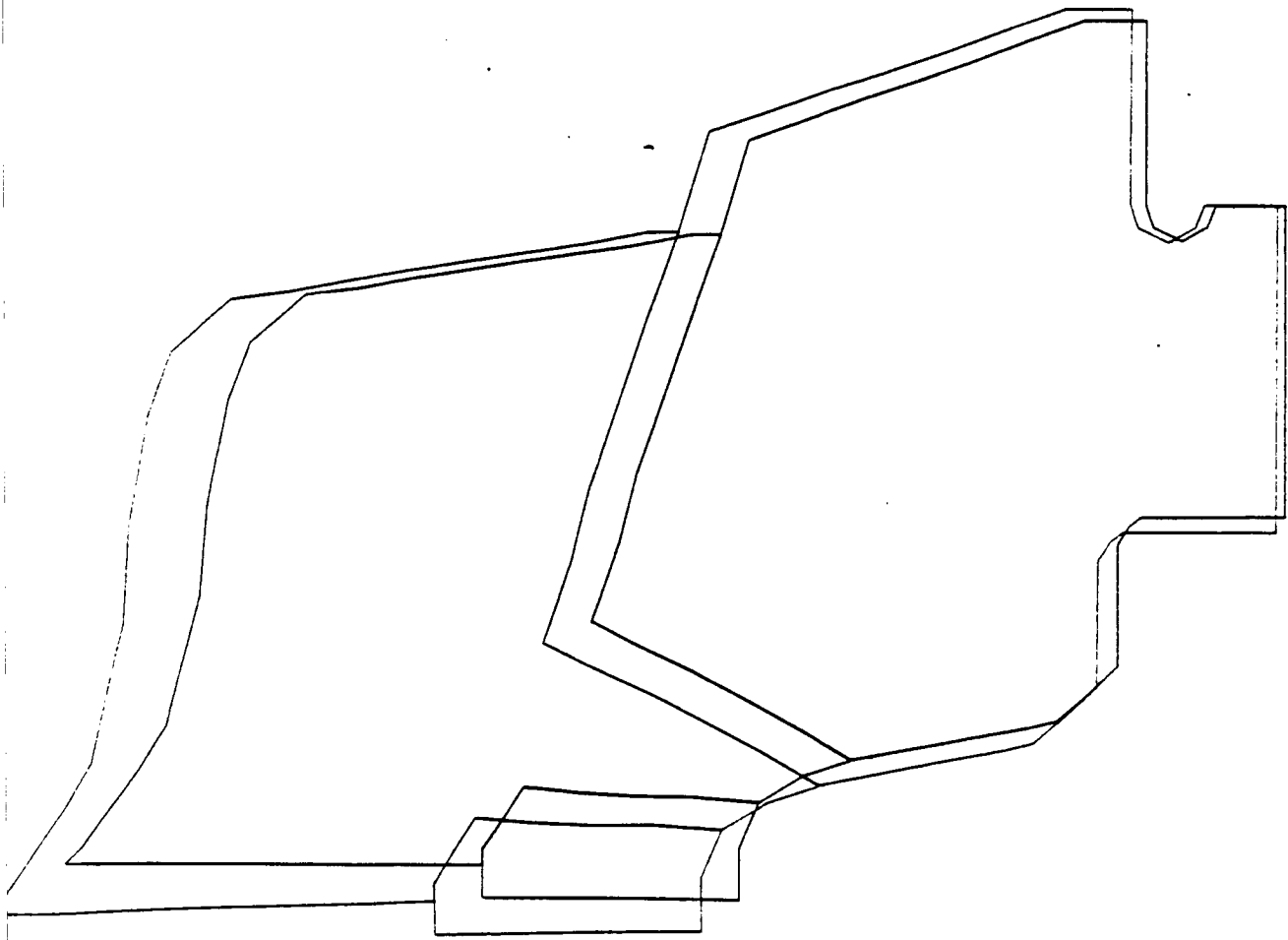


FIGURE 20

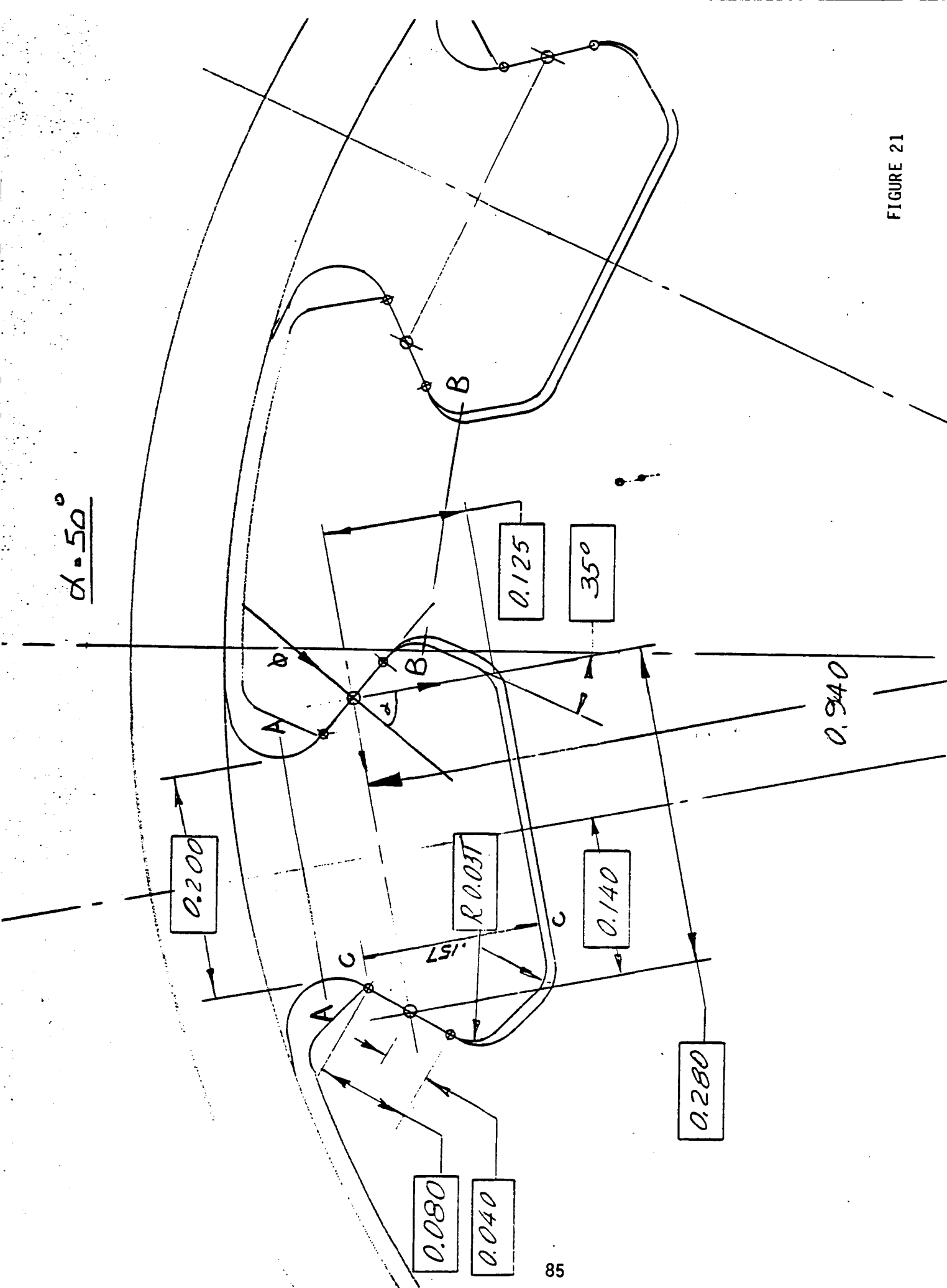


FIGURE 21

2D STRESS PROC.
PLOT TYPE 1
SCALE 20.00
MAX R 0.34
RPM 0.
ORIG. NODE NOS.

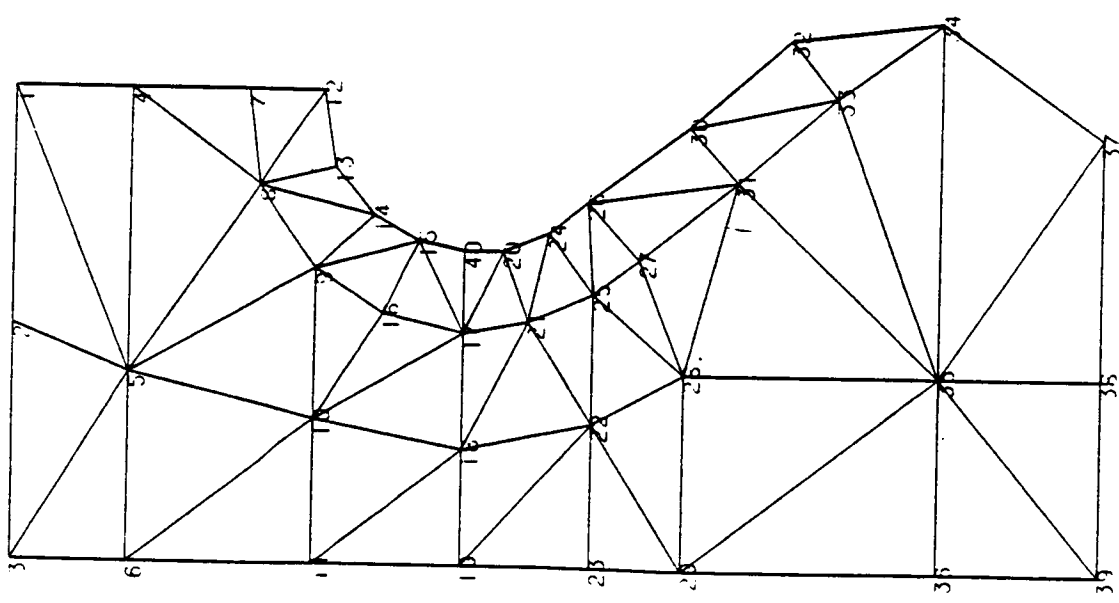


FIGURE 22

2D STRESS PROC.
PLOT TYPE 2
SCALE 20.00
MAX R 0.34
RPM 0.
ELEMENT NOS.

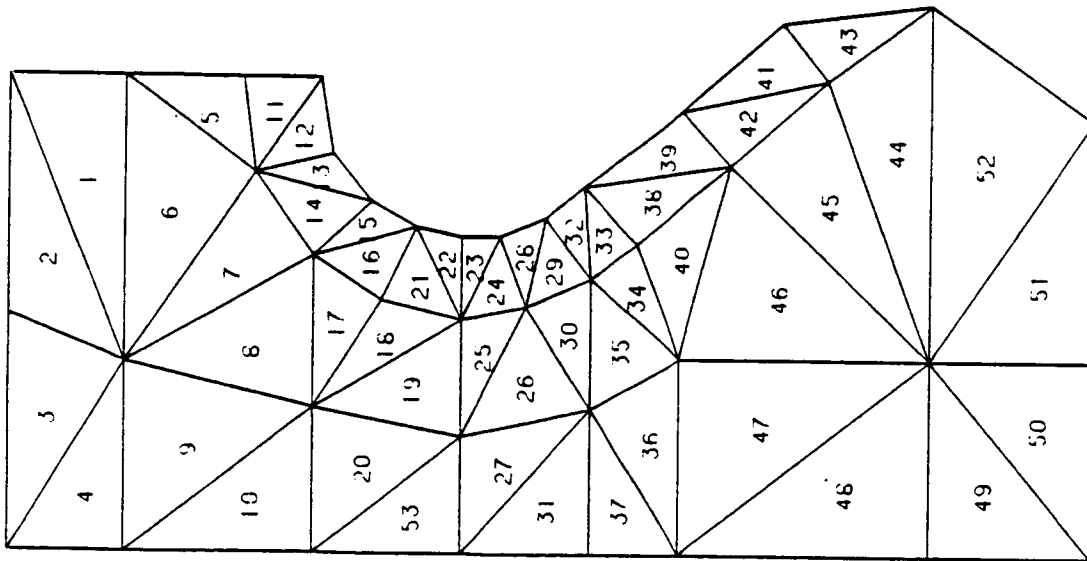
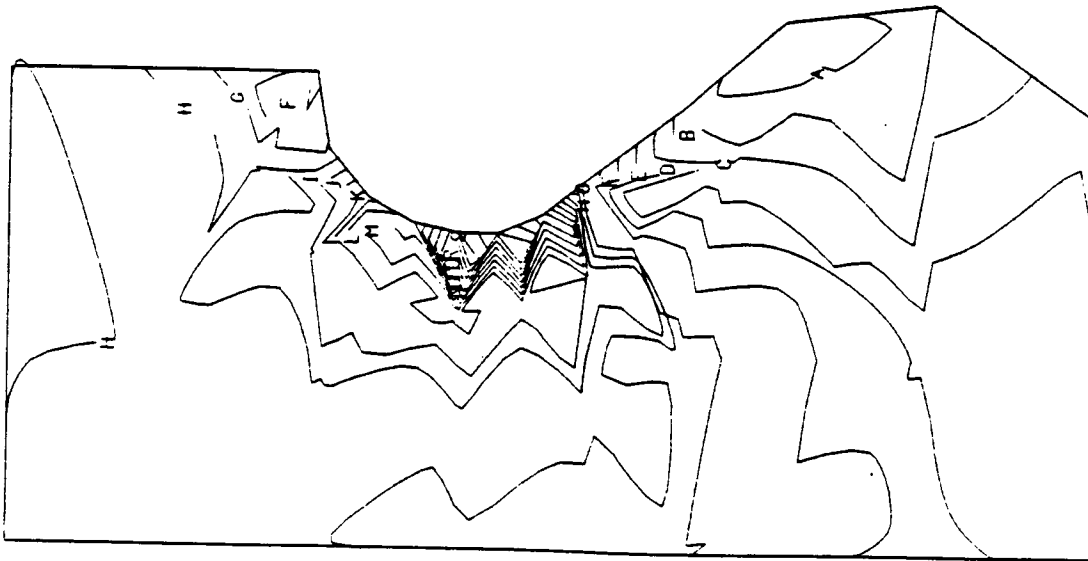


FIGURE 23

2D STRESS PROC.
PLOT TYPE 6
SCALE 20.00
MAX R 0.34
RPM 0.

RADIAL STRESS CONTOURS
PLATE STRESS:
A 30000
B 20000
C -10000
D 0
E 10000
F 20000
G 30000
H 40000
I 50000
J 60000
K 70000
L 80000
M 90000
N 100000
O 110000
P 120000
Q 130000
R 140000
S 150000



UNITED STATES GOVERNMENT PRINTING OFFICE: 1967 O 315-101

2D STRESS PROC.
PLOT TYPE 7
SCALE 20.00
MAX R 0.34
RPM 0.

AXIAL STRESS CONTOURS
PLATF STRESS
A -60000
B -55000
C -50000
D -45000
E -40000
F -35000
G -30000
H -25000
I -20000
J -15000
K -10000
L -5000
M 0
N 5000
O 10000
P 15000

ORIGINAL PAGE IS
OF POOR QUALITY

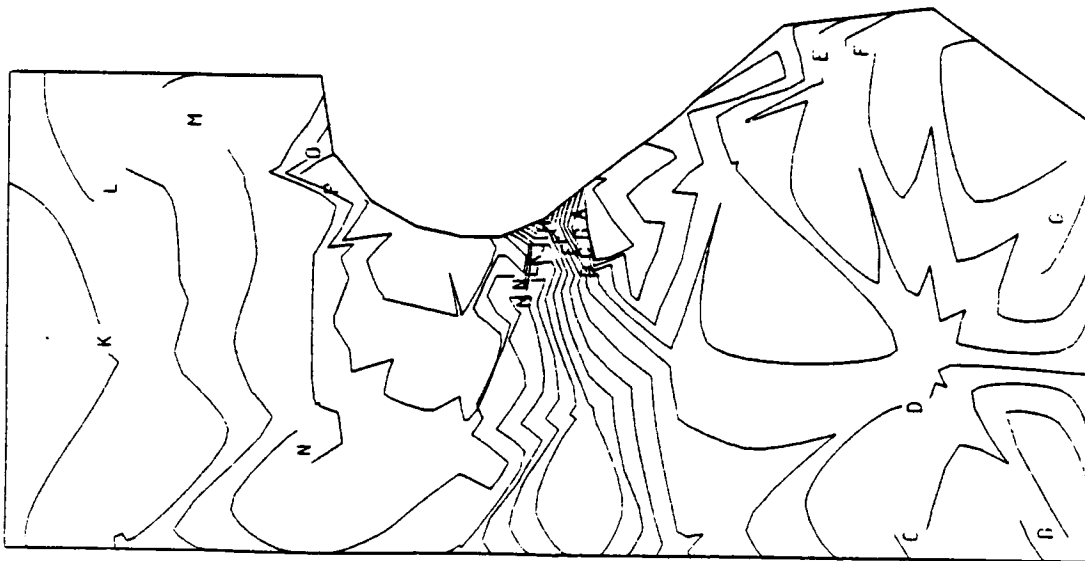


FIGURE 25

2D STRESS PROG.
PLOT TYPE 10
SCALE 20.00
MAX R 0.34
RPM 0.

EQUIV. STRESS CONTOURS
PLATE STRESS
A 30000
B 40000
C 50000
D 60000
E 70000
F 80000
G 90000
H 100000
I 110000
J 120000
K 130000
L 140000

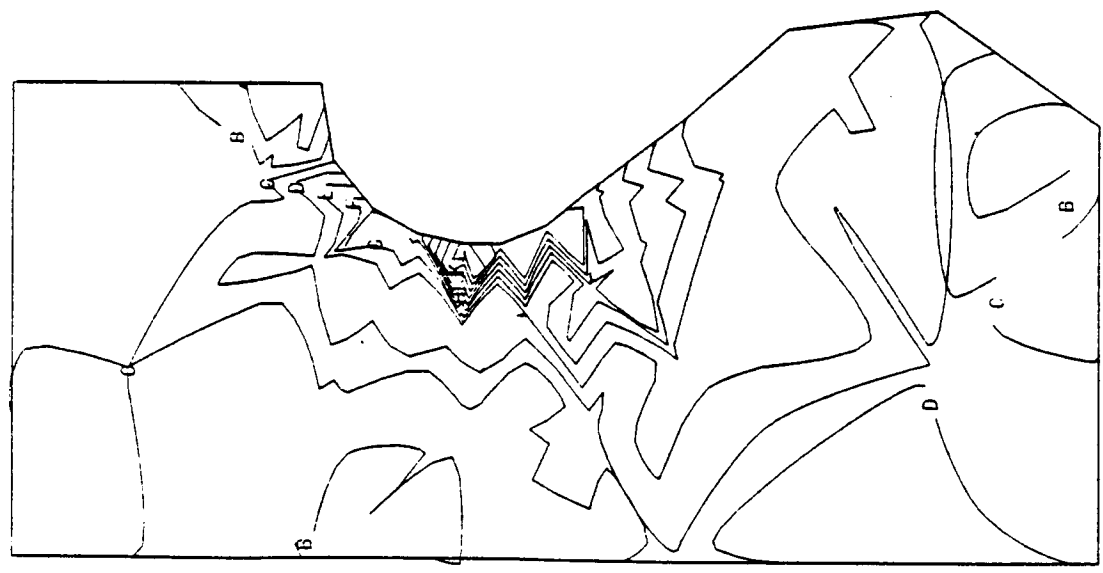


FIGURE 26

ORIGINAL PAGE IS
OF POOR QUALITY

ORIG. NODE NOS.

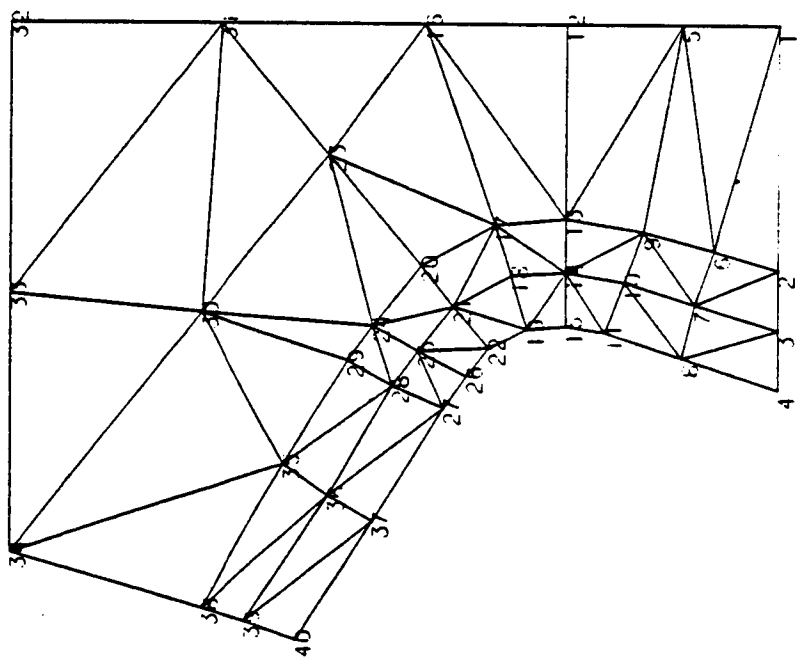
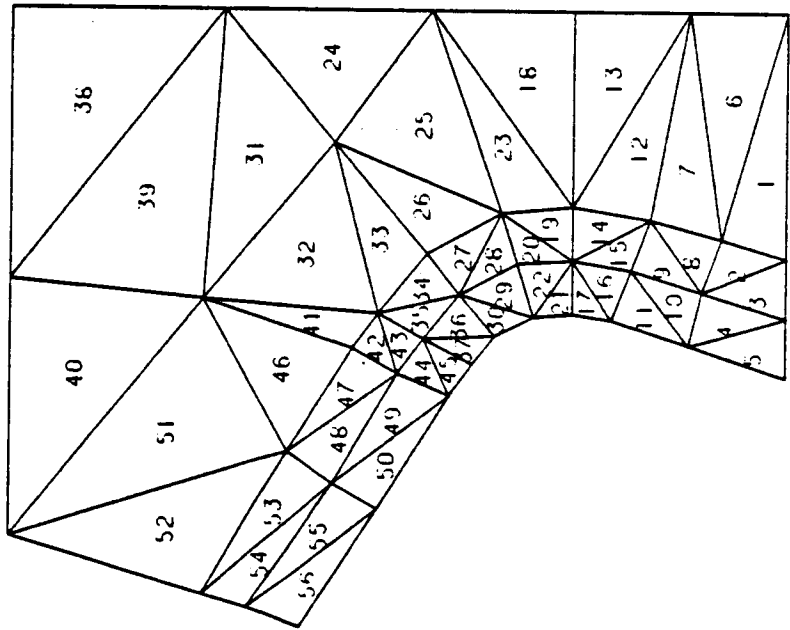


FIGURE 27

INVERTED BLADE DISC FIXING ANALYSIS 7-15-81 CRISFLOT.RJE P.BARROW 07/16/81 12.11.81

2D STRESS PROG
PLOT TYPE 2
SCALE 20.00
MAX R 0.24
RPH 0
ELEMENT NOS.



INSERTED BLADE DISC FIXING ANALYSIS 7-16-61 CRTS PLOT.RJE P.BARROW 07/16/61 14.42.22

2D STRESS PROC
PLOT TYPE 6
SCALE 20.00
MAX R 0.24
RPM 0.

RADIAL STRESS CONTOURS
PLATE STRESS
A -50000
B -40000
C -20000
D 0
E 20000
F 40000
G 60000
H 80000
I 100000
J 120000
K 140000

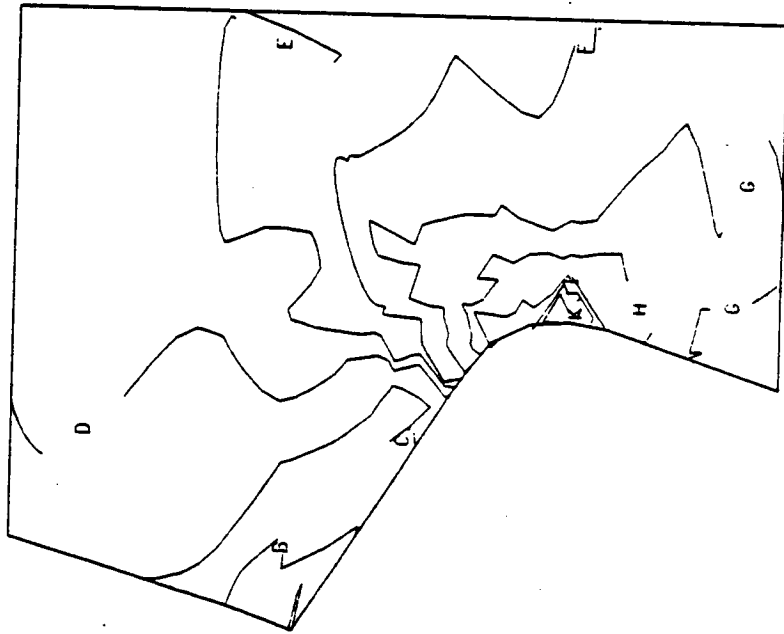
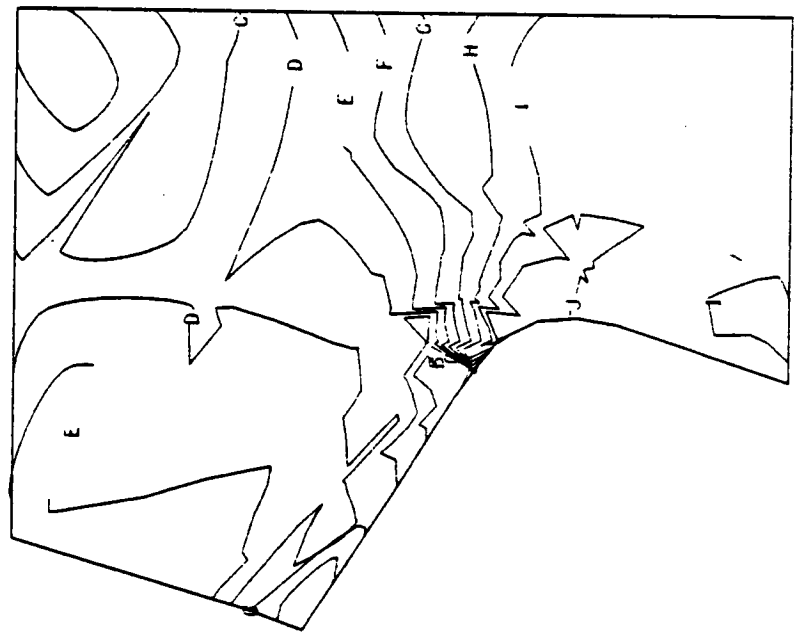


FIGURE 29

07/16/61 14.42.24
INSERTED BLADE DISC FIXING ANALYSIS 7-16-61 CRT&PLOT.RJE P.BARROW

2D STRESS PROC.
PLOT TYPE 7
SCALE 20.00
MAX R 0.24
RPM 0.



AXIAL STRESS CONTOURS
PLATE STRESS
A - 60000
B - 70000
C - 60000
D - 50000
E - 40000
F - 30000
G - 20000
H - 10000
I 0
J 10000

FIGURE 30

07/16/81 14.42.26
INSERTED BLADE DISC FIXING ANALYSIS 7-16-81 CRT8PLOT.RJE P.BARROW

2D STRESS PROG.
PLOT TYPE 10
SCALE 20.00
MAX R 0.24
RPM 0.

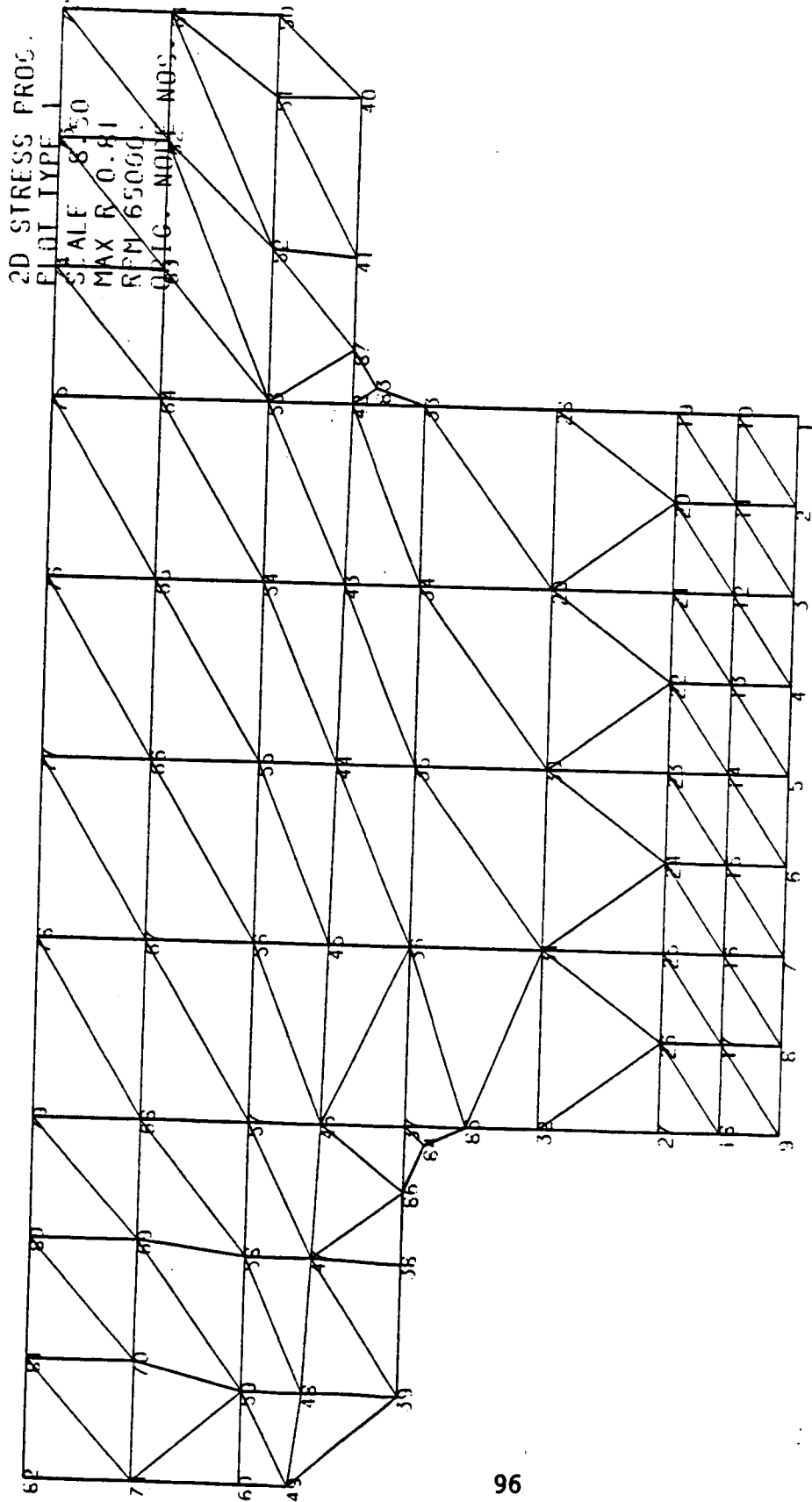
EQUIV. STRESS CONTOURS
PLATE STRESS
A 40000
B 50000
C 60000
D 70000
E 80000
F 90000
G 100000
H 110000
I 120000
J 130000
K 140000



FIGURE 31

INSERTED BLADE DISC ANALYSIS 7-14-81 CRT4PLOT.RJE P.BARROW

07/14/81 10.14.40



07/14/81 10.14.49

INSERTED BLADE DISC ANALYSIS 7-14-81 CRT4PLOT.RJE P.BARROW

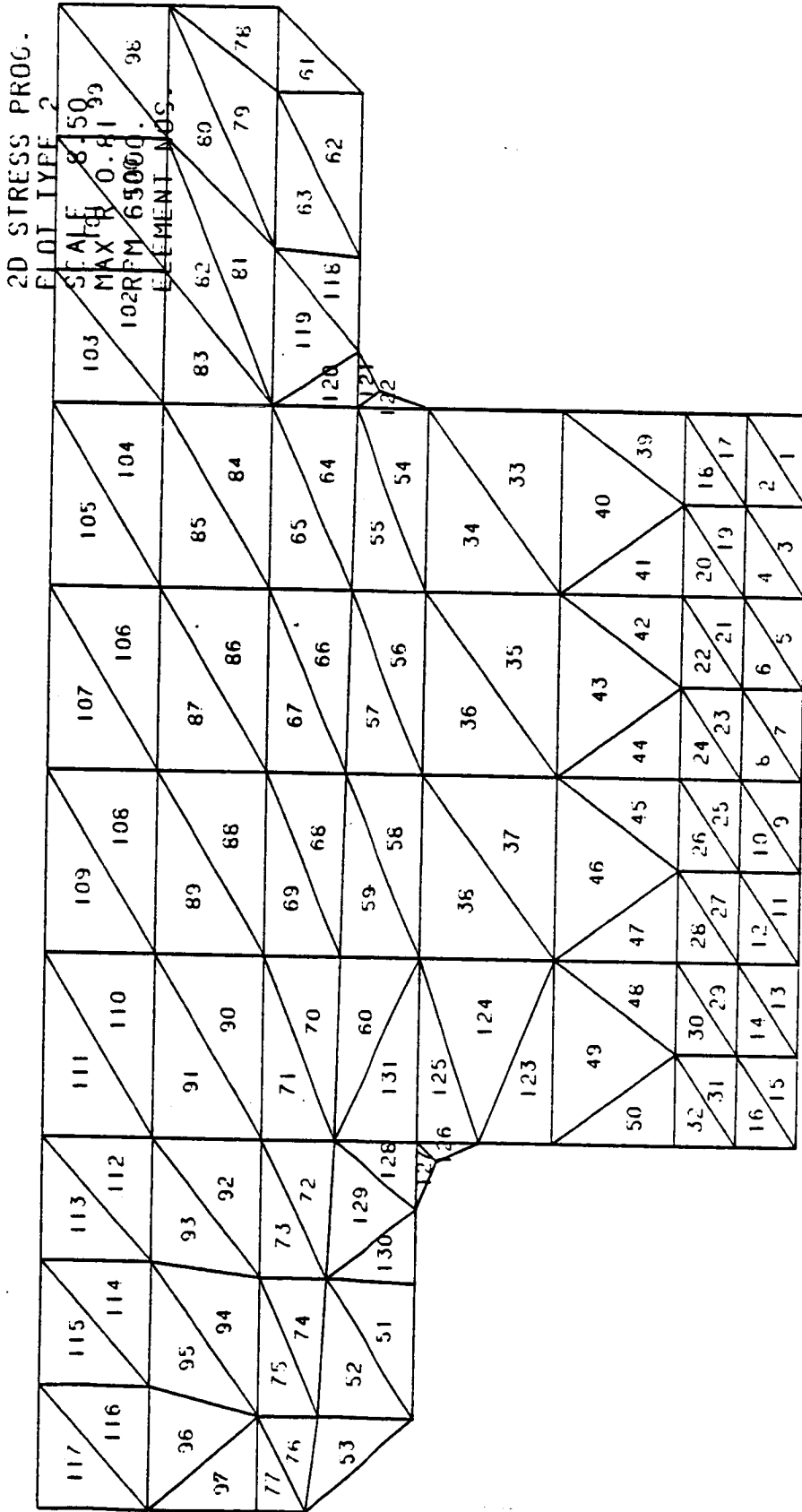


FIGURE 33

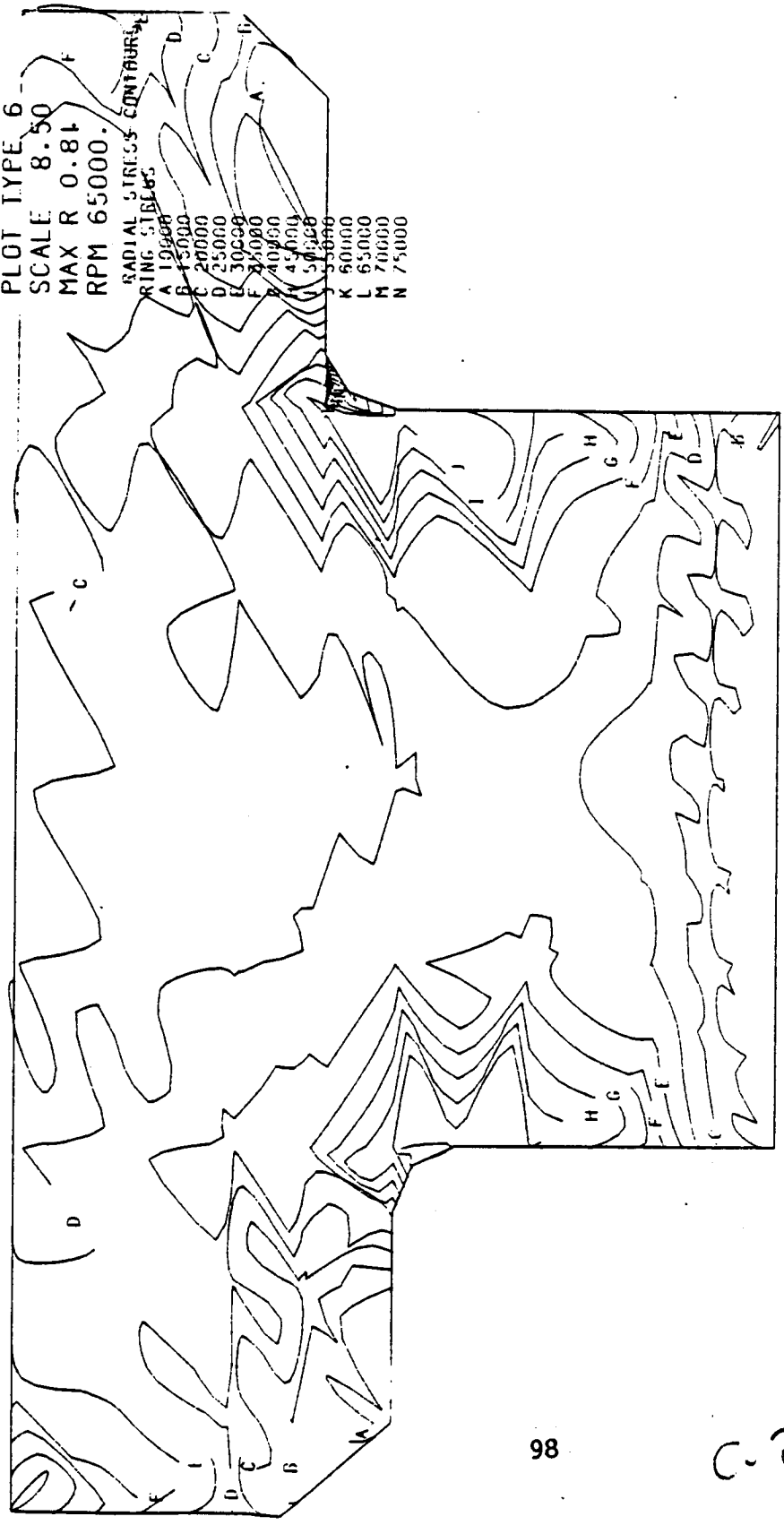
07/14/81 10.27.19

INSERTED BLADE DISC ANALYSIS 7-14-81 CRT4PLOT.RJE P.BARROW

2D STRESS PROG.
PLOT TYPE 6
SCALE 8.50
MAX R 0.81
RPM 65000.

RADIAL STRESS CONTOURS
RING STRESS

A	10000
B	15000
C	20000
D	25000
E	30000
F	35000
G	40000
H	45000
I	50000
J	55000
K	60000
L	65000
M	70000
N	75000



C.2

FIGURE 34

07/14/81 10.27.28

INSERTED BLADE DISC ANALYSIS 7-14-81 CRT4PLOT.RJE P.BARROW

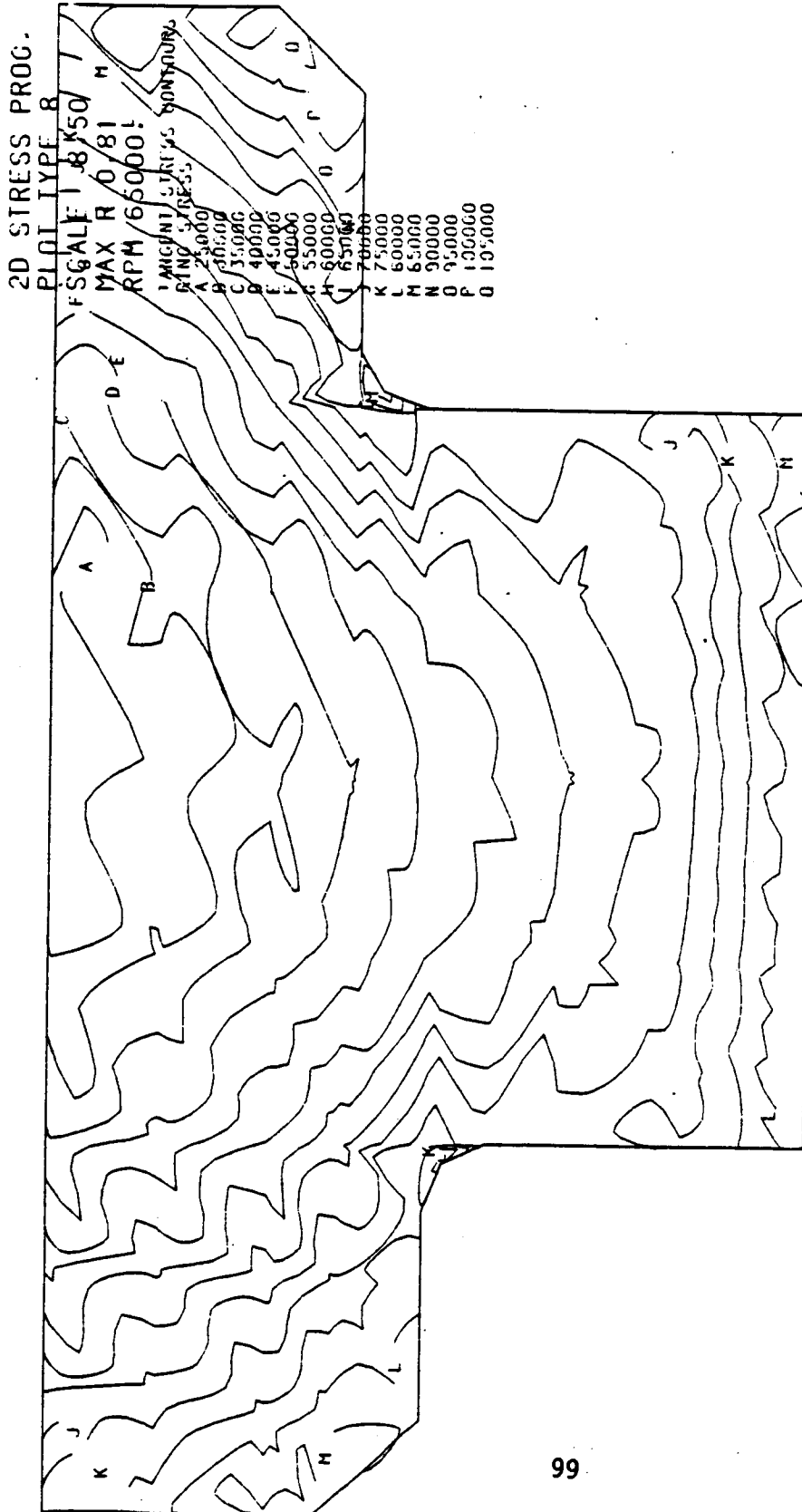


FIGURE 35

07/14/81 10.27.36

INSERTED BLADE DISC ANALYSIS 7-14-81 CRT4PLOT.RJE P.BARROW

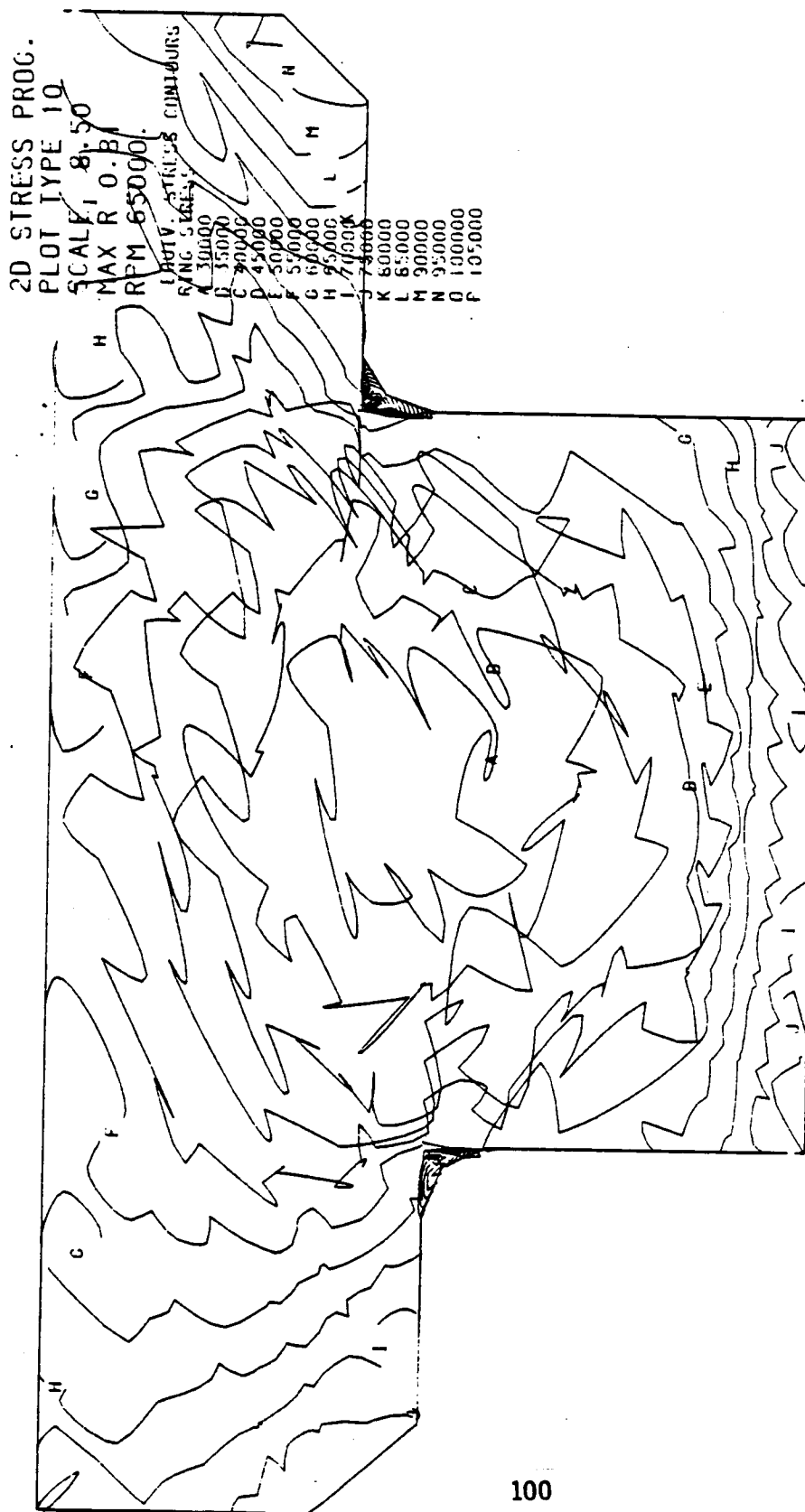
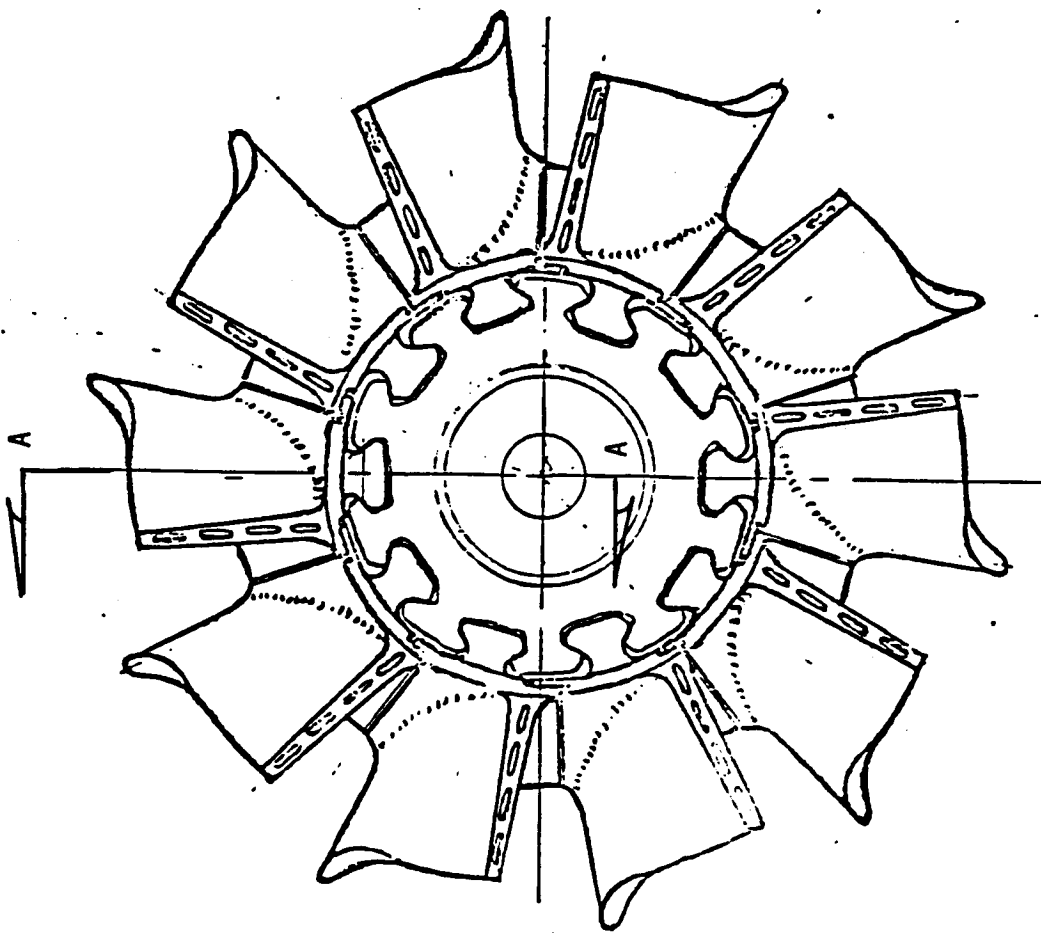
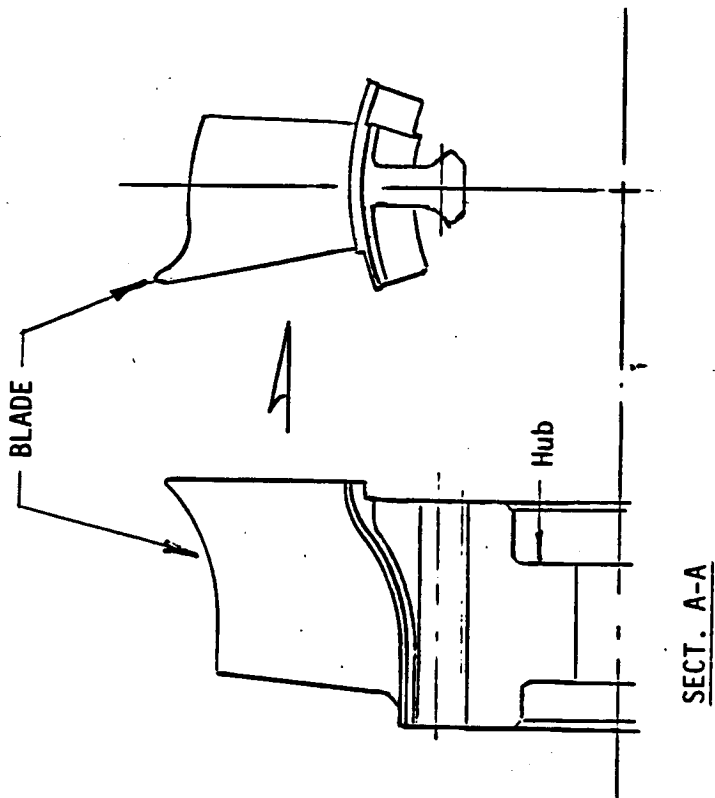


FIGURE 36



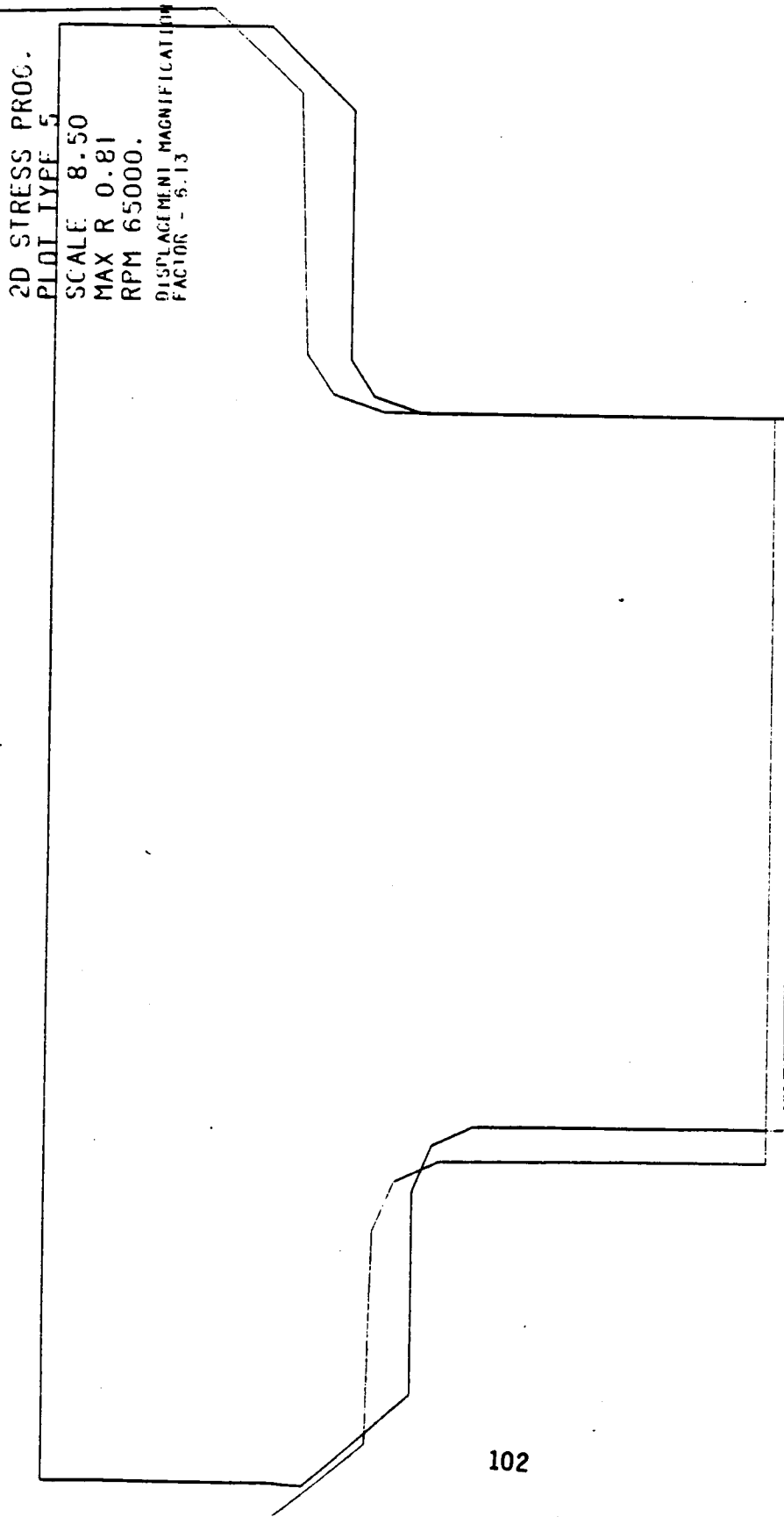
EXDUCER

BLADE-HUB ASSEMBLY

FIGURE 38

07/14/81 10.23.54

INSERTED BLADE DISC ANALYSIS 7-14-81 CRT4PLOT.RJE P.BARROW



2D STRESS PROC.

PLOT TYPE 5

SCALE 8.50

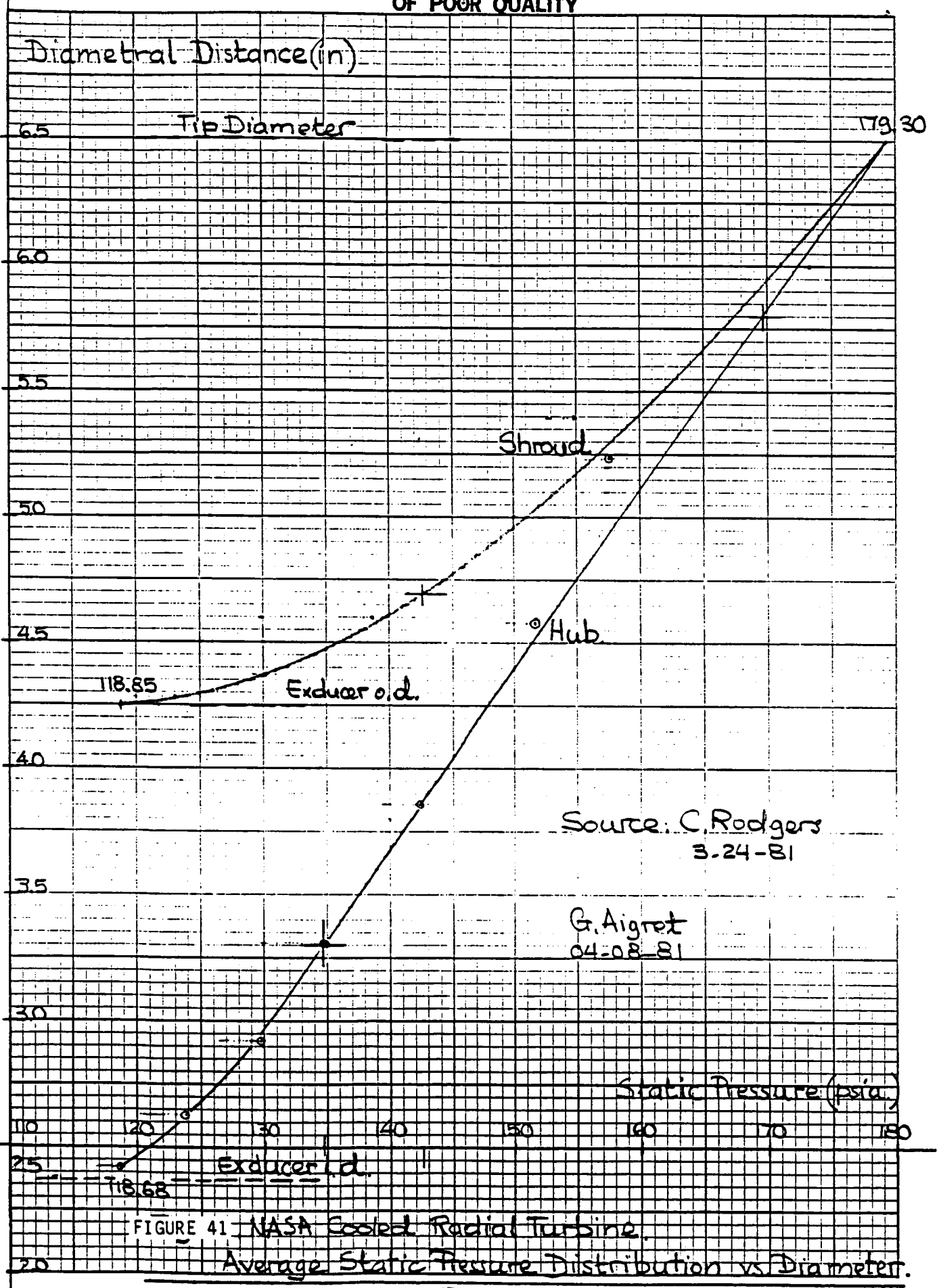
MAX R 0.81

RPM 65000.

DISPLACEMENT MAGNIFICATION
FACTOR - 5.13

102

FIGURE 37



ADDENDUM

These data are copies of the computer printout sheets showing:

- a) Radial and axial displacement at each node point.
- b) Stresses (radial, axial, tangential, shear and effective) at each element made up of three adjacent nodes.

Both a) and b) above are under operating conditions listed in para 3.0.4.1.

NOTE: The program performs node re-numbering (optimized wave front) to minimize computation time. Each output group has a re-numbered node diagram as a front sheet. This (re-numbered node) sheet should be used in determining the values of a and b above for each design.

PRECEDING PAGE BLANK NOT FILMED

*

3500

10 3000

NODES

AND

2500

NODES

NOS

2000

R VS

10

107

1500

1000

500

200

PRECEDING PAGE BLANK NOT FILMED

ORIGINAL PAGE IS OF POOR QUALITY

2865 284 283
 8 12 0 2 9 78 7
 27675274 2737271
 2709 268 26726665
 6 3 2 2 2 12 02 9
 2 5 5 2 4 2 32 22 1
 2570486 248 242 43242
 2481384 233 232 231230
 24029272 221 220 219 218
 228171508 207 206 205 204
 2 52030287 196 195 194 193
 2 73 2 6 1 29921918786 185 184 183 182
 2 7 6 4 2 3 1 1309218076175 174 173 172 171
 235233009 0090398118076175 174 173 172 171
 19 88 1 9 170 165 4 16 62 1 1 1 0
 178177 169 159 15453 152151 150 149
 16867 166 158 148 142 141 140
 157 156185 147 136 12928 127 130
 146 145 144 135 126 117 116 120 119
 143 134 133 126 115 114 105 107 118
 132 131 124 123 113 104 103 93 94106
 122 121 112 111 102 92 91 82 81
 110 109 101 100 90 80 79 69 68 67
 108 99 89 78 66 58 57
 98 97 88 77 65 56 49 48
 96 87 76 64 55 47 41 40
 85 75 63 54 46 39 34 33
 74 62 53 45 38 32 26 28 27 22
 85 73 61 37 31 25 20 16 12 17 13 10
 83 72 60 51 43 36 30 24 19 15 11 7 4 3
 71 60 51 43 36 30 24 19 15 11 7 4 3
 70 59 50 42 35 29 23 18 14 9 5 2 1

0 200 400 600 800 1000 1200 1400 1500 1800 2000 2200 2400

STAR WHEEL

*

DISPLACEMENTS AND REDUNDANT LOADS

NODE	RADIAL DISP.	AXIAL DISP.	RADIAL LOAD	AXIAL LOAD
1	0.150926E-02	0.0	0.115267D+02	-0.108336D-02
2	0.150488E-02	-0.102642E-02		
3	0.205931E-02	0.476131E-04		
4	0.213084E-02	-0.978606E-03		
5	0.170772E-02	-0.272347E-02		
6	0.325984E-02	0.148603E-03		
7	0.222625E-02	-0.265090E-02		
8	0.335095E-02	-0.880460E-03		
9	0.205017E-02	-0.408848E-02		
10	0.395260E-02	0.186212E-03		
11	0.254643E-02	-0.398409E-02		
12	0.340474E-02	-0.252259E-02		
13	0.399463E-02	-0.846174E-03		
14	0.249518E-02	-0.516281E-02		
15	0.298652E-02	-0.507360E-02		
16	0.374614E-02	-0.384756E-02		
17	0.402047E-02	-0.245577E-02		
18	0.267170E-02	-0.589468E-02		
19	0.315062E-02	-0.585729E-02		
20	0.429590E-02	-0.489814E-02		
21	0.434880E-02	-0.370384E-02		
22	0.474034E-02	-0.428668E-02		
23	0.266278E-02	-0.656401E-02		
24	0.312624E-02	-0.658202E-02		
25	0.443568E-02	-0.577371E-02		
26	0.587372E-02	-0.472381E-02		
27	0.500286E-02	-0.408142E-02		
28	0.563870E-02	-0.419637E-02		
29	0.251493E-02	-0.739704E-02		
30	0.297465E-02	-0.745231E-02		
31	0.437738E-02	-0.660248E-02		
32	0.595465E-02	-0.572146E-02		
33	0.780942E-02	-0.429971E-02		
34	0.230137E-02	-0.482649E-02		
35	0.275960E-02	-0.827216E-02		
37	0.419710E-02	-0.835181E-02		
38	0.586070E-02	-0.755654E-02		
39	0.776815E-02	-0.584260E-02		
40	0.945251E-02	-0.572074E-02		
41	0.941962E-02	-0.438477E-02		
42	0.202540E-02	-0.494235E-02		
43	0.248446E-02	-0.925815E-02		
44	0.594420E-02	-0.935432E-02		
45	0.564794E-02	-0.851173E-02		
46	0.760823E-02	-0.772272E-02		
47	0.936016E-02	-0.687871E-02		
48	0.112924E-01	-0.602567E-02		
49	0.112710E-01	-0.445765E-02		
50	0.169747E-02	-0.505899E-02		
51	0.215696E-02	-0.103835E-01		
52	0.357439E-02	-0.104817E-01		
53	0.534107E-02	-0.954801E-02		
54	0.731306E-02	-0.874071E-02		
55	0.917477E-02	-0.792407E-02		
56	0.112162E-01	-0.713963E-02		
57	0.131204E-01	-0.526010E-02		
58	0.142004E-02	-0.451015E-02		
59	0.142004E-02	-0.517161E-02		
60	0.888406E-02	-0.116381E-01		
61	0.323159E-02	-0.117280E-01		
62	0.495278E-02	-0.106865E-01		
63	0.629013E-02	-0.981669E-02		
64	0.893689E-02	-0.897771E-02		
65	0.110062E-01	-0.826087E-02		
66	0.132601E-01	-0.747173E-02		
67	0.144938E-01	-0.648931E-02		
68	0.147674E-01	-0.436082E-02		
69	0.148945E-01	-0.489720E-02		
70	0.123311E-02	-0.619771E-02		
71	0.170065E-02	-0.127736E-01		
72	0.277316E-02	-0.128607E-01		
73	0.334432E-02	-0.119232E-01		
74	0.435845E-02	-0.112662E-01		
75	0.633880E-02	-0.100850E-01		
76	0.834759E-02	-0.930124E-02		
77	0.105956E-01	-0.930124E-02		

70	0.130019E-01	-0.785734E-02
71	0.147982E-01	-0.702528E-02
72	0.146659E-01	-0.778322E-02
73	0.159836E-01	-0.618345E-02
74	0.160082E-01	-0.630878E-02
75	0.258725E-02	-0.130491E-01
76	0.314459E-02	-0.120926E-01
77	0.362339E-02	-0.115953E-01
78	0.573531E-02	-0.112437E-01
79	0.770804E-02	-0.105380E-01
80	0.100043E-01	-0.988436E-02
81	0.124538E-01	-0.919576E-02
82	0.144417E-01	-0.852152E-02
83	0.159189E-01	-0.720808E-02
84	0.157503E-01	-0.804774E-02
85	0.172143E-01	-0.647191E-02
86	0.170900E-01	-0.468069E-02
87	0.288151E-02	-0.131180E-01
88	0.285233E-02	-0.113549E-01
89	0.825171E-02	-0.111031E-01
90	0.899699E-02	-0.114772E-01
91	0.117696E-01	-0.104781E-01
92	0.141054E-01	-0.932307E-02
93	0.137837E-01	-0.993255E-02
94	0.154955E-01	-0.892690E-02
95	0.170935E-01	-0.745248E-02
96	0.168795E-01	-0.835066E-02
97	0.185373E-01	-0.569790E-02
98	0.174865E-01	-0.369161E-02
99	0.186907E-01	-0.490279E-02
100	0.109211E-01	-0.117254E-01
101	0.133126E-01	-0.106977E-01
102	0.124283E-01	-0.119100E-01
103	0.151124E-01	-0.965945E-02
104	0.147485E-01	-0.102991E-01
105	0.165798E-01	-0.918052E-02
106	0.183301E-01	-0.776752E-02
107	0.180538E-01	-0.872029E-02
108	0.200382E-01	-0.631770E-02
109	0.196231E-01	-0.813559E-02
110	0.189686E-01	-0.370369E-02
111	0.205632E-01	-0.387688E-02
112	0.202856E-01	-0.511974E-02
113	0.142188E-01	-0.110909E-01
114	0.134513E-01	-0.120874E-01
115	0.161414E-01	-0.100590E-01
116	0.157183E-01	-0.107062E-01
117	0.176938E-01	-0.959123E-02
118	0.192603E-01	-0.915169E-02
119	0.217571E-01	-0.596108E-02
120	0.212108E-01	-0.778843E-02
121	0.209460E-01	-0.055250E-02
122	0.222485E-01	-0.422131E-02
123	0.151273E-01	-0.115302E-01
124	0.144868E-01	-0.123076E-01
125	0.171948E-01	-0.105012E-01
126	0.160705E-01	-0.120137E-01
127	0.188252E-01	-0.100628E-01
128	0.204765E-01	-0.961668E-02
129	0.234278E-01	-0.453217E-02
130	0.229042E-01	-0.614293E-02
131	0.223405E-01	-0.781005E-02
132	0.221497E-01	-0.828235E-02
133	0.219650E-01	-0.870531E-02
134	0.220598E-01	-0.925100E-02
135	0.155849E-01	-0.125608E-01
136	0.182485E-01	-0.110083E-01
137	0.177196E-01	-0.117020E-01
138	0.167233E-01	-0.128375E-01
139	0.198846E-01	-0.107293E-01
140	0.213683E-01	-0.103872E-01
141	0.255658E-01	-0.527841E-02
142	0.249989E-01	-0.670243E-02
143	0.243781E-01	-0.818496E-02
144	0.239087E-01	-0.912773E-02
145	0.233107E-01	-0.101754E-01
146	0.230971E-01	-0.105806E-01
147	0.192746E-01	-0.116158E-01
148	0.213683E-01	-0.12891E-01
149	0.255658E-01	-0.131329E-01
150	0.249989E-01	-0.118487E-01
151	0.243781E-01	-0.116113E-01
152	0.239087E-01	-0.561688E-02
153	0.233107E-01	-0.698837E-02
154	0.230971E-01	
155	0.192746E-01	
156	0.213683E-01	
157	0.178537E-01	
158	0.207631E-01	
159	0.224542E-01	
160	0.263859E-01	
161	0.257923E-01	

162	0 251689E-01	0 839444E-02
163	0 244501E-01	0 972803E-02
164	0 256595E-01	0 109906E-01
165	0 233590E-01	0 113884E-01
166	0 201653E-01	0 124777E-01
167	0 195042E-01	0 133055E-01
168	0 192125E-01	0 136696E-01
169	0 217309E-01	0 125613E-01
170	0 225308E-01	0 124103E-01
171	0 272165E-01	0 58373E-02
172	0 266634E-01	0 736812E-02
173	0 258865E-01	0 878806E-02
174	0 250401E-01	0 102476E-01
175	0 241440E-01	0 115R15E-01
176	0 235895E-01	0 123643E-01
177	0 209408E-01	0 134213E-01
178	0 203640E-01	0 139737E-01
179	0 219331E-01	0 129111E-01
180	0 231789E-01	0 1286H1E-01
181	0 227550E-01	0 133224E-01
182	0 268037E-01	0 673925E-02
183	0 280070E-01	0 634325E-02
184	0 271378E-01	0 993514E-02
185	0 261698E-01	0 113746E-01
186	0 250833E-01	0 177868E-01
187	0 247820E-01	0 131539E-01
188	0 207756E-01	0 139794E-01
189	0 223215E-01	0 137485E-01
190	0 218805E-01	0 141685E-01
191	0 242678E-01	0 137308E-01
192	0 238165E-01	0 141648E-01
193	0 201070E-01	0 814008E-02
194	0 291912E-01	0 987017E-02
195	0 281813E-01	0 114167E-01
196	0 271025E-01	0 127893E-01
197	0 260254E-01	0 140462E-01
198	0 212215E-01	0 145992E-01
199	0 233274E-01	0 145805E-01
200	0 216644E-01	0 147015E-01
201	0 225928E-01	0 148465E-01
202	0 255437E-01	0 145574E-01
203	0 250258E-01	0 150180E-01
204	0 311466E-01	0 102024E-01
205	0 303209E-01	0 115148E-01
206	0 292598E-01	0 128902E-01
207	0 281298E-01	0 141361E-01
208	0 269790E-01	0 153290E-01
209	0 213405E-01	0 151302E-01
210	0 208336E-01	0 153256E-01
211	0 237098E-01	0 150988E-01
212	0 229911E-01	0 150109E-01
213	0 221796E-01	0 152097E-01
214	0 226359E-01	0 152656E-01
215	0 266624E-01	0 156244E-01
216	0 244068E-01	0 155104E-01
217	0 260800E-01	0 150955E-01
218	0 322960E-01	0 12069E-01
219	0 313922E-01	0 131915E-01
220	0 303439E-01	0 143486E-01
221	0 291115E-01	0 15507E-01
222	0 279900E-01	0 166111E-01
223	0 208516E-01	0 157595E-01
224	0 217788E-01	0 155755E-01
225	0 204434E-01	0 159762E-01
226	0 220163E-01	0 158143E-01
227	0 277576E-01	0 158113E-01
228	0 255177E-01	0 163084E-01
229	0 26205E-01	0 169206E-01
230	0 334024E-01	0 139123E-01
231	0 324403E-01	0 148922E-01
232	0 314454E-01	0 158310E-01
233	0 302395E-01	0 168790E-01
234	0 290364E-01	0 175074E-01
235	0 205672E-01	0 160835E-01
236	0 214043E-01	0 159555E-01
237	0 209160E-01	0 164370E-01
238	0 214489E-01	0 159545E-01
239	0 287983E-01	0 150982E-01
240	0 266606E-01	0 176183E-01
241	0 281772E-01	0 185565E-01
242	0 345779E-01	0 156323E-01
243	0 336161E-01	0 164834E-01
244	0 327036E-01	0 172480E-01
245	0 314245E-01	0 162560E-01

246 0.301380E-01
 247 0.211320E-01
 248 0.298861E-01
 249 0.278130E-01
 250 0.292158E-01
 251 0.351798E-01
 252 0.342195E-01
 253 0.333554E-01
 254 0.320527E-01
 255 0.306940E-01
 256 0.301494E-01
 257 0.289429E-01
 258 0.295281E-01
 259 0.367893E-01
 260 0.348963E-01
 261 0.340182E-01
 262 0.327049E-01
 263 0.313013E-01
 264 0.308206E-01
 265 0.370657E-01
 266 0.361522E-01
 267 0.352898E-01
 268 0.339685E-01
 269 0.326834E-01
 270 0.322483E-01
 271 0.383561E-01
 272 0.374058E-01
 273 0.365676E-01
 274 0.363613E-01
 275 0.341099E-01
 276 0.336780E-01
 277 0.389407E-01
 278 0.380462E-01
 279 0.371909E-01
 280 0.360129E-01
 281 0.347901E-01
 282 0.343608E-01
 283 0.395420E-01
 284 0.377925E-01
 285 0.395143E-01
 286 0.360512E-01

-0.192649E-01
 -0.166611E-01
 -0.194601E-01
 -0.188003E-01
 -0.199316E-01
 -0.164771E-01
 -0.172793E-01
 -0.179740E-01
 -0.189785E-01
 -0.199921E-01
 -0.203748E-01
 -0.201128E-01
 -0.207830E-01
 -0.172938E-01
 -0.180127E-01
 -0.187026E-01
 -0.197088E-01
 -0.207456E-01
 -0.210850E-01
 -0.188219E-01
 -0.195396E-01
 -0.202096E-01
 -0.212227E-01
 -0.221864E-01
 -0.225120E-01
 -0.202973E-01
 -0.210499E-01
 -0.217073E-01
 -0.226484E-01
 -0.236070E-01
 -0.239401E-01
 -0.219827E-01
 -0.217890E-01
 -0.224602E-01
 -0.233794E-01
 -0.243222E-01
 -0.246520E-01
 -0.218303E-01
 -0.232132E-01
 -0.249919E-01
 -0.253465E-01

REDUNDANT LOAD CALC. TIME (MIN.)= 0.0167

ELEMENT STRESSES

ELEMENT	STRESS-R	STRESS-Z	STRESS-Q	STRESS-RZ	EFF. STRESS
1	9	1587	1315	821	2039
2	-4839	582	1894	1917	7017
3	6990	9224	19074	1033	11939
4	-1143	7490	20941	6735	21686
5	1436	8609	52406	7299	43092
6	12574	9720	61935	-1726	50939
7	20476	-16346	98000	-6571	102588
8	26503	-7526	110846	-8478	106576
9	30823	-3387	143522	3680	156649
10	25788	-30261	136486	-2987	146126
11	36019	-29777	162609	6743	168297
12	24377	-29399	142218	-1246	152060
13	34017	-18409	159534	4412	168569
14	23809	-24077	133831	-669	140248
15	30588	-12789	141420	2761	137838
16	20232	-20296	114627	-620	119922
17	24712	-6248	113112	2259	109928
18	15083	-16500	87968	-116	92804
19	18037	-1519	80266	-116	74099
20	7758	-11721	64600	2473	59163
21	9749	5239	42993	2156	35715
22	3358	-3270	24423	-25	25098
23	1462	4036	10693	927	8674
24	-1599	-317	553	-1513	3201
25	1645	1353	711	1736	3201
26	-1167	315	284	2358	3117
27	6621	3220	11363	4335	4335
28	2975	3039	13338	7829	7829
29	15221	600	51173	1924	13609
30	30249	9795	35173	-8689	34505
31	34064	-17115	60880	-8620	38598
32	64177	-4986	74619	-12168	82367
33	67700	-23256	94874	-14902	92282
34	68116	-10502	118539	3124	124549
35	70329	-19610	117551	-1610	111893
36	65429	-8102	130312	6718	131220
37	66814	-13921	126306	1765	112597
38	58944	-10208	110558	5800	122323
39	60905	-9199	112591	1707	105000
40	48986	-10710	93752	3852	106989
41	51274	-4760	92158	2101	90852
42	36195	-10727	71335	3059	84446
43	38666	658	65786	3059	71512
44	17321	-11092	41986	3437	56987
45	20318	4948	34853	5917	47135
46	4594	-2153	18048	306	25908
47	3161	-3284	7834	1551	18015
48	1177	-1468	250	-3834	8086
49	5514	-1730	19508	-3185	5625
50	2765	-3696	10711	2673	19253
51	-1504	-515	3256	1453	12751
52	62	-3561	1008	-3096	6905
53	664	435	-1008	-1337	3964
54	-2595	-990	-1318	655	2060
55	1905	-3713	-1684	945	2151
56	-3562	-6284	4285	1707	7704
57	8990	-7586	5842	8159	17921
58	10312	-9933	24479	-7994	31036
59	24548	-2942	32762	848	37022
60	79717	-2125	57111	-22856	65484
61	9508	8668	88668	-20680	93779
62	52206	71053	71053	-31866	77654
63	112564	3231	106510	-56316	124369
64	111524	13279	108709	-11425	98874
65	89528	953	103092	-17940	100983
66	89734	-6546	111227	2043	107711
67	88043	11969	115179	-2223	92756
68	81437	-6832	112637	5092	107623
69	81329	7165	111372	672	92925
70	77257	-6362	106711	4248	101870
71	72199	1326	100736	1325	88330
72	4445	-4632	94870	3393	89885
73	60150	-2069	84689	2446	77577
74	53186	-2292	77921	2936	72860
75	44883	-3330	65031	3575	61160
76	44381	1221	55970	3607	60364
77	24001	-2997	37973	5266	37211

77	17200	-554	26773	-260	24022
78	12158	-421	20680	3049	19130
79	11539	5080	10402	-1640	14302
80	91716	9213	120025	3465	99902
81	80092	6757	108269	-3346	91916
82	86585	10568	116305	-4334	94753
83	74310	7270	103413	-7114	86284
84	80573	6514	110141	-2252	82216
85	68017	4617	96818	-5288	82546
86	74504	3097	101582	-45	88128
87	60109	1956	87344	-2156	76592
88	66890	1940	89946	2195	79136
89	49541	-1398	74515	1768	67086
90	56326	3915	74582	4839	64090
91	35410	-2285	57207	6447	53317
92	41730	7683	54832	5603	43258
93	23864	2992	40425	6398	34329
94	82567	1897	97589	-694	92937
95	77599	147	90245	-3958	84770
96	77625	-2716	90567	-2969	87687
97	75709	6835	86599	-9163	76829
98	74988	-4938	85445	-2868	76829
99	69008	1247	79593	-6614	95782
100	72786	-5139	80850	-557	74749
101	61008	-321	73374	-1883	82263
102	66503	-3257	73690	2200	68434
103	50604	1241	64033	3296	73719
104	56831	533	62894	5682	69978
105	38079	-233	50598	8067	60077
106	40193	4814	46936	12832	47953
107	33520	2668	41727	6283	44904
108	66637	-1150	87273	-693	36831
109	98632	10687	87083	-14359	80133
110	59364	10416	68488	-2746	76689
111	70819	3346	70199	-13177	70940
112	71032	-9503	69442	-927	79771
113	65908	5292	67711	6161	62456
114	65490	-7386	67708	1011	76023
115	58326	2630	63339	-252	58325
116	65078	-381	64382	4053	68448
117	48379	1223	56872	6369	53087
118	55787	2164	56531	7793	53087
119	37408	5661	46947	10183	55662
120	37667	-135	41173	8398	41588
121	44522	12030	62473	809	42356
122	57116	-3238	57338	-15505	67364
123	48082	5228	53052	66885	67364
124	69505	11373	55101	-9203	48255
125	60114	15782	54099	-7051	75770
126	63665	8181	54349	-1012	41690
127	65963	-6305	56164	1308	51515
128	59336	7625	55216	-7350	69087
129	66235	-4613	57726	-181	49782
130	84914	4321	57726	-552	67009
131	54243	2994	55037	50546	67009
132	60220	-1091	56910	52593	50546
133	48142	3219	52702	60143	60143
134	47124	5420	49756	5941	48475
135	106815	2082	44026	13208	48780
136	52129	12597	40228	8002	42053
137	51198	19998	36942	-4124	81838
138	55282	-3371	34977	11173	33907
139	57278	14630	38052	-700	48553
140	52200	-7393	38520	38341	48553
141	58595	9156	40145	-8126	68167
142	54506	-3607	44406	40947	40947
143	61396	6707	45141	56671	56671
144	52420	-3145	49148	-4279	44497
145	59759	3221	49148	-484	46551
146	50861	2714	61927	-408	46551
147	57816	-875	1849	1849	59380
148	42292	845	49769	4521	59380
149	50759	3208	53049	4531	48252
150	42292	5410	48773	6948	65305
151	37686	247	49733	12218	45134
152	79273	30039	42158	8011	49608
153	40016	4002	28407	8011	42211
154	52016	-3804	21567	4863	42211
155	51273	10407	20485	-16436	50776
156	45053	-3967	20485	-6624	50805
157	54874	10407	27903	-11032	49169
158	47310	8577	28350	-6593	35325
159	57012	-4042	28350	-8153	52281
160	49969	5864	36	-4447	36406
161	60347	-2402	431/2	-4429	54184
162				-1088	39801
163					56200

175	49817	3444	1713	186	42902
176	59748	-412	48122	2287	65416
177	46576	1556	4867	7067	45856
178	56355	3092	50749	5575	51507
179	43945	7918	47937	7667	40425
180	49491	5364	48571	11929	48327
181	36976	591	42402	6775	41055
182	28774	2882	-18910	7090	43150
183	23858	-1505	-24192	9588	44826
184	41008	-9633	-5618	12775	53194
185	53718	-6733	5708	-9126	56879
186	36869	7930	4747	-9340	34972
187	51655	5240	16872	-8620	52081
188	41641	5614	16674	-7823	34722
189	55214	-4538	27080	-5813	52748
190	46170	4916	20235	-3967	36483
191	58672	-2934	37070	-1797	54252
192	48805	3562	37071	310	50671
193	60867	237	45208	3669	54886
194	45474	93	38672	9840	45865
195	44953	-237	42333	3381	41717
196	31143	2358	42333	14253	48795
197	48155	3109	4126	5480	42102
198	40648	103	41573	4006	42363
199	16078	-24188	-44293	-9230	55596
200	105117	6188	-	14629	46494
201	105114	-4145	-6501	5626	52251
202	11415	-7387	8039	-8359	46294
203	115126	4805	19839	-5684	52251
204	118126	4805	22409	-5750	31689
205	125135	5461	31908	-2510	50612
206	133144	-3650	31908	-2410	31939
207	133144	4534	32798	714	51664
208	134145	2931	36730	4703	35005
209	134145	2518	39309	4505	52177
210	134145	3543	39229	13401	42934
211	134145	-1449	36046	10191	42553
212	134145	13895	-36749	11443	42737
213	134145	10506	-18140	-1017	50668
214	134145	-7881	-2300	6059	35880
215	134145	7666	2685	-2208	58794
216	134145	4387	14597	-4559	25960
217	134145	7430	18690	-248	45309
218	134145	1873	28287	-3091	26196
219	134145	4426	29985	2577	46226
220	134145	1622	39134	1151	32497
221	134145	5248	40708	8312	49778
222	134145	4837	47796	12717	38870
223	134145	37708	43495	8540	51278
224	134145	9177	32221	-9357	36170
225	134145	5554	-13549	1192	39797
226	134145	2137	-4826	-7673	32827
227	134145	25957	-2178	-1290	39122
228	134145	41057	9433	26484	26484
229	134145	31471	14340	-5777	40987
230	134145	48883	28977	1889	24210
231	134145	40559	33553	-3577	41397
232	134145	51618	41767	6117	31730
233	134145	46545	42222	2604	42792
234	134145	46545	42688	11107	40134
235	134145	46545	40791	4789	45090
236	134145	46545	13150	-6044	34744
237	134145	46545	-1910	4313	22707
238	134145	46545	15593	-7223	24685
239	134145	46545	17516	2411	17964
240	134145	46545	24432	7754	30737
241	134145	46545	35564	624	21358
242	134145	46545	34178	10242	33102
243	134145	46545	40898	6313	36326
244	134145	46545	42709	26940	26940
245	134145	46545	49542	4157	38205
246	134145	46545	49542	-769	39205
247	134145	46545	35100	-4707	30653
248	134145	46545	49542	-2426	31296
249	134145	46545	12727	-8900	33791
250	134145	46545	34566	-1769	33575
251	134145	46545	36267	-2180	33710
252	134145	46545	32613	-469	23959
253	134145	46545	-7445	-5616	17793
254	134145	46545	3311	4651	30390
255	134145	46545	9885	309	30390
256	134145	46545	309	13785	18727
257	134145	46545	309	8124	31175
258	134145	46545	28140	16074	30030
259	134145	46545	34807	20152	34973
260	134145	46545	18434	296	31175
261	134145	46545	-1579	8910	30030
262	134145	46545	38675	-50	34973
263	134145	46545	-3896	28378	37653
264	134145	46545	23556	24182	37653

325	189-190-199	36433	571	34184	707	34815
326	190-201-199	17363	-7569	29246	16632	43520
327	190-200-201	28511	1462	35376	-6602	35699
328	200-213-201	10099	-4240	34768	4038	34882
329	200-209-213	17483	3417	40184	-6912	34301
330	209-224-213	860	-8992	31679	618	36766
331	200-223-224	8481	3175	36862	-8645	38631
332	223-236-224	-1541	-3983	33011	-3911	36472
333	223-237-236	3283	-1342	36274	-2320	36758
334	223-235-237	-240	1677	34453	-2414	34034
343	186-187-197	13775	-8216	-8363	-6090	32096
344	187-181-197	25372	-8826	858	-5713	11307
345	191-202-197	20211	10969	7619	278	35389
346	191-192-202	37350	-3014	19723	-2820	23273
347	192-203-202	31016	4092	23211	4452	32096
348	192-199-203	39908	-1657	28059	2424	35389
349	199-211-203	30400	3873	28773	10553	25292
350	211-216-203	41338	6316	34083	10728	37324
351	199-212-211	41898	4060	37608	10553	31691
352	199-201-212	37666	-1243	34083	9083	37869
353	201-214-212	11603	17033	28551	9083	38101
354	201-213-214	-7603	-11121	28551	9969	31799
355	213-224-214	11886	-6374	28306	518	45171
356	224-226-214	2690	-17223	28306	-3112	37803
357	224-236-226	9231	-2249	26446	1888	36846
358	236-238-226	-1689	-8518	35734	-7323	38557
359	236-237-226	3118	267	32222	-1098	35048
360	237-247-238	-85	1481	37622	-2344	37840
369	197-202-208	8278	-7038	35058	-892	36244
370	202-216-208	21050	10088	-8860	-6023	35914
371	202-203-216	36242	837	9021	6632	19356
372	203-217-216	29040	4285	21724	-3249	18106
373	203-216-217	39648	2606	23270	6617	31338
374	216-228-217	35926	-7420	31061	376	25183
383	208-215-222	4601	2606	33642	7680	35707
384	215-227-222	18809	-7420	-7691	-3972	34876
385	215-217-227	30054	-2553	8619	4143	13971
386	217-229-227	24365	220	17826	-224	12195
387	217-228-229	36808	-3384	19571	5680	29074
388	228-240-229	29363	11541	29043	-2780	24208
397	222-227-234	458	-627	32267	1917	37235
398	227-239-234	9054	6410	-6923	-2690	19720
399	229-229-239	21102	3770	3797	5999	8689
400	229-241-239	18876	7488	14289	-2699	11390
401	229-240-241	26050	-6717	17771	5688	17067
402	240-249-241	25775	5646	21379	1830	16130
411	234-238-246	3003	-4309	26136	7072	30864
412	239-248-246	4483	3956	-5416	-2978	24154
413	239-241-248	11629	-8414	-1976	3283	9456
414	241-250-248	8690	2334	3188	-3611	8422
415	249-257-250	21180	-3593	7708	4590	18519
416	246-248-255	16503	7420	17860	-2382	9915
426	248-256-255	-425	-1019	16905	4293	23655
427	248-250-256	6115	-500	12736	-4745	13570
428	250-257-258	7636	-7352	-3527	5801	11944
429	250-258-256	7636	887	5698	-3736	10628
				4691	-1719	9114
				10944	2629	11025
						9977

ELEMENT STRESSES

ELEMENT	STRESS-Y	STRESS-X	STRESS-XY	EFF. STRESS
80	201951	8904	-28774	2038336
81	154606	-8459	-5619	157707
82	155623	-2092	-10922	157805
83	131940	-6398	-6000	136845
84	131942	-11325	-3442	138082
85	121317	-9537	-2644	126439
86	120518	-14750	-140	128579
87	107294	-12766	996	114227
88	108116	-13709	1719	115621
89	88432	-14408	5077	96846
90	91390	-9331	3367	96571
91	67697	-13159	9350	72046
92	67423	-1430	5980	68931
93	36145	-8222	11541	45506
198	78771	13931	21077	81451
199	63280	-4967	4067	67226
200	50203	-9881	4067	56247
201	49629	-11797	2354	56606
215	71681	-2573	-5811	73692
216	56873	2404	-1364	58160
217	45096	-2296	-9830	55039
218	32678	-6045	-2329	36307
231	71432	301	-7584	72482
232	40513	-2870	9173	44925
233	45086	979	-8020	46718
234	27210	-5821	-1492	40087
235	22346	-2293	-4870	25040
236	26269	3691	-1284	29570
249	53680	-3831	-7780	69621
250	31827	1694	-7074	33816
251	37705	-967	-16421	40115
252	24982	-3979	-3979	39349
253	27002	2154	-1143	26068
254	25097	6127	-10398	28948
255	29034	4225	-8428	30843
256	22560	965	4279	23303
257	8805	-7397	-10248	22637
258	26426	994	-3384	25523
259	25980	1955	-10445	31722
260	29037	6165	324	26836
261	35687	-2304	-5054	37917
262	38657	6072	4669	36904
263	45452	-3553	972	47369
264	45581	3919	8394	46106
265	49382	-4699	6188	52986
266	46552	5238	10894	48029
267	47150	-1421	11085	51610
268	46760	1282	-10816	49791
269	27898	172	-9368	32199
270	37828	-1465	-12657	44375
271	23272	3110	-14006	32672
272	33048	4236	-881	35339
273	28472	8432	-211	26361
274	37587	10586	-3707	34273
275	25950	457	4358	26819
276	9308	-4488	-6530	16628
277	22364	6085	-1962	20313
278	32639	6259	-8669	33604
279	25030	3382	2186	33825
280	39594	6302	-5365	38070
281	34004	3522	4647	33372
282	45121	3774	2846	40819
283	39450	3953	9134	43637
284	72924	13151	-11293	68712
285	46024	1898	-8970	51928
286	31198	3367	-14021	33481
287	41194	4228	-12479	46156
288	25186	6464	-10265	31313
289	39294	5316	-4114	40974
290	31509	8285	-3762	29175
291	42116	7879	-2485	39325
292	21821	-1980	-8561	23277
309	33049	-1064	-7619	25579
310	30532	2804	-13480	39024
311	19522	3211	-7020	21830

313	173-174-184	37897	2482	-11757	41987
314	174-185-184	32843	7163	-2144	30142
315	174-175-185	38978	6059	-6197	37882
316	175-186-185	20016	1163	3157	20214
318	182-183-193	27671	-689	-10006	32948
319	183-184-193	20869	1885	-6971	23065
320	183-184-194	27418	-3502	-12491	36443
321	184-195-194	20725	1182	-1761	20389
322	184-185-195	27163	25	-11717	42332
323	185-196-195	28503	2927	-884	27212
324	185-186-196	37463	7784	-6986	36312
325	186-197-196	14904	-187	1403	15195
326	193-194-204	36824	8564	-17197	44736
327	194-208-204	25150	2190	-7105	27086
328	194-198-205	28760	-464	-12057	38664
329	195-206-205	23611	1572	-416	22777
330	195-196-206	34703	-4887	-11380	42265
331	196-207-206	26837	1624	-48	26065
332	196-187-207	30861	4595	-7898	31910
333	197-208-207	7523	-179	2367	8648
334	204-208-218	40903	12058	-21134	51625
335	205-219-218	24761	1204	-4722	26627
336	205-206-219	24060	-2680	-12032	32938
337	206-220-219	19086	3171	-898	17783
338	206-207-220	28573	-2550	-10163	34917
339	207-221-220	19788	3788	923	18259
340	207-208-221	24097	7850	-6951	24456
341	208-222-221	4464	4089	2039	5556
342	219-231-230	42802	14996	-19343	50373
343	219-231-230	27557	179	-3433	28104
344	220-232-231	26966	4055	-1190	31776
345	220-232-231	22517	3886	-2667	21247
346	221-233-232	31485	3452	-8589	33378
347	221-233-232	18582	5512	-8589	17696
348	222-234-233	26482	13771	-5821	24273
349	222-234-233	1566	4398	-4842	9460
350	230-231-242	4398	13197	-14153	43751
351	231-232-243	28871	1014	-1824	29547
352	232-233-244	32783	6323	-8431	33481
353	232-233-244	27896	8039	-2809	26204
354	233-245-244	30985	8008	-6367	37328
355	233-245-244	24244	6936	-3997	22708
356	234-246-245	31244	18076	-4418	28125
357	242-243-251	4026	6682	6242	12244
358	243-252-251	44079	10315	-9841	43419
359	244-245-252	32609	584	-3082	32758
360	244-245-252	35668	5845	-3839	36631
361	244-245-253	34762	5731	939	32321
362	245-254-253	44983	7777	-2067	41796
363	245-254-253	30852	6981	912	28065
364	246-255-254	38989	14905	-621	34093
365	251-252-259	1159	3606	4730	8791
366	252-260-259	39660	64	-6530	38923
367	252-253-260	32126	64	-2096	32298
368	253-261-260	35439	2120	-120	34199
369	253-261-260	32984	3086	468	31211
370	254-262-261	38744	3941	-875	37171
371	254-262-262	39242	4499	-650	27182
372	255-263-262	34506	4809	2246	31164
373	255-263-262	24310	9311	2246	23278
374	255-268-263	37303	4276	3484	35026
375	258-264-263	29893	5740	2344	27418
376	259-260-265	29893	8549	3581	30860
377	260-266-265	31421	2415	-3421	27484
378	260-261-266	28789	2544	-1487	28111
379	261-267-266	28462	1667	277	26656
380	261-267-266	29830	4095	-277	29271
381	262-262-267	28330	1207	-712	24350
382	262-268-267	26479	5049	-43	26702
383	262-263-268	27320	1756	1965	24005
384	263-269-268	25932	4583	737	27870
385	263-264-269	23711	-6355	2796	20406
386	264-270-269	21952	3719	883	21737
387	265-266-271	21464	272	-180	21737
388	266-272-271	17917	532	-164	17809
389	266-267-272	20302	-532	-24	20786
390	267-273-272	17156	-935	-52	17127
391	268-274-273	19885	19	315	20507
392	268-274-273	16290	-133	-755	16409
393	268-269-274	18482	-1898	1245	15619
394	269-275-274	16696	-6	-870	16783
395	269-270-275	15348	-2508	1395	16917
396	270-276-277	13914	-168	-1	14015
397	271-272-277	11777	-1808	-1	12963
398	272-278-277	13001	801	-913	12718

-62	272-273-278	9879	-2309	-189	11562
463	273-279-278	12030	551	-438	11785
464	273-274-279	8847	-3379	154	10939
465	274-280-279	11149	510	-412	10927
466	274-275-280	7741	-3709	913	10242
467	275-281-280	10024	173	309	9953
468	275-276-281	7720	-82	1364	8113
469	276-282-281	11122	313	1233	11175
470	277-278-283	4372	160	-372	4342
471	278-284-283	3419	896	-457	3174
472	278-279-284	4508	245	-465	4462
473	279-280-284	4582	490	348	4400
474	280-285-284	1958	1266	116	1731
475	280-281-285	4782	540	64	4534
476	281-282-285	4539	270	438	4475
477	282-286-285	3029	768	1070	3298

STRESS CALCULATION TIME (MIN.) = 0.0833

MAXIMUM EFFECTIVE STRESS OCCURS AT ELEMENT 80 -28- -26- -33 AND IS EQUAL TO 2.0384E+05 PSI

MAXIMUM RADIAL DISPLACEMENT OCCURS AT NODE 283 AND IS EQUAL TO 3.9542E-02 INS.

MAXIMUM AXIAL DISPLACEMENT OCCURS AT NODE 286 AND IS EQUAL TO -2.5346E-02 INS.

AVERAGE STRESSES OF DISK - VOL. AVG. TANG. IS 47856.227 PSI
 AREA AVG. TANG. IS 59368.332 PSI
 AREA AVG. EQUIV. IS 61271.520 PSI

TOTAL WEIGHT OF BODY IS 4.804 LBS

DIAMETRAL INERTIA ABOUT ORIGIN IS 12.800 LB-IN**2

DIAMETRAL INERTIA ABOUT CENTROID IS 6.825 LB-IN**2

POLAR INERTIA OF BODY IS 12.553 LB-IN**2

CENTROID OF BODY FROM ORIGIN IS 1.1163 IN.

Category	10	20	30	40	50	60	70	80	90	100	110	120	130	140	150	160	170	180
2196																		
2175	213	212																
2141			208															
2107			204															
2062			198															
2016			186															
1954			173															
194	1820		160															
193181	169	158	148															
192180	168	157	146															
182176	163	153	141	134	1242	110												
175	167	156	140	139	130	129	128	118	117	107	106	97	98	99				
164	151	138	127	126	116	115	105	104	96	95	88	87	89	79	78			
			125	114	113	103	102	94	93	86	85	77	76	70	69	68		
			112	101														
			100	91														
			90	82														
			81	72														
			80	71	63													
			62	60	51													
			590															
			43	31														
			30	19														
			20	10														

DISPLACEMENTS AND REDUNDANT LOADS

NODE	RADIAL DISP	AXIAL DISP	RADIAL LOAD	AXIAL LOAD
1	0.501715E-02	0.328833E-03	0.583516D+01	-0.205454D-02
2	0.487302E-02	-0.858138E-04		
3	0.436575E-02	-0.383274E-03		
4	0.376511E-02	-0.198481E-03		
5	0.355173E-02	0.150909E-03		
6	0.290577E-02	0.714402E-04		
7	0.232815E-02	0.0		
8	0.242933E-02	-0.690132E-03		
9	0.258060E-02	-0.239640E-02		
10	0.273165E-02	0.422214E-02		
11	0.497826E-02	0.121940E-02		
12	0.522558E-02	0.124078E-02		
13	0.608482E-02	0.133559E-02		
14	0.619077E-02	-0.224540E-03		
15	0.513235E-02	-0.592322E-03		
16	0.406398E-02	-0.678215E-03		
17	0.300789E-02	-0.637725E-03		
18	0.314931E-02	-0.234637E-02		
19	0.329421E-02	-0.419045E-02		
20	0.281453E-02	-0.507026E-02		
21	0.486985E-02	0.223163E-02		
22	0.511837E-02	0.226087E-02		
23	0.597009E-02	0.236390E-02		
24	0.699099E-02	0.248212E-02		
25	0.728939E-02	0.145766E-02		
26	0.522539E-02	-0.218205E-02		
27	0.629482E-02	-0.212575E-02		
28	0.726623E-02	-0.999804E-04		
29	0.417098E-02	-0.226199E-02		
30	0.333613E-02	-0.503471E-02		
31	0.432600E-02	-0.411396E-02		
32	0.474663E-02	0.315729E-02		
33	0.499441E-02	0.318986E-02		
34	0.584695E-02	0.330074E-02		
35	0.687288E-02	0.357580E-02		
36	0.790366E-02	0.326858E-02		
37	0.802800E-02	0.264649E-02		
38	0.810095E-02	0.161371E-02		
39	0.536708E-02	-0.404984E-02		
40	0.644305E-02	-0.398102E-02		
41	0.738827E-02	-0.200988E-02		
42	0.839952E-02	-0.309748E-04		
43	0.445133E-02	-0.496847E-02		
44	0.467993E-02	0.365205E-02		
45	0.192750E-02	0.368602E-02		
46	0.577208E-02	0.379774E-02		
47	0.900785E-02	0.319323E-02		
48	0.916261E-02	0.273924E-02		
49	0.928113E-02	0.177172E-02		
50	0.559015E-02	-0.489168E-02		
51	0.601982E-02	-0.482898E-02		
52	0.677885E-02	0.558797E-02		
53	0.745920E-02	0.388110E-02		
54	0.845589E-02	-0.192283E-02		
55	0.947146E-02	0.187240E-03		
56	0.101416E-01	0.307942E-02		
57	0.102117E-01	0.280365E-02		
58	0.103890E-01	0.199379E-02		
59	0.887279E-02	-0.501356E-02		
60	0.615691E-02	-0.528516E-02		
61	0.661419E-02	-0.681163E-02		
62	0.634180E-02	-0.569177E-02		
63	0.700081E-02	-0.667705E-02		
64	0.763636E-02	-0.550771E-02		
65	0.849413E-02	-0.383309E-02		
66	0.956101E-02	-0.124527E-02		
67	0.106100E-01	0.324313E-03		
68	0.113738E-01	0.256234E-02		
69	0.115321E-01	0.223371E-02		
70	0.117152E-01	0.106192E-02		
71	0.709196E-02	-0.705861E-02		
72	0.775350E-02	-0.679938E-02		
73	0.850222E-02	-0.552962E-02		
74	0.954828E-02	-0.381354E-02		
75	0.106891E-01	-0.177840E-02		
76	0.118146E-01	-0.860309E-04		
77	0.118477E-01	-0.120600E-02		

78	0.127108E-01	0.281104E-02
79	0.129635E-01	0.118035E-02
80	0.744295E-02	0.730384E-02
81	0.777867E-02	0.736340E-02
82	0.855579E-02	0.690001E-02
83	0.956717E-02	0.554820E-02
84	0.106250E-01	0.381214E-02
85	0.116132E-01	0.228154E-02
86	0.117635E-01	0.331036E-02
87	0.130702E-01	0.803464E-05
88	0.130458E-01	0.116698E-02
89	0.136657E-01	0.760148E-03
90	0.852181E-02	0.696962E-02
91	0.943399E-02	0.562787E-02
92	0.105012E-01	0.420400E-02
93	0.116866E-01	0.524032E-02
94	0.115992E-01	0.214032E-02
95	0.129896E-01	0.228056E-02
96	0.129057E-01	0.352230E-02
97	0.143353E-01	0.987020E-03
98	0.143272E-01	0.828529E-04
99	0.143274E-01	0.734342E-03
100	0.933697E-02	0.785050E-02
101	0.103620E-01	0.712773E-02
102	0.117451E-01	0.613762E-02
103	0.113709E-01	0.693524E-02
104	0.128063E-01	0.436916E-02
105	0.126733E-01	0.534555E-02
106	0.141927E-01	0.229024E-02
107	0.140718E-01	0.342339E-02
108	0.156068E-01	0.120889E-02
109	0.153760E-01	0.287761E-02
110	0.151314E-01	0.441271E-02
111	0.156431E-01	0.461394E-03
112	0.103323E-01	0.823872E-02
113	0.111855E-01	0.700422E-02
114	0.125089E-01	0.802472E-02
115	0.123574E-01	0.626163E-02
116	0.139373E-01	0.711854E-02
117	0.137525E-01	0.469953E-02
118	0.168155E-01	0.218715E-03
119	0.167052E-01	0.144413E-02
120	0.167052E-01	0.301287E-02
121	0.148653E-01	0.556823E-02
122	0.162603E-01	0.507497E-02
123	0.151789E-01	0.570488E-02
124	0.115339E-01	0.871288E-02
125	0.122331E-01	0.783520E-02
126	0.121180E-01	0.959065E-02
127	0.135545E-01	0.641098E-02
128	0.133805E-01	0.721979E-02
129	0.132991E-01	0.759891E-02
130	0.183364E-01	0.274764E-04
131	0.182401E-01	0.176075E-02
132	0.180221E-01	0.317745E-02
133	0.146096E-01	0.663508E-02
134	0.153364E-01	0.563508E-02
135	0.175113E-01	0.721096E-02
136	0.169253E-01	0.529240E-02
137	0.190122E-01	0.710232E-02
138	0.130142E-01	0.930635E-02
139	0.129280E-01	0.864334E-02
140	0.141266E-01	0.951431E-02
141	0.192930E-01	0.739714E-02
142	0.196174E-01	0.306911E-03
143	0.193662E-01	0.196481E-02
144	0.151732E-01	0.339973E-02
145	0.155056E-01	0.869251E-02
146	0.188007E-01	0.865694E-02
147	0.163356E-01	0.558507E-02
148	0.151578E-01	0.878164E-02
149	0.128340E-01	0.745629E-02
150	0.120821E-01	0.987152E-02
151	0.141293E-01	0.98618E-02
152	0.138104E-01	0.85020E-02
153	0.212195E-01	0.979758E-02
154	0.210298E-01	0.65824E-03
155	0.207471E-01	0.226573E-02
156	0.147134E-01	0.366532E-02
157	0.156359E-01	0.100664E-01
158	0.201120E-01	0.103273E-01
159	0.172194E-01	0.592751E-02
160	0.194012E-01	0.974261E-02
161	0.194012E-01	0.786640E-02

162	0.126416E-01	-0.104691E-01
163	0.136412E-01	-0.102421E-01
164	0.118391E-01	-0.107035E-01
165	0.225906E-01	-0.112370E-02
166	0.224857E-01	-0.259652E-02
167	0.221423E-01	-0.395106E-02
168	0.144898E-01	-0.105742E-01
169	0.153288E-01	-0.109580E-01
170	0.158533E-01	-0.116273E-01
171	0.161292E-01	-0.117872E-01
172	0.214420E-01	-0.627786E-02
173	0.184039E-01	-0.102461E-01
174	0.206727E-01	-0.828840E-02
175	0.124718E-01	-0.109284E-01
176	0.114140E-01	-0.108202E-01
177	0.241383E-01	-0.54574E-02
178	0.238795E-01	-0.297584E-02
179	0.235495E-01	-0.427752E-02
180	0.142135E-01	-0.111917E-01
181	0.15025E-01	-0.116067E-01
182	0.157002E-01	-0.118938E-01
183	0.159494E-01	-0.120764E-01
184	0.172778E-01	-0.124244E-01
185	0.227457E-01	-0.671994E-02
186	0.196168E-01	-0.107460E-01
187	0.219195E-01	-0.874908E-02
188	0.132356E-01	-0.112416E-01
189	0.253601E-01	-0.314162E-02
190	0.251459E-01	-0.393951E-02
191	0.249461E-01	-0.463555E-02
192	0.140150E-01	-0.116073E-01
193	0.148094E-01	-0.120283E-01
194	0.154174E-01	-0.12654E-01
195	0.170934E-01	-0.12754E-01
196	0.184360E-01	-0.15224E-01
197	0.240186E-01	-0.150241E-01
198	0.207930E-01	-0.726919E-02
199	0.231561E-01	-0.112927E-01
200	0.255014E-01	-0.921288E-02
201	0.182573E-01	-0.480805E-02
202	0.19587E-01	-0.133284E-01
203	0.250936E-01	-0.136256E-01
204	0.219633E-01	-0.749158E-02
205	0.242853E-01	-0.118378E-01
206	0.193966E-01	-0.963543E-02
207	0.207129E-01	-0.139349E-01
208	0.230536E-01	-0.142665E-01
209	0.238145E-01	-0.126312E-01
210	0.205035E-01	-0.125867E-01
211	0.219123E-01	-0.145907E-01
212	0.210893E-01	-0.14939E-01
213	0.237158E-01	-0.138124E-01
214	0.216850E-01	-0.147460E-01
215	0.232882E-01	-0.153658E-01
216	0.247980E-01	-0.157453E-01
217	0.230938E-01	-0.163208E-01
218	0.246108E-01	-0.161685E-01
219	0.250484E-01	-0.167538E-01
		-0.169410E-01

REDUNDANT LOAD CALC. TIME (MIN.) = 0.0167

ELEMENT STRESSES

ELEMENT	STRESS-R	STRESS-Z	STRESS-Q	STRESS-RZ	EFF. STRESS
1					
2					
3					
4					
5					
6					
7					
8					
9					
10					
11					
12					
13					
14					
15					
16					
17					
18					
19					
20					
21					
22					
23					
24					
25					
26					
27					
28					
29					
30					
31					
32					
33					
34					
35					
36					
37					
38					
39					
40					
41					
42					
43					
44					
45					
46					
47					
48					
49					
50					
51					
52					
53					
54					
55					
56					
57					
58					
59					
60					
61					
62					
63					
64					
65					
66					
67					
68					
69					
70					
71					
72					
73					
74					
75					
76					

77	25-28-38	10615	11106	17150	5854	18361
78	28-42-38	18135	4240	20681	2001	15715
79	28-41-42	20328	712	25380	6993	26870
80	41-54-42	23122	688	29725	3387	21092
81	41-53-54	32669	3268	41332	3847	36385
82	53-65-54	26885	9084	45060	2647	31485
83	53-64-65	47535	6417	69011	3763	55476
84	64-73-65	26667	12166	70734	2295	52983
85	64-72-73	53830	7174	102985	-6013	83639
86	72-82-73	36539	15382	104417	5292	81266
87	72-81-82	8397	8397	124405	-8382	102648
88	81-90-82	51182	4260	108549	-6283	94982
89	36-37-47	29105	2483	5336	1984	7597
90	37-48-47	1641	1927	8142	1720	6186
91	37-38-48	6258	1906	9583	3660	11631
92	38-49-48	12084	1962	11707	10089	10089
93	38-42-49	10636	12545	6189	17626	17626
94	42-55-49	16874	4266	15509	12084	12084
95	54-66-55	17999	2440	18906	893	24808
96	54-66-55	20172	6348	18906	7664	16267
97	54-65-66	29445	2332	3352	2817	33589
98	65-74-66	24368	8339	3758	2314	25518
99	65-73-74	42170	1987	86420	-743	48910
100	73-83-74	29377	12828	11062	-2236	42630
101	73-82-83	51269	1431	84714	-4030	72928
102	82-91-83	42221	15226	85589	66429	66429
103	82-90-91	52516	3075	101480	-7990	86325
104	90-100-91	3824	5028	93682	-8181	78784
105	47-48-56	2674	2294	3719	1820	6396
106	48-57-56	5870	4316	6809	-3368	6228
107	48-49-57	6374	2323	6442	3445	10528
108	48-58-57	14375	6175	9841	-2840	18650
109	49-55-58	8515	3329	6645	6931	18911
110	55-67-58	14667	5250	9392	-553	8231
111	55-66-67	14955	4516	11496	7986	22696
112	66-75-67	16299	4809	15278	2337	11736
113	66-74-75	26030	2762	28451	6400	30654
114	74-84-75	19352	6215	28458	20131	20131
115	74-83-84	38194	570	46616	3046	3046
116	83-92-84	29138	13294	51155	2001	42609
117	83-91-92	16634	1981	68711	-1774	33079
118	91-101-92	55209	12441	73984	-3941	63016
119	91-100-101	40931	2894	88369	-8174	55359
120	100-112-101	40624	8939	84332	-8501	76082
121	56-67-68	9159	3456	-233	10248	67689
122	57-58-68	7221	4617	1458	1188	11537
123	58-68-68	6410	5459	-1458	4609	13284
124	58-70-69	5071	5883	-765	8573	8573
125	58-67-70	12677	3702	-1961	5234	11748
126	67-76-70	3900	2292	554	2603	16306
127	67-77-76	13160	2356	-2566	3495	8358
128	67-75-77	17931	1995	2035	7169	18605
129	75-85-77	10804	1985	8621	17588	17588
130	75-86-85	18732	644	8093	7804	17033
131	84-85-75	21781	359	14023	7173	22889
132	84-93-86	23371	1871	21385	1431	22185
133	84-94-93	24670	3893	26211	5857	24950
134	84-92-94	25133	3301	25579	5313	30453
135	92-102-94	27161	33027	33027	-2163	33371
136	92-103-102	40706	2662	39750	4115	33491
137	101-103-92	38997	1519	53517	-1179	46995
138	101-113-103	46410	2556	62103	-9491	54655
139	101-114-113	51015	11072	71480	-4027	53005
140	101-112-114	51738	7956	75487	-6554	60299
141	68-69-78	11109	5261	78466	10455	66671
142	69-79-78	1528	17090	14207	811	22659
143	69-70-79	8855	2202	-18329	3251	20974
144	70-76-79	7389	7209	-12951	-3093	20305
145	76-87-79	5376	-9033	-1222	3488	19813
146	76-77-87	15013	-15009	-18009	-369	17675
147	77-88-87	8298	-1592	-5802	3634	26023
148	77-85-88	17278	-6953	-2316	6245	14029
149	85-95-88	8470	656	8279	6522	23780
150	85-86-95	13855	-8336	8279	4431	23675
151	86-96-95	17132	-1452	10554	3621	14792
152	86-93-96	21118	-5856	16798	3621	12773
153	93-104-96	19520	1477	15936	2970	26687
154	93-94-104	21711	-9023	20089	2126	18137
155	94-105-104	14983	-2360	30089	1085	30016
156	94-102-105	25418	-6443	30089	2455	21302
157	102-103-105	27185	5748	38213	1683	34560
158	102-103-115	36265	-3863	46001	3650	29300
159	103-116-115	32828	7620	48976	-1623	46651
160	103-113-115	43377	1054	59254	-1084	36952
161						52916

162	113-126-116	42862	7535	52022	-3393	48236
163	113-114-126	52365	6218	70840	-5510	59386
164	78-79-89	5048	7408	-	-3583	20362
165	79-87-89	13695	-7824	-16386	326	26781
166	87-97-89	2082	1836	-13294	1669	15627
167	88-98-97	9538	-8604	-11704	-82	19876
168	88-95-97	14156	-9526	-5650	6510	24956
169	95-106-106	1501	-8090	-9025	7763	29556
170	96-107-106	11672	-10411	-570	4610	16812
171	96-104-107	6998	-2382	510	4030	20699
172	104-117-107	15751	-10070	7880	2449	10861
173	104-108-117	11107	-3600	8993	23315	23315
174	105-118-117	23307	-3947	19669	2960	14661
175	105-115-118	13411	-656	18100	2883	26113
176	115-128-118	23424	-5921	29566	5350	19200
177	115-116-128	19190	355	27322	3611	31661
178	116-129-128	30202	-4942	36907	4374	25129
179	116-130-129	26096	2384	38703	185	38935
180	116-126-130	33992	-1490	52144	1344	32025
181	138-150-140	39052	1411	63703	587	41216
182	138-151-150	1378	1378	52144	-3777	48800
183	151-162-150	21298	1289	63862	-3183	54766
184	151-164-162	2320	246	63994	-9417	57731
185	164-175-162	3950	-1916	53491	264	52520
186	97-106-110	-3148	-20	47907	2179	53728
187	106-107-110	-2888	-6597	47907	1016	49711
188	107-117-110	2842	-8148	-1963	6990	13051
189	117-118-112	14042	6804	6017	152	13051
190	117-122-110	10525	-7265	11168	1842	6969
191	118-128-112	15328	-7937	9208	3209	18407
192	128-134-122	18468	-9913	17500	7610	18557
193	128-129-134	12781	-6012	16832	3829	24701
194	129-141-134	23599	-10016	26274	4832	28688
195	129-130-141	19525	-4323	27899	819	35037
196	140-150-153	30812	-6992	37892	3222	29525
197	150-162-153	32452	31	60334	-1604	41941
198	150-162-163	17672	-580	56231	-9199	54818
199	162-175-175	20537	4253	83272	-1398	47500
200	175-188-176	4561	-1147	56231	-5358	46977
201	110-122-124	6424	856	46011	-633	44594
202	122-134-124	6434	-476	47263	-2166	44051
203	134-135-124	12483	9936	40088	1370	42316
204	134-141-135	8810	6404	6404	4206	17926
205	153-163-157	15100	523	16316	25127	25127
206	153-168-157	26037	-9653	16383	4143	20563
207	163-176-168	15410	-2439	22930	-560	29203
208	176-180-168	18019	2457	50468	-2300	46033
209	188-192-180	5801	1081	46063	1147	38840
210	188-192-180	5592	2617	47410	-3200	38840
211	197-168-168	3435	592	41009	-160	40981
212	168-168-168	20646	384	39997	-7465	37037
213	168-180-169	12125	176	34399	1589	37404
214	180-181-169	10210	12477	43515	1589	36169
215	180-181-169	4504	1120	42754	483	37563
216	192-193-181	3278	8370	39121	2464	30754
217	158-169-170	-2633	903	36773	-2857	34726
218	169-181-170	4896	506	34173	-2464	30819
219	181-182-170	2541	-9513	29955	-3176	32617
220	181-194-182	10201	-11609	18587	-590	31156
221	60-62-52	7975	-170	15871	-3222	24971
222	50-59-51	1317	-228	15273	2857	25700
223	59-60-51	7956	344	31490	572	29553
224	59-60-51	73960	8089	29631	-3340	28887
225	59-60-51	29485	21388	92136	-18609	98960
226			5216	75260	-30346	82540
227					-17912	68979

ELEMENT STRESSES

ELEMENT	STRESS-Y	STRESS-X	STRESS-XY	EFF. STRESS
141	43314	11175	-24152	57157
142	34598	7897	-18151	44498
143	36269	3064	-12201	40423
144	39036	12871	-19175	47854
145	24776	2004	-4214	24929
146	24159	5940	-3395	22584
147	37586	-2127	-9673	42164
148	20791	995	-9525	26098
149	26576	1294	-6187	28078
150	9756	3334	-16553	29930
151	21211	-257	-2929	21936
152	17920	-621	-1071	18341
153	12297	1178	-3164	12967
154	15056	-4917	10565	25612
155	29719	-4979	3887	33117
156	29519	-7816	-8000	35187
157	13702	-4152	-6101	19327
158	6511	-6742	-6463	31472
159	23591	-1801	-3980	10242
160	17664	1662	-3073	24514
161	18974	1375	-3336	17973
162	20017	-6831	5651	24436
163	27858	-7614	2304	20124
164	14071	2308	3482	32901
165	36739	-7873	7301	23643
166	16505	-5825	5171	39639
167	10253	-2701	11953	44136
168	18450	-6570	-609	22300
169	4004	-1802	-1167	21597
170	22028	1480	-1874	22559
171	13126	376	-1258	4777
172	19019	-4172	2648	23085
173	15644	3255	-321	14402
174	27516	-466	6385	14772
175	21185	3677	6011	31974
176	30182	-3892	11141	22199
177	34306	-12135	2522	39066
178	21374	-14946	268	36412
179	8877	8330	-6331	28381
180	9592	-5678	-284	50399
181	35343	-5284	1620	28381
182	4104	-4929	-4005	15542
183	22619	-1202	-677	38090
184	8503	4183	-3079	28437
185	18270	3747	2910	25501
186	14408	-7141	11022	11022
187	25542	-13529	2192	21287
188	17925	-1084	6394	13493
189	20778	-11603	3147	31756
190	26268	-6382	5494	18614
191	11131	-13631	3241	39534
192	20938	-52237	-256	27863
193	39321	-13631	1619	47664
194	19405	-3842	-10007	24912
195	14276	-12142	24507	43330
196	35745	-3902	2155	66520
197	12732	-12031	-12142	24507
198	20293	7243	-12031	41298
199	7814	-4564	-2264	23596
200	15393	-1765	-2351	23251
201	12426	-7568	1934	9724
202	23340	2210	1934	20558
203	14360	-270	2134	12062
204	27053	-555	5236	29996
205	37014	-13559	2519	15139
206	34017	-12270	1662	36614
207	39361	-555	4377	22671
208	27915	-1489	518	44447
209	31652	-18386	-3918	35441
210	29667	-6577	147	51098
211	19985	-4176	-12794	38693
212	9921	2711	-3368	32936
213	9921	-721	-2812	28823
214	9921	1350	-418	21740
215	9921	1350	2146	9393

284	155	156-166	13348	-5565	1152	16953
285	156-167-166	13143	5974	1896	11862	11862
286	156-159-167	20739	-6702	4692	26077	26077
287	159-172-167	13550	3107	2380	12951	12951
288	159-161-172	23947	-11172	2380	32020	32020
289	161-174-172	23828	280	2270	22899	22899
300	161-173-174	37148	-10510	440	43376	43376
301	173-196-174	32760	1881	-4781	32906	32906
302	173-184-186	38088	-6694	-530	42740	42740
303	184-195-186	26286	-1852	-7232	30000	30000
304	184-195-196	27958	-1287	1318	28751	28751
305	195-201-196	28116	2211	-37	27079	27079
306	165-166-177	11804	-768	13082	13082	13082
307	166-178-177	2224	1585	-2564	4864	4864
308	166-157-178	9129	-3514	854	11400	11400
309	167-179-178	7336	4679	1789	7141	7141
310	167-172-179	17556	-3425	4489	21357	21357
311	172-185-179	8006	4697	2958	2642	2642
312	172-174-185	19628	-8349	3557	28628	28628
313	174-187-185	16284	4348	2780	15377	15377
314	174-186-187	29079	-7861	-240	33707	33707
315	186-198-187	25834	4681	-4701	25202	25202
316	186-196-198	31851	-2059	-772	32962	32962
317	196-202-198	23142	2446	-5731	24155	24155
318	196-201-202	22474	-1583	366	23205	23205
319	201-206-202	21174	1569	2113	20760	20760
320	177-178-199	1597	-127	5632	10059	10059
321	178-190-189	-182	2156	3728	6839	6839
322	178-179-190	1684	-5063	-1312	5553	5553
323	179-191-190	1684	1605	2060	3529	3529
324	179-185-191	12224	-2214	4381	15458	15458
325	185-197-191	2457	3066	3840	7221	7221
326	185-187-197	15514	-7349	3971	21358	21358
327	187-199-197	6263	2324	4920	10133	10133
328	187-198-199	22598	-6256	-280	25638	25638
329	188-204-199	17685	6108	17016	17016	17016
330	198-202-204	25454	2073	24519	24519	24519
331	202-207-204	18197	5003	-7229	20678	20678
332	202-206-207	15797	-1111	-954	16464	16464
333	206-210-207	13371	8370	3746	13380	13380
334	189-190-200	-8409	2615	3340	10769	10769
335	190-191-200	3415	-2833	5210	5210	5210
336	191-197-200	4930	-4970	2629	9735	9735
337	197-203-200	-4209	-7878	386	6861	6861
338	187-199-203	7878	-14134	5657	22498	22498
339	199-205-203	10925	-16859	19371	19371	19371
340	199-204-205	1477	-12602	1414	23619	23619
341	204-208-205	686	-16764	-788	16176	16176
342	204-207-208	25140	311	1526	25434	25434
343	207-211-208	10450	5432	-13559	25172	25172
344	207-210-211	19593	-1179	-2437	20635	20635
345	210-214-211	11333	21378	1496	18706	18706
346	205-208-209	1741	-24861	7615	28954	28954
347	208-212-209	-593	-18664	-246	18193	18193
348	208-213-212	3376	-4461	13066	22985	22985
349	208-211-213	15093	19918	-3256	30926	30926
350	211-215-213	1029	42	12613	20871	20871
351	211-214-215	16542	-4732	455	19363	19363
352	214-217-215	10687	11183	-11746	23146	23146
353	212-213-216	1760	-19866	-3317	19894	19894
354	213-215-216	5942	-14572	742	18327	18327
355	215-217-216	8563	-5047	5278	15528	15528
356	217-218-216	12095	1381	2819	12463	12463
357	216-218-219	-19	-2272	0	2263	2263

STRESS CALCULATION TIME (MIN.) = 0.0667

MAXIMUM EFFECTIVE STRESS OCCURS AT ELEMENT 64 61- 71- 63 AND IS EQUAL TO 1.3380E+05 PSI

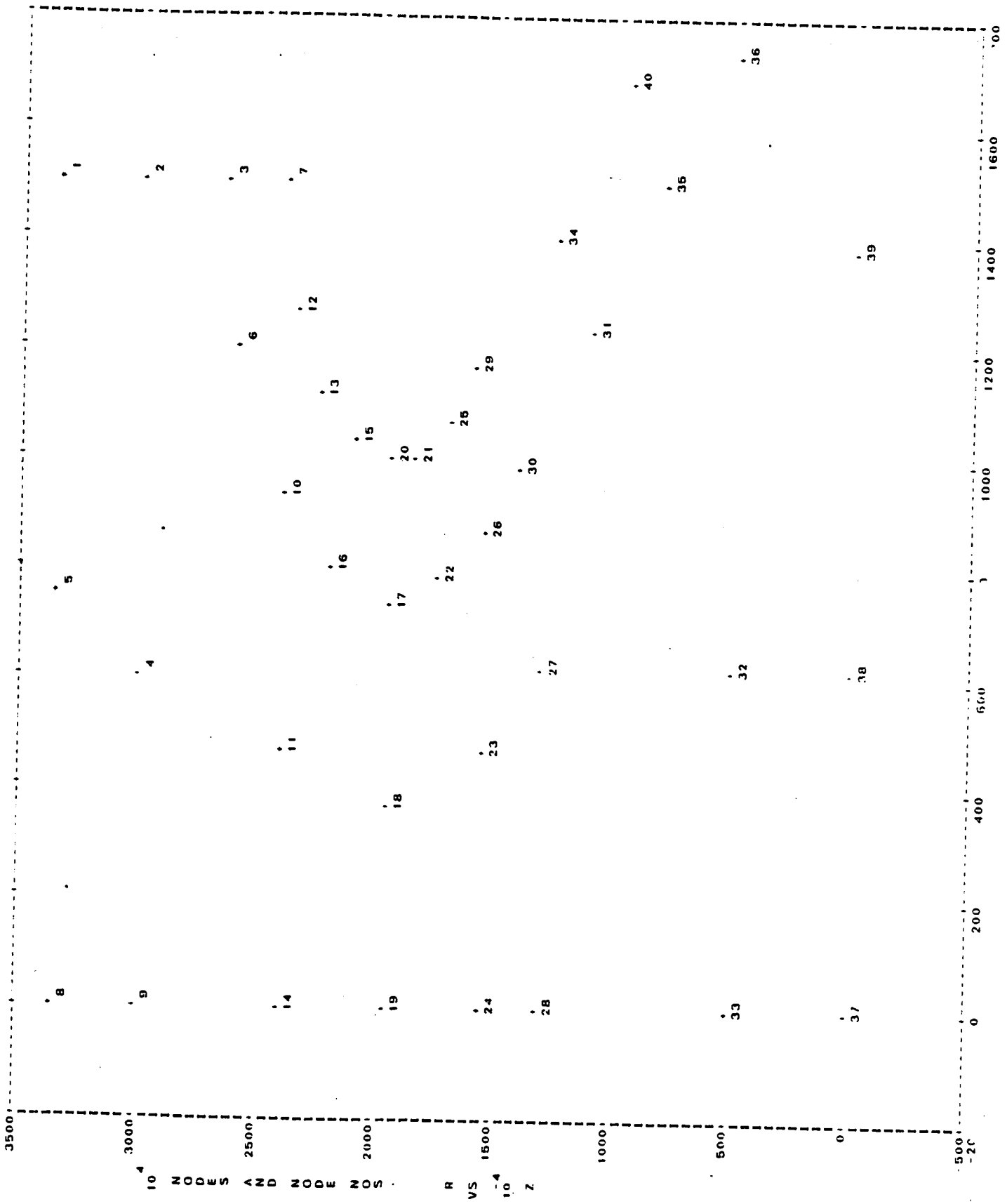
MAXIMUM RADIAL DISPLACEMENT OCCURS AT NODE 200 AND IS EQUAL TO 2.6501E-02 INS.

MAXIMUM AXIAL DISPLACEMENT OCCURS AT NODE 219 AND IS EQUAL TO -1.6941E-02 INS.

AVERAGE STRESSES OF DISK - VOL. AVG. TANG. IS 35625.488 PSI
 AREA AVG. TANG. IS 1248.711 PSI
 AREA AVG. EQUIV. IS 334.590 PSI

*

TOTAL WEIGHT OF BODY IS 2.388 LBS
DIAMETRAL INERTIA ABOUT ORIGIN IS 3.257 LB-IN²
DIAMETRAL INERTIA ABOUT CENTROID IS 2.006 LB-IN²
POLAR INERTIA OF BODY IS 3.255 LB IN²
CENTROID OF BODY FROM ORIGIN IS 0.7235 IN.





DISPLACEMENTS AND REDUNDANT LOADS

NODE	RADIAL DISP.	AXIAL DISP.	RADIAL LOAD	AXIAL LOAD
1	0.506701E-02	0.172208E-02	0.258700D-04	0.275196D+03
2	0.452590E-02	0.177064E-02	-0.225780D-01	0.425275D+03
3	0.400837E-02	0.181706E-02		
4	0.433535E-02	0.700942E-03		
5	0.487915E-02	0.834167E-03		
6	0.336804E-02	0.144954E-02		
7	0.368560E-02	0.186439E-02		
8	0.490382E-02	0.0		
9	0.435152E-02	0.115990E-02		
10	0.352166E-02	0.571636E-03		
11	0.347484E-02	0.155491E-02		
12	0.355783E-02	0.138485E-02	0.208126D-01	-0.434457D+03
13	0.329874E-02	0.0		
14	0.349318E-02	0.129577E-02		
15	0.301412E-02	0.100133E-02		
16	0.317374E-02	0.930718E-03		
17	0.277195E-02	0.460714E-03		
18	0.280631E-02	0.0	0.168209D-02	-0.362173D+03
19	0.292919E-02	0.122696E-02		
20	0.274507E-02	0.122128E-02		
21	0.250384E-02	0.122128E-02		
22	0.245899E-02	0.938858E-03		
23	0.221006E-02	0.525005E-03		
24	0.223817E-02	0.0	-0.137290D-02	0.742165D+03
25	0.219662E-02	0.123343E-02		
26	0.209910E-02	0.956461E-03		
27	0.174655E-02	0.645045E-03	0.154304D-02	0.232650D+04
28	0.183337E-02	0.0		
29	0.187924E-02	0.121129E-02		
30	0.179685E-02	0.100957E-02		
31	0.125344E-02	0.124979E-02		
32	0.613755E-03	0.623410E-03		
33	0.689326E-03	0.0		
34	0.135213E-02	0.143497E-02	-0.258191D-02	0.403891D+04
35	0.787013E-03	0.157122E-02		
36	0.344704E-03	0.191513E-02		
37	0.0	0.0	0.239958D-02	0.223464D+04
38	0.616953E-04	0.61388E-03		
39	-0.210753E-03	0.146451E-02		
40	0.888009E-03	0.175262E-02		

REDUNDANT LOAD CALC. TIME (MIN.) = 0.0

sk

ELEMENT STRESSES

ELEMENT	STRESS-Y	STRESS-X	STRESS-XY	EFF. STRESS
1	45907	-4092	6282	49300
2	23681	-11507	10078	35642
3	45333	-19980	-10032	50697
4	31585	-6589	-2142	55300
5	34696	3640	11698	38747
6	42002	-5264	9783	47959
7	56901	-2132	12590	61969
8	38665	1381	1960	38160
9	41586	6621	-6835	48582
10	14261	-608	7252	41782
11	21242	6340	11282	19240
12	39001	21436	11308	27210
13	47947	-1797	33959	68274
14	102014	24322	13323	54044
15	73329	15693	38723	111133
16	69570	10392	6	66878
17	64582	10392	2829	64212
18	43675	14775	5071	59350
19	40067	12128	-6846	40811
20	67138	5342	-3327	38120
21	143674	19008	2845	60141
22	157740	15081	9840	137816
23	51497	19298	-6051	149399
24	67859	2116	-11754	54423
25	38465	19381	10702	63114
26	43790	568	-1636	38289
27	148442	6973	4524	142762
28	46902	16507	-8989	60275
29	75664	-13121	1472	48092
30	36842	-23319	9272	92415
31	111271	16575	-31316	81869
32	19498	-60876	84122	75947
33	79631	-80267	-33630	77182
34	36321	-55972	-38835	81142
35	52237	-35123	-41810	68614
36	272814	32814	-35765	59727
37	29661	-18730	-28181	83513
38	18624	-51535	-31771	59385
39	16309	-56168	-8027	66676
40	22348	50146	-9689	59332
41	35458	-55354	-54143	55530
42	35458	-39792	-6422	41839
43	38478	-34392	-14055	33831
44	-24858	-32605	-13468	35192
45	4788	-36565	-4857	
46	21439	-60677	-46339	
47	24282	-41200	-37777	
48	25181	-48142	81869	
49	5179	-54143	84122	
50	-2080	-59494	75947	
51	6211	-30168	77182	
52	6211	-27030	81142	
53	36208	4716	-35765	

STRESS CALCULATION TIME (MIN.) = 0.0167

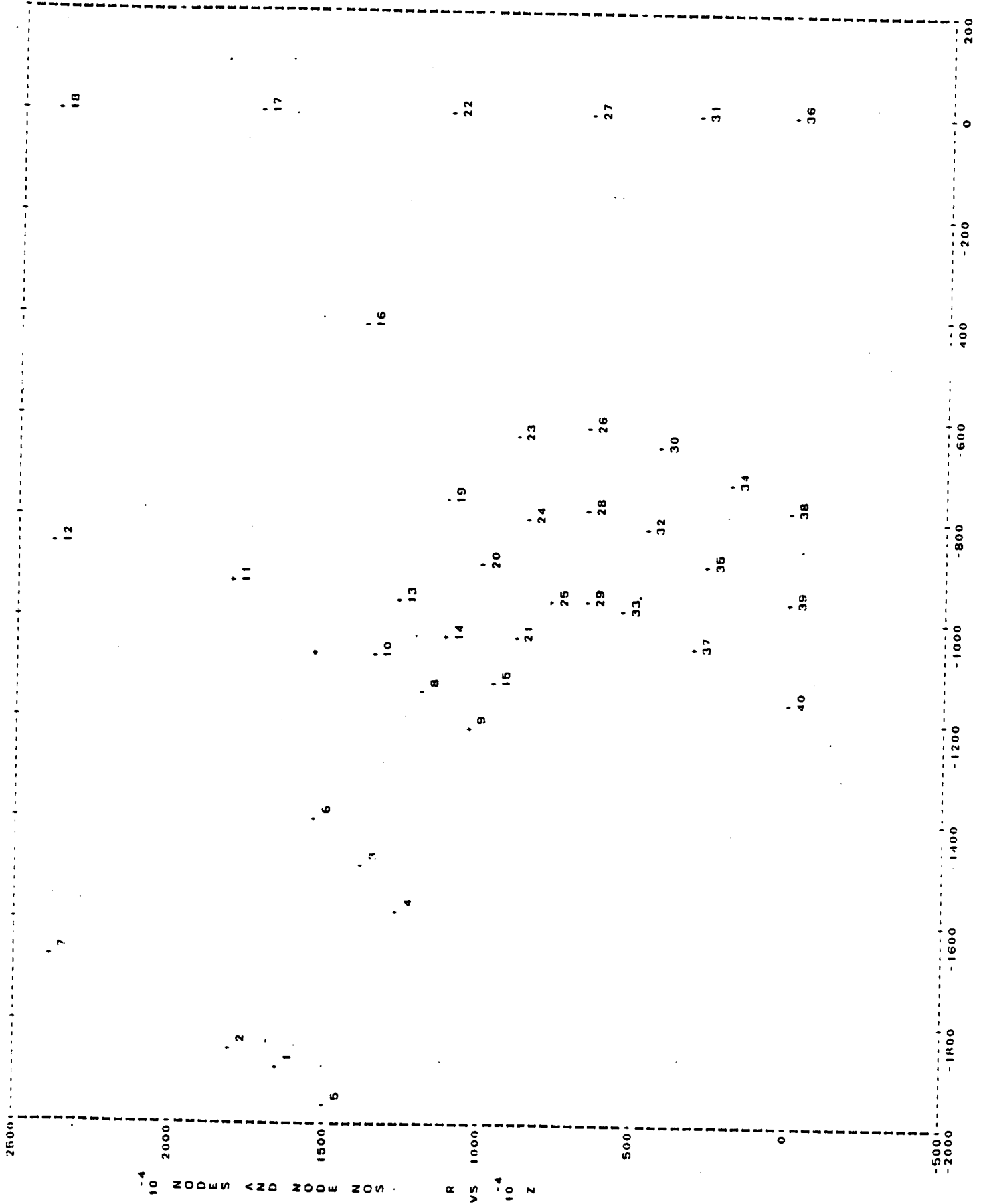
MAXIMUM EFFECTIVE STRESS OCCURS AT ELEMENT 32 -29 -26 -25 AND IS EQUAL TO 1.5124E+05 PSI
 MAXIMUM RADIAL DISPLACEMENT OCCURS AT NODE 1 AND IS EQUAL TO 5.0670E-03 INS.
 MAXIMUM AXIAL DISPLACEMENT OCCURS AT NODE 36 AND IS EQUAL TO 1.9151E-03 INS.

AVERAGE STRESSES OF DISK - VOL. AVG. TANG. IS 0.0 PSI
 AREA AVG. TANG. IS 0.0 PSI
 AREA AVG. EQUIV. IS 0.0 PSI

TOTAL WEIGHT OF BODY IS 0.0 LBS

*

DIAMETRAL INERTIA ABOUT ORIGIN IS	0.0	LB-IN**2
DIAMETRAL INERTIA ABOUT CENTROID IS	0.0	LB-IN**2
POLAR INERTIA OF BODY IS	0.0	LB-IN**2
CENTROID OF BODY FROM ORIGIN IS	0.0	IN.



10⁻⁴ NODES AND NODE NOS

R VS Z

*

DISPLACEMENTS AND REDUNDANT LOADS

NODE	RADIAL DISP.	AXIAL DISP.	RADIAL LOAD	AXIAL LOAD
1	0.363918E-02	-0.180495E-02	-0.968993D-03	-0.446177D+04
2	0.375987E-02	-0.176702E-02	-0.235628D-03	-0.446560D+04
3	0.303641E-02	-0.141004E-02		
4	0.293816E-02	-0.151000E-02		
5	0.352771E-02	-0.185141E-02		
6	0.311960E-02	-0.129276E-02		
7	0.438254E-02	-0.142179E-02		
8	0.246973E-02	-0.109007E-02		
9	0.237355E-02	-0.120281E-02		
10	0.256835E-02	-0.989872E-03		
11	0.309089E-02	-0.768866E-03		
12	0.390440E-02	-0.595313E-03		
13	0.231816E-02	-0.909023E-03		
14	0.218463E-02	-0.103504E-02		
15	0.206263E-02	-0.123778E-02		
16	0.223633E-02	-0.401968E-03		
17	0.263415E-02	0.0		
18	0.364459E-02	0.0		
19	0.193043E-02	-0.809506E-03		
20	0.183378E-02	-0.978270E-03		
21	0.178779E-02	0.119037E-02		
22	0.168465E-02	0.0		
23	0.146135E-02	-0.752714E-03		
24	0.145211E-02	-0.951689E-03		
25	0.145783E-02	-0.118083E-02		
26	0.109368E-02	-0.767001E-03		
27	0.102905E-02	0.0		
28	0.114412E-02	-0.980117E-03		
29	0.117701E-02	-0.115556E-02		
30	0.702476E-03	0.809016E-03		
31	0.475702E-03	0.0		
32	0.820862E-03	-0.998649E-03		
33	0.919713E-03	-0.118471E-02		
34	0.335249E-03	-0.867327E-03		
35	0.435081E-03	-0.106480E-02		
36	0.0	0.0		
37	0.472501E-03	-0.126434E-02		
38	0.0	-0.931409E-03		
39	0.0	-0.114809E-02		
40	0.0	-0.137386E-02		
			-0.289813D-02	-0.131571D+04
			0.336791D-02	0.276115D+03
			-0.414839D-02	0.528143D+03
			-0.246017D+04	0.181516D+03
			-0.379063D+04	0.663900D-04
			-0.128577D+04	0.118188D-02
			-0.224424D+03	-0.654497D+03

REDUNDANT LOAD CALC TIME (MIN.) = 0.0

ELEMENT STRESSES

ELEMENT	STRESS-Y	STRESS-X	STRESS-XY	EFF. STRESS
1				
2				
3				
4				
5				
6				
7				
8				
9				
10				
11				
12				
13				
14				
15				
16				
17				
18				
19				
20				
21				
22				
23				
24				
25				
26				
27				
28				
29				
30				
31				
32				
33				
34				
35				
36	63234	5624	-2221	60328
37	60650	-390	-1260	61194
38	60065	-2520	-1784	61443
39	52931	-948	7273	54877
40	45964	546	-1820	45802
41	48578	3829	-1477	46851
42	64803	10096	-6118	61314
43	59512	-2000	-2672	60714
44	70403	6903	-8328	76987
45	64826	1556	6540	65057
46	88106	6470	1312	85086
47	58102	9129	-4358	54642
48	42060	6832	-6121	40506
49	66327	16785	-19516	69955
50	83198	6154	-8855	81752
51	79925	1661	-1932	78178
52	138949	4589	-7099	137263
53	34161	4452	-6121	33865
54	60849	14991	-7022	56241
55	79531	7804	-15425	80497
56	163331	12038	-18575	161346
57	84342	25551	-18438	81432
58	55280	-7258	-3059	59480
59	18993	-42840	-14904	60631
60	41142	929	929	49407
61	58320	-13619	-16181	86193
62	61736	-34015	-15884	79459
63	84922	-17786	-3086	85797
64	85185	-1400	-2831	76168
65	127019	13483	-51023	146081
66	42985	25707	-61023	79459
67	16881	-52783	-15159	146081
68	66228	-54199	-20140	87132
69	67699	-47100	-13072	72576
70	36813	-34497	-7851	101176
71	66001	-66370	-44104	91068
72	67632	-22803	-22184	88688
73	13614	-4093	-56051	119553
74	3145	-84886	-17739	97420
75	670	-68968	-12360	67915
76	23016	-38477	-23170	58694
77	4082	-59331	-56715	119705
78	51512	-58022	-60827	121326
79	18990	-54631	-53258	130254
80	45713	-82934	-74341	149204
81	10600	-114633	-42833	161166
82	20218	-37352	-38751	80052
83	19711	-47628	-45885	89607
84	49308	-49554	-45885	90112
85	31276	-48615	-45611	92944
86	20469	-58106	-39743	85298
87	12170	-48601	-31612	69168
88	34989	-24971	-27535	52367
89	44005	-43678	-39347	79048
90	33636	-52621	-44209	90847
91	60636	-43173	-38577	77509
92		-79303	-54971	119258

STRESS CALCULATION TIME (MIN.) = 0.0167

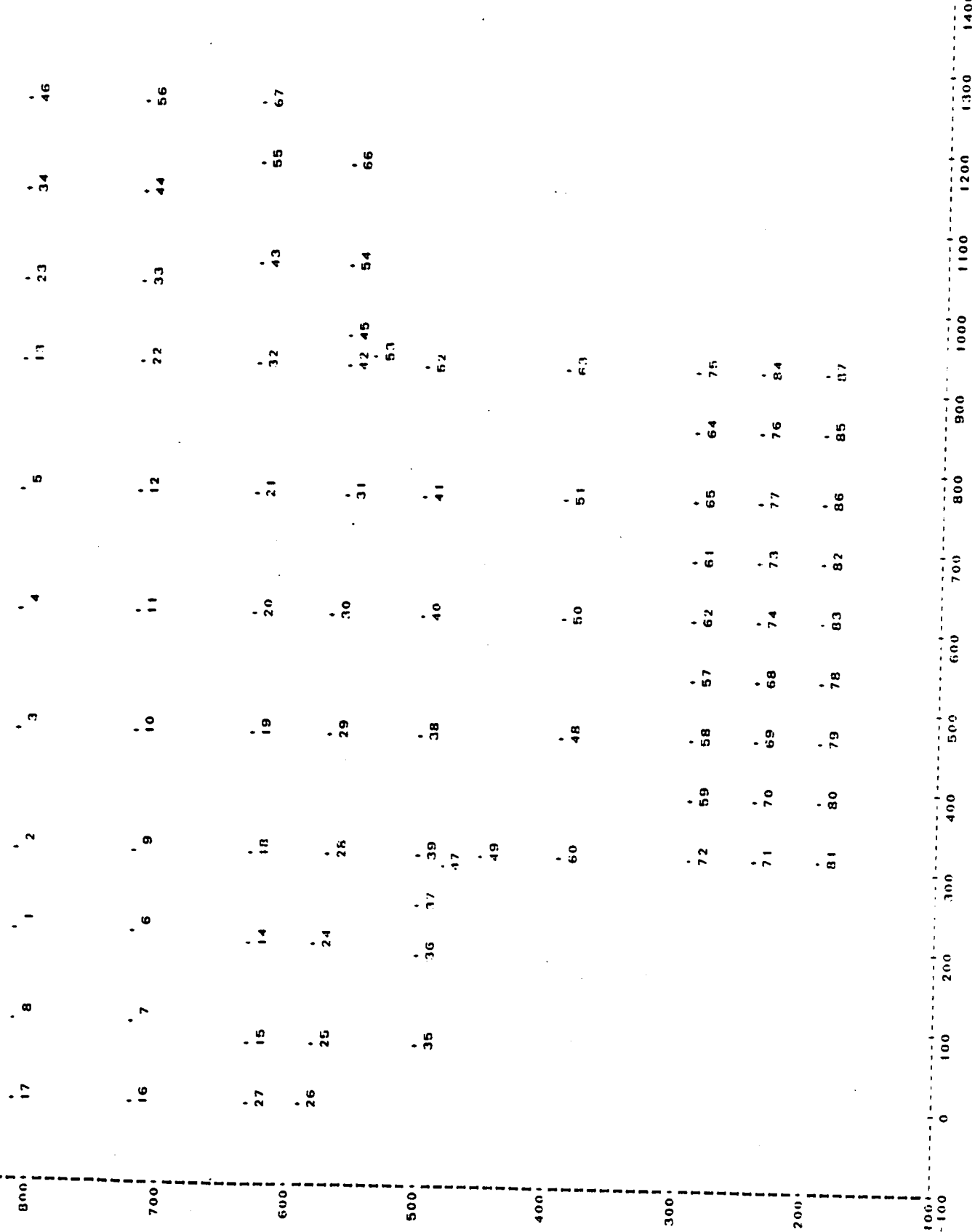
MAXIMUM EFFECTIVE STRESS OCCURS AT ELEMENT 21 -28- -29- -25 AND IS EQUAL TO 1.6135E+05 PSI

MAXIMUM RADIAL DISPLACEMENT OCCURS AT NODE 7 AND IS EQUAL TO 4.3825E-03 INS.

MAXIMUM AXIAL DISPLACEMENT OCCURS AT NODE 5 AND IS EQUAL TO -1.8514E-03 INS.

AVERAGE STRESSES OF DISK - VOL. AVG. TANG. IS 0.0 PSI
 AREA AVG. TANG. IS 0.0 PSI
 AREA AVG. EQUIV. IS 0.0 PSI

TOTAL WEIGHT OF BODY IS 0.0 LBS
DIAMETRAL INERTIA ABOUT ORIGIN IS 0.0 LB-IN**2
DIAMETRAL INERTIA ABOUT CENTROID IS 0.0 LB-IN**2
POLAR INERTIA OF BODY IS 0.0 LB-IN**2
CENTROID OF BODY FROM ORIGIN IS 0.0 IN.



4

DISPLACEMENTS AND REDUNDANT LOADS

NODE	RADIAL DISP.	AXIAL DISP.	RADIAL LOAD	AXIAL LOAD
------	--------------	-------------	-------------	------------

1	0.829528E-02	-0.506498E-02		
2	0.799572E-02	-0.438197E-02		
3	0.773715E-02	-0.388955E-02		
4	0.766766E-02	-0.239389E-02		
5	0.778704E-02	-0.141234E-02		
6	0.746743E-02	-0.629993E-02		
7	0.82124E-02	-0.604085E-02		
8	0.862833E-02	-0.677583E-02		
9	0.715493E-02	-0.455966E-02		
10	0.689947E-02	-0.347381E-02		
11	0.682688E-02	-0.238008E-02		
12	0.691670E-02	-0.128776E-02		
13	0.806913E-02	-0.451767E-03		
14	0.670838E-02	-0.558130E-02		
15	0.711579E-02	-0.644054E-02		
16	0.818817E-02	-0.678131E-02		
17	0.903501E-02	-0.646516E-02		
18	0.632850E-02	-0.471034E-02		
19	0.607955E-02	-0.354446E-02		
20	0.600918E-02	-0.236269E-02		
21	0.609940E-02	-0.117647E-02		
22	0.723272E-02	-0.204956E-03		
23	0.851816E-02	0.238614E-03		
24	0.623991E-02	-0.569892E-02		
25	0.670427E-02	-0.657361E-02		
26	0.707302E-02	-0.713512E-02		
27	0.739986E-02	-0.701598E-02		
28	0.578337E-02	-0.480143E-02		
29	0.522207E-02	-0.358526E-02		
30	0.543243E-02	-0.235667E-02		
31	0.550146E-02	-0.110806E-02		
32	0.640660E-02	0.251844E-04		
33	0.771109E-02	0.566738E-03		
34	0.601291E-02	0.974406E-03		
35	0.608151E-02	-0.652455E-02		
36	0.568167E-02	-0.593219E-02		
37	0.538924E-02	-0.537924E-02		
38	0.492183E-02	-0.362480E-02		
39	0.515568E-02	-0.428068E-02		
40	0.486583E-02	-0.235736E-02		
41	0.495714E-02	-0.108836E-02		
42	0.577562E-02	0.163931E-03		
43	0.704921E-02	0.103407E-02		
44	0.824178E-02	0.137193E-02		
45	0.602116E-02	0.580681E-03		
46	0.952238E-02	0.174443E-02		
47	0.508228E-02	-0.501512E-02		
48	0.395593E-02	-0.361935E-02		
49	0.467922E-02	-0.486261E-02		
50	0.390944E-02	-0.235584E-02		
51	0.397820E-02	-0.111122E-02		
52	0.518333E-02	0.125578E-03		
53	0.565719E-02	0.270252E-03		
54	0.648921E-02	0.129317E-02		
55	0.772131E-02	0.202076E-02		
56	0.879015E-02	0.215288E-02		
57	0.306589E-02	-0.297931E-02		
58	0.308658E-02	-0.358576E-02		
59	0.311883E-02	-0.418154E-02		
60	0.409189E-02	-0.478842E-02		
61	0.307126E-02	-0.174596E-02		
62	0.305462E-02	-0.236211E-02		
63	0.409185E-02	0.207286E-04		
64	0.312495E-02	-0.561263E-03		
65	0.309761E-02	-0.114793E-02		
66	0.720458E-02	0.234766E-02		
67	0.807055E-02	0.252306E-02		
68	0.264977E-02	-0.297455E-02		
69	0.265800E-02	-0.357774E-02		
70	0.269332E-02	-0.416548E-02		
71	0.270092E-02	-0.473041E-02		
72	0.314206E-02	-0.473305E-02		
73	0.265164E-02	-0.176070E-02		
74	0.264120E-02	-0.236128E-02		
75	0.315231E-02	-0.731810E-05		
76	0.269860E-02	0.571469E-03		
77	0.267675E-02	-0.116236E-02		

78 0.226228E-02
 79 0.237780E-02
 80 0.239855E-02
 81 0.239678E-02
 82 0.226592E-02
 83 0.225509E-02
 84 0.272415E-02
 85 0.230528E-02
 86 0.228587E-02
 87 0.233650E-02

-0.297554E-02
 -0.357934E-02
 -0.416308E-02
 -0.472704E-02
 -0.174656E-02
 -0.235977E-02
 -0.795899E-06
 -0.566844E-03
 -0.114809E-02
 0.0

0.494406D+01

-0.13762D-02

REDUNDANT LOAD CALC. TIME (MIN.)= 0.0

ELEMENT STRESSES

ELEMENT	STRESS-R	STRESS-Z	STRESS-Q	STRESS-RZ	EFF. STRESS
87-85-84	8012	3680	89190	2406	82723
84-85-76	8004	1149	78544	2333	75644
35-86-76	14581	9902	69416	1559	77331
76-86-77	8310	4603	78667	1838	71557
86-82-77	14777	15371	88652	1599	73634
77-82-73	7906	19567	76815	2116	68201
82-82-73	14192	19724	87604	568	70818
73-82-74	8225	19724	87604	1279	65667
83-78-74	13207	20006	86741	-1197	70415
74-78-68	9728	18367	77490	-889	65147
78-79-68	12609	18367	86577	-1766	72476
68-79-68	10562	12615	78498	-1992	67025
79-80-60	11839	9047	86524	-2308	76199
69-80-70	11839	8501	80124	-3656	70181
80-81-70	17103	2667	86512	-240	79488
71-71-71	12269	1809	80085	-1609	72726
04-76-75	25724	3166	75207	3745	64091
19952	19952	-4322	74800	4713	63014
76-76-64	26498	7187	73168	4396	69502
64-77-65	21095	13461	67933	4718	55650
77-73-65	24545	7187	73168	3862	55419
65-73-61	19713	9918	65986	4233	52307
73-74-61	23615	16986	71937	2480	52134
61-74-62	19337	15727	65916	1939	48623
74-68-62	20914	15670	70343	-1240	51779
62-68-57	21421	1623	67056	-2338	48152
69-69-57	21544	13623	70876	-3215	54023
57-69-58	21915	13875	67782	-4150	50883
69-70-58	21472	18715	71468	-4735	58032
70-71-59	25972	12556	70990	-7161	54450
71-59-72	23078	1882	72018	4047	62699
59-71-72	29190	-1380	69697	3431	62043
51-52	60911	12048	69032	16331	59863
52-51-41	31139	13077	55336	16292	46317
51-50-41	32272	18080	54110	6335	33297
41-50-40	25437	18263	48225	5624	28796
50-48-40	25881	18013	49954	-3064	29309
40-48-38	22313	19278	49591	-4006	27838
63-64-63	45475	4504	70368	6147	58582
64-65-61	34558	2287	60748	8706	52916
65-61-51	29325	7941	62215	6977	48874
61-51-50	29407	12159	62502	6852	45674
61-62-50	23770	18558	5530	5530	37099
62-57-50	23688	14777	58336	2702	40107
50-57-48	28879	15161	58348	-820	39580
57-58-48	27910	21572	58653	-3728	34662
58-58-48	26681	13678	61132	-5838	43376
59-60-48	35951	9759	60955	7303	46916
59-60-48	48239	9370	62641	-1071	49734
36-35-24	5406	4674	70828	8247	69972
24-35-25	9781	12743	79339	-7485	71736
35-26-25	10705	8972	81152	-5411	72392
42-41-42	64222	3521	89605	4803	83227
41-40-31	27918	20778	73757	20439	53615
41-40-30	24894	17438	52891	15626	39811
40-38-30	21791	11617	48019	2724	26110
30-38-29	23819	16851	40851	5828	27617
38-28-29	26192	1615	43211	-3429	24973
66-55-67	27630	10297	42206	1382	27739
66-54-55	4196	10218	47243	-9441	36010
55-54-43	7079	520	105511	3069	103208
32-31-32	2637	14226	100448	5674	90548
31-30-21	24028	25480	81896	7864	80153
21-30-20	26093	4453	59751	-352	29901
30-29-20	20321	12904	43686	10479	38223
20-29-19	23034	27	42120	4797	25920
29-28-19	21260	8196	34522	5144	31158
19-28-18	27546	-1248	38389	-144	27633
28-24-18	29727	9582	35046	840	31893
18-24-14	38716	45155	46171	-893	34375
24-25-14	17227	15345	62823	-1100	38691
14-25-15	26812	-430	55945	-1977	53520
25-26-15	15930	11068	74737	-11201	63487
26-15	20748	1380	72257	-14704	62834
25-26-15	20748	3631	85691	-8473	66459
25-26-15	20748	3631	85691	-8839	76380

77	15-26-27	17367	-1444	84644	-5504	78975
78	67-55-56	21970	6200	106962	8423	95007
79	55-43-55	15768	10673	93543	7064	81373
80	56-43-44	18695	-3747	83440	15767	83040
81	43-32-44	9373	70866	70866	9006	59065
82	43-32-33	-3534	63422	63422	18223	66621
83	32-22-33	20184	-12428	51009	17229	63300
84	32-21-22	36103	10357	51292	-5217	36964
85	22-21-12	19435	-18657	32912	7396	48066
86	21-20-12	27281	2987	37426	-6841	32865
87	12-20-11	17020	-19951	25810	3806	42578
88	20-19-11	25640	-18977	34639	-6294	33035
89	11-19-10	18331	-348	27140	3004	42725
90	19-18-10	27226	-15520	40156	-8116	38612
91	10-18-9	24093	-4731	36873	-9	47319
92	18-14-9	35672	-12667	55198	-15664	51761
93	9-14-6	19294	4731	47734	-7946	54120
94	14-15-6	32370	6135	68245	-13315	54120
95	6-15-7	23511	-6410	63845	-8095	59473
96	15-16-7	29574	-1064	75968	-9304	62656
97	15-27-16	34222	4108	86292	-9072	69084
98	56-44-46	43358	8473	86292	4296	73713
99	46-44-34	25107	-6045	80866	8181	79893
100	44-33-34	24223	2820	72094	3918	76909
101	34-33-23	24168	-1946	59164	8191	64440
102	33-22-23	23000	-13848	51770	6759	69854
103	23-22-13	20421	-37602	37458	12881	58215
104	22-12-13	27910	-14254	39100	-6443	71720
105	13-12-5	15581	-42846	22927	6368	50000
106	12-11-5	25698	-16129	29891	-7647	63398
107	5-11-4	14700	-41176	17917	4160	46018
108	11-10-4	25270	-16457	28471	-6052	58004
109	4-10-3	15145	-38366	19455	-2774	53099
110	10-9-3	23974	-16500	32234	61260	61260
111	3-9-2	19710	-34721	28184	-7074	47687
112	9-6-2	31031	-8558	46692	2682	56372
113	2-6-1	21500	-28122	40020	-10094	59292
114	1-7-8	34479	-4520	54764	-2774	61260
115	1-7-8	33062	-16302	54764	-2678	57244
116	7-16-8	1247	71527	71527	-5829	61896
117	8-16-17	6791	77542	77542	-5926	63854
118	5-15-43	15195	46904	86176	1457	75220
119	45-32-43	31228	12114	68670	20253	60950
120	45-32-32	54372	55254	81063	32266	60950
121	53-42-45	77666	66165	94136	61188	61751
122	52-42-53	74753	48584	84798	108748	108748
123	48-60-49	50561	18738	70300	60294	109314
124	48-49-38	16821	16821	54853	-20622	59130
125	49-39-38	56580	31693	64853	-12862	59130
126	49-47-39	67195	62056	69041	40322	40322
127	47-37-39	45367	83939	83939	-18026	45382
128	39-37-28	50500	48149	79458	-60796	92221
129	37-24-28	23180	49277	78072	-44913	84423
130	37-24-24	14323	11226	63079	-29217	57934
131	38-39-28	36681	39064	78920	-15928	54527
			22811	58418	-18876	65238
					-3859	32044

STRESS CALCULATION TIME (MIN.) = 0.0333

MAXIMUM EFFECTIVE STRESS OCCURS AT ELEMENT 122 52-42-53 AND IS EQUAL TO 1.0931E+05 PSI

MAXIMUM RADIAL DISPLACEMENT OCCURS AT NODE 46 AND IS EQUAL TO 9.5924E-03 INS.

MAXIMUM AXIAL DISPLACEMENT OCCURS AT NODE 26 AND IS EQUAL TO -7.1351E-03 INS.

AVERAGE STRESSES OF DIK VOL. AVG. TANG. IS 54967.166 PSI
 AREA AVG. TANG. IS 57492.172 PSI
 AREA AVG. EQUIV. IS 52473.430 PSI

TOTAL WEIGHT OF BODY IS 0.650 LBS

DIAMETRAL INERTIA ABOUT ORIGIN IS 0.372 LB-IN**2

DIAMETRAL INERTIA ABOUT CENTROID IS 0.169 LB-IN**2

POLAR INERTIA OF BODY IS 0.219 LB-IN²
CENTROID OF BODY FROM ORIGIN IS 0.6092 IN.

APPENDIX B

ENGINEERING REPORT

**2800 F R.T.I. NASA COOLED RADIAL TURBINE ROTOR HEAT
TRANSFER AND AERODYNAMICS DESIGN STATUS REPORT**


Engineering Report

2800⁰F R.I.T. NASA COOLED RADIAL TURBINE ROTOR
HEAT TRANSFER AND AERODYNAMICS DESIGN STATUS REPORT

REPORT T-5500


ISSUED 5/8/81

PREPARED BY


N. Anderson, Advanced Analysis

G. Aigret, Advanced Analysis

APPROVED BY


R. G. Mills, Vice President
Research & Advanced Development

PRECEDING PAGE BLANK NOT FILMED

CUSTOMER REF NAS 3-22513
SOLAR REF SO 6-4938-7
COPY NO

**SOLAR TURBINES
INCORPORATED**

145

PAGE 144 INTENTIONALLY BLANK

TABLE OF CONTENTS

<u>Section</u>		<u>Page</u>
	NOMENCLATURE	1
I	INTRODUCTION	5
II	CONTRIBUTORS	5
III	FLUID PROPERTIES	6
IV	FLOW PATH DESCRIPTION	6
V	DISCUSSION OF THE AERODYNAMIC DESIGN	8
VI	COOLING SCHEME SELECTION	9
VII	INTERNAL AERODYNAMICS OF COOLING CIRCUITS	12
	7.1 Analytical Coolant Flow Models	12
	7.1.1 Purpose	12
	7.1.2 Major Assumptions	12
	7.1.3 Methods of Analysis	12
	7.1.4 Results	14
	7.2 Experimental Static Cold Flow Models	14
	7.2.1 Purpose	14
	7.2.2 Test Apparatus	14
	7.2.3 Static Flow Models	15
	7.2.4 Test Results	15
	7.3 Prototype Hardware Cold Flow Testing	16
VIII	DETAILED HEAT TRANSFER ANALYSIS	17
	8.1 Gas Side Heat Transfer Coefficients	17
	8.2 Relative Total Gas Temperatures	18
	8.3 Approximate Heat Load on Turbine Wheel	19
	8.4 Film Cooling	20
IX	HEAT TRANSFER MODELS AND RESULTS	21
	9.1 Disc Model	21
	9.2 Blade Model	21
	9.3 Calculated Temperatures	22
X	FINAL DIMENSIONS	23
XI	CLOSING REMARKS	23

TABLE OF CONTENTS (Cont)

FIGURES 1-a Through 31-b

TABLES

APPENDICES

- A ROTOR EXTERNAL FLOW ANALYSIS
- B COOLED RADIAL TURBINES LITERATURE CONSULTED
- C THERMAL ANALYSIS RESULTS FOR DISC
- D THERMAL ANALYSIS RESULTS FOR BLADES
- E LIST OF DRAWINGS

NOTE: There is no Figure 20

NOMENCLATURE

SYMBOLS	UNITS	DEFINITIONS
<u>Stations</u>		
0		Stator entrance
1		Stator exit
2		Rotor entrance
3		Rotor exit
4		Exhaust diffuser exit
T, p	°F, psia	Static values of gas temperature and pressure
T ₀ , P ₀	°F, psia	Total values of gas temperature and pressure
T ₀ , rel	°F	Relative total gas temperature
b	in.	Flow path width
c	ft/s	Absolute velocity
c _p	Btu/lb°F	Constant pressure specific heat
C	-	Film turbulence factor (J.M.)
C _D	-	Discharge coefficient
d	in.	Leading edge diameter
D	in.	Diameter
D _H	in.	Hydraulic diameter
e	in.	Wall thickness
g _c	$\frac{\text{ft} \cdot \text{lb}_m}{\text{lb}_f \cdot \text{s}^2}$	Conversion factor
h	Btu/hft ² F	Heat transfer coefficient
h	Btu/lb	Enthalpy
J	$\frac{\text{ft} \cdot \text{lb}_f}{\text{Btu}}$	Energy conversion factor (778.161)
k	Btu/hftF	Thermal conductivity

NOMENCLATURE (Cont)

SYMBOLS	UNITS	DEFINITIONS
K	-	Total pressure loss factor
L	in.	Flow path length
l	in.	Meridional length
\dot{m}	lb/s	Mass flow rate
m	-	Film blowing parameter
M	lb/lb mole	Molecular mass
N	RPM	Rotation, speed
Nu	-	Nusselt number
N_s	$\left(\frac{\text{ft lb}_m}{\text{lb}_f}\right)^{3/4} \frac{1}{\text{min. s}^{1/2}}$	Specific speed
P	hp	Shaft power
Pr	-	Prandtl number
q''	Btu/hft ²	Heat flux
Q	Btu/s	Heat load
R_n	$\frac{\text{ft} \cdot \text{lb}_f}{\text{lb}_m \cdot R}$	Gas constant
r	in , ft	Current radius
R_p, R_T	-	Ratios defined on page 13
Re	-	Reynolds number
R_2	in.	Rotor tip radius
R.I.T.	°F	Rotor inlet total temperature
s	in.	Film slot height
t	in.	Airfoil normal thickness
u, U_2	ft/s	Tangential wheel speed

NOMENCLATURE (Cont)

SYMBOLS	UNITS	DEFINITIONS
U	$\frac{\text{Btu}}{\text{h.ft}^2.\text{F}}$	Overall heat transfer coefficient
W	ft/s	Relative velocity
x	in.	Distance from film injection point
z	-	Number of blades (z_2) or vanes (z_1)

Greek Symbols

α_2	degree	Rotor flow inlet angle (w.r.t. tang.)
β_3	degree	Blade exit angle (w.r.t. axial)
γ	-	Ratio of specific heats
Δ	-	Difference
η_c	-	Metal cooling effectiveness
η_f	-	Film cooling effectiveness
η	-	Isentr. efficiency
θ	degree	Angular position
λ	-	Work factor
μ	lb/ft.h	Dynamic viscosity
ν	ft ² /h	Kinematic viscosity
ρ	lb/ft ³	Density
ϕ	-	Coolant flow ratio
ω	rad/s	Angular speed

Subscripts

r	Rotor
c	Coolant
f	Film
g	Gas

NOMENCLATURE (Cont)

SYMBOLS	UNITS	DEFINITION
$\left\{ \begin{array}{l} e \\ m \\ i \end{array} \right.$		External
		Metal
		Internal
$\left\{ \begin{array}{l} tt \\ ts \end{array} \right.$		Total-to-total
		Total-to-static
$\left\{ \begin{array}{l} b \\ d \end{array} \right.$		Blading
		Disc
$\left\{ \begin{array}{l} h \\ s \end{array} \right.$		Hub
		Shroud
R.M.S.		Root mean square value
$\left\{ \begin{array}{l} o \\ i \end{array} \right.$		Outer
		Inner
-		Average

I. INTRODUCTION

NASA-Lewis awarded Manufacturing Contract NAS3-22513 (Solar S.O. 6-4938-7) to Solar Turbines International to design and manufacture a high-temperature cooled radial inflow turbine rotor characterized by (Figs. 1-a, 1-b and 2).

- Shaft power: $P = 1000$ hp
- Stator inlet total pressure; $P_{00} = 280$ psia
- Rotor inlet total gas temperature selected: $T_{02} = 2800^{\circ}\text{F}$
(2420°F is the lowest acceptable to NASA)
- Rotor inlet gas flow: $\dot{m}_{g2} \approx 5$ lb/s
- Cooling air available at 280 psia and 950°F
- Primary flow total-total isentropic efficiency: $\eta_{tt} \geq 0.85$
0-3
- Heat transfer promoters in the internal cooling passages for more effective use of the coolant expenditure that should not exceed 1 lb/s for the rotor and the stationary rotor shroud. The stator vanes and associated shrouds are assumed to be made out of ceramic material, i.e., are uncooled.
- Parts designed to be castable
- 1500 hours life.

II. CONTRIBUTORS

NASA Program Manager - H. E. Rohlik

Solar Project Director - A. G. Metcalfe

Solar Project Manager - A. N. Hammer

External Aerodynamic Design - C. Rodgers

Heat Transfer Design and Internal Aerodynamics - G. Aigret and N. Anderson

Configuration and Stress Design - T. P. Psychogios and R. P. Barrow

Mechanical Design - A. W. August and T. P. Psychogios

Manufacturing Engineers - J. R. Woodward and A. N. Hammer

III. FLUID PROPERTIES

The products of combustion at 2800°F of air at 950°F with a liquid fuel such as ASTM-A-1 (H/C = 0.168; L.H.V. = 18,700 Btu/lb_m) result from a fuel-air ratio of f/a = 0.0315. Per NASA TN D-7488 (see App. B for references), the transport properties at 20 atmospheres pressure are:

	γ_g	C_{pg} (Btu/lbF)	μ_g (lb/ft.h)	k_g (Btu/hftF)	Pr_g	M_g (lb/lb mole)
At rotor entrance	1.2699	0.3232	0.1485	0.06870	0.699	28.966
At rotor exit	1.2828	0.3113	0.1345	0.05975	0.702	28.968
Average	1.2751	0.3182	0.1430	0.06483	0.701	28.967

Likewise, per the same source, the coolant properties at pressure are:

	γ_c	C_{pc}	μ_c	k_c	Pr_c
At 950°F (fresh)	1.3537	0.2626	0.0876	0.03266	0.706
At 1500°F (spent)	1.3288	0.2773	0.1076	0.04233	0.705
Average	1.3413	0.2700	0.0976	0.03750	0.705

IV. FLOW PATH DESCRIPTION

After several iterations involving the aerodynamics, heat transfer, applied mechanics, manufacturing and design disciplines, the flow path of Figures 1-a, 1-b, and 2 and shown on the drawings listed in Appendix E was found to satisfy the design requirements. Main features are:

Stator: O.D.: $D_0 = 9$ inches
 I.D.: $D_1 = 7.4$ inches
 Width: $b_0 = b_1 = 0.29$ inch
 $z_1 = 17$ vanes

Rotor: Tip diameter: $D_2 = 6.5$ inches ($R_2 = 3.25$ inches)
 Inlet blade width: $b_2 = 0.30$ inch
 Exducer O.D.: $D_{3s} = 4.25$ inches
 Exducer I.D.: $D_{3h} = 2.40$ inches
 Exducer $D_{3,RMS} = 3.45$ inches
 $D_2/D_{3,RMS} = 1.88$

$z_2 = 10$ full blades
 $N = 65,000$ RPM
 Tip speed: $U_2 = 1844$ ft/s
 Rotor flow inlet angle: $\alpha_2 = 22.31^\circ$ (w.r.t. tang.)
 Exducer R.M.S. blade exit angle: $\beta_3 = 55^\circ$ (w.r.t. axial)
 Rotor tip leading edge thickness: $t_2 = 0.110$ inch
 Exducer R.M.S. trailing edge thickness: $t_3 = 0.15$ inch
 Mean meridian flow path length: $l_2 = 2.366$ inch
 Solidity factor: $z_2 l_2 / D_2 = 3.64$
 Nozzle hot throat area: 2.2 inch²

Figure 2 also shows the main aerothermodynamic parameters such as pressures and temperatures. These are for an uncooled turbine;

Rotor inlet total temperature: $T_{O2} = 2800^\circ\text{F}$
 Rotor inlet static temperature: $T_2 = 2510^\circ\text{F}$
 Rotor inlet pressure: total: $P_{O2} = 276.1$ psia
 static: $p_2 = 179.3$ psia
 Exhaust gas temperature: $T_{O3} = 2363^\circ\text{F}$
 Enthalpy drop: $\Delta h_0 = 139.0$ Btu/lb
 Exit total pressure: $P_{O3} = 126.1$ psia
 Exit static pressure: $p_3 = 118.8$ psia
 Total-to-total rotor pressure ratio: $P_{O2}/P_{O3} = 2.19$
 Overall total-to-static pressure ratio: $P_{O0}/P_3 = 2.36$
 Gas flow rate: $\dot{m}_{g2} = 4.98$ lb/s

$$\text{Velocity ratio: } \frac{U_2}{C_{\text{spouting, isentrop}}(0-4)} \approx 0.65$$

$$\frac{U_2}{\sqrt{T_{O2}}} = 32.3 \text{ ft/s} \cdot R^{1/2}$$

$$\text{Work factor: } \lambda = \frac{\Delta h_0}{U_2^2} = 1.023$$

$$\text{Rotor Reynolds number: } Re = \frac{\dot{m}_{g2}}{\mu_g R_2} = 4.63 \cdot 10^5$$

$$\text{Flow function: } \frac{\dot{m}_{g2} \sqrt{T_{O2}}}{P_{O2}} = 1.03 \frac{\text{lb} \cdot R^{1/2}}{\text{S} \cdot \text{psia}}$$

Shaft power: $P = 980$ hp (uncooled; no mechanical losses)

$$\text{Specific speed (02-03): } N_s = 64.2 \left(\frac{\text{ft} \cdot \text{lb}_m}{\text{lb}_f} \right)^{3/4} \frac{1}{\text{min} \cdot \text{s}^{1/2}}$$

Reaction: ≈ 0.44

Expected primary flow (uncooled) efficiency (0-3): $\eta_{tt} \approx 0.848$

V. DISCUSSION OF THE AERODYNAMIC DESIGN

The turbine rotor was designed for a low solidity ($z_2 \ell_2 / D_2$) and a small inlet relative width ($b_2 / D_2 = 0.046$) to minimize the blading area to be cooled. The results of initial geometry optimizations at the design conditions are listed below:

Effect of Blade Height b_2 (inch)

b_2	0.25	0.30 [●]	0.35
$\% \Delta \eta_{tt}$	-1.1	0	+0.2
$\% P$	0	0	+0.8

Effect of Blade Number z_2

z_2	8	10 [●]	12	14
$\% \Delta \eta_{tt}$	-1.4	0	0.75	1.3
$\% P$	-0.2	0	0.4	1.0

Effect of Blade Exit Angle β_3 (deg)

β_3	55.0 [●]	60.0	65.0
$\% \Delta \eta_{tt}$	-0.9	0	+0.8
$\% P$	+2.0	0	-3.3

Effect of Hub Diameter D_{3h} (inch)

D_{3h}	2.2	2.4 [●]	2.6
$\% \Delta \eta_{tt}$	-0.3	0	+0.1
$\% P$	+1.0	0	-1.4

Effect of Trailing Edge Thickness t_3 (inch)

t_3	0.06	0.08	0.10	0.15 [●]
$\% \Delta \eta_{tt}$	+0.2	0	-0.2	-0.6
$\% P$	+0.1	0	-0.1	-0.5

● indicates selected parameters

From manufacturing and cooling constraints, the final geometry selected is shown in Figures 1-a and 1-b (see App. E for drawing numbers) and employs ten blades with a relatively large exducer hub diameter to minimize exit blade height. A relatively thick exducer trailing edge (RMS) blade thickness of 0.15 inch is needed to permit trailing edge ejection of the largest rotor cooling flow fraction. Estimated total-to-total primary flow (uncooled) adiabatic efficiency from stator inlet to exducer outlet (i.e., 0-3) is 84.8 percent compared to the design goal of 85 percent.

Design rotational speed is 65,000 RPM; reducing this to 60,000 RPM would reduce the blade stresses by approximately 15 percent at the expense of a 2 percent points reduction in total-to-total efficiency.

Figure 3 shows the velocity triangles. Note a 10-degree positive incidence at the entrance and nearly axial leaving velocities. Figures 4, 5 and 6 give the surface velocity distributions on the blades near the shroud, at mid-passage and near the hub, respectively. The flow path was modified several times to obtain the desirable zero or negative surface pressure gradients at the expected airfoil and hub film injection points. The flow path was further assumed continuous without any flow ejection at the star/exducer blade interface (see Fig. 1-b).

Figure 7 provides the average static pressure distributions necessary to find the sink pressures for coolant ejection. A smooth acceleration is shown along both the shroud and hub. The velocity distribution output listing from external flow program P-229 is included in Appendix A.

VI. COOLING SCHEME SELECTION

Using the formula proposed by J. W. Gauntner in NASA TM 81453, the allowable bulk metal temperature for the blades of an axial turbine using a 1970 material such as Inconel 792 (Mod. 5A) and a 1500-hour life would be 1582°F.

The average blade metal cooling effectiveness, based on a relative total gas temperature of 2600°F and a target bulk average metal temperature of 1500°F, is:

$$\bar{\eta}_c = \frac{2600-1500}{2600-950} = 0.667$$

From the axial turbine cooling experience of Solar, with a blading coolant-to-gas flow ratio of $\phi_{gb} = 0.10$, we expect to achieve for the blading;

$$\bar{\eta}_{cb} = \frac{1}{1 + 0.0641 \phi_{gb}^{-0.8296}} = 0.698$$

This approximation and more detailed calculations (presented later), based on the heat loads on the blading and the hub exposed area lead to the following cooling airflow requirements for the rotor:

For the blading: $\phi_{gb} = 0.10$ or 0.50 lb/s

For the disc hub: $\phi_{gd} = 0.03$ or 0.15 lb/s

Corresponding quantities per blade are 0.05 and 0.015 lb/s, respectively, for a total of $\phi_g = 0.13$ or 0.065 lb/s per blade (Fig. 10).

A double-pass convective scheme in the blade tip region is required to avoid massive tip ejection with resulting poor aerodynamic performances and to

achieve the proper cooling effectiveness; Figure 1-a shows that the net coolant flow area near the blade tip is quite reduced (see also Fig. 11 and Table 1): for a passage gap of 0.050 inch between walls, we have the following passage widths: 0.160 inch for the outflow (Sec. S₆) and 0.070 inch for the inflow (Sec. S₉) channels! Likewise, the feed holes S₂ (Fig. 11) are rapidly choked. Obviously then, the coolant to the exducer portion has to be introduced through the feed holes E₁ near the bore. The limited amount of spent air from the radial blade portion has to be ejected in the form of films on the exducer surfaces (see Fig. 1-b). Disc cooling can be achieved by impingement cooling on the back side of the rim (holes A₁) and subsequent veil cooling from A₂ along the hub surface. Such a film will quickly lose its effectiveness; hence, it is necessary to supply another film on the hub between the blades in the exducer region through slots E₃₂. The advantages of a two-piece rotor now become apparent, both from the aerothermodynamic and manufacturing viewpoints. The bore holes E₁ feed air to the exducer blades through holes E₄ and to the exducer hub through metering slots E₃₁. The spent air from the star portion blades is ejected to film cool the leading edges of the exducer blades (Fig. 1-b). The effect of a possible misalignment of the exducer blades with respect to the star blades is discussed next.

An uncooled two-piece radial inflow turbine of similar construction and dimensions has been tested at Solar (Ref. 27, Fig. 3 of pg. 7) with the following characteristics:

- . Tip diameter: 6.25 inches
- . Exducer maximum O.D.: 4.16 inches
- . Exducer minimum I.D.: 1.00 inch
- . Speed: 56,700 RPM
- . Number of blades: 12

The effect of an exducer blading misalignment with respect to the star blading was systematically investigated for this simplified tandem arrangement (see pgs. 5 and 6 of Ref. 27).

The effects of exducer position on overall turbine efficiency indicated maximum overall turbine efficiency with direct alignment to the star blades and minimum efficiency with maximum misalignment. The efficiency variation from maximum to minimum was almost four percentage points. When the exducer was misaligned a quarter of a pitch against the direction of rotation, the efficiency penalty was less than one percentage point (see Fig. 3 of Ref. 27).

Preferred misalignment is also against the direction of rotation for the cooled turbine presented here, as it will result in more film cooling flow to the suction side of the exducer blades where the heat load is the highest.

Heat transfer promotion is logically obtained by staggered trip strips in the passages of the star blades and by a variable density array of pin fins in the triple-pass convectively cooled passages of the exducer blades. The gap between the internal blade walls is kept everywhere at a constant value of 0.050 inch to ease the casting process. The final flow split is shown in Figure 10. Note that a small percentage of air (1%) is bled at the rotor tip (radius R₂) to protect it by convection in the holes and by some external

filming from the impinging external flow. Special attention has been paid to the thick blade roots cooling: this is achieved by flowing fresh coolant in the root passages (e.g., through orifices S_4 and E_6 [Fig. 11] and outflow along the hub passages S_5 of the star blades) and by cooling the blades by conduction to the impingement - (jets A_1 and E_2) and film-cooled (films A_2 and E_{32}) hub surfaces.

The cooling flow usage can be summarized as follows on a per blade basis (see Fig. 10):

	Area To Be Cooled (in. ²)	Coolant Flow (lb/s)	Specific Coolant Flow (lb/s. in. ²)	Percentage of Gas Flow
<u>Star portion</u>				
Blade (with edges)	1.343	0.015	0.0112	3.0
Hub (net)	1.458	0.010	0.0069	2.0
<u>Exducer portion</u>				
Blade (with edges)	2.310	0.035	0.0152	7.0
Hub (net)	0.930	0.005	0.0054	1.0
Total for Rotor	6.041	0.065	(0.0108)	13.0

It is seen that the largest portion of the spent coolant is ejected at the exducer blade trailing edges ($\approx 5.46\%$): the next most important portion ($\approx 2\%$) is ejected as films on the exducer blade leading edges (Fig. 1-b) in a region of favorable external pressure gradients, as can be seen from Figures 4, 5 and 6.

Some coolant ($\approx 1.54\%$) is ejected in the exducer blade-shroud gap for several reasons:

- To reduce the blade-tip clearance losses where they are most detrimental.
- To partly cool the shroud: as a total of one lb/s was assigned for the rotor and its shroud cooling, there remains 0.35 lb/s for further back cooling of this shroud.
- To completely flow-fill the blade internal cavities (corners).
- To provide core support locations.

The last two reasons also justify the tip leading edge film cooling holes.

The cooling flow ratios mentioned here are referred to the radial turbine total inlet flow of 5 lb/s. The engine inlet flow would be of the order of

6.6 lb/s as the downstream turbine would require about 0.75 lb/s of cooling air. (The mass balance is: $6.6 - 1.0 - 0.75 + 0.15$ fuel flow = 5 lb/s gas flow.) Using the engine inlet air flow as a reference, we get the following ratios for this project:

$$\text{Rotor cooling: } \phi_{c,r} = \frac{0.65}{6.6} \times 100 = 9.85\%$$

$$\text{Rotor and shroud cooling: } \phi_{c,t} = \frac{1.00}{6.6} \times 100 = 15.15\%$$

Again, it is assumed that a ceramic distributor is used.

VII. INTERNAL AERODYNAMICS OF COOLING CIRCUITS

7.1 ANALYTICAL COOLANT FLOW MODELS

7.1.1 Purpose

An analytical model (Fig. 12) of the blade cooling circuits was developed in order to gain a better understanding of the stationary flow models, to predict flow distribution within the rotating cooling circuits, and to predict internal heat transfer coefficients for the heat transfer analysis.

7.1.2 Major Assumptions

The analysis assumed that pre-swirl nozzles would not be used and that the star blade cooling air would be pumped radially outward between the rotor and a stationary shroud from near the exducer inlet port (E_1) to the star blade inlet port (S_2) (see Fig. 11). The analysis superimposed the effects of heat transfer and forced vortex pumping on a conventional compressible flow network of orifices, frictional passages, and turning losses. It was assumed that the cooling air will be available at a total temperature of 950°F and a total pressure of 280 psia.

7.1.3 Methods of Analysis

A block diagram of the cooling circuit model is illustrated in Figure 12.

7.1.3.1 Star Internal Cooling Circuit

The flow characteristics between the turbine wheel and shroud were modeled from graphical data in Reference 34. The analysis assumed a 0.030-inch gap

between the shroud and turbine wheel. This small gap was sized to prevent inflow near the stationary shroud. It was found that a total pressure rise of 10 psi occurred between the inlet to the shroud and the inlet to the star cooling circuit. The core velocity of the fluid was found to be approximately one-half of the turbine wheel velocity when the throughflow effects are included. It was then assumed that the total pressure in the star blade entry port was equal to the static pressure in the gap between the turbine wheel and the shroud.

The frictional effects of the star circuit trip strips were estimated from graphical data presented in Reference 35. The pressure loss at the star tip turn is estimated by applying a loss coefficient of 2.1 to the maximum dynamic head.

The holes (S_4) near the bottom of the partition between the star blade cooling passages and the star blade tip holes (S_{g1} through S_{g4}) were sized using a discharge coefficient of 0.80 applied to the isentropic orifice equation.

Effects of forced vortex pumping were estimated from the following equations:

$$R_p = \left[1 + \frac{\omega^2 (r_0^2 - r_i^2)}{2g_c J C_p T_0} \right]^{\frac{\gamma}{\gamma-1}}$$

$$R_T = \left[1 + \frac{\omega^2 (r_0^2 - r_i^2)}{2g_c J C_p T_0} \right]$$

7.1.3.2 Exducer Internal Cooling Circuit

The exducer cooling circuit analytical model combines the traditional compressible flow elements, the forced vortex pumping, and the heat transfer effects as in the star cooling circuit. A discharge coefficient of 0.8 was applied to the orifice elements (E_6 , E_{24} , E_{15}). The pressure drop due to the pin fin array was estimated from experimental data in reference one (pg 10) expressed as:

$$\Delta p_c = \frac{1}{2} K \cdot \gamma \cdot p \cdot M^2 \quad \text{with } K = 0.605$$

where the Mach number and static pressure are defined at the minimum flow area.

7.1.4 Results

The results of the analytical flow model are illustrated and tabulated in Figure 10 and Table 1, respectively. In summary, cooling passages were sized to provide the following flows per turbine wheel:

Star internal cooling circuit: 0.15 lb/sec
Star hub film cooling: 0.10 lb/sec
Star blade film cooling: 0.05 lb/sec
Exducer blade internal cooling circuit: 0.35 lb/sec
Exducer hub film cooling: 0.05 lb/sec
Exducer shroud cooling: 0.077 lb/sec
Exducer blade film cooling: 0.10 lb/sec

The total flow used for cooling the turbine wheel, neglecting seal leakage, is 0.65 lb/sec which is approximately 10 percent of the total compressor mass flow. This leaves 0.35 lb/sec for additional shroud cooling.

7.2 EXPERIMENTAL STATIC COLD FLOW MODELS

7.2.1 Purpose

One-to-one scale models of the star blade and exducer blade internal cooling passages were fabricated from brass, aluminum and clear plastic. Pieces of steel wire (\varnothing 0.013 in.) were glued with lacquer to form the trip strips. The curvature of the exducer flow passage was removed in order to ease the fabrication. Static cold airflow tests were performed with various combinations of turbulence promoters, tip holes, and internal division schemes until a satisfactory design was achieved.

The flow tests provided a flow function which must be corrected for inlet losses and the effects of forced vortex pumping before applying the results to a design calculation. These flow tests were then used to verify portions of the analytical model of the internal flow network.

Cold air flow tests will also provide a basis for determining the extent of plugging or voidage in the castings.

7.2.2 Test Apparatus

A block diagram of the flow bench is illustrated in Figure 13-a. Figure 13-b is a sample data sheet with the accuracies of each gauge shown. The sonic orifice was not operating under choked conditions for all but the highest flows; consequently, it was disconnected for the tests.

The flow bench as well as each test model was checked for leaks before the tests.

7.2.3 Static Flow Models

Photographs of the flow models are provided in Figures 14, 15, 16 and 17. Upon completion of flow testing, several measurements were made in order to determine differences between the models and the design drawings. These differences are tabulated in Figure 19 for the final flow models. The lack of dimensional accuracy is due to the fact that the models were fabricated before the final design was completed.

Analysis indicates that the star piece flow function is most sensitive to dimension "F" and dimension "C" in Figure 18. Analysis also indicates that the exducer flow function is sensitive to dimension "K" and to the pin density. The results of the flow tests were corrected for dimensional inaccuracies before they were applied to design calculations.

7.2.4 Test Results

7.2.4.1 Final Test Results, Exducer Blade Model

The results of the final test of the exducer passage is illustrated in Figure 21. Results of the analytical model indicate a flow of 0.035 lb/sec per blade at an upstream pressure of 234 psia, a downstream pressure of 120 psia, an upstream temperature of 960°C and a speed of 65,000 RPM (6807 rad/sec). The pressure rise due to forced vortex pumping is calculated from an inlet radius of 1.05 inches and an outlet radius of 1.477 inches by the expression:

$$\Delta P_B = \frac{p_i \cdot \omega^2 \cdot (r_o^2 - r_i^2)}{2g_c R_n T_o} .$$

The resulting pressure rise due to pumping through the exducer is 16 psi. In order to relate the analytical results to the experimental results obtained with a stationary passage, the pressure rise due to pumping is subtracted from the inlet pressure to obtain an equivalent pressure of 218 psia. The resulting analytical flow function per blade is 0.0061 lb_m °R^{1/2} (sec.psia) at a pressure ratio of 1.82. Since the endwall spacing was 0.05 inch in this analytical model and the test piece endwall spacing was measured to be 0.06 inch, the analytical model should yield a flow function that is 0.05/0.06 or 0.833 times the experimental results.

The experimental results from Figure 21 indicate a flow function of 0.0076 lb_m °R^{1/2} (s.piai) at a pressure ratio of 1.82. Multiplying 0.0076 by 0.833 gives a flow function that is 3 percent higher than the analytical model. This is a fortunate occurrence since the discrepancy between the methods is well within the uncertainties of the measurements and the analytical model.

7.2.4.4 Final Test Results, Star Blade Model

The results of the final test of the star passage are illustrated in Figure 21. Results of the analytical model indicate a flow of 0.015 lb/sec/blade at an inlet pressure of 270 psia, an exit pressure of 140 psia, and an inlet temperature of 1410°R. Forced vortex pumping effects are not considered in the star piece since most of the flow exits at the same radius as it enters.

The flow function per blade at design point from the analytical model is $0.0021 \text{ } ^\circ\text{R}^{1/2} \text{ lb}_m/\text{sec}/\text{psia}$ at a pressure ratio of 1.93. The results of the experimental hardware model indicate a flow function of $0.0027 \text{ } ^\circ\text{R}^{1/2} \text{ lb}_m/(\text{s.psia})$ at the same pressure ratio. Correcting the experimental hardware results for dimensional inaccuracies, we obtain a flow function of $0.0025 \text{ } ^\circ\text{R}^{1/2} \text{ lb}_m/\text{sec}/\text{psia}$ at a pressure ratio of 1.93. Consequently, the corrected hardware model results are 19 percent larger than the analytical model results. This is considered quite satisfactory considering the uncertainty in the loss coefficients used in the analytical models.

7.3 PROTOTYPE HARDWARE COLD FLOW TESTING (See Fig. 11)

Number the blades 1 through 10.

- a) Flow with water: to make sure all holes are open

Part	Feedpoint	Plug	Observe
Star Exducer Assembly	S ₂ ; <u>each</u> hole E ₄ ; <u>each</u> hole E ₁ ; <u>all</u> holes S ₂ ; <u>each</u> hole	E ₄	S ₈₁ -S ₈₄ , S ₁₁ -S ₁₄ E ₉₁ -E ₉₄ , E ₁₆ -E ₂₀ Flow at E ₃₂ in each passage Flow around exducer leading edge

- b) Flow with air: at a pressure ratio of 1.4083 or 6 psig plenum

Part	Feedpoint	Plug	Acceptable flow function limits $\left(\frac{\text{lb } ^\circ\text{R}^{1/2}}{\text{s.psia}}\right)$
Star Exducer Assembly	S ₂ ; <u>each</u> hole E ₄ ; <u>each</u> hole E ₁ ; <u>all</u> holes together	E ₄	0.0022 \pm 0.0002 0.0055 \pm 0.0005 To calibrate slots E ₃₁
Assembly	S ₂ ; <u>each</u> hole		0.0022 \pm 0.0002

VIII. DETAILED HEAT TRANSFER ANALYSIS

8.1 GAS SIDE HEAT TRANSFER COEFFICIENTS

The primary aim of this project being to prove the feasibility of manufacturing a highly cooled, high pressure radial inflow turbine rotor, and the literature (see App. B) being relatively sparse on the subject of heat loading of such a turbine, it has been decided to not distinguish between the blading suction and pressure side heat transfer coefficient distributions, but rather to use an average distribution, variable along the mean line, but constant from hub to shroud (see Figs. 9-1, 9-2, 9-3). Likewise, the film cooling heat transfer coefficients were assumed to be those calculated for gas flow only.

a) Flow field in the rotor

The surface velocities were nevertheless duly calculated (see App. A) in five streamsheets during the course of the aerodynamic design and the results are used here to properly assess the static pressure distributions near the film and trailing edge ejection ports. Figures 4, 5 and 6 show the surface velocities in the shroud, mid, and hub streamsheets, respectively. The exducer leading edge and the aft hub film cooling air flows are seen to be injected in regions of constant or accelerating external flow, as they should be.

b) Blading heat transfer coefficients

All the available literature resources (see App. B) and a boundary layer analysis were utilized to generate the distributions of Figures 9-1, 9-2 and 9-3.

Important numbers are listed here:

- Exit Reynolds number based on rotor throat area and mean flow length of $L_2 = 2.8$ inch; $Re_{g,L_2} = 1.814 \cdot 10^6$
- Reynolds number based on mean relative velocity of $\bar{w}_{2-3} = 1009$ ft/s and $L_2 = 2.8$ inch; $Re_g = 0.871 \cdot 10^6$
- Leading edge Reynolds number based on a diameter of $d = t_2 = 0.10$ inch; $Re_{g,t_2} = 23,425$
- Leading edge stagnation h.t.c: $h_{g2} = 1246$ Btu/h.ft².F
- Exit h.t.c.
 - Per Swartwout: $h_{g3} = 743$ Btu/h.ft².F
 - Per Hamed-Baskharone-Tabakoff: $h_{g3} = 647$ Btu/h.ft².F

• Average h.t.c.

- Per flat plate formula: $\bar{h}_{g2-3} = 903 \text{ Btu/h.ft}^2\text{.F}$
- Per Halls plot (axial): $611 \text{ Btu/h.ft}^2\text{.F}$
- Per Russian method 1 (mean velocity; factor of 2 for turbulence): $626 \text{ Btu/h.ft}^2\text{.F}$
- Per Russian method 2 (accounts for RPM): $657 \text{ Btu/h.ft}^2\text{.F}$

The boundary layer analysis (per NASA TND-5681), together with the leading edge classical formula, gives a blading distribution (Fig. 9-1) whose average is $611 \text{ Btu/h.ft}^2\text{.F}$ as obtained from the Halls plot. Figure 9-2 provides the detailed external h.t.c. distribution used on the star blade.

c) Hub surface heat transfer coefficient

The following Russian formula was used:

$$\text{Nu}_{g,L_2} = 0.1 \text{ Re}_{g,L_2}^{0.65} \text{ which yields } \bar{h}_{g,h} = 325 \text{ Btu/h.ft}^2\text{.F}$$

This low value is well justified considering the lower and more constant surface velocities prevailing near the hub (see Fig. 6). Figure 9-3 shows the actual distribution of the star disc hub h.t.c. that has been used.

8.2 RELATIVE TOTAL GAS TEMPERATURE

For an uncooled purely radial inflow turbine, this temperature can be calculated from:

$$T_{o,rel}(r) = \text{R.I.T.} - 3.0416 \cdot 10^{-9} \frac{N^2}{\bar{c}_{pg}} \left[R_2^2 - \frac{r^2}{2} \right] (\text{°F})$$

In our design, however, the flow enters with a 10° positive incidence (see Fig. 3), and it is thus necessary near the tip to use the results of the external flow analysis to calculate:

$$T_{o,rel}(r) = T + 1.997 \cdot 10^{-5} \frac{w^2}{\bar{c}_{pg}} (\text{°F})$$

For the 2800°F R.I.T., we find (see Figs. 2 and 8-a):

at the tip (6.5 inch diameter): $T_{O,rel,2} = 2553^\circ\text{F}$

at the exducer O.D. (4.25 inch diameter): 2455°F

I.D. (2.419 inch diameter): 2395°F

for a rotor average relative total gas temperature of 2490°F (i.e., 310°F below the R.I.T.). To be conservative, we used the full total relative gas temperature distribution of Figure 8-a for the source temperatures to calculate the heat loads at non-film cooled locations, and the adiabatic wall film temperatures (see Figs. 8-b and 8-c) on the film-cooled portions.

8.3 APPROXIMATE HEAT LOAD ON TURBINE WHEEL (See Also Page 11)

Exposed Portion	Net Total Area (in. ²)	Average Gas-Side h.t.c. (Btu/hft ² F)	$[\overline{T_{O,rel}} - \overline{T_m}]^*$ (°F)	Q(Btu/s)	Total Coolant Flow (lb/s)	Coolant Temp. Rise (°F)
Blading Hub Surface (net)	36.53	611.0	900.0	38.750	0.50	287.0
	23.88	325.0	900.0	13.474	0.15	333.0
	60.41			52.224	0.65	
* $\overline{T_{O,rel}} = 2490^\circ\text{F}$ $\overline{T_m} = 1590^\circ\text{F}$ (surface)						

Typical Blading Heat Flux

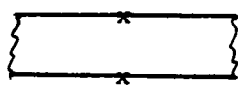
$$\times \overline{T_{O,rel}} = 2490^\circ\text{F}$$

$$\dot{h}_g = 611 \text{ Btu/h.ft}^2.\text{F}$$

IN-792 blade wall

$$T_{me} = 1590^\circ\text{F}$$

$$k_m = 13.5 \frac{\text{Btu}}{\text{hftF}}$$



$$e = 0.025 \text{ to } 0.040 \text{ inch}$$

$$T_{mi}$$

$$h_c$$

Cooling air $\times T_c$

To achieve a wall external temperature of 1590°F with a local gas total relative temperature of 2490°F, the cooling flow must remove a heat flux of:

$$q'' = (2490 - 1590)611 = 549,900 \text{ Btu/h.ft}^2 \text{ and a wall gradient of}$$

$$\frac{\Delta T_m}{\Delta e} = \frac{549,900}{13.5 \cdot 12} = 3,394 \text{ }^\circ\text{F/in. results}$$

The wall thermal differential ($T_{me} - T_{mi}$) amounts to 102, 136, 170 and 204°F for a 0.030, 0.040, 0.050 and 0.060 inch thick wall, respectively! It is thus mandatory to cast the walls as thin as feasible. For example, with the 0.060-inch wall, the internal surface would be at $T_{mi} = 1386^\circ\text{F}$ and with a coolant-side h.t.c. of $h_c = 2000 \text{ Btu/hft}^2\text{F}$, the local coolant temperature T_c must not be higher than 1111°F , i.e., 161°F above the supply temperature. This explains the moderate global coolant temperature rises shown in the last column of the table above.

For the 0.060-inch thick wall, the resistances to heat flow are:

$$\cdot \text{ Gas side: } \frac{1}{h_g} = 0.001637 \frac{\text{hft}^2\text{F}}{\text{Btu}}$$

$$\cdot \text{ Wall: } \frac{e}{k_m} = 0.000370 \frac{\text{hft}^2\text{F}}{\text{Btu}}$$

$$\cdot \text{ Coolant side: } \frac{1}{h_c} = 0.000500 \frac{\text{hft}^2\text{F}}{\text{Btu}}$$

$$\text{for a total of } \frac{1}{U} = 0.002507 \frac{\text{hft}^2\text{F}}{\text{Btu}} \text{ or } U = 398.883 \frac{\text{Btu}}{\text{hft}^2\text{F}}$$

The wall resistance for a thin 0.060-inch wall is clearly of the same order of magnitude as the coolant side resistance. For a thicker wall (say 0.18"), the wall resistance approaches the gas-side one.

8.4 FILM COOLING

This technique is used at four locations (see Figs. 10, 11), namely to protect the hub by injections at points A_2 and E_{32} , to evacuate the spent air out of the star blades through slots S_{11} to S_{14} , thereby film cooling the leading edge of the exducer blades (see Fig. 1-b) and at the blade tip leading edges (holes S_{g1} to S_{g4}). Figures 8-b and 8-c show the adiabatic wall film temperatures versus the distance from the injection points used in the two analytical heat transfer models.

IX. HEAT TRANSFER MODELS AND RESULTS

Two steady-state analytical thermal models were devised: one for a 1/10 pie-shaped segment of the assembled disc (see Fig. 22), and one for the two components (star and exducer) of half a blade (see Fig. 23). The disc model has boundary nodes that simulate one full blade, and the half blade model has boundary nodes that simulate the disc; the two models were run several times until agreement was found at the blade-disc interfaces where the heat leaving the blade walls must equal the heat entering the disc.

9.1 DISC MODEL (Fig. 22; Appendix C)

Characterized as follows:

- Axisymmetric pie-shaped ($\Delta\theta = 360^\circ/10 = 36^\circ$) per Figure 22.
- 359 nodes total, of which 267 are metal nodes
- 632 conductances per network of Appendix C
- Material conductivity of IN-792 per Figure 24.
- Cooling heat transfer coefficients:
 - on back face per Figure 25
 - in holes A (Fig. 22); $\bar{h}_c = 765 \text{ Btu/hft}^2\text{F}$

B	808	"	"
C	449	"	"
D	701	"	"
 - no contact resistance between the two disc parts
 - adiabatic wall film temperatures per Figure 8-b
 - the heat exchange with the blade takes place between each disc surface node and a blade boundary node

9.2 BLADE MODEL (Fig. 23; Appendix D)

Only half a blade was modeled using the external streamwise h.t.c. distribution of Figures 9-1 and 9-2 for both suction and pressure sides, and from hub to shroud. This is realistic as the cooling air, the blade cavity end caps, the webs, the pin fins and the disc altogether tend to equalize the leading and trailing wall metal temperatures. A three-layer model (see Fig. 23) was used for each wall (star and exducer) including the associated edges with the nodes placed on the external and internal surfaces and at mid-wall

thickness, thereby accounting for the full wall resistance to heat flow. In the vicinity of the disc hub, each layer is connected to a single local disc node whose temperature has been iteratively calculated with the disc model. The disc model ($\Delta\theta = 360^\circ/10 = 36^\circ$) concerns one full blade, and each of the hub surface nodes is connected to a single equivalent local blade node (in fact, the mid-wall layer node) through a conductance equivalent to six conductances of the blade model (three layers and two half blades).

Each half blade region is cooled by half of the local cooling air flow. The effect of rotation on the coolant temperature has been neglected.

Figures 26 and 27 show the internal heat transfer coefficients used inside the star and exducer blade passages, respectively. Figure 28 gives the several coolant flow networks used to simulate coolant temperature rise, to calculate mixed flow temperatures,.....

The blade model is characterized by a total of 271 nodes, of which 159 are metal nodes.

9.3 CALCULATED TEMPERATURES

These can be consulted in Appendices C and D for the disc and blading models of Figures 22 and 23, respectively.

A few predicted temperatures are shown in Figure 29 for the two-piece disc and in Figures 30, 31-a and 31-b for the two-piece blade.

Maximum disc temperature has been estimated at 1592°F at node 74 (Fig. 29). The star disc rim is well cooled by backside impingement and film-cooled on the gas-side ($T_2 \sim 1400^\circ\text{F}$).

Maximum blade temperature occurs at node 76 (Fig. 30) where the external wall is at 1825°F and the internal at 1529°F, i.e., a differential of 296°F exists across a wall 0.170 inch thick. The star blade temperature in this attachment region could be reduced by changing the star blade flow split, i.e., by opening the S_4 orifices (see Fig. 11). It is also conceivable to add a radial row of film cooling holes where needed in the attachment region of the star blade.

X. FINAL DIMENSIONS (Figs. 11 and 1-a)

S ₂	10 holes	dia. 0.110	E ₈	0.430 x 0.050
S ₃	10 holes	0.160 x 0.050	E ₁₀	0.275 x 0.050
S ₄	2 holes	dia. 0.026	E ₁₂	0.430 x 0.050
S ₅		0.220 x 0.050	E ₁₃	0.360 x 0.050
S ₆		0.150 x 0.050	E ₆	0.050 x 0.050
S ₇		0.063 x 0.050	E ₁₄	0.260 x 0.050
S ₉		0.070 x 0.050	E ₂₄	dia. 0.050
S _{81-S₈₄}	4 holes	dia. 0.0235	E ₁₅	dia. 0.050
S ₁₀		0.160 x 0.050	E ₂₀	0.15 x 0.050
S ₁₁		0.080 x 0.050	E ₁₉	0.14 x 0.050
S ₁₂		0.125 x 0.050	E ₁₈	0.15 x 0.050
S ₁₃		0.100 x 0.050	E ₁₇	0.14 x 0.050
S ₁₄		0.095 x 0.050	E ₁₆	0.125 x 0.050
E _{1-E₂}	10 holes	dia. 0.160	E _{91-E₉₄}	2 holes dia. 0.050
E ₃₁	10 slots	0.037 x 0.0625	Trip strips:	height 0.010
E ₃₂		gap 0.025		spacing 0.100
E ₄		dia. 0.160	88 pin fins:	dia. 0.025
E ₅		0.325 x 0.050	Tip thickness:	t ₂ = 0.110

XI. CLOSING REMARKS

Every attempt has been made in this design to flow fresh cooling air in the highly stressed attachment region of the blades. This is the case (Fig. 11) for the passages S₅-S₆, S₄-S₁₄, and E₆. Highest calculated metal temperatures occur in the star piece in the S₁₄ region where the blade roots are quite thick; note that the S₄ holes could be opened and that a larger number of the E₃₁ slots could be used to improve the cooling effectiveness in that region. Airfoil film-cooling could also be considered by means of a radial row of film holes drilled in the S₄-S₁₄ region.

The present design achieves a minimum blading external wall cooling effectiveness (Fig. 30) based on the entrance relative total gas temperature of;

$$\eta_{b,e} = \frac{2553-1825}{2553-950} = 0.454$$

which could be improved, as explained above.

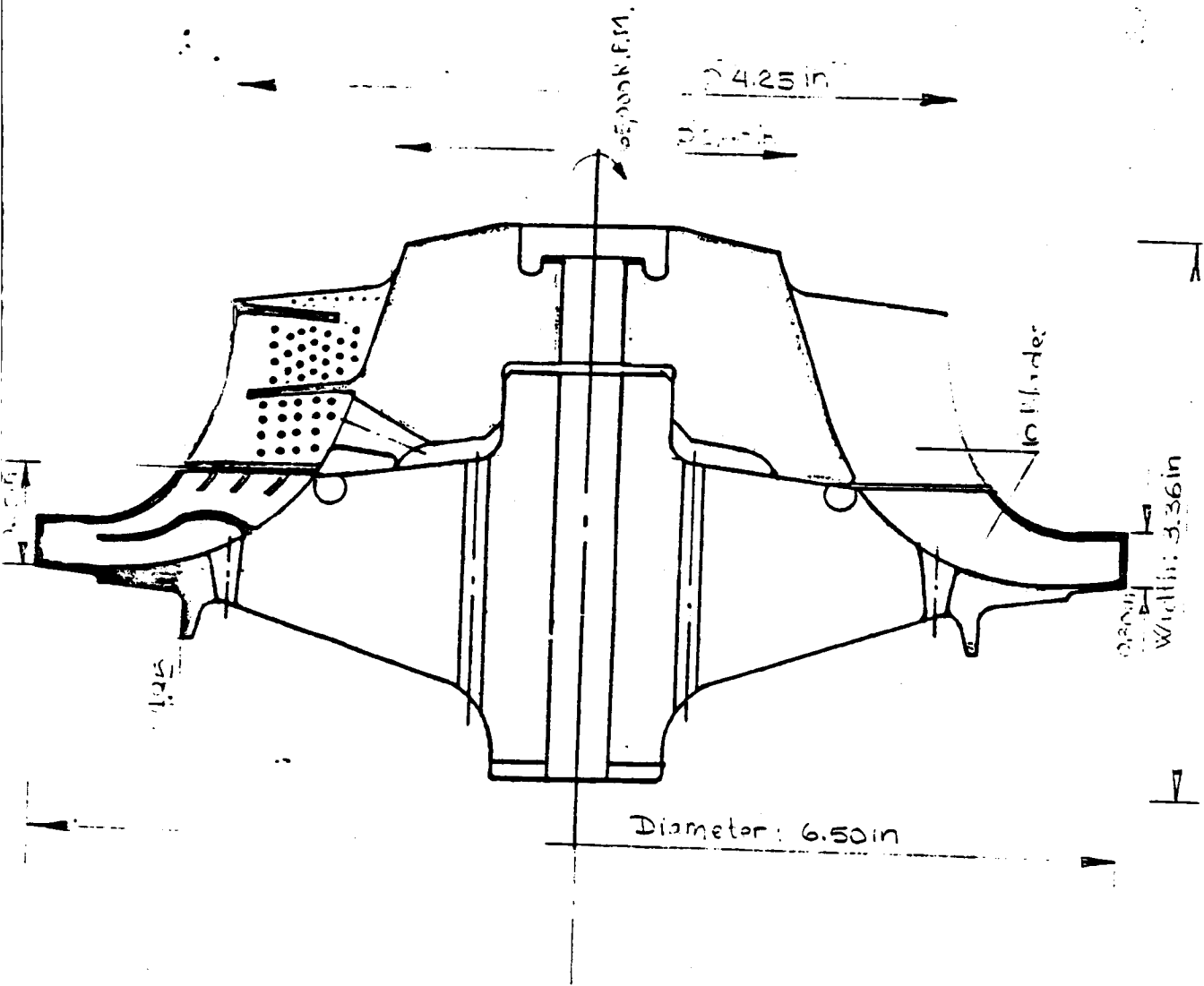
Another approach would be to run the rotor at 2200°F relative total temperature, i.e., at 2450°F R.I.T. (minimum NASA goal being 2420°F), with the maximum blading temperature left below 1630°F for longer life; the minimum cooling effectiveness would still be:

$$\eta_{b,e} = \frac{2200-1630}{2200-950} = 0.456$$

The aerodynamic penalties associated with coolant flow reinjection have been estimated to be 3.4 percentage points which would reduce the total-total isentropic efficiency η_{tt0-3} from 0.848 for the uncooled turbine to 0.814 for the cooled turbine.

A logical extension of this program would, of course, be to measure the performances of this cooled rotor and to compare them to those of the uncooled version.

ORIGINAL PAGE IS
OF POOR QUALITY



ORIGINAL PAGE IS
OF POOR QUALITY

Full size photo of the M14 engine cooled piston and ring assembly. Part number 516/s.

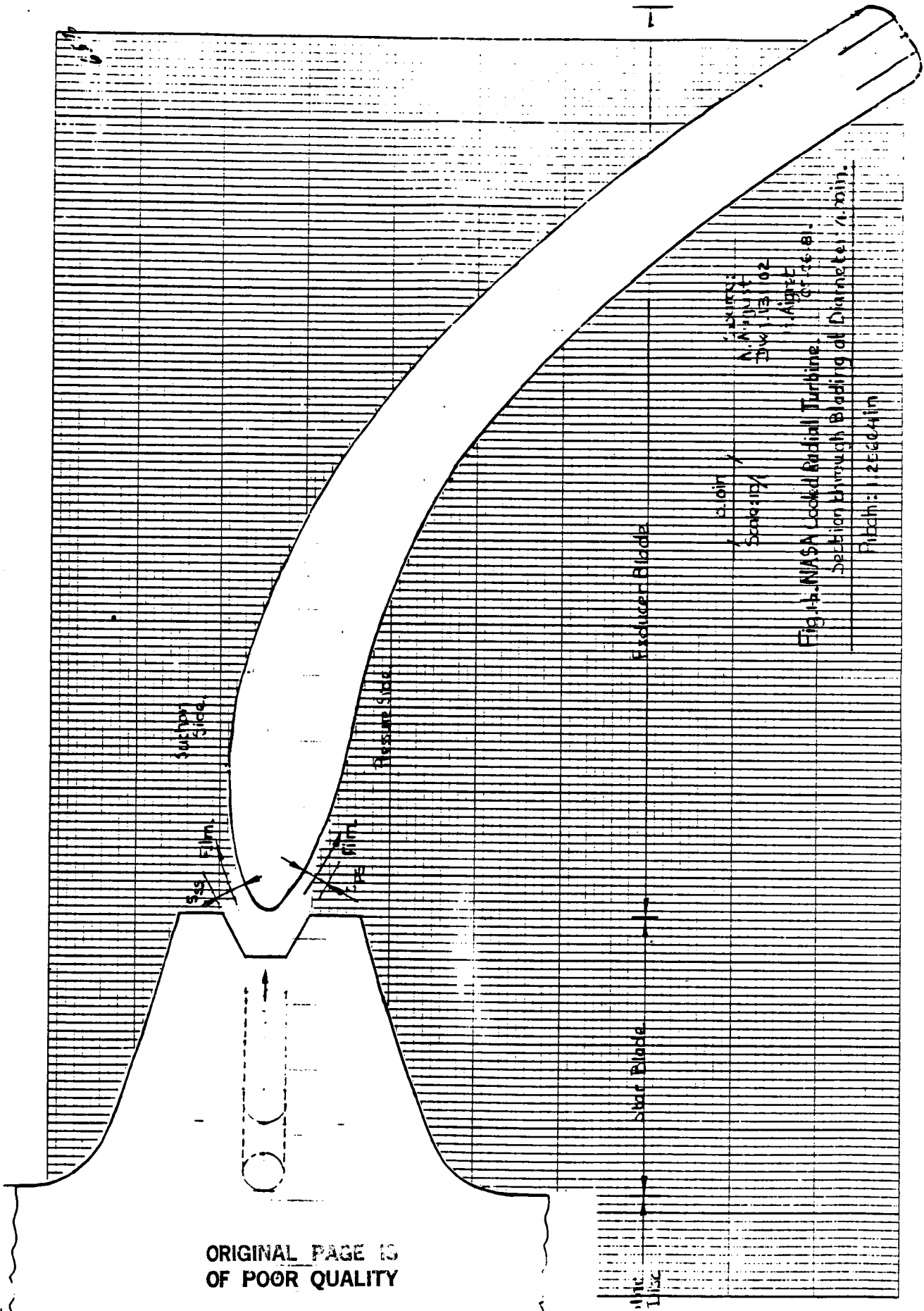


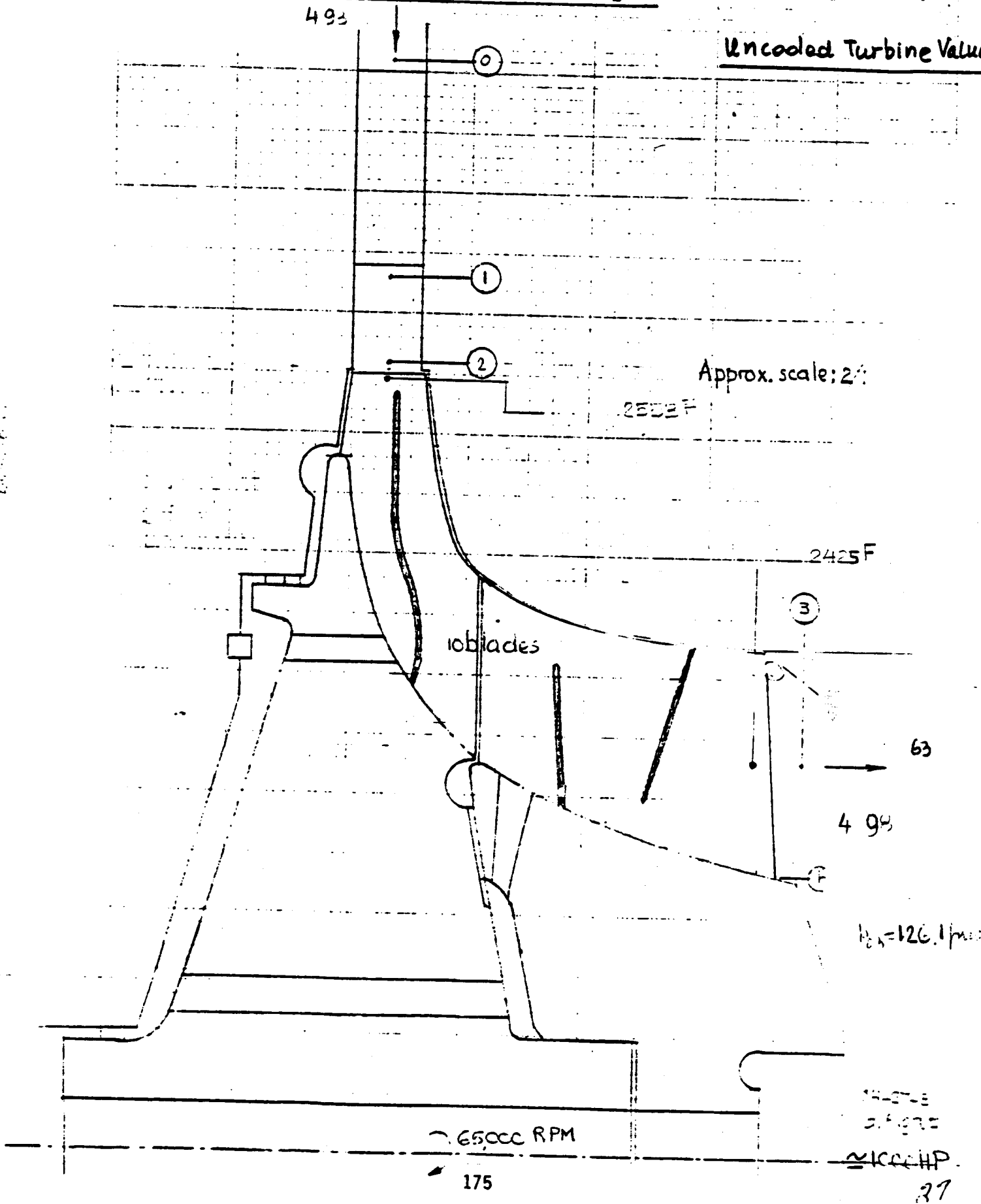
Fig. 1. NASA Lockheed Radial Turbine.
 Section through Blade of Diameter: 1.0 in.
 Pitch: 1.25 in

ORIGINAL PAGE IS
 OF POOR QUALITY

Fig.2 .NASA Cooled Radial Turbine Project.

ORIGINAL PAGE IS
OF POOR QUALITY

Uncooled Turbine Values



R.P.M. 65000

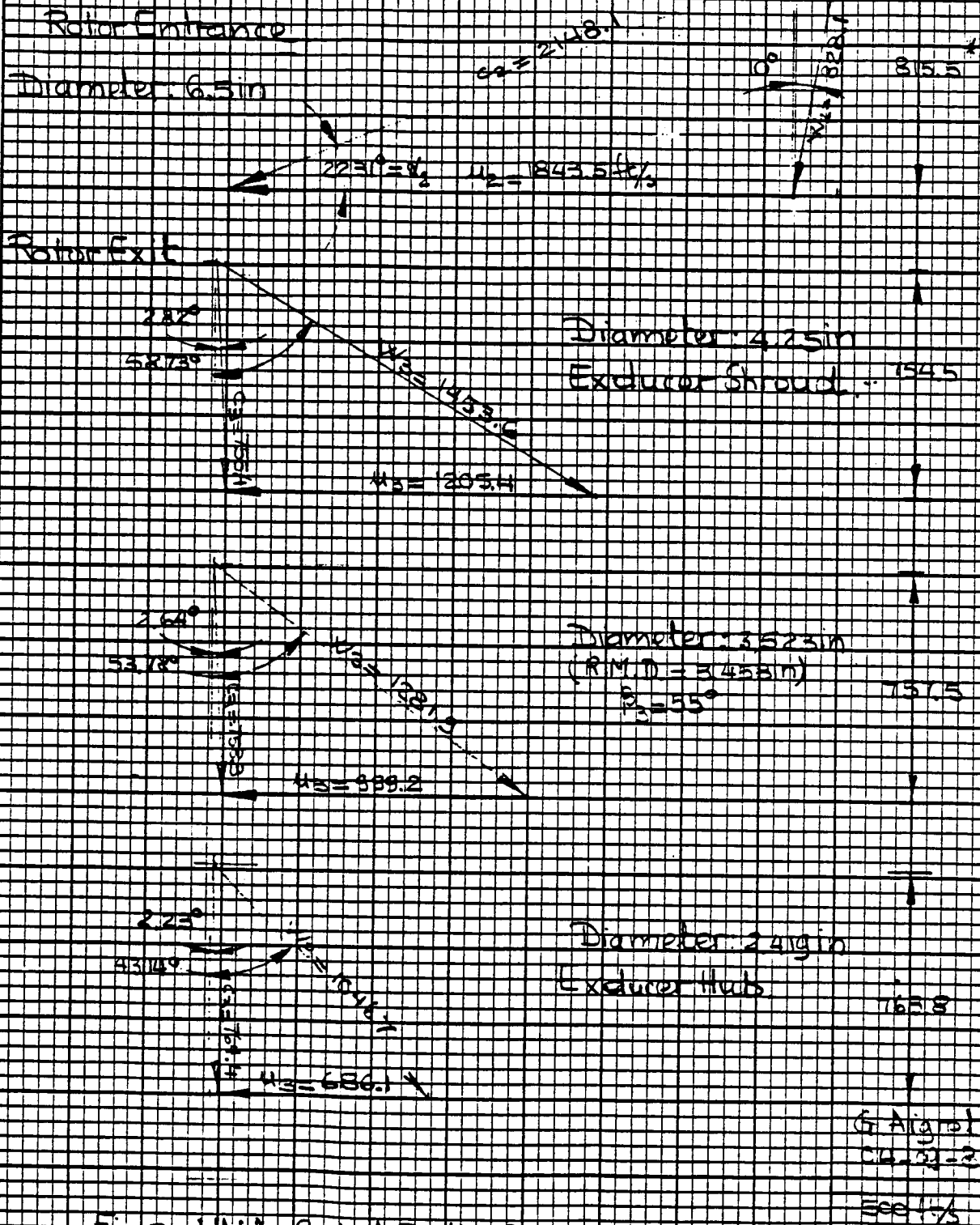
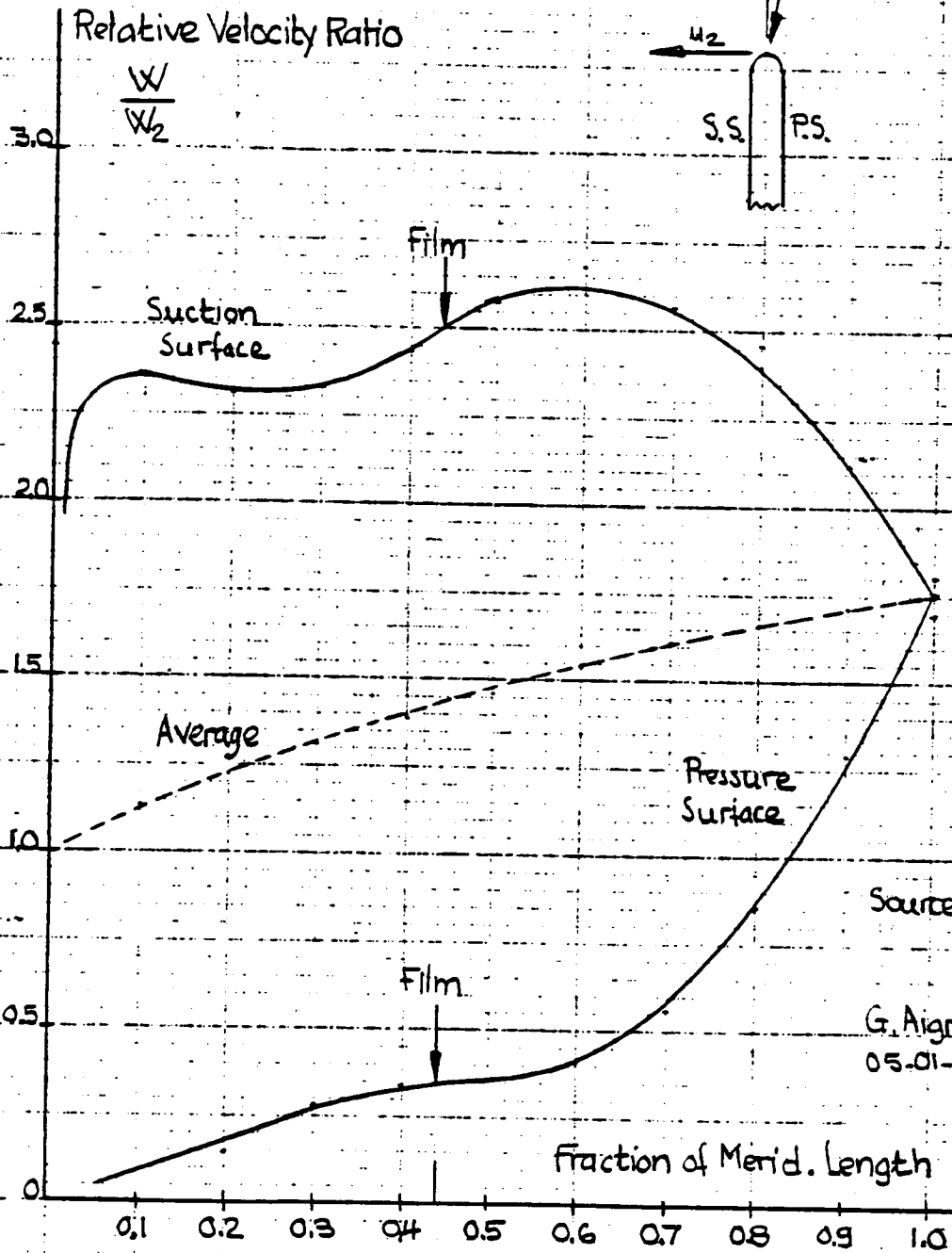


Fig 3 NASA Cooled Radial Turbine
Blocked Velocity Triangles.

Source: C. Radgort
Uncooled Turbine Analysis.

ORIGINAL PAGE IS
OF POOR QUALITY



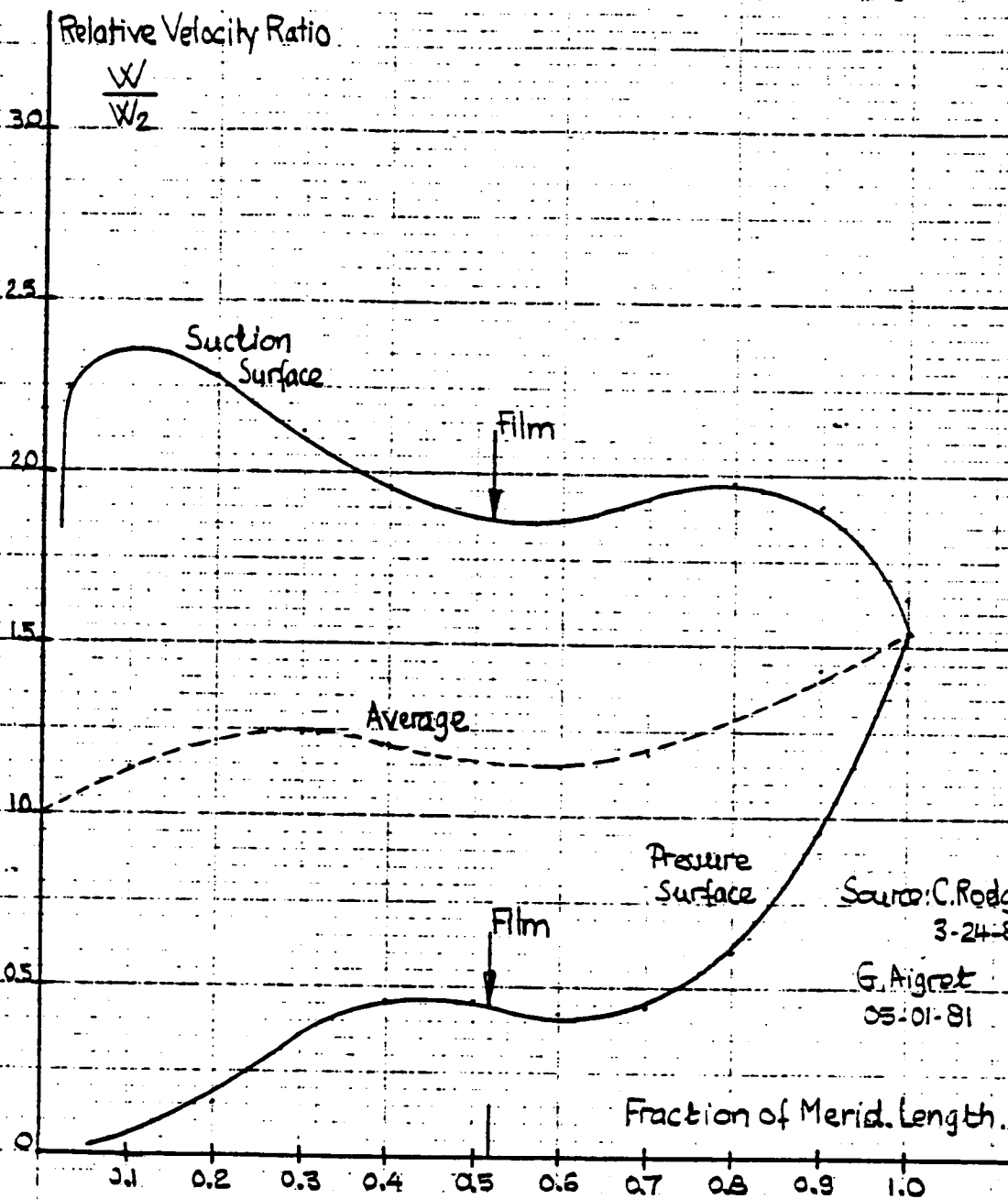
Source: C. Rodgers
3-24-81

G. Aigret
05-01-81

Fig. 4. NASA Cooled Radial Turbine.

Blade Relative Velocity Distribution near Shroud.

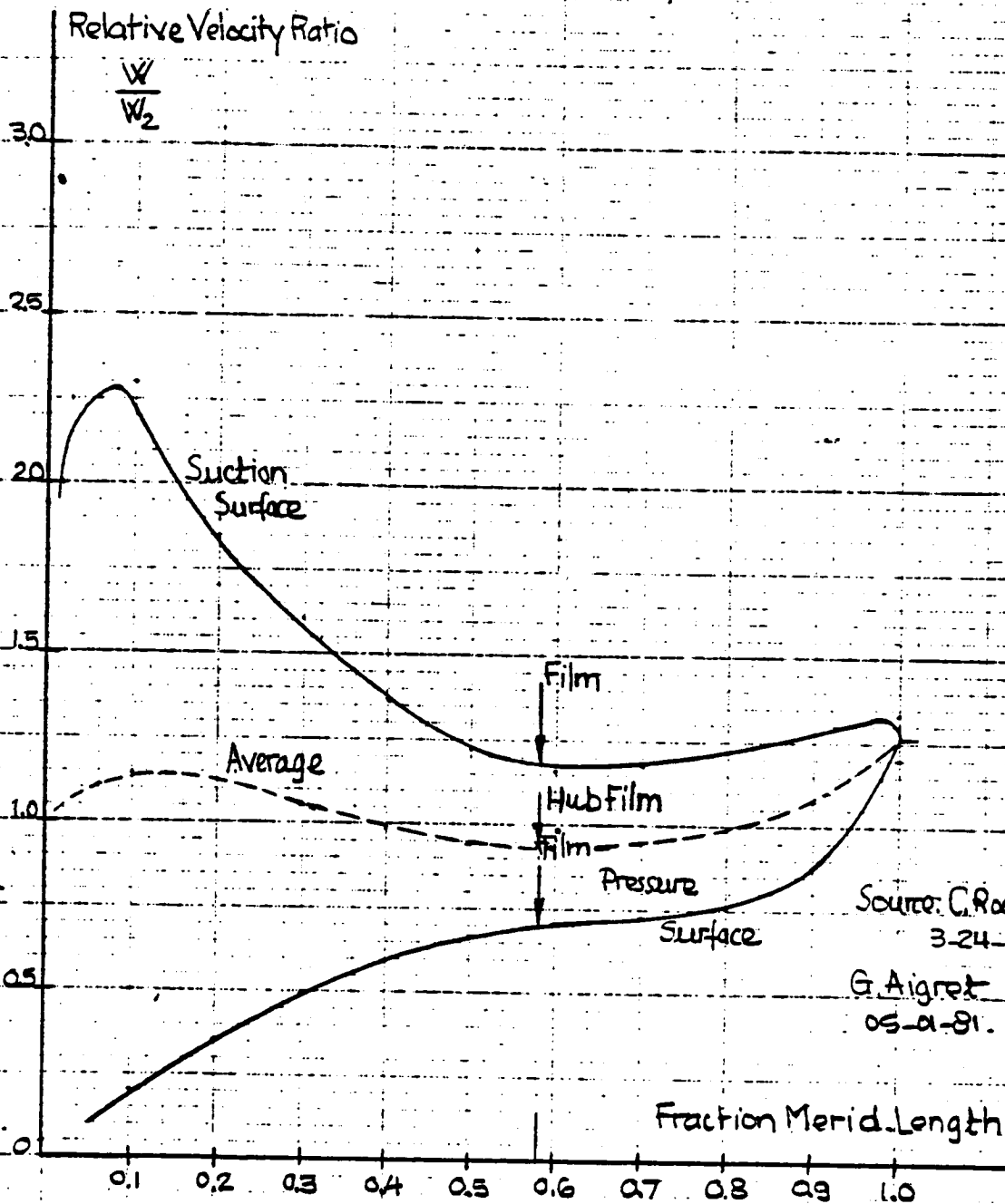
- Meridional Line Length: 2.059 in.
- Actual length:
- Entrance Relative Velocity: $W_2 = 823.1 \text{ ft/s}$ (blocked)



Source: C. Rodgers
3-24-81
G. Aigret
05-01-81

Fig. 5. NASA Cooled Radial Turbine.
Blade Relative Velocity Distribution near Mid. Passage.

- Merid. Line Length: 2.366 in
- Actual Length;
- Entrance Relative Velocity: $W_2 = 228.1 \text{ ft/s}$ (blocked)

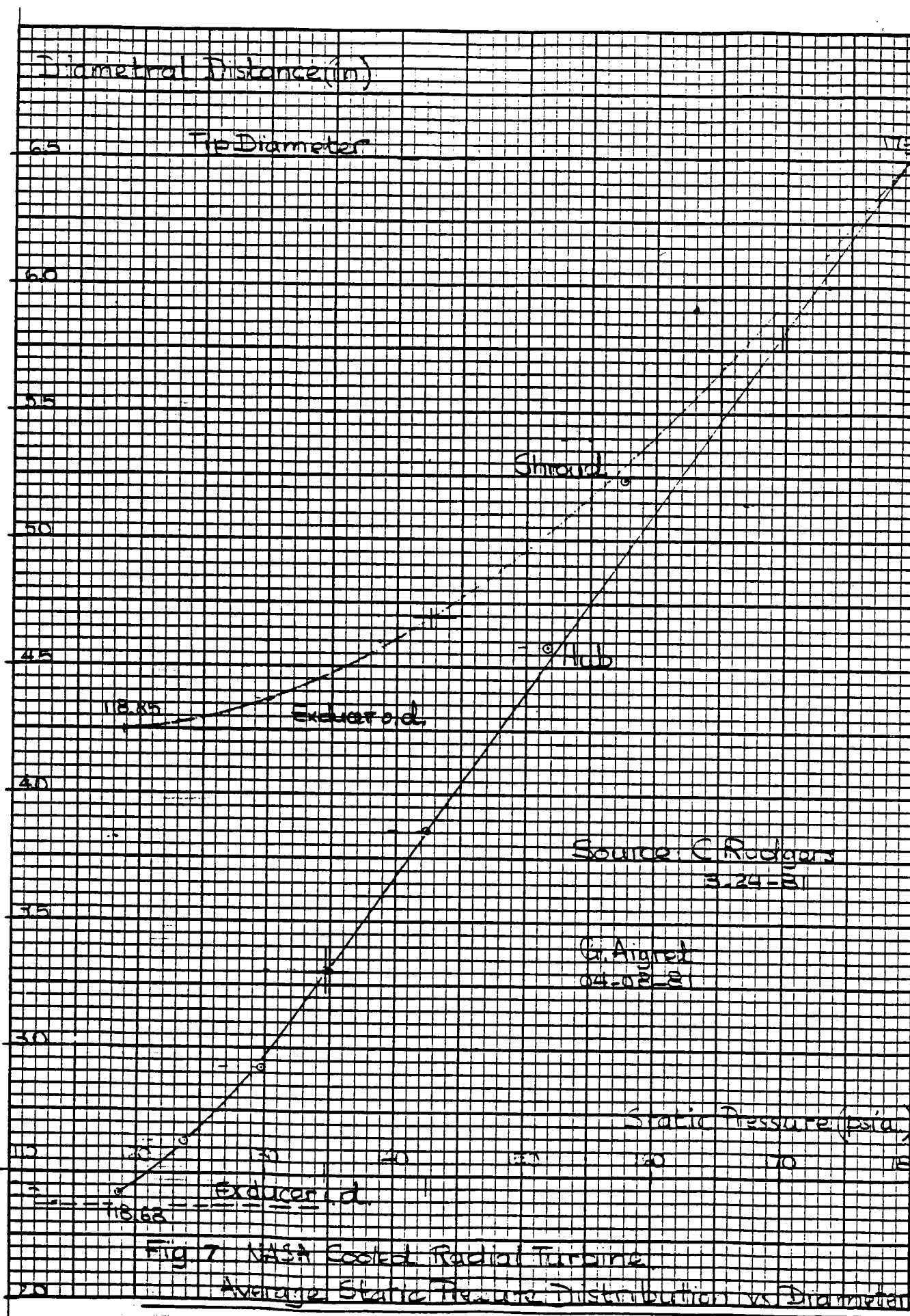


Source: C. Rodgers
3-24-81
G. Aigret
05-2-81.

Fig. 6, NASA Cooled Radial Turbine.
Blade Relative Velocity Distribution near Hub.

- Merid. Line Length: 2,918 in.
- Actual Length:
- Entrance Relative Velocity: $W_2 = 228.1 \text{ ft/s}$ (blocked)

K-E 5 X 5 TO 1/2 INCH 46 0863
 7 X 10 INCHES MADE IN U.S.A.
 KEUFFEL & ESSER CO.



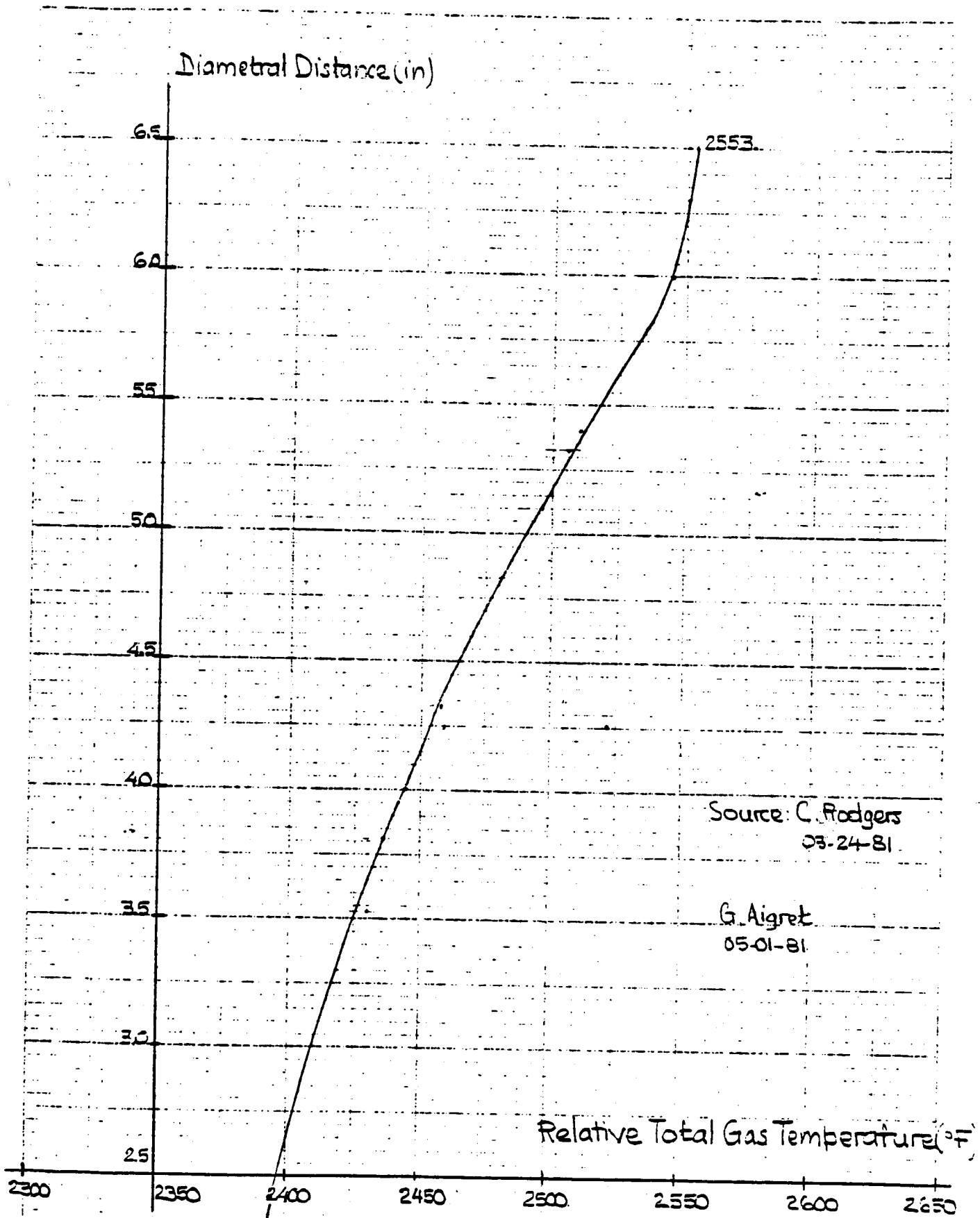
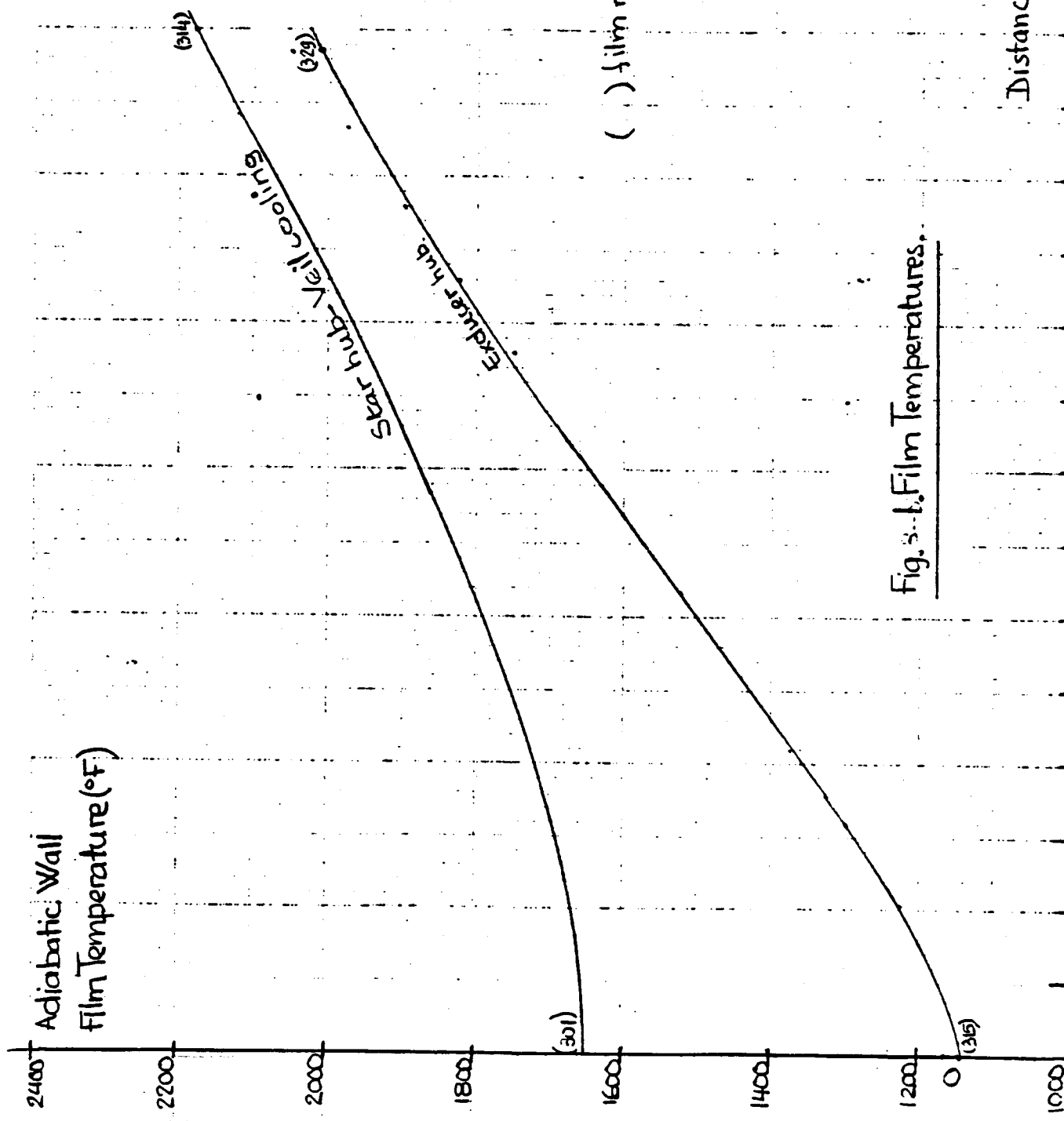


Fig. 8-a NASA Cooled Radial Turbine.

Relative Total Gas Temperatures (without cooling)



() film nodes per Fig. 22

G. Aigret
05-01-81

Fig. 3-1. Film Temperatures.

Distance from Injection Point (in)

ORIGINAL PAGE IS OF POOR QUALITY

Adiabatic Wall

Film Temperature (°F)

() film node number per Fig. 23

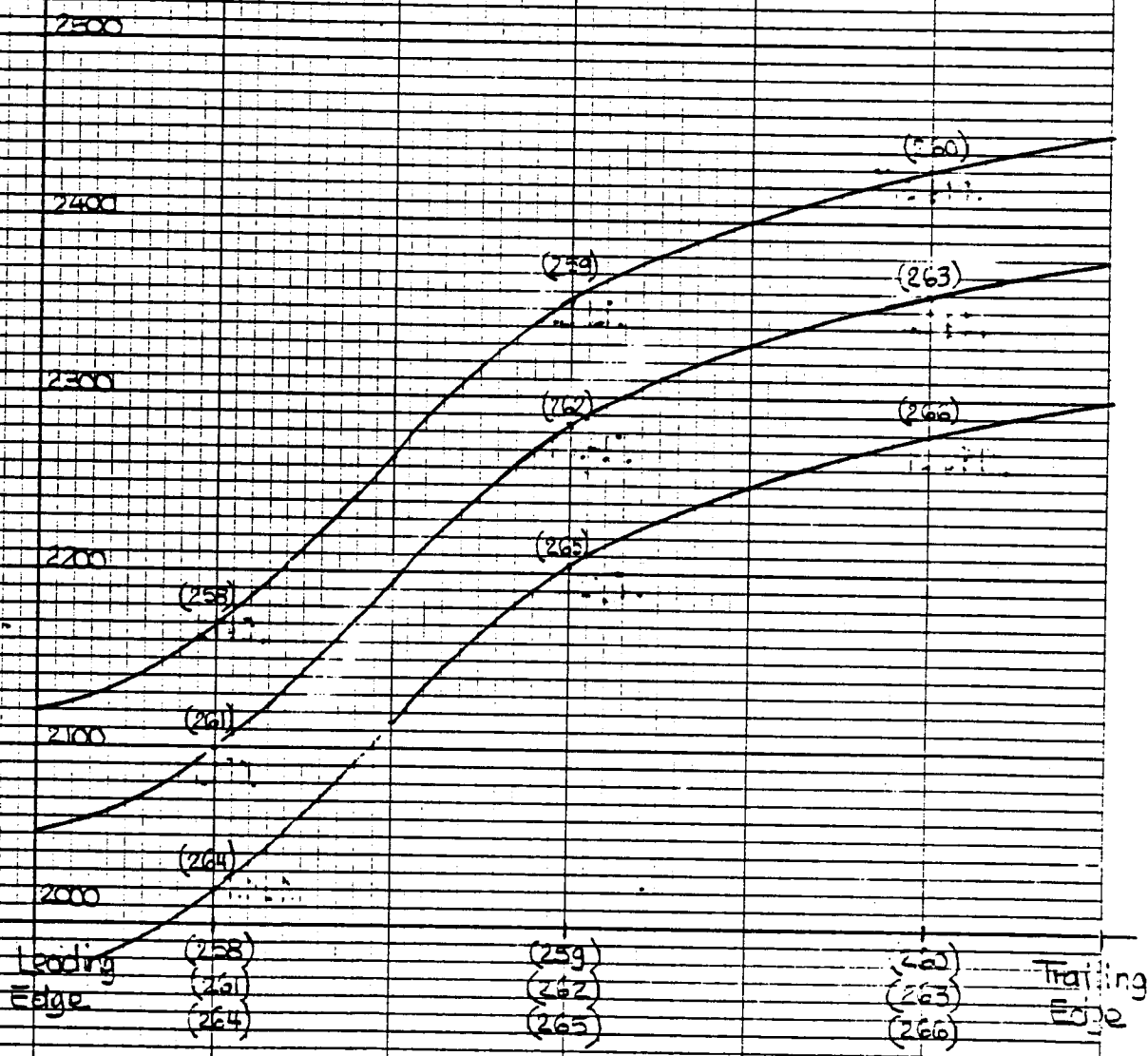


Fig. 3-c, Exducer Blade Film Temperatures.

- Algren
05-22-81

use 1246
for L.E.

S.S. and P.S.
Average Gas-Side
Heat Transfer Coefft.
(Btu/h.ft².F)

ORIGINAL PAGE IS
OF POOR QUALITY

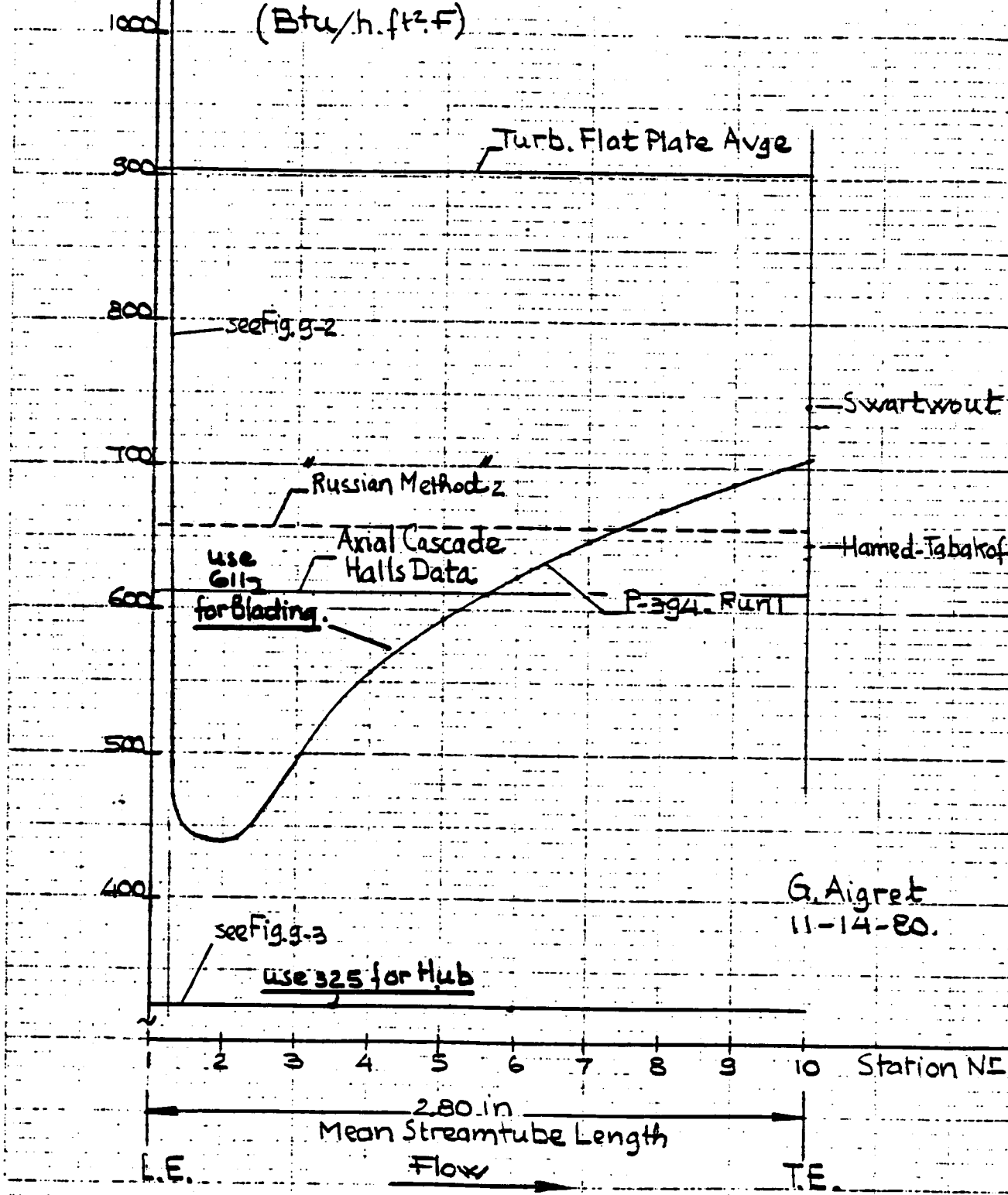


Fig. 9-1. NASA Cooled Radial Turbine.
Gas-Side Heat Transfer Coefficient.

46 0702

K&E 10 X 10 TO THE INCH .7 X 10 INCHES
KEUFFEL & ESSER CO. MADE IN U.S.A.

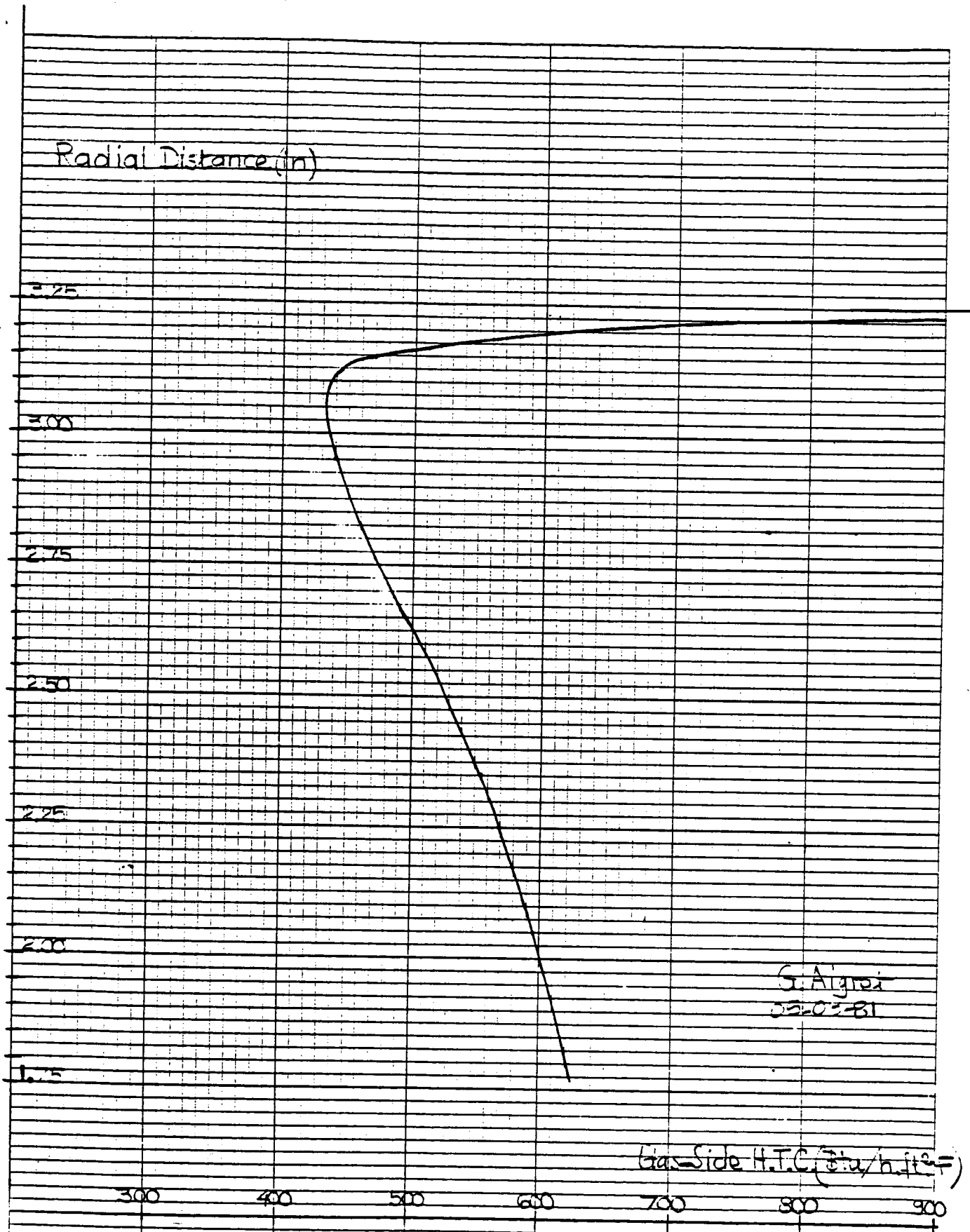


Fig. 32. NASA Cooled Radial Turbine.
Star Blade External Heat Transfer Coefficient.

46 0702

K&E 10 X 10 TO THE INCH • 7 X 10 INCHES
KEUFFEL & ESSER CO. MADE IN U.S.A.

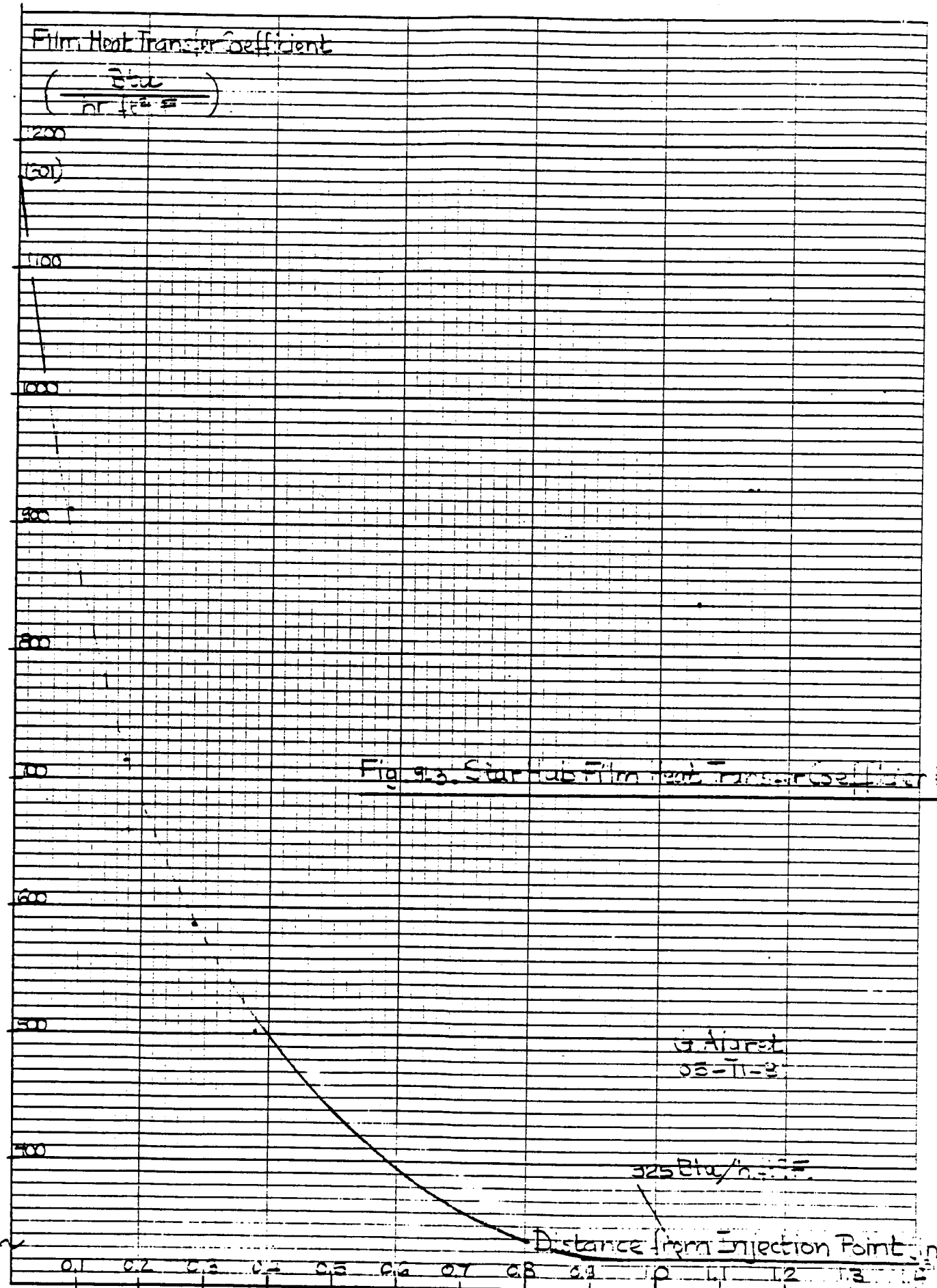
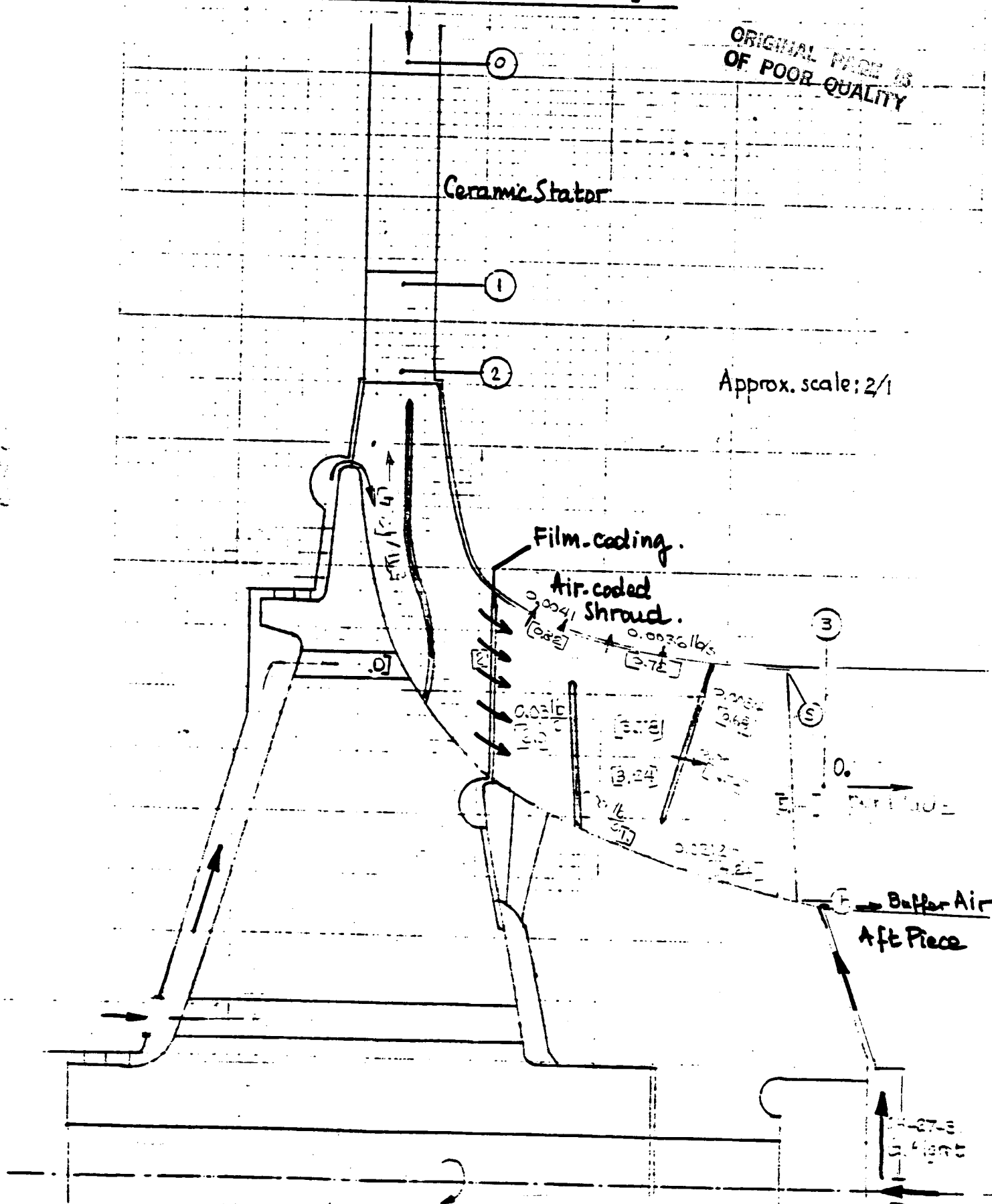


Fig.10. NASA Cooled Radial Turbine Project.

ORIGINAL PAGE IS
OF POOR QUALITY



Ceramic Stator

Approx. scale: 2/1

Film-cooling.

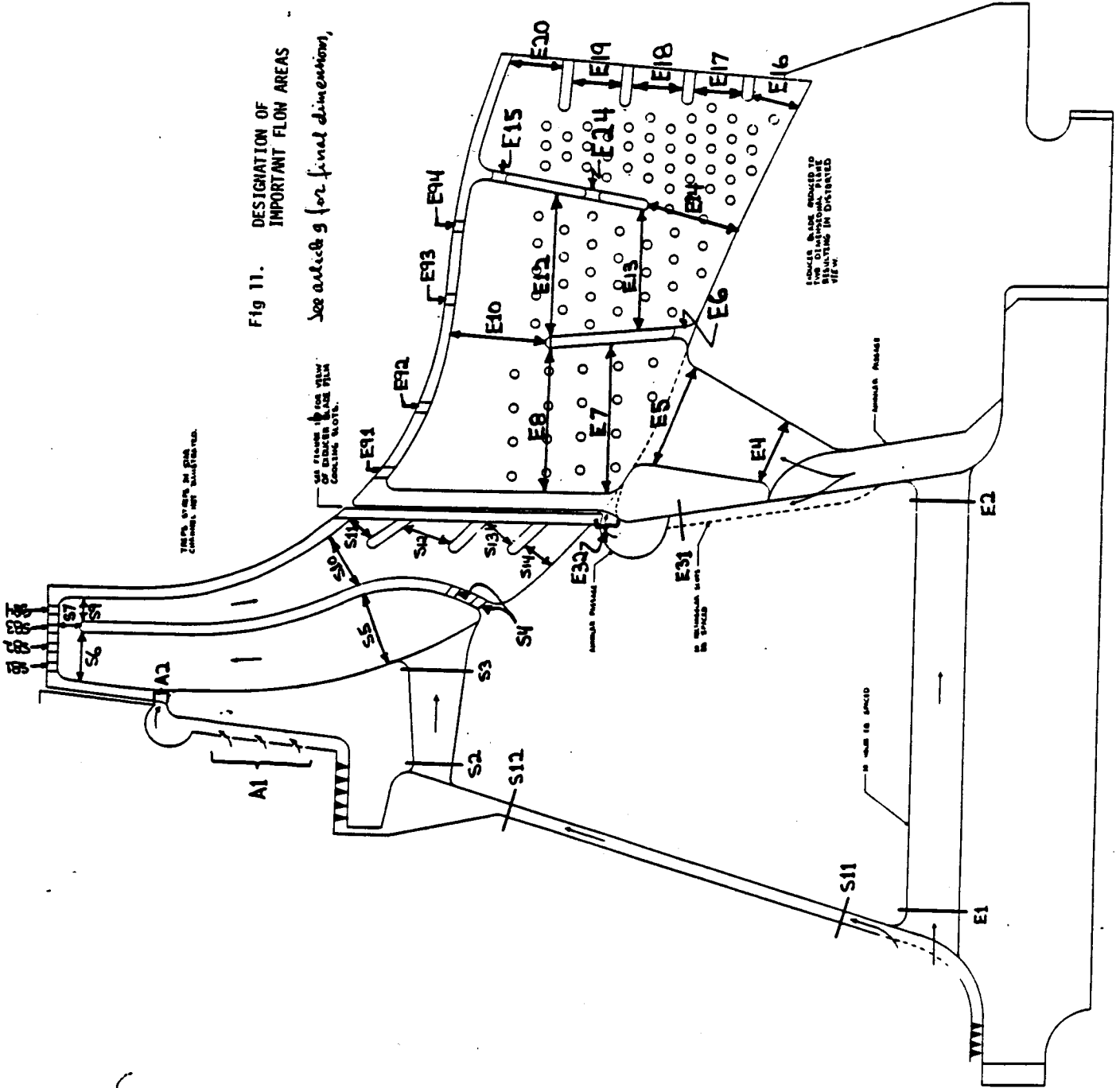
Air-cooled Shroud.

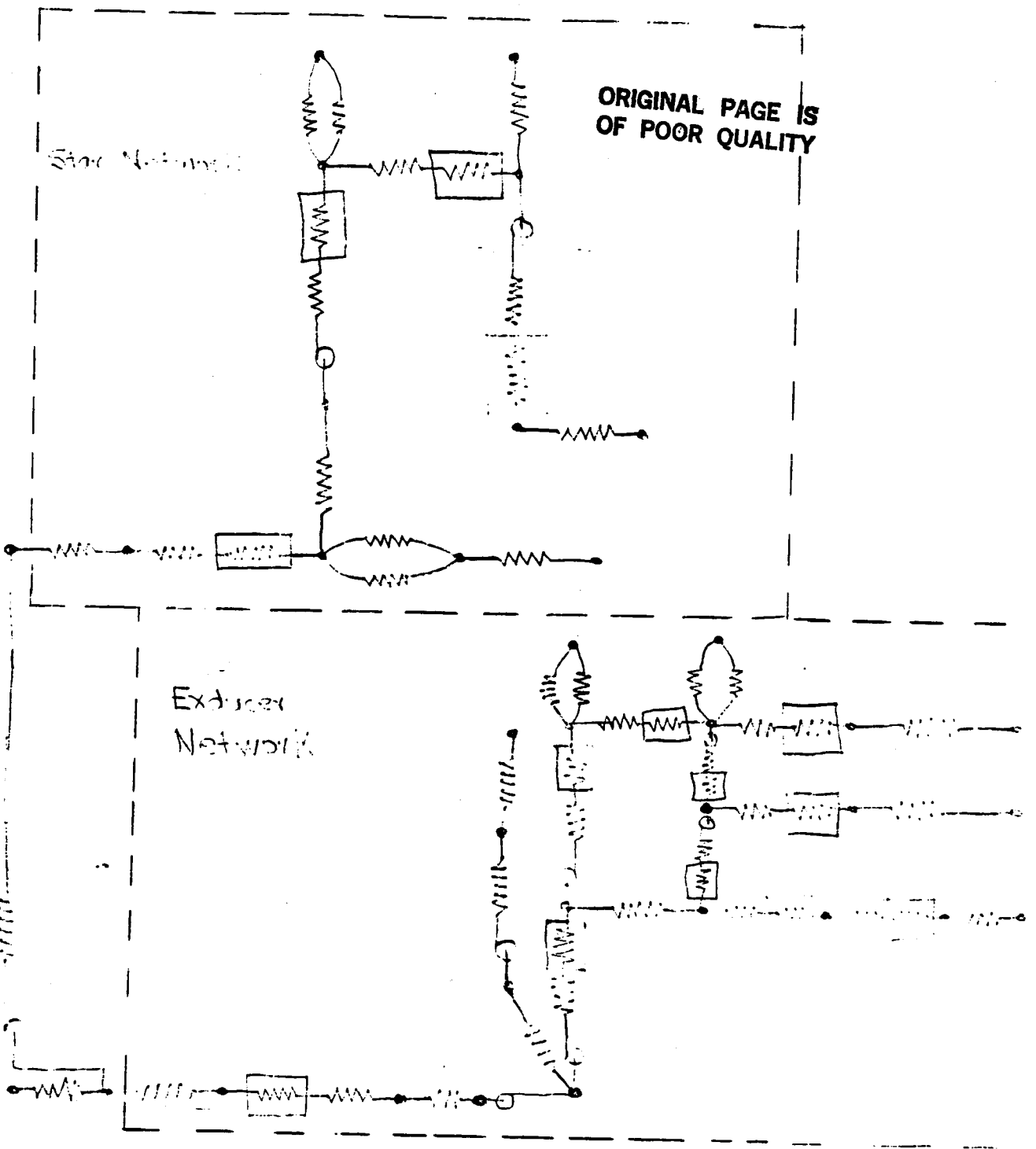
Buffer Air Aft Piece

4210

Fig 11. DESIGNATION OF IMPORTANT FLOW AREAS

See article 9 for final dimensions,





ORIGINAL PAGE IS
OF POOR QUALITY

Star Network

External
Network

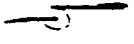
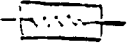
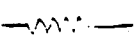
-  Pin
-  Half Bridge
-  Impedance Flow Resistive Element

Figure 12 - Star Network. Star Network
Check Table.

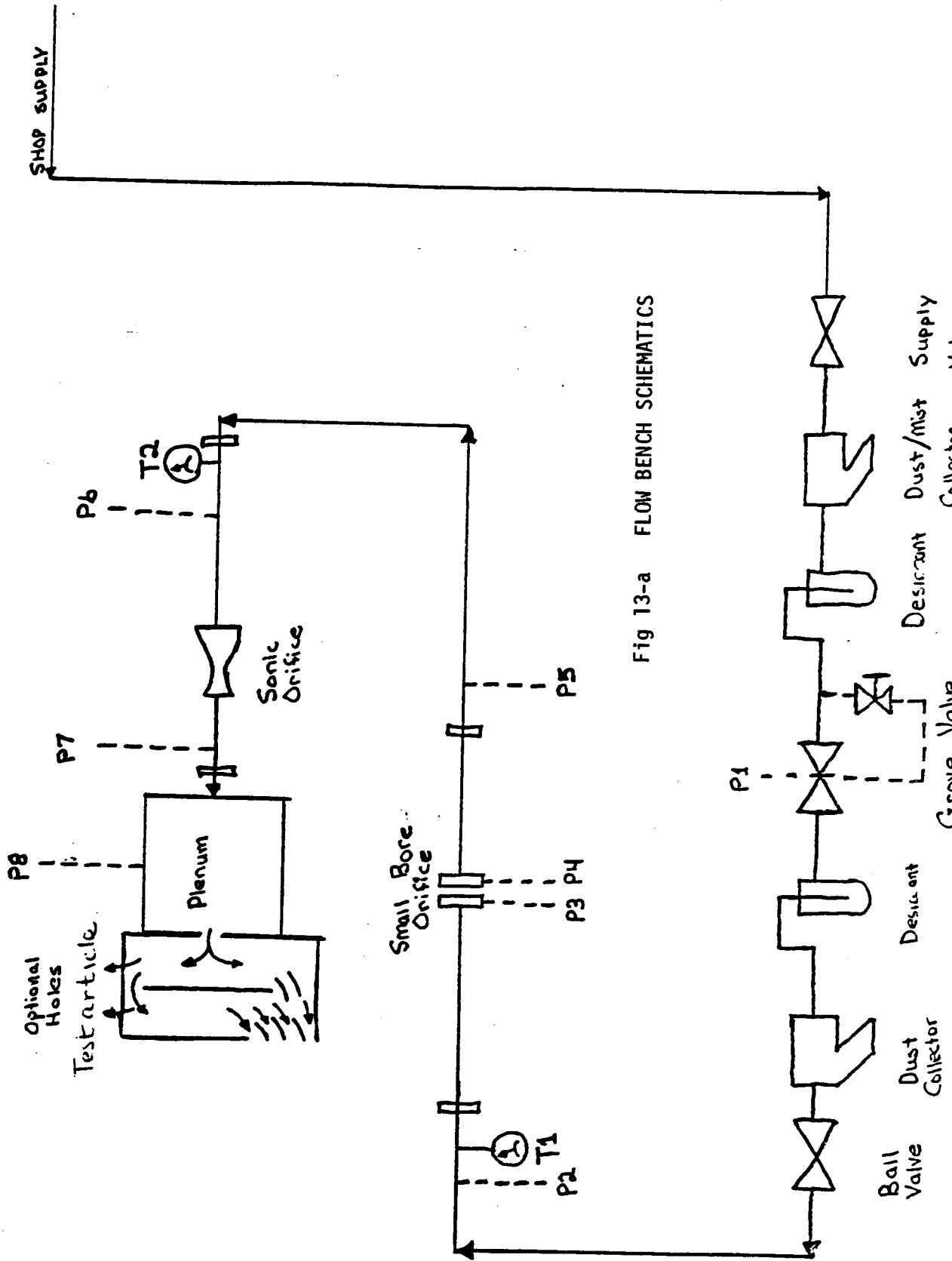


Fig 13-a FLOW BENCH SCHEMATICS

TEST:
DATE:

TIME:

Bench Temps		Bench Gauges					Bench Manometers				Barometer		
Bench Amb. (°F)	S. B. Upst. (°F)	Grove Press. (PSIG)	S. Bore Downstr. (PSIG)	S. Bore Upstream (PSIG)	S. B. Inlet Flange (PSIG)	Test Plenum (in Hg)	Sonic Orifica ΔP (in Hg)	Sonic Upstr. (in Hg)	S. B. ΔP (in H ₂ O)	Press (in Hg)	Temp. (°F)	Corrected Press. (in Hg)	
T1 ±1°F	T2 ±1°F	P1 ±1psi	P5 ±1psi	P2 ±1psi	P3 ±1/2 psi	P8 ±1in	P6-P7 ±1in	P6 ±1in	P3-P4 ±1in				

COMMENTS:
Fig 13-b COLD FLOW DATA SHEET

43

ORIGINAL PAGE IS
OF POOR QUALITY

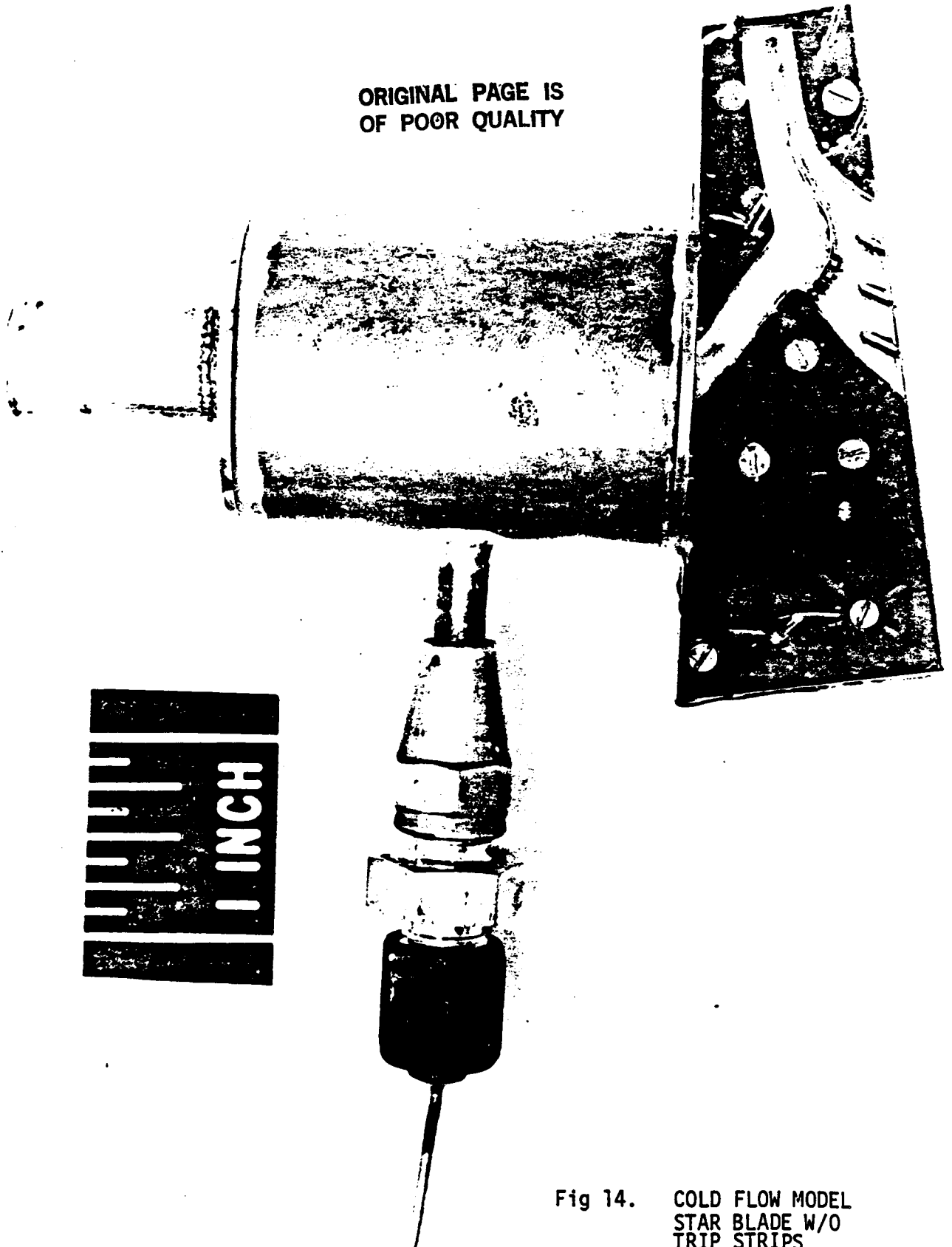


Fig 14. COLD FLOW MODEL
STAR BLADE W/O
TRIP STRIPS

ORIGINAL PAGE IS
OF POOR QUALITY

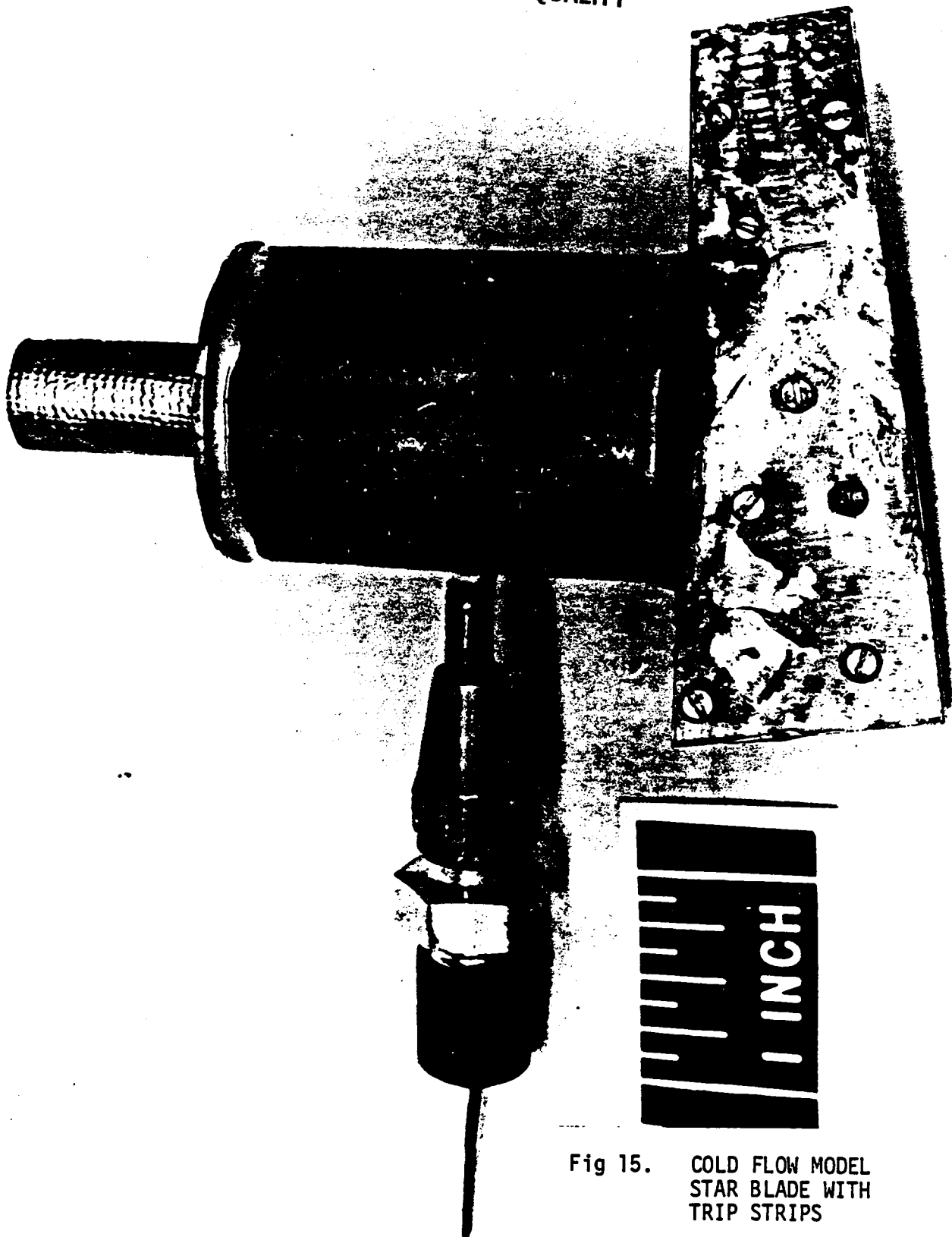


Fig 15. COLD FLOW MODEL
STAR BLADE WITH
TRIP STRIPS

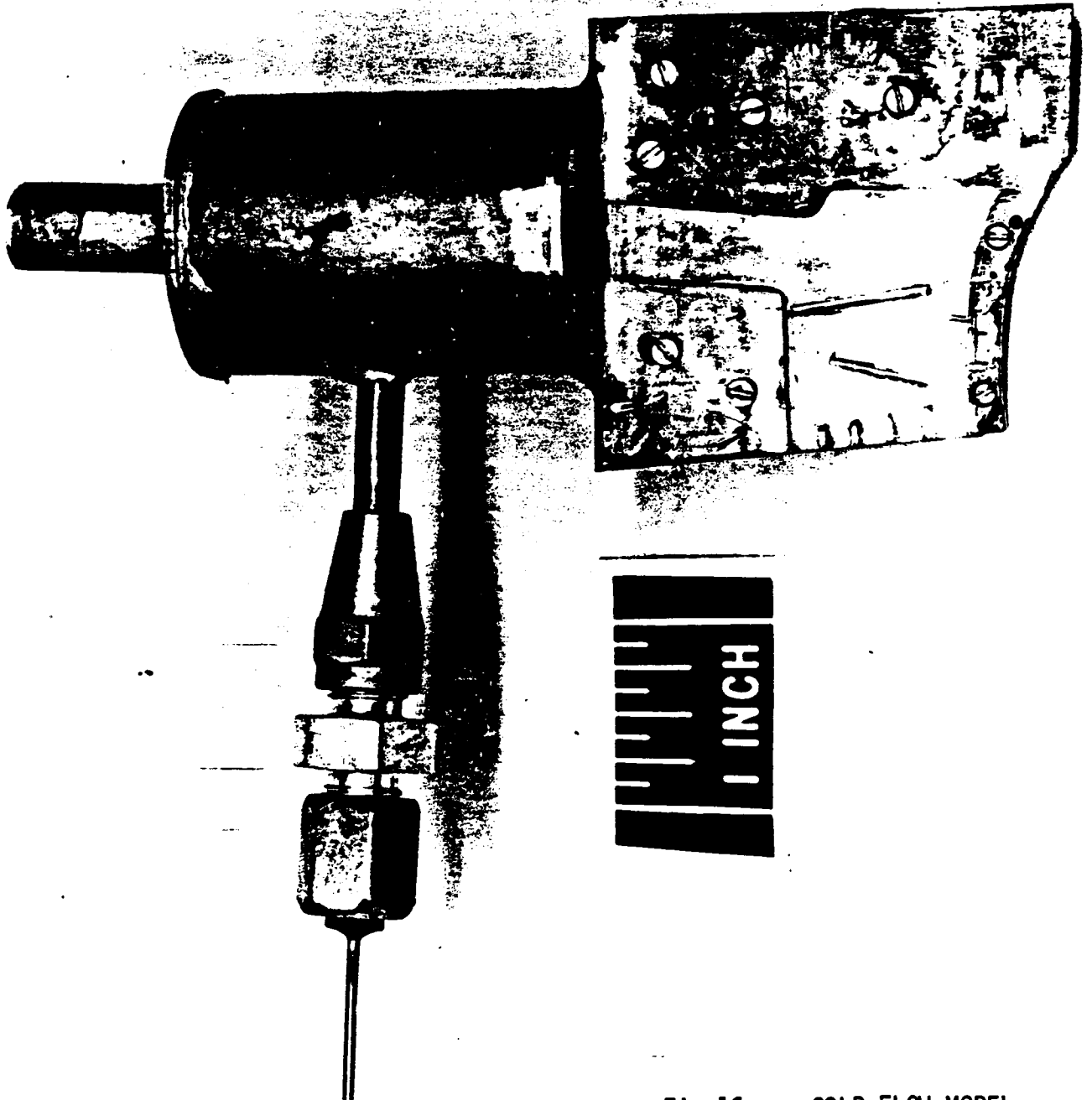


Fig 16. COLD FLOW MODEL
EXDUCER BLADE W/O
PIN FINS

ORIGINAL PAGE IS
OF POOR QUALITY

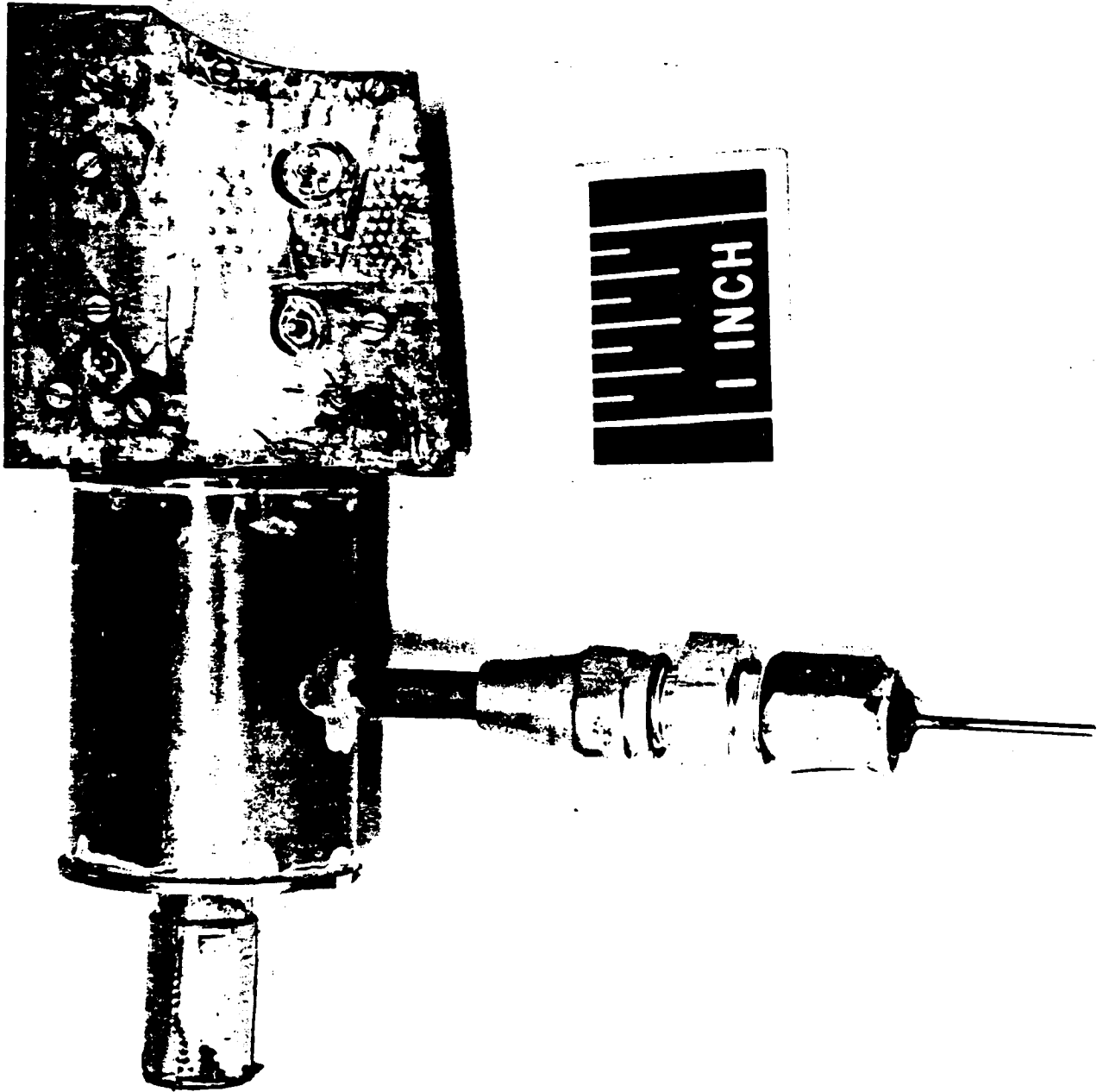


Fig 17. COLD FLOW MODEL
EXDUCER BLADE WITH
PIN FINS

12910

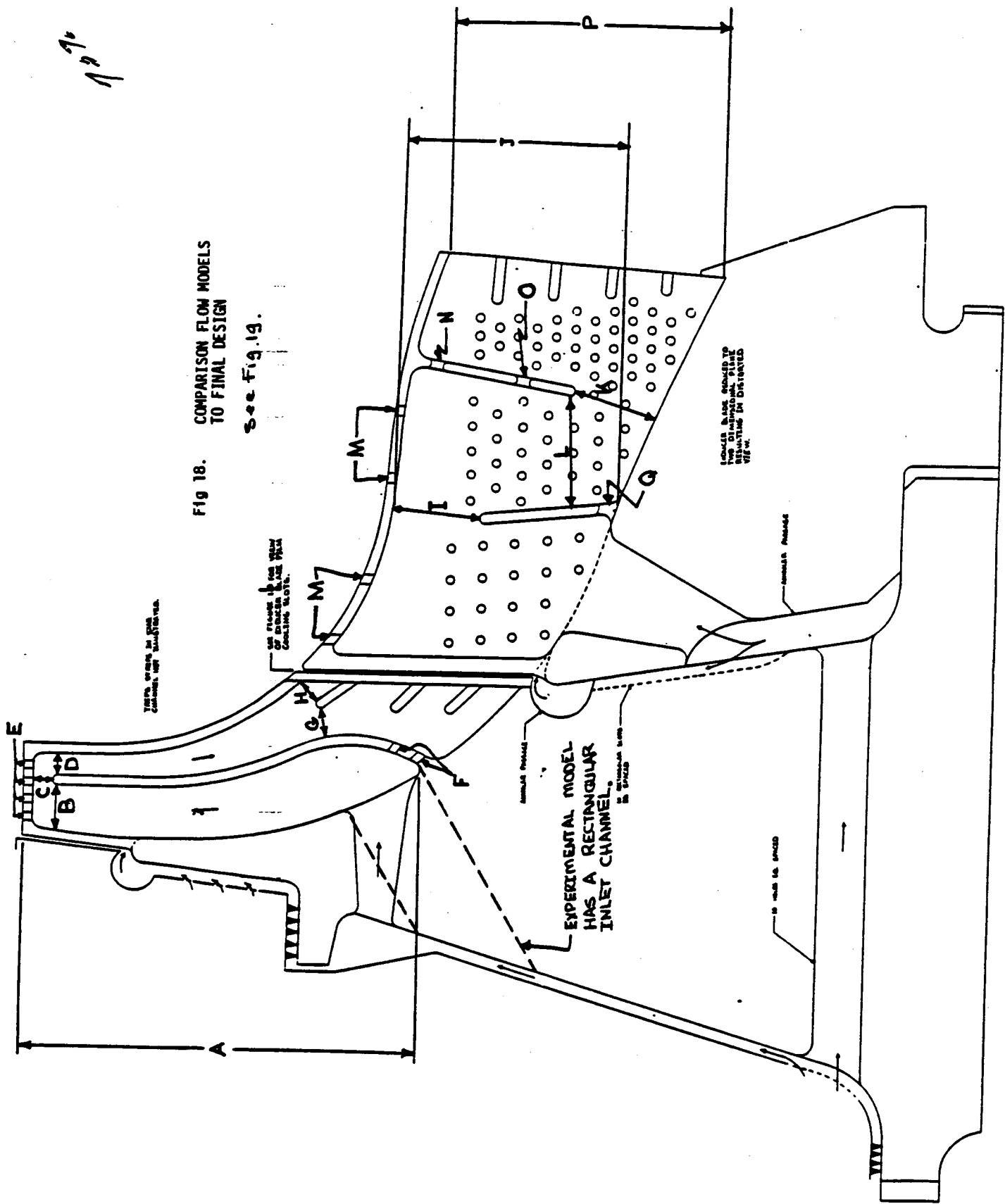


Fig 18. COMPARISON FLOW MODELS TO FINAL DESIGN See Fig. 19.

COMPARISON OF DIMENSIONAL ACCURACIES BETWEEN
EARLY
 EXPERIMENTAL FLOW MODELS AND THEIR DESIGN DRAWINGS.

LOCATION	EXPERIMENTAL FLOW MODELS				DESIGN DRAWINGS			
	DIMENSION (in)	AREA (in ²)	C _D	A·C _D (in ²)	DIMENSION (in)	AREA (in ²)	C _D	A·C _D (in ²)
A	1.35	—			1.22	—		
B	.135 x .060	.00810			.144 x .050	.00666		
C	.044 x .060	.00264			.061 x .050			
D	.070 x .060	.00420			.069 x .050	.00345 .00297		
E	3∅ .030	.00212 .00871	.8	.00170	4∅ .024	.00181	.8	.00145
F	.032 x .060	.00192	.6	.00115	2∅ ^{.026} .050	.00106 .00393	.8	.00085
G	.093 x .060	.00558			.094 x .050	.00416		
H	.125 x .060	.00750			.081 x .050	.00351		
I	.270 x .060	.01620			.278 x .050	.01336		
J	.925	—			.73	—		
K	.265 x .060	.01590			.269 x .050	.01291		
L	.265 x .060	.01590			.363 x .050	.0176		
M	4∅ .030	.00283	.8	.00226	4∅ .030	.00283	.8	.00226
N	.032 x .060	.00192	.6	.00115	∅ .040	.00126	.8	.00101
O	.030 x .060	.00180	.6	.00108	∅ .040	.00126	.8	.00101
P	.906	—			.870			
Q	.054 x .060	.00324	.6	.00194	∅ .050	.00196	.8	.00157

FOR FINAL DIMENSIONS; REFER TO THE SPECIFICATIONS LISTED IN APPENDIX E.
 A SUMMARY APPEARS IN SECTION 10 OF THE REPORT.

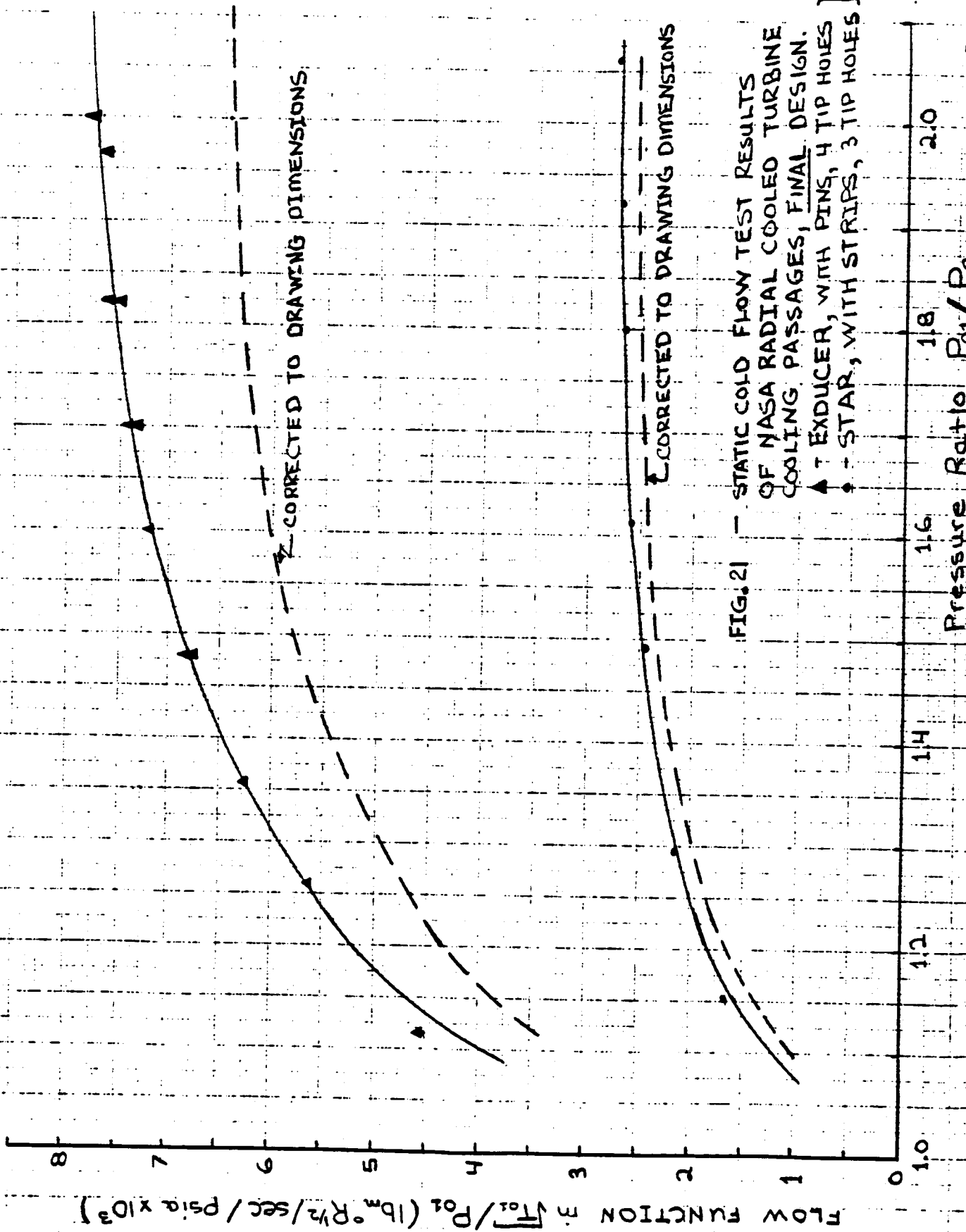
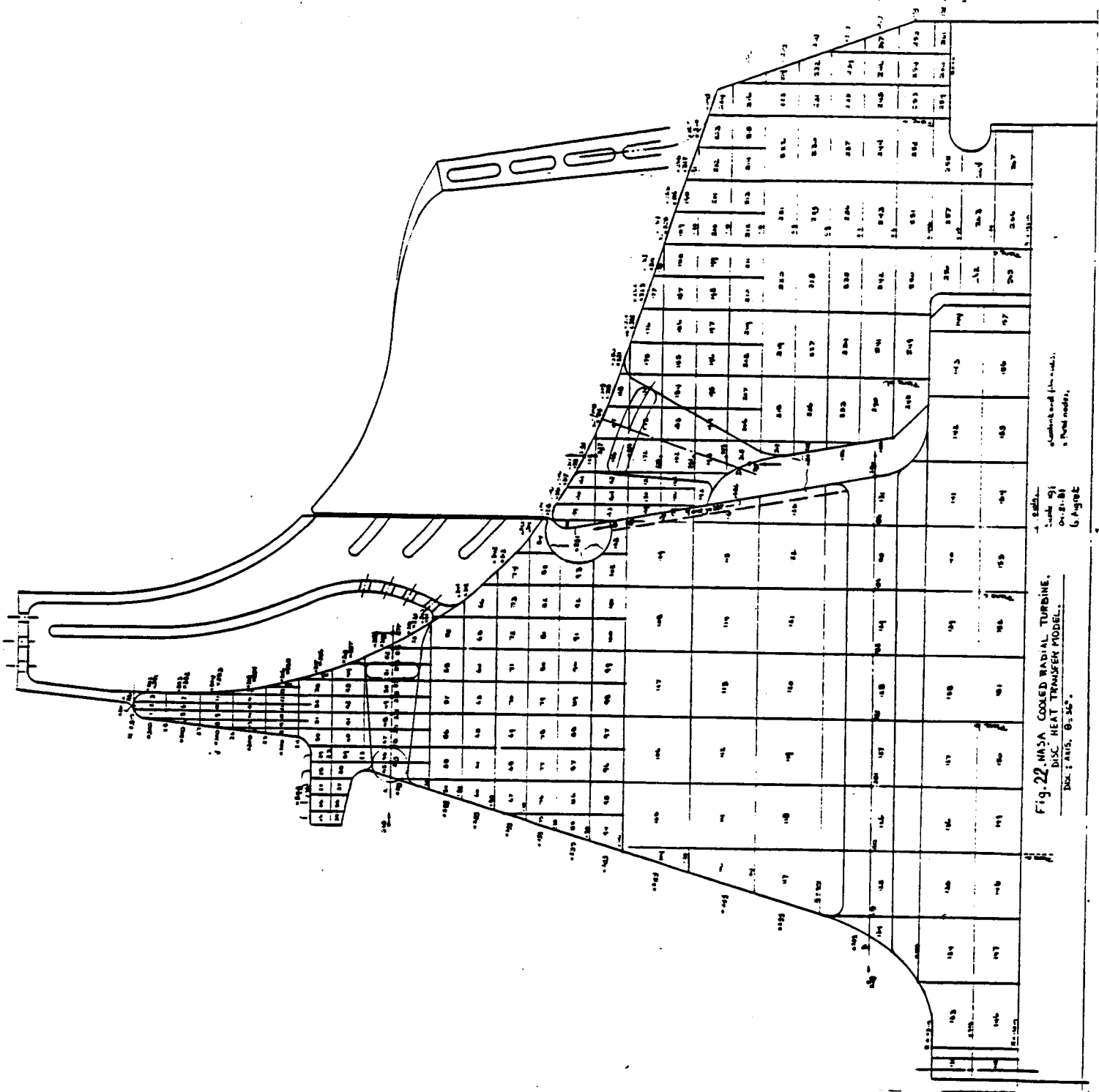
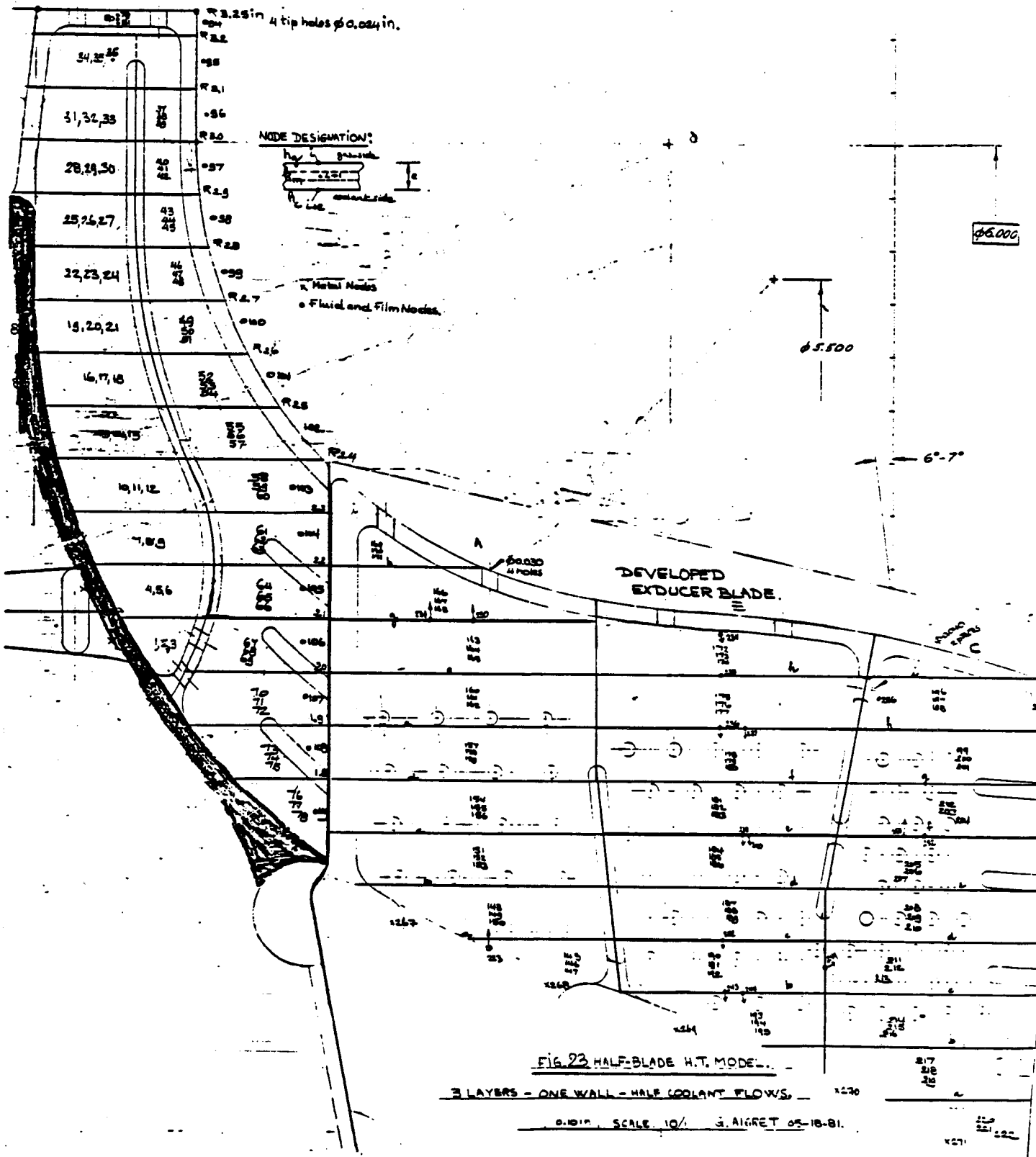


FIG. 21 - STATIC COLD FLOW TEST RESULTS OF NASA RADIAL COOLED TURBINE COOLING PASSAGES, FINAL DESIGN.



C-3

ORIGINAL PAGE IS
OF POOR QUALITY



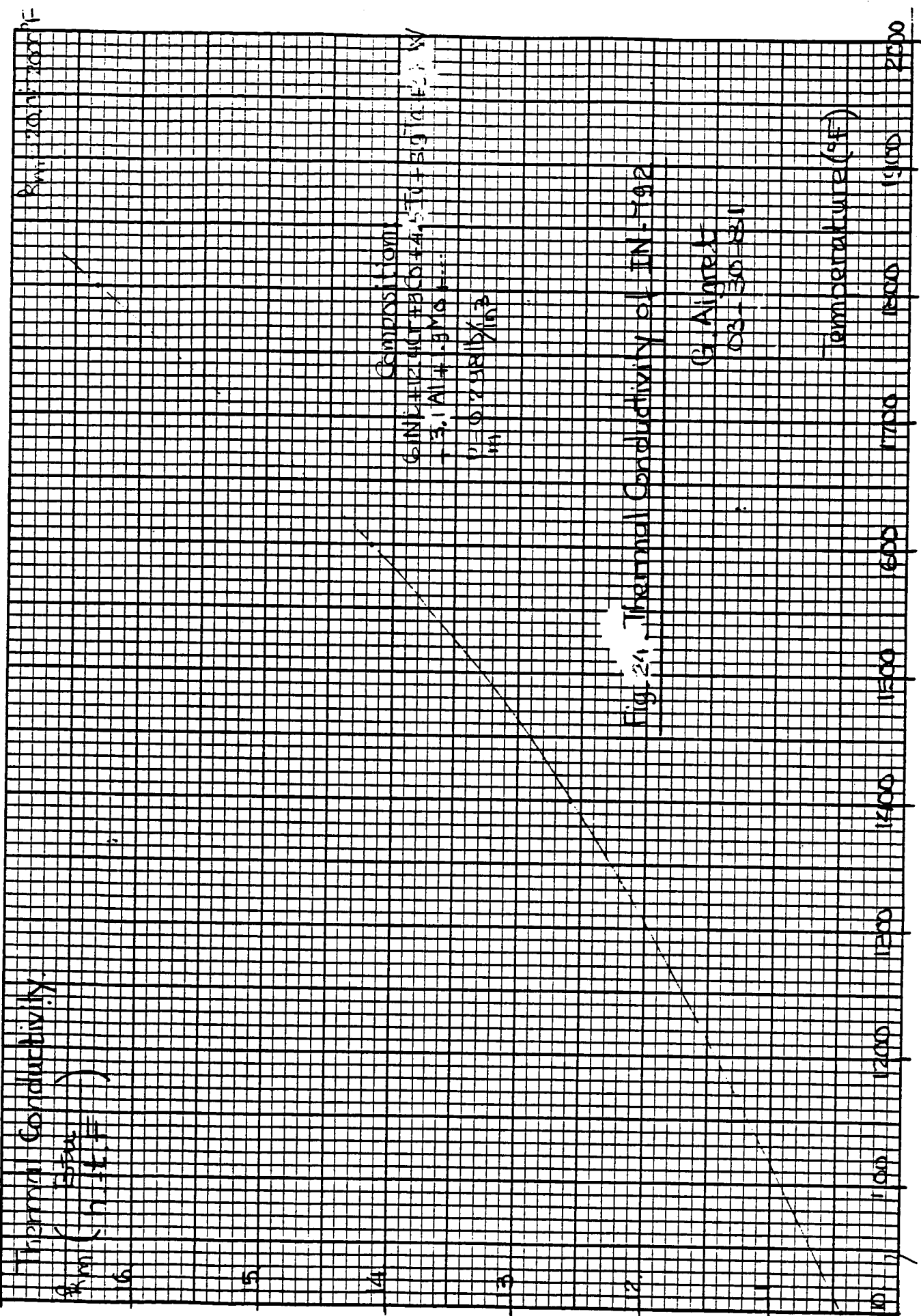


Fig. 24 Thermal Conductivity of IN-600

Diametral Distance (in)

Convection only per
 $Nu_{Re} = 0.0159 Re^{0.8} Pr^{0.333}$
 $RPM = 65020$
 $Re = \frac{W \cdot \mu}{\rho}$

Gauglet
 03-25-51

(Beu
 (112.3))

Fig. 3 Back-Fane Heat Transfer Coef.

0 100 200 300 400 500 600 700

46 0702

K^o2
KEUFFEL & ESSER CO. MADE IN U.S.A.

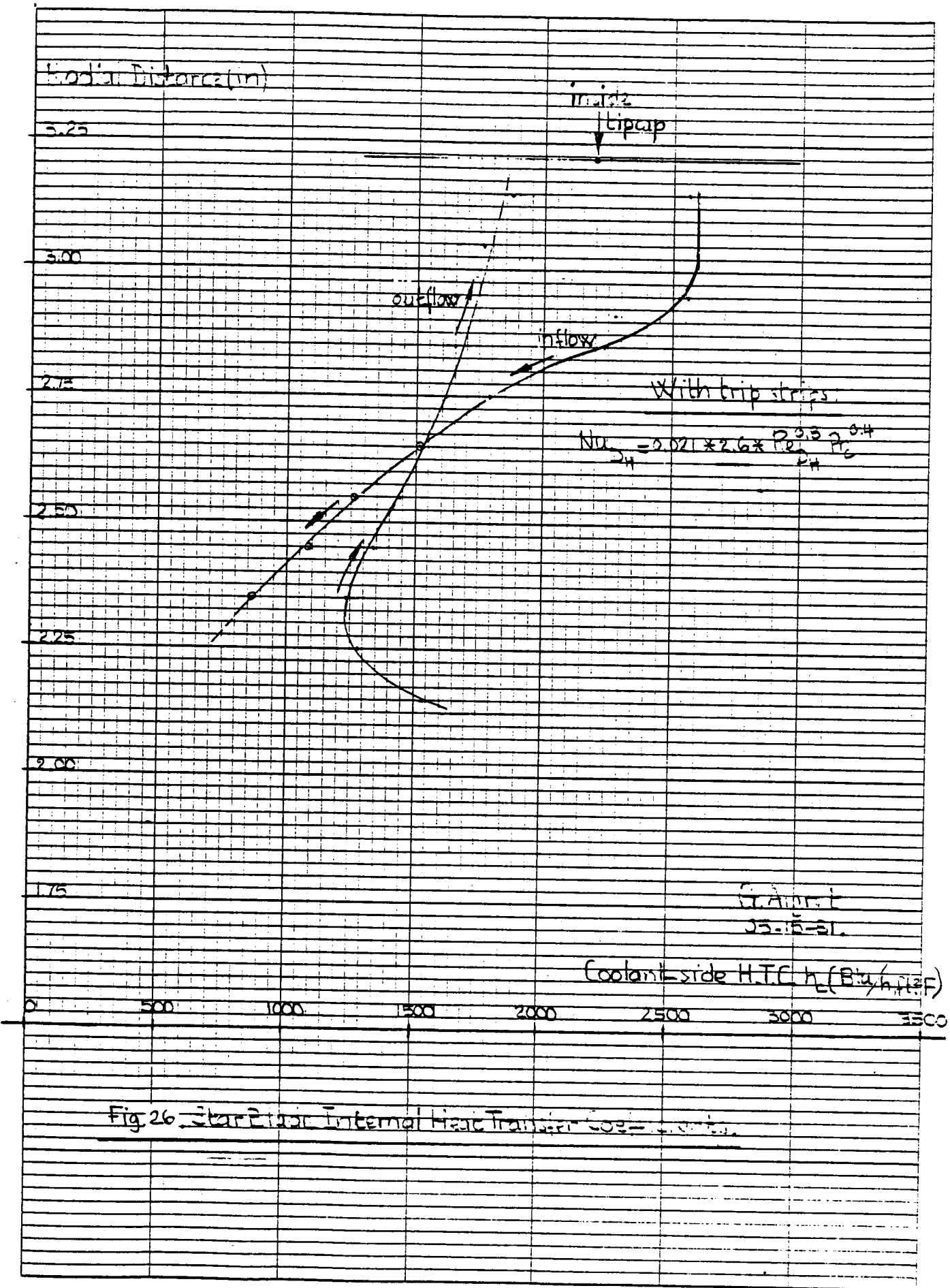


Fig 26 Star Fin Internal Heat Transfer Coe =

Internal Heat Transfer Coeff. h
($Btu/h \cdot ft^2 \cdot ^\circ F$)

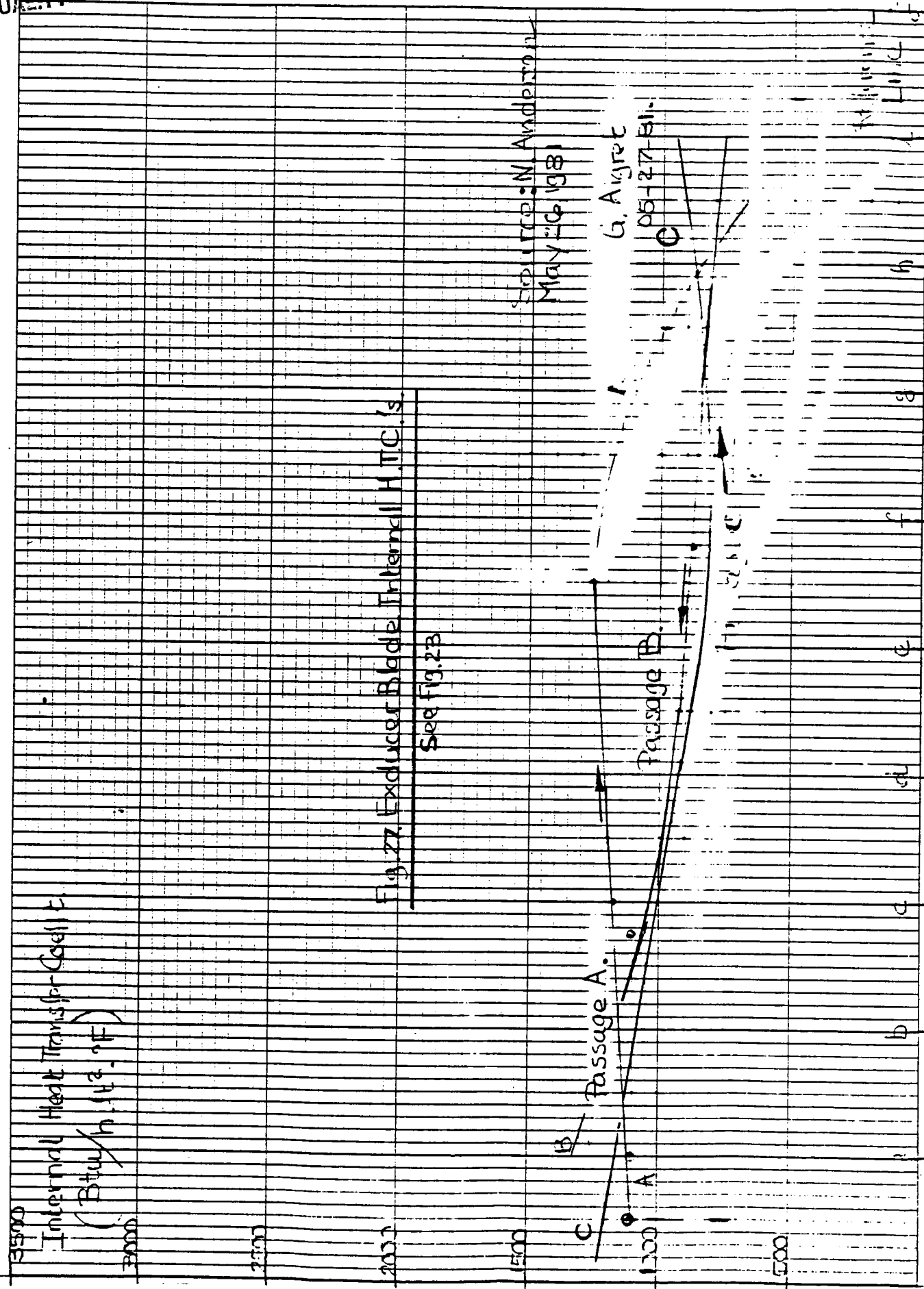


Fig. 27. Exducer Blade Internal H.T.C.'s

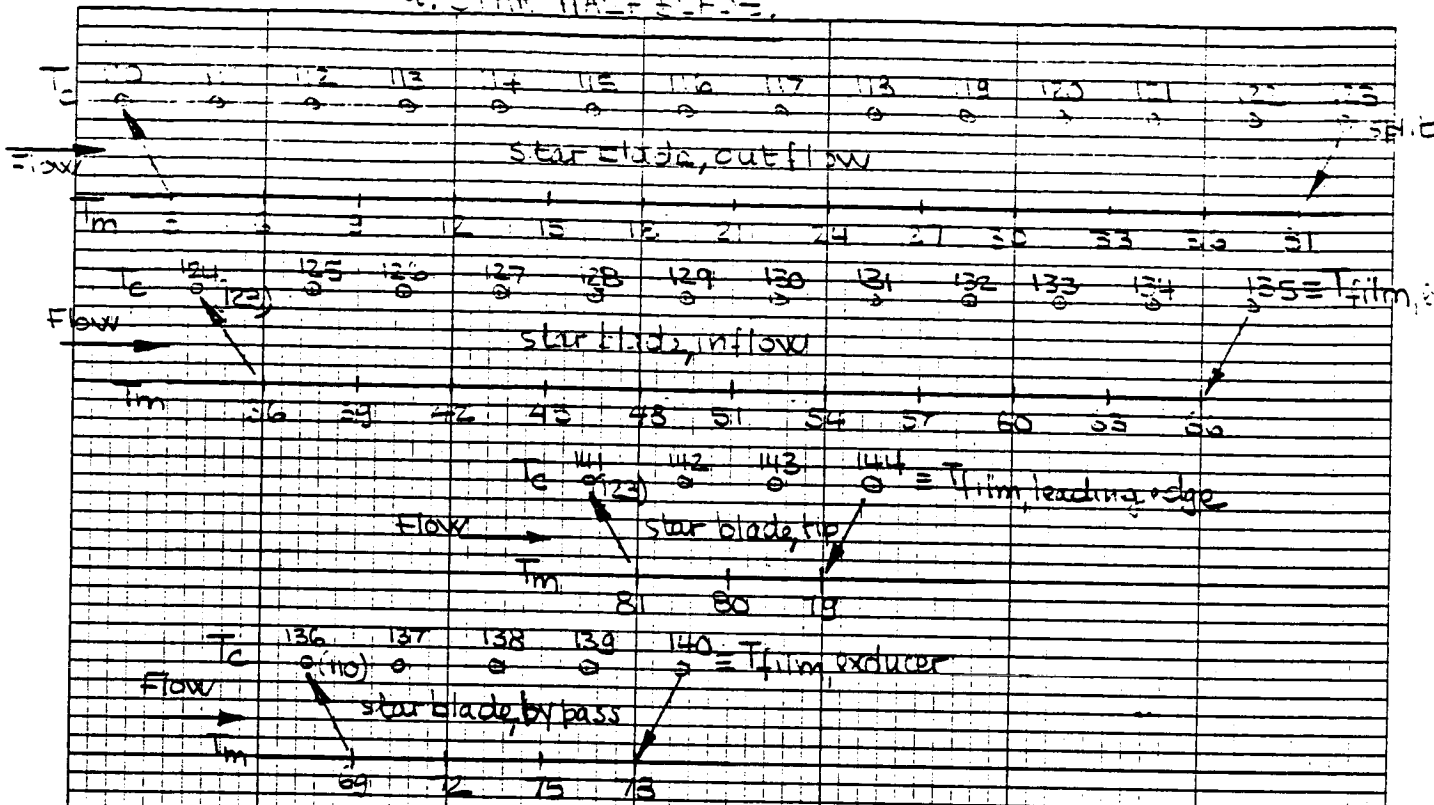
See Fig. 23

SOURCE: N. Anderson
May 16, 1981

G. Aigret

05-27-81

1. STAR HALF BLADE



2. EXDUCER HALF BLADE

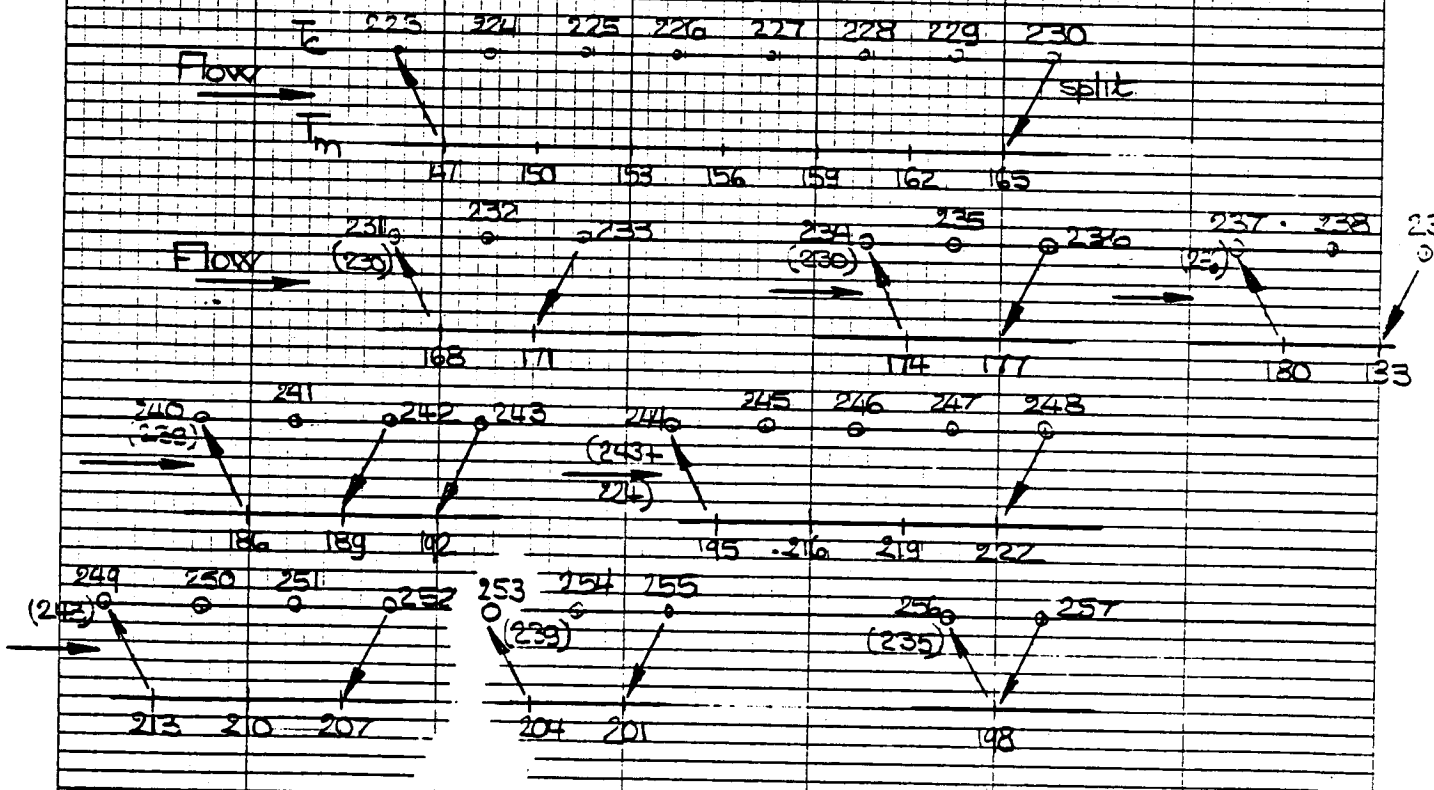


Fig. 28. Blade Heat Transfer Models: Coolant Flow Networks.

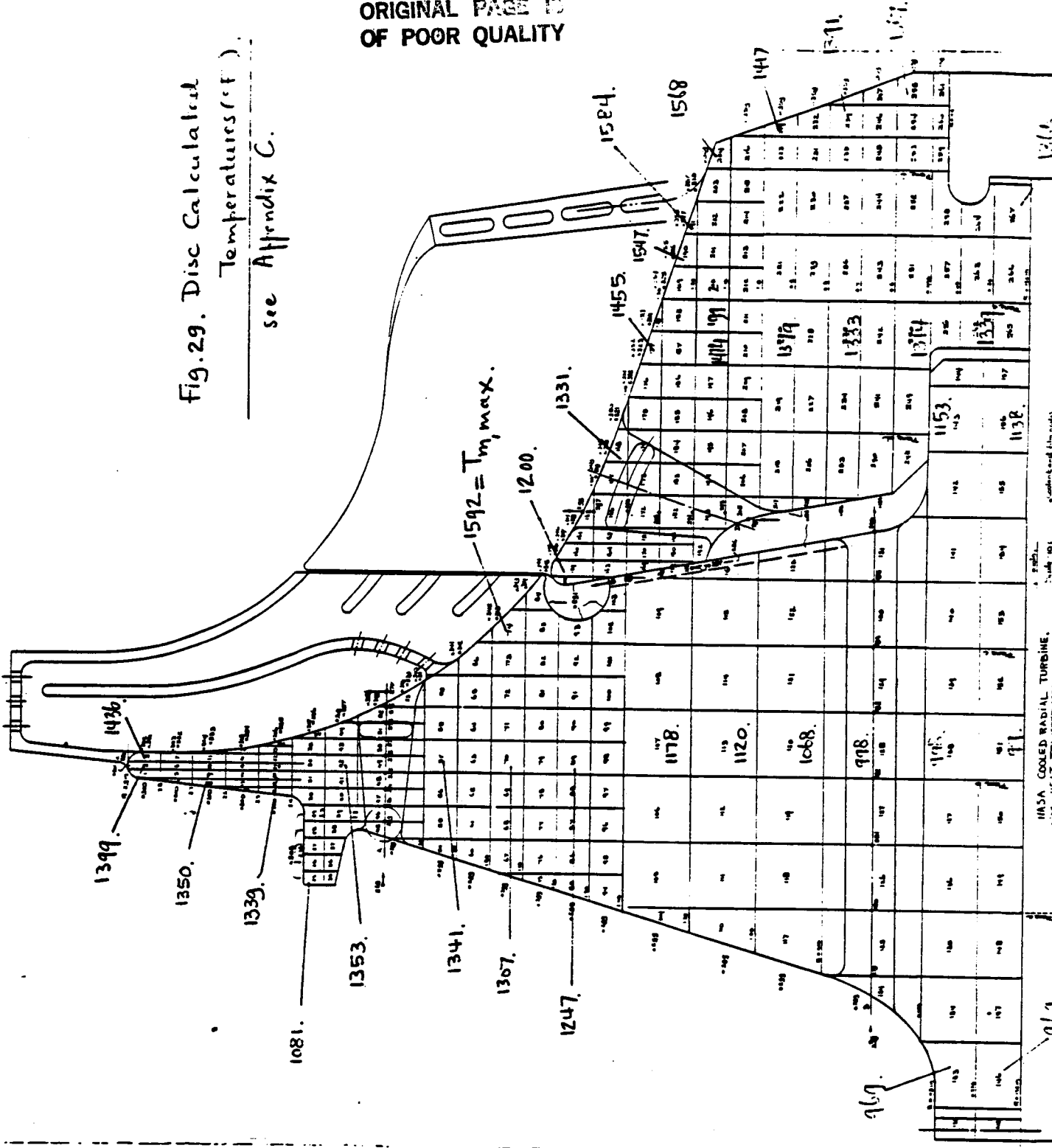
Continued
05-13-21

46 0702

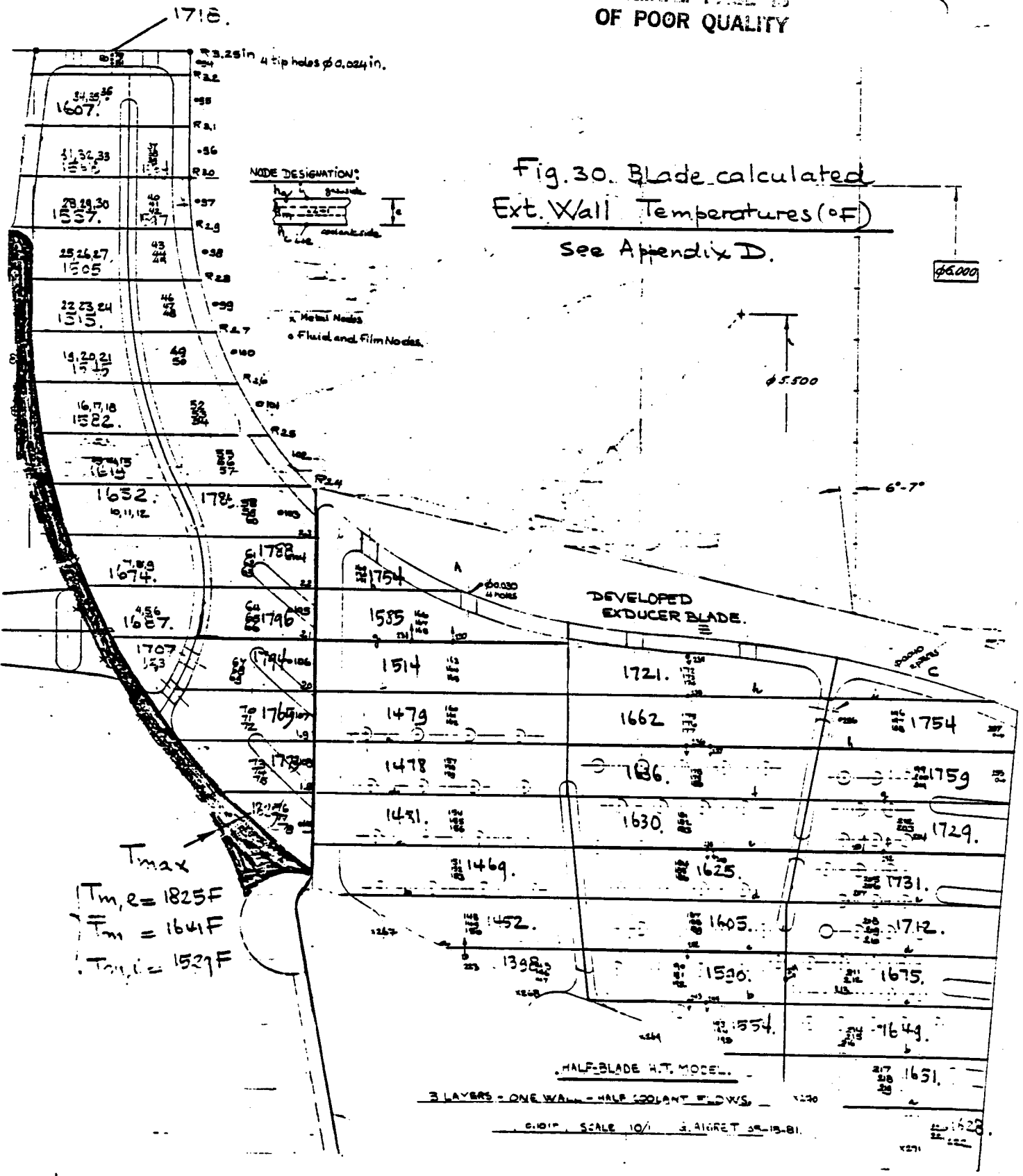
K&E
10 X 10 TO THE INCH, 7 X 10 INCHES
KEUFFEL & ESSER CO. MADE IN U.S.A.

ORIGINAL PAGE IS
OF POOR QUALITY

Fig. 29. Disc Calculated
Temperatures (°F).
see Appendix C.



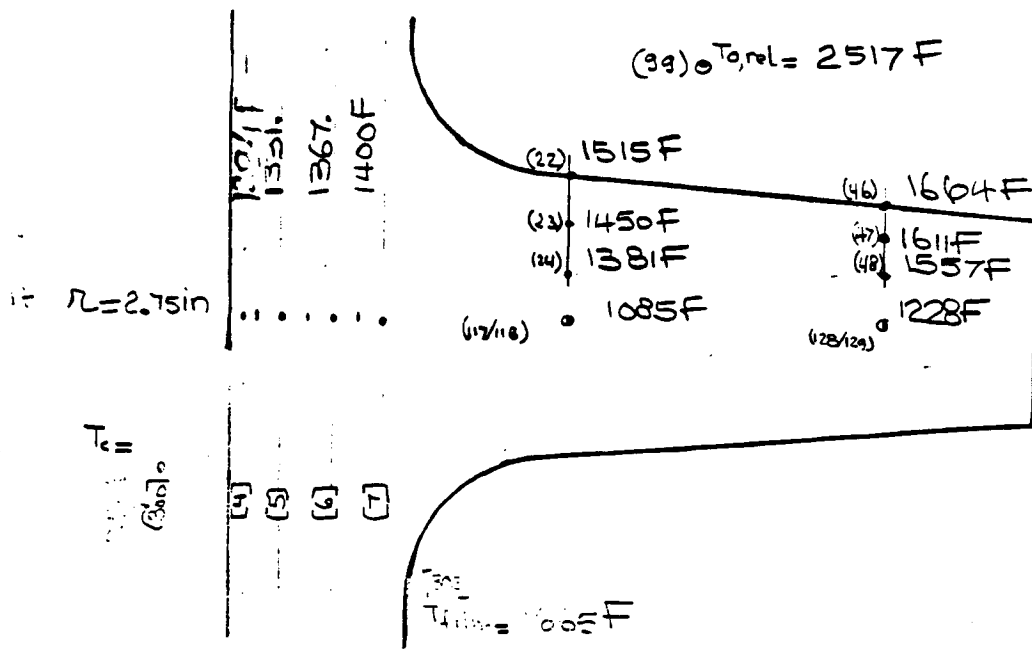
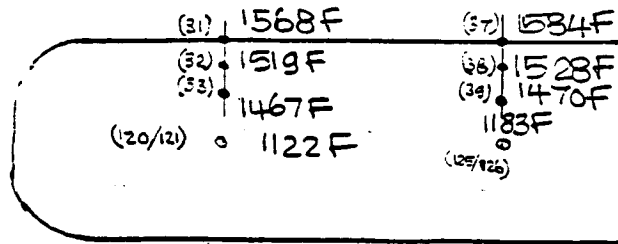
ORIGINAL PAGE IS
OF POOR QUALITY



ORIGINAL PAGE IS
OF POOR QUALITY

$T_{0,r} = 2546 F$

Section
at $r = 3.05 \text{ in}$



- () ... number from blade model.
- [] " " " " disc model.

8/1/67
3/1/68

Fig. 1.1.1.1. ...
...
...

ORIGINAL PAGE IS
OF POOR QUALITY

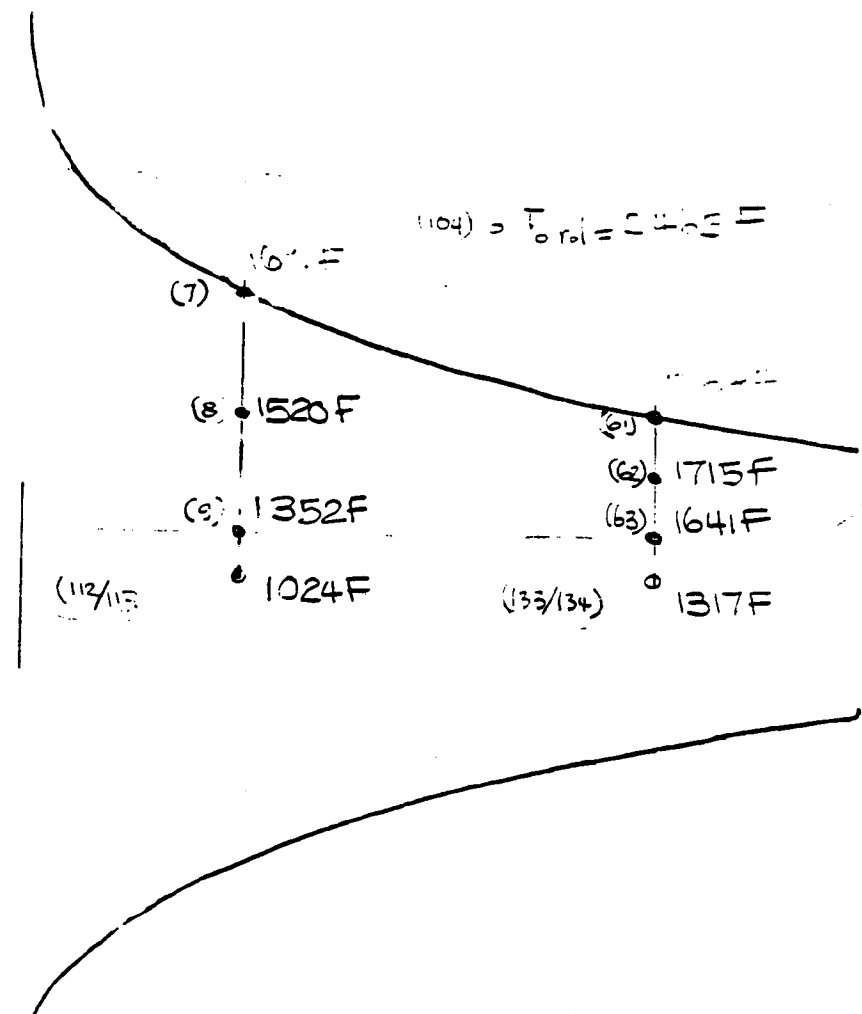
[40] 1259 F.

[41] 1306.

[42] 1353.

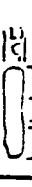
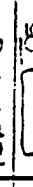

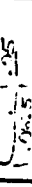

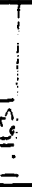
[43] 1402.

[44] 1454.



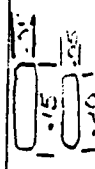


$(104) = T_{0rel} = 2465 =$

from data made
 $T_{film} = 2000$
 due to
 a factor
 5-10-51

Plane	Profile	Area in ²	Perimeter in	Hyd. Diam in	Mass Flow (lb/sec)	Mass Flux lb/sec/in ²	Temp OF	Press psia	Dyn Hd. Psi	Comments
S1	.030 gap				.15	.40	750	270	20	Flow rate to H.P.M. 2.23 (0.0014) (0.001)
S2	φ .11	.0095	.346	.11	.015	1.6	760	260	10	
S3		.0077	.3746	.08	.015	1.9	780	255	13	
S4	2φ .026	.0010			.003	3.0	970			$C_p = 1.7, C_{Df} = .3$
S5		.0104	.495	.084	.012	1.2	1020	243	9	
S6		.0015	.377	.080	.012	1.6	1260	235	10	
S7		.0016	.182	.057	.0036	3.5	1260	290	45	
S8	φ .0275	.0008	.086	.057	.0018	3.0	1260			$R_p = 1.92, C_{Df} = .3$
S9	φ .0275	.0006	.086	.075	.0016	3.7	1260			$R_p = 1.67, C_{Df} = .3$
S10	φ .0275	.0006	.086	.077	.0015	2.5	1260			$R_p = 1.67, C_{Df} = .3$
S11		.005	.171	.061	.0071	2.3	1260	237	32	
S12		.0076	.384	.079	.0071	1.2	1270	149	9	
S13	.61x .040	.023			.010	.36				
S14	.61x .032	.022			.010	.45				
A1	70x .030	.047			.10	2.0				$m = .01 / blade$
A2	70x .05	.173			.10	.58				$m = .01 / blade$

Plane	Profile	Area in ²	Perimeter in	Hyd. Diam. in	Mass Flow (lb/sec)	Mass Flux lb/sec/in ²	Temp OF	Press psia	Dyn Hd. Psi	Comments
E1	Ø.15	.0057	.471	.15	.010	2.26	950	247	25	Mach = .80 !?
E2	Ø.15	.0057	160	.15	.040	2.26	953	242	25	
E3	Ø.15	.02102	160	.0255	.005	4.90	970	135	87	
E4	Ø.16	.0057	.503	.16	.005	.011	954	237	0	
E5	Ø.16	.0057	.717	.01	.035	1.74	980	226	16	
E6	Ø.050	.0007	.1575	.05	.005	2.19	1005	229	28	
E7	Ø.050	.02176	.957	.05	.030	2.54	1005			
E8	Ø.050	.01996	.877	.091	.030	1.37	1010	243	11	Re = 1.57
E9	Ø.030	.00971	.094	.030	.021	2.96	1110			WALL THICKNESS, A = .017 PE = .757, d = .031
E10	Ø.030	.00971	.094	.030	.020	2.82	1070		13	WALL THICKNESS, A = .015 PE = .617, d = .031
E11	Ø.030	.00971	.094	.030	.0018	2.54	1110			Re = 1.35, Cp = .3
E12	Ø.030	.01321	.607	.037	.026	1.97	1100	219	18	Re = 1.90, Cp = .3
E13	Ø.030	.0235	1.017	.092	.0187	.80	1120	216	4	Re = 1.77, Cp = .3
E14	Ø.030	.00971	.094	.030	.0018	2.54	1150	155	10	Re = 1.77, Cp = .3
E15	Ø.010	.00126	.126	.040	.0034	2.70	1155	127	28	Re = 1.77, Cp = .8
E16	Ø.010	.00116	.357	.078	.0105	1.51	1160	120	24	WALL THICKNESS, A = .014 PE = .732, d = .031
E17	"				.0070	1.01	1180	120	14	WALL THICKNESS, A = .012 PE = .527, d = .031
E18	"				.0035	.50	1200	120	3	WALL THICKNESS, A = .006 PE = .317, d = .076
E19	"				.0027	.39	1220	120		Re = 1.80, Cp = .3
E20	"						1230	120		

ORIGINAL PAGE IS
OF POOR QUALITY

Plane	Profile	Area in ²	Perimeter in	Hyd. Diam in	Mass Flow (lb/sec)	Mass Flux lb/sec/in ²	Temp OF	Press psia	Dyn Hd. Psi	Comments
E100		.0004	3.57	.073	.0024	.49	1320	120		
E101		.0015	4.57	.083	0.0					
E102		.0115	5.37	.085	0.0					
E104	Ø .040	.00126	12.6	.070	-.0027	2.14	1000			Pg 1-55

ORIGINAL PAGE IS
OF POOR QUALITY

Engineering Report

REPORT T-5500
ISSUED 5/8/81

APPENDIX A

ROTOR EXTERNAL FLOW ANALYSIS

FROM PROGRAM P-229 PER C. RODGERS (03-24-81)

ORIGINAL PAGE IS
OF POOR QUALITY

ID	DS	TS	A	DELTA	GAMMA	UM	UH	LAM	ETA	NS	NM	N	O	Z
4	5.00	0.100	0.430	0.0	60.00	0.2000	0.7500	0.990	1.100	0.110	0.150	0.430	1.00	10.
AS	D	N	ALPHA	BETA	TT	TS	PT	PS	RO	VR	VW	U	VA	M REL
0.0	5.000	0.0	-0.50	-0.50	3077.2	2875.3	205.46	150.00	0.141	1085.0	1427.5	1410.1	1095.8	0.4329
1.568	4.946	0.108	-1.03	-1.03	3073.5	2872.6	204.21	149.25	0.140	1086.0	1422.2	1402.8	1085.8	0.4331
1.720	4.829	0.126	-1.42	-1.42	3062.8	2880.3	200.56	159.86	0.142	982.0	1394.0	1369.6	981.7	0.3911
2.049	4.670	0.192	-0.29	-0.29	3044.0	2891.5	194.34	153.12	0.143	815.6	1328.7	1324.6	815.6	0.3242
0.0	4.574	0.0	1.33	1.33	3031.3	2887.0	190.20	151.70	0.142	815.8	1278.5	1297.3	815.6	0.3246

ID	DS	TS	A	DELTA	GAMMA	UM	UH	LAM	ETA	NS	NM	N	O	Z
5	4.60	0.100	0.640	0.0	45.00	0.7800	0.6500	0.990	1.120	0.130	0.220	0.530	1.00	10.
AS	D	N	ALPHA	BETA	TT	TS	PT	PS	RO	VR	VW	U	VA	M REL
0.0	4.600	0.0	5.57	5.57	3017.4	2837.2	184.38	138.57	0.132	1215.0	1186.6	1304.6	1210.1	0.4880
1.500	4.519	0.114	3.95	3.95	3015.9	2833.9	183.88	137.76	0.131	1213.0	1198.2	1281.8	1210.1	0.4871
1.863	4.330	0.154	0.97	0.97	3010.0	2861.9	182.00	144.03	0.136	943.8	1212.2	1228.1	943.7	0.3772
2.231	4.040	0.257	-1.40	-1.40	2990.7	2866.7	175.95	144.60	0.136	786.1	1164.9	1145.7	785.8	0.3139
0.0	3.858	0.0	-1.58	-1.58	2976.4	2859.5	171.59	142.49	0.135	786.1	1115.9	1094.2	785.8	0.3143

ID	DS	TS	A	DELTA	GAMMA	UM	UH	LAM	ETA	NS	NM	N	O	Z
6	4.37	0.100	0.860	0.0	30.00	0.7800	0.6500	0.990	1.140	0.150	0.280	0.620	1.00	10.
AS	D	N	ALPHA	BETA	TT	TS	PT	PS	RO	VR	VW	U	VA	M REL
0.0	4.370	0.0	18.69	18.69	2951.1	2813.2	162.45	130.14	0.125	1301.3	822.4	1239.4	1232.6	0.5245
1.493	4.261	0.126	16.37	16.37	2951.5	2811.2	162.58	129.71	0.125	1284.7	846.4	1208.6	1232.6	0.5180
1.873	4.003	0.172	11.38	11.38	2957.3	2853.7	164.31	137.81	0.130	980.5	941.8	1135.3	961.2	0.3930
2.279	3.580	0.316	5.01	5.01	2943.6	2847.2	160.25	137.32	0.130	804.8	945.2	1015.4	801.7	0.3224
0.0	3.307	0.0	2.14	2.14	2930.0	2837.9	156.32	134.81	0.128	802.2	907.9	937.9	801.7	0.3219

ID	DS	TS	A	DELTA	GAMMA	UM	UH	LAM	ETA	NS	NM	N	Q	Z
7	4.28	0.080	1.070	0.0	15.00	0.700	0.6500	0.990	1.160	0.160	0.320	0.710	1.00	10.
AS	D	N	ALPHA	BETA	TT	TS	PT	PS	RO	VR	VW	U	VA	M REL
0.0	4.280	0.0	34.05	34.05	2890.2	2795.7	143.48	122.99	0.119	1382.1	440.0	1213.9	1145.2	0.5588
1.490	4.141	0.144	37.02	32.02	2890.7	2795.2	143.62	122.91	0.119	1350.7	458.3	1174.4	1145.2	0.5461
1.898	3.811	0.198	27.23	27.23	2907.4	2833.1	140.23	131.47	0.125	1004.6	621.0	1080.7	893.3	0.4035
2.401	3.271	0.361	19.82	19.82	2899.9	2837.9	146.15	132.21	0.126	790.8	659.4	927.6	744.0	0.3174
0.0	2.922	0.0	15.51	15.51	2887.8	2828.8	142.85	129.80	0.124	772.1	622.1	928.8	744.0	0.3183

ID	DS	TS	A	DELTA	GAMMA	UM	UH	LAM	ETA	NS	NM	N	Q	Z
8	4.25	0.070	1.300	0.0	0.0	0.9000	0.8000	0.990	1.160	0.200	0.330	0.820	1.00	10.
AS	D	N	ALPHA	BETA	TT	TS	PT	PS	RO	VR	VW	U	VA	M REL
0.0	4.250	0.0	47.55	47.55	2852.2	2796.0	133.42	121.66	0.118	1373.0	192.3	1205.4	926.7	0.5551
1.522	4.068	0.182	46.30	46.30	2849.8	2793.7	132.79	121.12	0.117	1341.3	184.0	1153.7	926.7	0.5425
1.746	3.656	0.230	43.24	43.24	2856.0	2808.4	134.40	124.32	0.120	1144.6	252.7	1036.8	833.8	0.4617
2.116	3.026	0.400	37.90	37.90	2851.5	2814.1	133.75	125.40	0.120	938.5	281.8	858.3	740.6	0.3782
0.0	2.626	0.0	34.04	34.04	2846.0	2807.8	131.83	123.83	0.119	893.7	244.6	744.9	740.6	0.3606

ID	DS	TS	A	DELTA	GAMMA	UM	UH	LAM	ETA	NS	NM	N	Q	Z
9	4.25	0.060	1.600	0.0	0.0	1.0000	1.0000	0.990	1.160	0.240	0.340	0.925	1.00	10.
AS	D	N	ALPHA	BETA	TT	TS	PT	PS	RO	VR	VW	U	VA	M REL
0.0	4.250	0.0	58.73	58.73	2823.1	2787.3	126.10	118.85	0.115	1453.6	-37.1	1205.4	754.5	0.5886
1.485	4.021	0.229	57.31	57.31	2823.1	2787.3	126.10	118.85	0.115	1396.9	-35.1	1140.6	754.5	0.5656
1.619	3.523	0.282	53.78	53.78	2823.1	2787.0	126.10	118.79	0.115	1281.9	-34.9	999.3	757.5	0.5191
1.831	2.836	0.418	47.70	47.70	2823.1	2786.4	126.10	118.68	0.115	1134.9	-35.0	804.4	763.8	0.4596
0.0	2.419	0.0	43.14	43.14	2823.1	2786.4	126.10	118.68	0.115	1046.7	-29.0	685.9	763.8	0.4239

NASA CRT 55

2-13-61

NASACRT.RJE

03/24/MI 16.06.51

190

F. M. L.	M. L.	D	VRB	VRM	VRP	VRB/VRT	VRM/VRT	VRP/VRT	ALPHA	PS/PI	DF
0.00	0.00	499	594.4	822.3	50.1	1.925	0.993	0.061	10.60	0.651	0.0
0.10	0.570	6563	718.0	895.9	172.0	1.908	1.000	0.257	9.85	0.627	0.0
0.20	0.810	5485	562.1	949.0	396.0	1.616	0.970	0.050	9.25	0.601	0.0
0.30	1.050	4396	172.5	818.6	451.0	1.276	0.937	0.021	8.65	0.575	0.0
0.40	1.290	3358	045.5	777.2	551.0	1.000	0.900	0.000	8.05	0.549	0.0
0.50	1.530	3102	045.5	730.4	551.0	0.740	0.867	0.000	7.45	0.523	0.0
0.60	1.770	2436	173.5	691.0	1020.2	0.561	0.832	0.000	6.85	0.497	0.0
0.70	2.010			651.0					6.25	0.471	0.0
0.80	2.250			611.0					5.65	0.445	0.0
0.90	2.490			571.0					5.05	0.419	0.0
1.00				531.0					4.45	0.393	0.0

F. M. L.	M. L.	D	VRB	VRM	VRP	VRB/VRT	VRM/VRT	VRP/VRT	ALPHA	PS/PI	DF
0.00	0.00	9	627.1	822.3	100.0	0.977	0.977	0.048	10.59	0.651	0.0
0.10	0.292	910	571.1	875.0	100.0	0.897	0.925	0.055	10.00	0.627	0.0
0.20	0.585	925	571.1	927.0	100.0	0.817	0.852	0.052	9.40	0.601	0.0
0.30	0.877	940	571.1	979.0	100.0	0.737	0.787	0.050	8.80	0.575	0.0
0.40	1.170	955	571.1	1031.0	100.0	0.657	0.724	0.048	8.20	0.549	0.0
0.50	1.462	970	571.1	1083.0	100.0	0.577	0.661	0.046	7.60	0.523	0.0
0.60	1.755	985	571.1	1135.0	100.0	0.497	0.598	0.044	7.00	0.497	0.0
0.70	2.047	1000	571.1	1187.0	100.0	0.417	0.535	0.042	6.40	0.471	0.0
0.80	2.340	1015	571.1	1239.0	100.0	0.337	0.472	0.040	5.80	0.445	0.0
0.90	2.632	1030	571.1	1291.0	100.0	0.257	0.409	0.038	5.20	0.419	0.0
1.00		1045	571.1	1343.0	100.0	0.177	0.346	0.036	4.60	0.393	0.0

hub

APPENDIX B

COOLED RADIAL TURBINES LITERATURE CONSULTED

1. Aigret, G., "Heat Transfer Promotion by Means of Triangularly Spaced Pins Between Plates", Solar Report T-4737 (Sept. 25, 1974).
2. Calvert, G.S. and Okapuu, U., "Design and Evaluation of a High-Temperature Radial Turbine", USAAVLABS Tech. Report 68-69, AD688164 (Jan. 1969).
3. Calvert, G.S., Beck, S.C. and Okapuu, U., "Design and Experimental Evaluation of a High-Temperature Radial Turbine", USAAMRDL Tech. Report 71-20, AD726466 (May 1971).
4. Okapuu, U. and Calvert, G.S., "An Experimental Cooled Radial Turbine", AGARD CP-73 (1970).
5. Monson, D.S. and Ewing, B.A., "High-Temperature Radial Turbine Demonstration", USA AVRADCOM-TR-80-D-6 (also AIAA 80-0301) (Apr. 1980).
6. Hamed, A., Baskharone, E. and Tabakoff, W., "A Numerical Study of the Temperature Field in a Cooled Radial Turbine Rotor", NASA CR137951 (also AIAA 76-44) (Mar. 1977).
7. Hamed, A., Sheoran, Y. and Tabakoff, W., "Stress Analysis Study in Cooled Radial Inflow Turbine", AIAA 78-94.
8. Branger, Vanle and Von der Nuell, "Veil Cooling of Radial Inflow Turbines", AiResearch Report K-500, Office of Naval Research Contract NONR 3685(00).
9. Petrick, E.N. and Smith, R.D., "Experimental Cooling of Radial Flow Turbines", ASME 54-A-245.
10. Swartwout, T.R., "Experimental Investigation of Heat Transfer by Forced Convection from the Hot Gas to a Cooled Stainless Steel Radial Inflow Gas Turbine Rotor", Report F-58-2, Jet Propulsion Center, Purdue Univ. (Jan. 1958).
11. Hogge, M.A., "Thermal Fields and Stresses in Cooled Turbine Blades by the Finite Element Method", V.K.I., Lecture Series 83 (1976).
12. LeGrives, E. and Genot, J., "Refroidissement des Aubes de Turbines par Metaux Liquides", AGARD CP-73 (1970).
13. Rogo, C., "High Tip Speed Radial Turbine", SAE 710552.
14. Dyban, "Cooled Diesel Supercharging Turbine", H.T. Soviet Research, Vol. 5, No. 3 (May 1973).
15. Rohlik, H.E., "Radial Inflow Turbines", Turbine Design and Application, Chapt. 10, Vol. 3, NASA SP-290.

16. Gusak, Y.M., "The Thermal and Stressed States of Rotors of Centripetal Gas Turbines", NASA TT-F-16,148 (1973-75).
17. Arnold, D.J. and Balje, O.E., "High Temperature Potential of Uncooled Radial Turbines", ASME 77-GT-46.
18. Poferl, D.J. and Svehla, R.A., "Thermodynamic and Transport Properties of Air and its Products of Combustion with ASTM-A-1 Fuel and Natural Gas at 20, 30 and 40 Atmospheres", NASA TN D-7488 (Dec. 1973).
19. Watanabe, I., Ariga, I. and Mashimo, T., "Effect of Dimensional Parameters of Impellers on Performance Characteristics of a Radial Inflow Turbine", ASME 70-GT-90.
20. Kostors, C.H., "Radial Flow Turbines", Elliott Company.
21. Rodgers, C., "Efficiency and Performance Characteristics of Radial Turbines", SAE 660754.
22. Mizumachi, N., "A Study of Radial Gas Turbines", IP-476, Univ. of Michigan (Nov. 1960).
23. Jaggi, H., "Temperaturverhältnisse im Laufrad einer Zentripetalturbine", M.T.Z. 22, Heft 5, pp. 175-181 (May 1961).
24. Bayley, F.J. and Turner, A.B., "High Temperature Turbines", 1970 AGARD Conference Proceedings No. 73, p. 12-6.
25. Prihodko, M. and Gologorski, I., "Diesel Turbine Combined Unit", Energomashinostroenie, No. 11, pp. 40-42 (1976).
26. McLallin, K.L. and Haas, J.E., "Experimental Performance and Analysis of 15.04 Centimeter Tip Diameter, Radial Inflow Turbine with Work Factor of 1.126 and Thick Blading", NASA Tech. Paper 1730 (Oct. 1980).
27. Rodgers, C., "Performance and Application of the Exducer Power Turbine", SAE 750208 (Feb. 1975).
28. Benson, R.S., Cartwright, W.G. and Woollatt, G., "Calculations of the Flow Distribution Within a Radial Turbine Rotor", Inst. of Mechanical Engineers, London (1970).
29. Rodgers, C., "Performance Development History - 10 kW Turboalternator", SAE 740849.
30. Takizawa, M., Sasaki, S. and Mizumachi, N., "A Study of an Advanced Automotive Radial Turbine - A Design Procedure Considering Rotor Loss Distributions and Exit Flow Patterns", ASME 77-GT-6 (Mar. 1977).
31. Lane, J.M., "Cooled Radial Inflow Turbines for Advanced Gas Turbine Engines", ASME 81-GT-213.

32. Van Fossen, G.J., "Heat Transfer Coefficients for Staggered Arrays of Short Pin Fins", ASME 81-GT-75.
33. Jen, H.F. and Sobanik, J.B., "Cooling Air Flow Characteristics in Gas Turbine Components", ASME 81-GT-76.
34. Daily, J.W., Ernst, W.D. and Asbedian, V.V., "Enclosed Rotating Disks with Superimposed Throughflow: Mean Steady and Periodic Unsteady Characteristics of the Induced Flow", MIT Hydrodynamics Laboratory Report 64 (April 1964).
35. Burggraf, F., "Experimental Heat Transfer and Pressure Drop with Two-Dimensional Discrete Turbulence Promoters Applied to Two Opposite Walls of a Square Tube", Augmentation of Convective Heat and Mass Transfer, ASME, pp. 70-79 (1970).
36. Norris, R.H., "Some Simple Approximate Heat-Transfer Correlations for Turbulent Flow in Ducts with Rough Surfaces", Augmentation of Convective Heat and Mass Transfer, ASME, pp. 16-26 (1970).

TEMPERATURE NODES AND CAPACITANCES

MODE	INC	CAP	CURV	RXC	EVX	NO.	TEMP	CAP. VAL.
1	1	1	1	1	1	99	1.5000E+03	0.0
100	1	1	1	1	1	99	1.5000E+03	0.0
199	1	1	1	1	1	69	1.5000E+03	0.0
268	1	2	0	1	0	9	9.6500E+02	0.0
277	1	2	0	0	0	8	9.5000E+02	0.0
278	1	2	0	0	0	8	9.5000E+02	0.0
286	1	2	0	0	0	8	9.5000E+02	0.0
287	1	2	0	0	0	8	9.5000E+02	0.0
291	1	2	0	0	0	4	9.5000E+02	0.0
292	1	2	0	0	0	6	9.5000E+02	0.0
298	0	0	0	0	0	9	9.5000E+02	0.0
299	0	0	0	0	0	9	9.5000E+02	0.0
300	0	0	0	0	0	9	9.5000E+02	0.0
301	0	0	0	0	0	9	9.5000E+02	0.0
302	0	0	0	0	0	9	9.5000E+02	0.0
303	0	0	0	0	0	9	9.5000E+02	0.0
304	0	0	0	0	0	9	9.5000E+02	0.0
305	0	0	0	0	0	9	9.5000E+02	0.0
306	0	0	0	0	0	9	9.5000E+02	0.0
307	0	0	0	0	0	9	9.5000E+02	0.0
308	0	0	0	0	0	9	9.5000E+02	0.0
309	0	0	0	0	0	9	9.5000E+02	0.0
310	0	0	0	0	0	9	9.5000E+02	0.0
311	0	0	0	0	0	9	9.5000E+02	0.0
312	0	0	0	0	0	9	9.5000E+02	0.0
313	0	0	0	0	0	9	9.5000E+02	0.0
314	0	0	0	0	0	9	9.5000E+02	0.0
315	0	0	0	0	0	9	9.5000E+02	0.0
316	0	0	0	0	0	9	9.5000E+02	0.0
317	0	0	0	0	0	9	9.5000E+02	0.0
318	0	0	0	0	0	9	9.5000E+02	0.0
319	0	0	0	0	0	9	9.5000E+02	0.0
320	0	0	0	0	0	9	9.5000E+02	0.0
321	0	0	0	0	0	9	9.5000E+02	0.0
322	0	0	0	0	0	9	9.5000E+02	0.0
323	0	0	0	0	0	9	9.5000E+02	0.0
324	0	0	0	0	0	9	9.5000E+02	0.0
325	0	0	0	0	0	9	9.5000E+02	0.0
326	0	0	0	0	0	9	9.5000E+02	0.0
327	0	0	0	0	0	9	9.5000E+02	0.0
328	0	0	0	0	0	9	9.5000E+02	0.0
329	0	0	0	0	0	9	9.5000E+02	0.0
330	0	0	0	0	0	9	9.5000E+02	0.0
331	0	0	0	0	0	9	9.5000E+02	0.0
332	0	0	0	0	0	9	9.5000E+02	0.0
333	0	0	0	0	0	9	9.5000E+02	0.0
334	0	0	0	0	0	9	9.5000E+02	0.0
335	0	0	0	0	0	9	9.5000E+02	0.0
336	0	0	0	0	0	9	9.5000E+02	0.0
337	0	0	0	0	0	9	9.5000E+02	0.0
338	0	0	0	0	0	9	9.5000E+02	0.0
339	0	0	0	0	0	9	9.5000E+02	0.0
340	0	0	0	0	0	9	9.5000E+02	0.0
341	0	0	0	0	0	9	9.5000E+02	0.0
342	0	0	0	0	0	9	9.5000E+02	0.0
343	0	0	0	0	0	9	9.5000E+02	0.0
344	0	0	0	0	0	9	9.5000E+02	0.0
345	0	0	0	0	0	9	9.5000E+02	0.0
346	0	0	0	0	0	9	9.5000E+02	0.0
347	0	0	0	0	0	9	9.5000E+02	0.0
348	0	0	0	0	0	9	9.5000E+02	0.0
349	0	0	0	0	0	9	9.5000E+02	0.0
350	0	0	0	0	0	9	9.5000E+02	0.0
351	0	0	0	0	0	9	9.5000E+02	0.0
352	0	0	0	0	0	9	9.5000E+02	0.0
353	0	0	0	0	0	9	9.5000E+02	0.0
354	0	0	0	0	0	9	9.5000E+02	0.0
355	0	0	0	0	0	9	9.5000E+02	0.0
356	0	0	0	0	0	9	9.5000E+02	0.0
357	0	0	0	0	0	9	9.5000E+02	0.0
358	0	0	0	0	0	9	9.5000E+02	0.0
359	0	0	0	0	0	9	9.5000E+02	0.0

PRECEDING PAGE BLANK NOT FILMED 223

COND	INC	MODE	INC	MODE	INC	CURV	EXV	NO.	COND.	VAL.
602	0	357	0	203	0	0	0	2	8940E-02	
603	1	358	0	25	1	0	0	2	7190E-01	
612	0	291	0	103	0	0	0	1	2650E-01	
613	0	291	0	93	0	0	0	1	3530E-01	
614	0	291	0	84	0	0	0	2	7950E-01	
615	0	286	0	240	0	0	0	7	8540E-01	
616	0	286	0	233	0	0	0	2	6180E-01	
617	0	286	0	225	0	0	0	1	4840E-01	
618	0	286	0	227	0	0	0	8	2900E-02	
620	0	286	0	123	0	0	0	1	5710E-01	
621	0	359	0	116	0	0	0	1	5010E-01	
622	0	359	0	261	0	0	0	2	1800E-02	
623	0	359	0	255	0	0	0	6	7700E-02	
624	0	359	0	247	0	0	0	8	6400E-02	
625	0	359	0	239	0	0	0	1	2070E-01	
626	0	359	0	232	0	0	0	1	2070E-01	
627	0	359	0	224	0	0	0	1	4640E-01	
632	0	158	0	291	0	0	0	2	3250E-01	
								1	6232E-01	

OTHER VALUES

LOC. INC NO. VALUE

228

VARIABLE LINES

ANS	INC	PRMA	INC	PRMP	INC	PRMC	INC	CODE	CURV	EXV	NO.	PARAM.	A	PARAM.	B	PARAM.	C
20268	1	41003	0	0	0	0	0	0	6	0	1	9	0.0	1	4580E+01	0.0	
20278	1	41003	0	0	0	0	0	0	6	0	1	8	0.0	3	8880E+01	0.0	
20287	1	41003	0	0	0	0	0	0	6	0	1	4	0.0	4	8600E+00	0.0	
20292	1	41003	0	0	0	0	0	0	6	0	1	6	0.0	3	4020E+01	0.0	
10292	0	10286	0	0	0	0	0	0	4	0	1	0	0.0	5	0000E+00	0.0	
10287	0	10286	0	0	0	0	0	0	4	0	1	0	0.0	5	0000E+00	0.0	

CURVE NO. 41 IN-792 THER.CON

0.0	0.0
8.0000E+02	7.9200E+00
1.0000E+03	1.0000E+01
1.2000E+03	1.0420E+01
1.4000E+03	1.1420E+01
1.6000E+03	1.2580E+01
1.8000E+03	1.4170E+01
2.0000E+03	1.6330E+01
0.0	0.0

OUTPUT CODES

I.D.	INC	NO.
10001	1	359
0	0	0

P-315 RMAL TRANSIENT ANALYSIS
NASA COOLING
PSEUDO SE-

P-315 THERMAL TRANSIENT ANALYSIS
NASA COOLING

REVISION NO.
RADIAL TURBINE

P-315 THERMAL TRANSIENT ANALYSIS
NASA COOLING
REVISION NO.
AXIAL TURBINE

CAP.	COND.	NODE	RCX	STU	DCND
1	1	2	0	0	0
	142	5			
	545	300			
2	1	1	0	0	0
	143	6			
	546	301			
	575	330			
3	2	2	0	0	0
	144	7			
	547	302			
	576	331			
4	3	3	0	0	0
	139	8			
	544	300			
5	3	4	0	0	0
	142	1			
	629	9			
6	4	5	0	0	0
	143	2			
	630	10			
7	5	6	0	0	0
	144	3			
	548	303			
	577	332			
	631	11			
8	6	9	0	0	0
	139	4			
	140	13			
	543	300			
9	6	8	0	0	0
	145	14			
	629	5			
10	7	9	0	0	0
	146	15			
	630	6			
11	8	10	0	0	0
	147	16			
	549	304			
	578	333			
	631	7			
12	9	13	0	0	0
	138	18			
	542	300			
13	9	12	0	0	0
	10	14			
	140	18			

CAP.	COND.	NODE	RCX	STU	DCND
14	10	13	0	0	0
	11	15			
	145	9			
	149	20			
15	11	14	0	0	0
	12	16			
	146	10			
	150	21			
16	12	15	0	0	0
	13	17			
	147	11			
	151	22			
17	13	16	0	0	0
	152	23			
	550	305			
	579	334			
18	14	19	0	0	0
	138	12			
	153	30			
	541	300			
19	14	18	0	0	0
	15	20			
	148	13			
	154	31			
20	15	19	0	0	0
	16	21			
	149	14			
	155	31			
21	16	20	0	0	0
	17	22			
	150	15			
	156	32			
22	17	21	0	0	0
	18	23			
	151	16			
	157	32			
23	18	22	0	0	0
	19	24			
	152	17			
	158	33			
24	19	23	0	0	0
	159	33			
	551	306			
	580	335			
25	20	26	0	0	0
	160	35			
	603	358			
26	20	25	0	0	0
	1	27			
	1	36			
	140	18			

CAP.	COND.	NODE	RCX	STU	DCND
27	21	26	0	0	0
	22	28			
	162	37			
	605	358			
28	22	27	0	0	0
	23	29			
	163	38			
	606	358			
29	23	28	0	0	0
	24	30			
	164	39			
	607	358			
30	24	29	0	0	0
	25	31			
	165	18			
	165	40			
31	25	30	0	0	0
	26	32			
	164	19			
	165	20			
	166	41			
32	26	31	0	0	0
	27	33			
	166	21			
	167	22			
	167	42			
33	27	32	0	0	0
	28	34			
	168	23			
	169	24			
	168	43			
34	28	33	0	0	0
	169	44			
	552	307			
	581	336			
35	29	36	0	0	0
	160	25			
36	29	35	0	0	0
	30	37			
	161	26			
37	30	36	0	0	0
	31	38			
	162	27			
38	31	37	0	0	0
	32	39			
	163	28			
	170	45			
39	32	38	0	0	0
	33	40			
	164	29			
	171	46			

ORIGINAL PAGE IS
OF POOR QUALITY

P-315 THERMAL TRANSIENT ANALY
NASA COOLED

CAP. COND. NODE RCX STU DCND

40 33 39 0 0 0
34 41
165 30
172 47

41 34 40 0 0 0
35 42
166 31
173 48

42 35 41 0 0 0
36 43
167 32
174 49

43 36 42 0 0 0
37 44
168 33
175 50

44 37 43 0 0 0
38 45
169 34
176 51
177 52
178 53
179 54
180 55
181 56
182 57
183 58
184 59
185 60
186 61
187 62
188 63
189 64
190 65
191 66
192 67
193 68
194 69
195 70
196 71
197 72
198 73
199 74
200 75
201 76
202 77
203 78
204 79
205 80
206 81
207 82
208 83
209 84
210 85
211 86
212 87
213 88
214 89
215 90
216 91
217 92
218 93
219 94
220 95
221 96
222 97
223 98
224 99
225 100

45 38 46 0 0 0
39 47
170 38
171 39
172 40
173 41
174 42
175 43
176 44
177 45
178 46
179 47
180 48
181 49
182 50
183 51
184 52
185 53
186 54
187 55
188 56
189 57
190 58
191 59
192 60
193 61
194 62
195 63
196 64
197 65
198 66
199 67
200 68
201 69
202 70
203 71
204 72
205 73
206 74
207 75
208 76
209 77
210 78
211 79
212 80
213 81
214 82
215 83
216 84
217 85
218 86
219 87
220 88
221 89
222 90
223 91
224 92
225 93
226 94
227 95
228 96
229 97
230 98
231 99
232 100

46 39 45 0 0 0
40 47
171 39
172 40
173 41
174 42
175 43
176 44
177 45
178 46
179 47
180 48
181 49
182 50
183 51
184 52
185 53
186 54
187 55
188 56
189 57
190 58
191 59
192 60
193 61
194 62
195 63
196 64
197 65
198 66
199 67
200 68
201 69
202 70
203 71
204 72
205 73
206 74
207 75
208 76
209 77
210 78
211 79
212 80
213 81
214 82
215 83
216 84
217 85
218 86
219 87
220 88
221 89
222 90
223 91
224 92
225 93
226 94
227 95
228 96
229 97
230 98
231 99
232 100

47 39 46 0 0 0
40 48
172 40
173 41
174 42
175 43
176 44
177 45
178 46
179 47
180 48
181 49
182 50
183 51
184 52
185 53
186 54
187 55
188 56
189 57
190 58
191 59
192 60
193 61
194 62
195 63
196 64
197 65
198 66
199 67
200 68
201 69
202 70
203 71
204 72
205 73
206 74
207 75
208 76
209 77
210 78
211 79
212 80
213 81
214 82
215 83
216 84
217 85
218 86
219 87
220 88
221 89
222 90
223 91
224 92
225 93
226 94
227 95
228 96
229 97
230 98
231 99
232 100

P-315 THERMAL TRANSIENT ANALYSE
NASA COOLED RADIAL TURB.

CAP. COND. NODE RCX STU DCND

51 43 50 0 0 0
44 52
176 44
183 58
482 274
491 275

52 44 51 0 0 0
45 53
184 58
483 275
492 276
584 309
583 338

53 45 52 0 0 0
46 55
185 59
484 276
493 277
555 310
584 339

54 46 55 0 0 0
47 56
177 45
178 46
187 61

55 46 54 0 0 0
47 56
177 45
178 46
187 61

56 47 55 0 0 0
48 57
179 47
180 48
188 62

57 48 56 0 0 0
49 58
181 49
182 50
189 63

58 49 57 0 0 0
50 59
183 51
184 52
190 64

P-315 THERMAL TRANSIENT ANALYSE
NASA COOLED RADIAL TURB.

CAP. COND. NODE RCX STU DCND

62 52 61 0 0 0
53 63
188 66
194 69

63 53 62 0 0 0
54 64
189 67
195 70

64 54 63 0 0 0
55 65
190 68
196 71

65 55 64 0 0 0
56 65
191 69
197 72

66 56 65 0 0 0
198 73
557 312
586 341

67 57 68 0 0 0
192 60
199 76
537 299

68 57 67 0 0 0
58 69
193 61
200 77

69 58 68 0 0 0
194 62
201 78

P-315 THERMAL TRANSIENT ANALYSE
NASA COOLED RADIAL TURB.

CAP. COND. NODE RCX STU DCND

70 59 69 0 0 0
60 71
195 63
202 79

71 60 70 0 0 0
61 72
196 64
203 80

72 61 71 0 0 0
62 73
197 65
204 81

73 62 72 0 0 0
63 74
198 66
205 82

74 63 73 0 0 0
64 75
199 67
206 83

75 64 74 0 0 0
65 76
200 77

76 65 75 0 0 0
66 77
201 78

77 66 76 0 0 0
67 78
202 79

P-315 ERMAL TRANSIENT ANALYSER REVISION NO
NASA COOLED RADIAL TURB.DI

P-315 THE L TRANSIENT ANALYSER
NASA COOLED RA

P-315 ERMAL TRANSIENT ANALYSER REVISION
NASA COOLED RADIAL TURB.

CAP. COND. NODE RCX STU DCND

75 64 76 0 0 0
207 85
536 299

76 64 75 0 0 0
65 77
199 67
208 86

77 65 76 0 0 0
66 78
200 68
209 87

78 66 77 0 0 0
67 79
201 69
210 88

79 67 78 0 0 0
68 80
202 70
211 89

80 68 79 0 0 0
69 81
203 71
212 90

81 69 80 0 0 0
70 82
204 72
213 91

82 70 81 0 0 0
71 83
205 73
214 92

83 71 82 0 0 0
72 84
206 74
215 93

84 72 83 0 0 0
73 85
559 314
588 343
614 291

85 73 86 0 0 0
74 87
216 94
535 299

86 73 85 0 0 0
74 87
208 76
217 95

87 74 86 0 0 0
75 88
209 77
218 96

CAP. COND. NODE RCX STU DCND

88 75 87 0 0 0
76 88
210 78
219 97

89 76 88 0 0 0
77 90
211 79
220 98

90 77 89 0 0 0
78 91
212 80
221 99

91 78 90 0 0 0
79 92
213 81
222 100

92 79 91 0 0 0
80 93
214 82
223 101

93 80 92 0 0 0
81 93
215 83
224 102
613 291

94 81 95 0 0 0
82 96
216 85
225 105
534 299

95 81 94 0 0 0
82 96
217 86
226 105

96 82 95 0 0 0
83 97
218 87
227 106

97 83 96 0 0 0
84 98
219 88
228 106

98 84 97 0 0 0
85 99
220 89
229 107

99 85 98 0 0 0
86 100
221 90
230 107

100 86 99 0 0 0
87 101
222 91
231 108

CAP. COND. NODE RCX STU DCND

101 87 100 0 0 0
88 102
223 92
232 108

102 88 101 0 0 0
89 103
224 93
233 109

103 89 102 0 0 0
90 104
225 94
226 95
234 109
470 163
612 291

104 90 105 0 0 0
91 106
227 96
228 97
235 110
533 299

105 90 104 0 0 0
91 105
92 107
227 96
228 97
237 112

106 91 105 0 0 0
92 106
93 108
229 98
230 99
238 113

107 92 106 0 0 0
93 107
94 109
231 100
232 101
239 114

108 93 107 0 0 0
94 108
95 109
233 102
234 103
240 115
471 169
472 179

109 94 108 0 0 0
95 110
96 112
236 105
242 118

110 95 111 0 0 0
96 112
97 113
237 106
243 119

111 95 110 0 0 0
96 111
97 112
236 105
242 118

112 96 111 0 0 0
97 113
98 114
237 106
243 119

P-315		RMAL TRANSIENT ANALYSER REVISION		P-315		RMAL TRANSIENT ANALYSER REVI		P-315		RMAL TRANSIENT ANALYSER REVI	
		NASA COOLED RADIAL TURB				NASA COOLED RADIAL				NASA COOLED RADIAL TURB O	
CAP. COND.	MODE	MODE	ROX	MODE	ROX	MODE	ROX	MODE	ROX	MODE	ROX
113	97 112	0	0	0	0	0	0	0	0	0	0
	98 114										
	238 107										
	244 120										
114	98 113	0	0	0	0	0	0	0	0	0	0
	99 115										
	239 108										
	245 121										
115	99 114	0	0	0	0	0	0	0	0	0	0
	100 116										
	240 109										
	246 122										
	473 192										
116	100 115	0	0	0	0	0	0	0	0	0	0
	247 123										
	620 286										
117	101 118	0	0	0	0	0	0	0	0	0	0
	241 110										
	248 125										
	531 299										
118	101 117	0	0	0	0	0	0	0	0	0	0
	102 119										
	242 111										
	249 126										
119	102 118	0	0	0	0	0	0	0	0	0	0
	103 120										
	243 112										
	250 127										
120	103 119	0	0	0	0	0	0	0	0	0	0
	104 121										
	244 113										
	251 128										
121	104 120	0	0	0	0	0	0	0	0	0	0
	105 122										
	245 114										
	252 129										
122	105 121	0	0	0	0	0	0	0	0	0	0
	106 123										
	246 115										
	253 130										
123	106 122	0	0	0	0	0	0	0	0	0	0
	247 116										
	254 131										
	619 286										
124	107 125	0	0	0	0	0	0	0	0	0	0
	255 134										
	494 278										
	502 279										
	530 299										
125	107 124	0	0	0	0	0	0	0	0	0	0
	107 126										

P-315 FORMAL TRANSIENT ANALYSER REVISION
NASA COOLED RADIAL TURB

CAP. COND. NODE RCX STU DCND

152 132 151 0 0 0
133 153
270 139

153 133 152 0 0 0
134 154
271 140

154 134 153 0 0 0
135 155
272 141

155 135 154 0 0 0
136 156
273 142

156 136 155 0 0 0
137 157
274 143

157 137 156 0 0 0
275 144

158 276 159 0 0 0
632 291

159 276 158 0 0 0
277 160
372 163
560 315
589 344

160 277 159 0 0 0
278 161
373 164
561 316
590 345

161 278 160 0 0 0
279 162
374 165
562 317
591 346

162 279 161 0 0 0
375 166
523 297
529 298
563 318
592 347

163 280 164 0 0 0
372 159
376 169
470 103
513 290
517 291

164 280 163 0 0 0
281 165
373 160
377 170

P-315 THERM/

RANSIENT ANALYSER REV
NASA COOLED RADIAL

CAP. COND. NODE RCX STU DCND

165 281 164 0 0 0
282 166
374 161
378 171

166 282 165 0 0 0
283 167
375 162
379 172
522 296
528 297

167 283 166 0 0 0
284 168
380 173
564 319
593 348

168 284 167 0 0 0
381 174
565 320
594 349

169 285 170 0 0 0
376 163
382 179
471 109
512 289
516 290

170 285 169 0 0 0
286 171
377 164
383 180

171 286 170 0 0 0
287 172
378 165
384 181

172 287 171 0 0 0
288 173
379 166
385 182
521 295
527 296

173 288 172 0 0 0
289 174
380 167
386 183

174 289 173 0 0 0
290 175
381 168
387 184

175 290 174 0 0 0
291 176
388 185
566 321
595 350

176 290 175 0 0 0
291 177
389 186
596 351

P-315

ORMAL TRANSIENT
NASA

ALYSER REVISION
LED RADIAL TURB

CAP. COND. NODE RCX STU DCND

177 389 186 0 0 0
567 322
596 351

178 292 176 0 0 0
391 187
568 323
597 352

179 392 188 0 0 0
569 324
598 353

180 294 180 0 0 0
382 169
472 109
511 288
515 289

181 294 179 0 0 0
295 181
383 170
393 192

182 296 181 0 0 0
297 183
385 172
395 193
520 294
526 295

183 297 182 0 0 0
298 184
386 173
396 194

184 298 183 0 0 0
299 185
387 174
397 195

185 299 184 0 0 0
300 186
388 175
398 196

186 300 185 0 0 0
301 187
399 197

187 301 186 0 0 0
302 188
391 177
400 198

188 302 187 0 0 0
303 189
392 178
401 199

P-315 THERMAL TRANSIENT ANALYSER REVISION 1
NASA COOLED RADIAL TL

CAP. COND. NODE RCX STU DCND

189 0 0 0 0
303 188
304 190
402 200
570 325
599 354

190 0 0 0 0
304 189
403 201
571 326
600 355

191 0 0 0 0
404 202
572 327
601 356

192 0 0 0 0
306 193
393 180
394 181
473 115
510 287
514 288

193 0 0 0 0
306 192
307 194
395 182
405 205
512 293
525 294

194 0 0 0 0
307 193
308 195
396 183
406 206

195 0 0 0 0
308 194
309 196
397 184
407 207

196 0 0 0 0
309 195
310 197
398 185
408 208

197 0 0 0 0
310 196
311 198
399 186
409 209

198 0 0 0 0
311 197
312 199
400 187
410 210

199 0 0 0 0
312 198
313 200
401 188
411 211

P-315 THERMAL TRANSIENT ANALYSER REV
NASA COOLED RADIAL

CAP. COND. NODE RCX STU DCND

201 0 0 0 0
314 200
315 202
403 190
413 213

202 0 0 0 0
315 201
316 203
404 191
414 214

203 0 0 0 0
316 202
317 204
415 215
573 328
602 357

204 0 0 0 0
317 203
416 216
574 329

205 0 0 0 0
318 205
405 193
417 217
518 292
524 293

206 0 0 0 0
318 205
319 207
406 194
418 218

207 0 0 0 0
319 206
320 208
407 195
628 218

208 0 0 0 0
320 207
321 209
408 196
419 219

209 0 0 0 0
321 208
322 210
409 197
420 219

210 0 0 0 0
322 209
323 211
410 198
421 220

211 0 0 0 0
323 210
324 212
411 199
422 220

P-315 THERMAL TRANSIENT ANALYSER REVISION 1
NASA COOLED RADIAL TURB. D

CAP. COND. NODE RCX STU DCND

214 0 0 0 0
326 213
327 215
414 202
425 222

215 0 0 0 0
327 214
328 216
415 203
426 222

216 0 0 0 0
328 215
416 204
427 223
627 359

217 0 0 0 0
329 218
417 205
428 225
618 286

218 0 0 0 0
329 217
330 219
418 206
429 226
628 207

219 0 0 0 0
330 218
331 220
419 208
420 209
430 227

220 0 0 0 0
331 219
332 221
421 210
422 211
431 228

221 0 0 0 0
332 220
333 222
423 212
424 213
432 229

222 0 0 0 0
333 221
334 223
425 214
426 215
433 230

223 0 0 0 0
334 222
335 224
427 216
434 231

224 0 0 0 0
335 223
435 232
626 359

P-315 THERMAL TRANSIENT ANALYSER REVISION 1
NASA COOLED RADIAL TL

CAP. COND. NODE RCX STU DCND

212 0 0 0 0
324 211
325 213
412 200
423 221

213 0 0 0 0
325 211
326 212
413 201
424 222

214 0 0 0 0
326 212
327 214
414 202
425 223

215 0 0 0 0
327 215
328 217
415 203
426 224

216 0 0 0 0
328 218
329 220
416 204
427 225

217 0 0 0 0
329 219
330 221
417 205
428 226

218 0 0 0 0
330 220
331 222
418 206
429 227

219 0 0 0 0
331 221
332 223
419 207
430 228

220 0 0 0 0
332 222
333 224
420 208
431 229

221 0 0 0 0
333 223
334 225
421 209
432 230

222 0 0 0 0
334 224
335 226
422 210
433 231

P-316 THERMAL TRANSIENT ANALYSER REVISED NASA COOLED RADIAL TURBINE		P-315 THERMAL TRANSIENT ANALYSER REVISED NASA COOLED RADIAL TURBINE		P-315 THERMAL TRANSIENT ANALYSER REVISED NASA COOLED RADIAL TURBINE	
CAP.	COND. NODE RCX STU DCND	CAP.	COND. NODE RCX STU DCND	CAP.	COND. NODE RCX STU DCND
226	336 225 337 227 429 218 436 233	239	348 238 442 232 449 246 624 359	253	360 252 361 254 454 244 460 258
227	337 226 338 228 430 219 437 234	240	349 241 443 233 450 248 615 286	254	361 253 362 255 456 246 462 260
228	338 227 339 229 431 220 438 235	241	349 240 350 242 444 234 451 249	255	362 254 457 247 463 261 622 359
229	339 228 340 230 432 221 439 236	242	350 241 351 243 445 235 452 250	256	363 257 458 250 464 262
230	340 229 341 231 433 222 440 237	243	351 242 352 244 446 236 453 251	257	363 258 364 258 459 231 465 263
231	341 230 342 232 434 223 441 238	244	352 243 353 245 447 237 454 252	258	364 257 365 259 460 252 466 264
232	342 231 435 224 442 239 625 359	245	353 244 354 246 448 238 455 253	259	365 258 366 260 461 253
233	343 234 436 226 443 240 616 286	246	354 245 355 247 449 239 456 254	260	366 259 367 261 462 254
234	343 233 344 235 437 227 444 241	247	355 246 457 255 623 359	261	367 260 463 255 621 359
235	344 234 345 236 438 228 445 242	248	356 249 450 240	262	368 263 464 256 467 265
236	345 235 346 237 439 229 446 243	249	356 248 357 250 451 241 474 143	263	368 262 369 264 465 257 468 266
237	346 236 347 238 440 230 447 244	250	357 249 358 251 452 242 458 256	264	369 263 466 258 469 267
238	347 237 348 239 441 231 448 245	251	358 250 359 252 453 243 459 257	265	370 266 467 262
		252	251	266	370 265 371 267

ORIGINAL PAGE IS
OF POOR QUALITY

P-315 THERMAL TRANSMISSION ANALYSER (REV. 11/69) B
DATA COOLED RADIAL

P-315 THERMAL TRANSMISSION ANALYSER (REV. 11/69) B
DATA COOLED RADIAL

GAP COND. NODE RCX STU DCOND

GAP	COND.	NODE	RCX	STU	DCOND	GAP	COND.	NODE	RCX	STU	DCOND
267	471	266	1	1	1	296	521	162	1	1	1
	464	264				296	522	166			
268	476	45	1	1	1	297	523	162	1	1	1
269	477	46	1	1	1						
270	478	47	1	1	1						
271	479	48	1	1	1						
272	480	49	1	1	1						
273	481	50	1	1	1						
274	482	51	1	1	1						
275	483	52	1	1	1						
276	484	53	1	1	1						
278	494	124	1	1	1						
279	495	125	1	1	1						
280	496	126	1	1	1						
281	497	127	1	1	1						
282	498	128	1	1	1						
283	499	129	1	1	1						
284	500	130	1	1	1						
285	501	131	1	1	1						
287	510	192	1	1	1						
288	511	179	1	1	1						
289	512	169	1	1	1						
290	513	163	1	1	1						
292	518	205	1	1	1						
293	519	193	1	1	1						
294	520	182	1	1	1						

COUNT PREV INC NEXT INC MIN RC
300 3.7500E-01 3.7500E-01 1.5000E+00

311 ALY TEMPERATURES (°F)

1	1.3512E+03	1.3992E+03	1.4359E+03	1.2935E+03	1.3306E+03	1.3665E+03	1.4003E+03	1.2829E+03	1.3172E+03	1.3504E+03
11	1.3825E+03	1.2507E+03	1.3128E+03	1.3128E+03	1.3428E+03	1.3720E+03	1.4001E+03	1.2515E+03	1.2810E+03	1.3101E+03
21	1.3385E+03	1.3667E+03	1.3944E+03	1.4216E+03	1.0811E+03	1.0925E+03	1.1147E+03	1.1479E+03	1.1948E+03	1.2678E+03
31	1.3141E+03	1.3616E+03	1.4102E+03	1.4594E+03	1.0976E+03	1.1129E+03	1.1397E+03	1.1757E+03	1.2128E+03	1.2591E+03
41	1.3055E+03	1.3530E+03	1.4021E+03	1.4535E+03	1.1560E+03	1.1959E+03	1.2375E+03	1.2784E+03	1.3219E+03	1.3654E+03
51	1.4123E+03	1.4591E+03	1.4928E+03	1.5124E+03	1.1898E+03	1.2624E+03	1.3407E+03	1.4258E+03	1.5195E+03	1.6125E+03
61	1.1893E+03	1.2566E+03	1.3282E+03	1.4049E+03	1.4880E+03	1.5789E+03	1.6778E+03	1.7832E+03	1.8438E+03	1.9067E+03
71	1.3723E+03	1.4409E+03	1.5130E+03	1.5918E+03	1.0786E+03	1.1234E+03	1.1735E+03	1.2256E+03	1.2787E+03	1.3316E+03
81	1.3828E+03	1.4293E+03	1.4647E+03	1.4770E+03	1.0742E+03	1.1159E+03	1.1600E+03	1.2036E+03	1.2474E+03	1.2878E+03
91	1.3230E+03	1.3463E+03	1.3461E+03	1.0710E+03	1.1044E+03	1.1450E+03	1.1787E+03	1.2162E+03	1.2447E+03	1.2693E+03
101	1.2792E+03	1.2662E+03	1.2013E+03	1.0382E+03	1.0731E+03	1.1301E+03	1.1778E+03	1.2072E+03	1.1866E+03	1.0194E+03
111	1.0504E+03	1.0896E+03	1.1198E+03	1.1323E+03	1.1183E+03	1.0867E+03	9.9883E+02	1.0243E+03	1.0493E+03	1.0681E+03
121	1.0751E+03	1.0664E+03	1.0421E+03	9.6255E+02	9.7049E+02	9.8106E+02	9.9843E+02	1.0281E+03	1.0025E+03	1.0022E+03
131	9.9758E+02	9.6906E+02	9.6900E+02	9.6856E+02	135	136	137	138	139	140
141	1.0370E+03	1.0952E+03	1.1531E+03	1.1505E+03	9.6919E+02	9.6927E+02	9.7013E+02	9.7485E+02	9.8221E+02	9.9045E+02
151	9.9875E+02	1.0078E+03	1.0210E+03	1.0464E+03	1.0941E+03	1.1383E+03	1.1433E+03	1.1899E+03	1.2003E+03	1.0160E+03
161	1.2221E+03	1.2258E+03	1.1860E+03	1.1951E+03	1.2033E+03	1.2145E+03	1.2828E+03	1.3306E+03	1.3701E+03	1.4176E+03
171	1.1839E+03	1.1956E+03	1.2612E+03	1.3200E+03	1.3798E+03	1.4203E+03	1.4554E+03	1.5059E+03	1.5585E+03	1.6191E+03
181	1.1670E+03	1.1776E+03	1.2405E+03	1.2978E+03	1.3506E+03	1.3961E+03	1.4401E+03	1.4849E+03	1.5220E+03	1.5472E+03
191	1.5842E+03	1.1479E+03	1.1627E+03	1.2221E+03	1.2738E+03	1.3250E+03	1.3699E+03	1.4143E+03	1.4539E+03	1.4904E+03
201	1.5220E+03	1.5524E+03	1.5727E+03	1.5681E+03	205	206	207	208	209	210
211	1.4218E+03	1.4596E+03	1.4829E+03	1.5048E+03	1.5108E+03	1.4910E+03	1.5222E+03	1.3023E+03	1.3404E+03	1.3895E+03
221	1.4400E+03	1.4678E+03	1.4464E+03	1.4170E+03	225	226	227	228	229	230
231	1.4220E+03	1.4036E+03	1.1085E+03	1.2380E+03	235	236	237	238	239	240
241	1.2125E+03	1.3186E+03	1.3746E+03	1.3971E+03	245	246	247	248	249	250
					1.3916E+03	1.3815E+03	1.3688E+03	1.0918E+03	1.1919E+03	1.3138E+03

251	1.3639E+03	252	1.3849E+03	253	1.3832E+03	254	1.3766E+03	255	1.3667E+03	256	1.3289E+03	257	1.3589E+03	258	1.3762E+03	259	1.3801E+03	260	1.3752E+03
261	1.3667E+03	262	1.3386E+03	263	1.3865E+03	264	1.3692E+03	265	1.3428E+03	266	1.3557E+03	267	1.3660E+03	268	9.6500E+02	269	9.6599E+02	270	9.6719E+02
271	9.6859E+02	272	9.7021E+02	273	9.7204E+02	274	9.7408E+02	275	9.7636E+02	276	9.7887E+02	277	9.8155E+02	278	9.8500E+02	279	9.8500E+02	280	9.5039E+02
281	9.6076E+02	282	9.5123E+02	283	9.5180E+02	284	9.5240E+02	285	9.5299E+02	286	9.5352E+02	287	9.5852E+02	288	9.6267E+02	289	9.6696E+02	290	9.7140E+02
291	9.7610E+02	292	9.5852E+02	293	9.5952E+02	294	9.6054E+02	295	9.6164E+02	296	9.6281E+02	297	9.6408E+02	298	9.6540E+02	299	9.5800E+02	300	9.5000E+02
301	1.6500E+03	302	1.6530E+03	303	1.6650E+03	304	1.6860E+03	305	1.7140E+03	306	1.7470E+03	307	1.7840E+03	308	1.8280E+03	309	1.8750E+03	310	1.9240E+03
311	1.9800E+03	312	2.0390E+03	313	2.1030E+03	314	2.1720E+03	315	2.2400E+03	316	2.3100E+03	317	2.3800E+03	318	2.4500E+03	319	2.5200E+03	320	2.5900E+03
321	1.4500E+03	322	1.5250E+03	323	1.6000E+03	324	1.6800E+03	325	1.7600E+03	326	1.8250E+03	327	1.8900E+03	328	1.9500E+03	329	2.0100E+03	330	2.0700E+03
331	1.4670E+03	332	1.4640E+03	333	1.4750E+03	334	1.4900E+03	335	1.5080E+03	336	1.5180E+03	337	1.5240E+03	338	1.5220E+03	339	1.5280E+03	340	1.6000E+03
341	1.6200E+03	342	1.6400E+03	343	1.6500E+03	344	1.6300E+03	345	1.6490E+03	346	1.6680E+03	347	1.6870E+03	348	1.7050E+03	349	1.7240E+03	350	1.7430E+03
351	1.4620E+03	352	1.4810E+03	353	1.5000E+03	354	1.5180E+03	355	1.5370E+03	356	1.5560E+03	357	1.5750E+03	358	1.5940E+03	359	1.6130E+03	360	1.6320E+03

CAPACITANCES

271	5.4675E+00	272	5.4675E+00	273	5.4675E+00	274	5.4675E+00	275	5.4675E+00	276	5.4675E+00	278	5.4675E+00	279	5.4675E+00	280	5.4675E+00	281	5.4675E+00
282	1.4580E+01	283	1.4580E+01	284	1.4580E+01	285	1.4580E+01	287	1.4580E+01	288	1.4580E+01	289	1.4580E+01	290	1.4580E+01	292	1.4580E+01	293	1.4580E+01
294	1.2758E+01	295	1.2758E+01	296	1.2758E+01	297	1.2758E+01	298	1.2758E+01	299	1.2758E+01	300	1.2758E+01	301	1.2758E+01	302	1.2758E+01	303	1.2758E+01

CONDUCTANCES

7.423	0	2	7.5922E+00	3	6.9519E+00	4	7.0737E+00	5	7.1901E+00	6	6.66	7	6.7690E+00	8	6.8740E+00	9	6.3046E+00	10	6.4008E+00
-------	---	---	------------	---	------------	---	------------	---	------------	---	------	---	------------	---	------------	---	------------	----	------------

121	122	123	124	125	126	127	128	129	130
1.2330E-04	1.1221E-04	5.6432E-05	1.2999E-04	4.9203E-05	8.4925E-05	5.7856E-05	7.7591E-05	7.7089E-05	7.9936E-05
131	132	133	134	135	136	137	138	139	140
6.1549E-05	9.2339E-03	3.0437E-03	5.5634E-06	1.1521E-04	1.8967E-04	2.0657E-04	5.2540E-04	3.1370E-04	2.0020E-04
141	142	143	144	145	146	147	148	149	150
1.0899E-04	1.9213E-04	3.6665E-04	2.3664E-03	9.1833E-03	1.8330E-03	3.1251E-04	2.6807E-04	2.3812E-04	4.4604E-04
151	152	153	154	155	156	157	158	159	160
3.4062E-04	3.6760E-04	2.6451E-04	2.3827E-04	3.0472E-04	4.7508E-04	1.4873E-03	6.4206E-05	4.7291E-05	7.8090E-06
161	162	163	164	165	166	167	168	169	170
1.0134E-04	4.8512E-05	2.3385E-04	2.8508E-05	3.1703E-04	1.5514E-06	5.0951E-05	4.7512E-05	2.8316E-04	3.5339E-04
171	172	173	174	175	176	177	178	179	180
2.9717E-04	8.9782E-05	7.6853E-05	8.9634E-05	4.4123E-05	8.8188E-05	6.8023E-05	1.2028E-04	3.9256E-04	3.6944E-04
181	182	183	184	185	186	187	188	189	190
4.9892E-04	1.1991E-04	9.5699E-05	1.1416E-04	1.0666E-04	1.1715E-04	1.2725E-04	8.7041E-05	8.2348E-05	8.9791E-05
191	192	193	194	195	196	197	198	199	200
7.0987E-05	1.9879E-04	1.4091E-04	1.3549E-04	1.4964E-04	1.6326E-04	1.5638E-04	1.6943E-04	1.3929E-04	1.7087E-04
201	202	203	204	205	206	207	208	209	210
1.6129E-04	1.2135E-04	7.1566E-05	6.3759E-05	1.2572E-04	1.8552E-04	1.6412E-04	2.1216E-04	1.9986E-04	2.6707E-04
211	212	213	214	215	216	217	218	219	220
2.5069E-04	2.4232E-04	2.1700E-04	2.2715E-04	2.1323E-04	1.0909E-04	1.3897E-04	1.5547E-04	2.1132E-04	2.3381E-04
221	222	223	224	225	226	227	228	229	230
2.9331E-04	2.5066E-04	2.8649E-04	2.6402E-04	6.5613E-05	1.1953E-04	2.0168E-04	3.3349E-04	3.7692E-04	4.2434E-04
231	232	233	234	235	236	237	238	239	240
5.3039E-04	4.8555E-04	7.6479E-05	2.1702E-04	4.1435E-04	5.9412E-04	6.3585E-04	9.6400E-04	6.4335E-04	5.7687E-05
241	242	243	244	245	246	247	248	249	250
2.2627E-04	5.2979E-04	7.5850E-04	1.0476E-03	1.3596E-03	1.3636E-03	8.1943E-04	1.2500E-04	2.0040E-04	6.2542E-04
251	252	253	254	255	256	257	258	259	260
1.1838E-03	1.5587E-03	3.1580E-03	2.3931E-03	1.7596E-03	1.0617E-03	1.9337E-03	1.8994E-03	3.7967E-03	3.7241E-03
261	262	263	264	265	266	267			
2.4864E-03	1.9822E-03	3.3567E-03	2.7945E-03	2.8874E-03	3.7771E-03	3.7932E-03			

ORIGINAL PAGE IS
OF POOR QUALITY

CONDUCTANCES

COND INC NODE INC CURV EVX NO. COND. VAL.

COND INC NODE	INC CURV EVX NO.	COND. VAL.
1	1	6.940E-03
291	79	9.1667E-02
293	79	3.5900E-03
3	4	2.0964E-02
5	7	3.0769E-02
7	10	3.8993E-02
9	13	4.5098E-02
11	16	5.1961E-02
13	19	6.1728E-02
15	22	7.2868E-02
17	25	8.4259E-02
19	28	1.1217E-01
21	31	1.1222E-01
23	34	1.7111E-01
25	37	6.4444E-02
27	40	6.456E-02
29	43	6.6697E-02
31	46	7.0476E-02
33	49	7.4561E-02
35	52	7.5000E-02
37	55	8.0208E-02
39	58	7.2620E-02
41	61	5.6771E-02
43	64	4.7587E-02
45	67	4.5185E-02
47	70	4.4753E-02
49	73	2.8205E-02
51	76	1.3084E-02
53	79	7.0710E-03
55	82	8.8800E-03
57	85	8.1600E-03
59	88	6.2810E-03
61	91	4.6660E-03
63	94	3.5080E-03
65	97	2.6130E-03
67	100	2.0670E-03
69	103	1.7420E-03
71	106	1.6670E-03
73	109	9.6700E-04
75	112	6.7700E-04
77	115	1.1020E-03
79	118	1.5170E-03
81	121	1.6440E-03
83	124	2.0840E-03
85	127	2.7340E-03
87	130	3.6690E-03
89	133	3.7670E-03
91	136	4.1420E-03
93	139	5.2020E-03
95	142	7.4250E-03
97	145	7.7400E-03
99	148	6.7530E-03
101	151	1.9650E-03
103	154	1.4570E-03
105	157	1.0780E-03
107	160	8.4900E-04
109	163	7.7000E-04
111	166	7.1700E-04
113	169	6.7300E-04
115	172	6.3700E-04
117	175	6.0800E-04
119	178	5.0700E-04
121	181	4.2100E-04
123	184	3.7730E-03
125	187	4.440E-03
127	190	3.0870E-03
129	193	2.3560E-03
131	196	1.9680E-03
133	199	1.6260E-03
135	202	1.3690E-03
137	205	1.2570E-03
139	208	1.1600E-03
141	211	8.2E-04
143	214	4.1220E-03
145	217	1.0420E-02
147	220	1.6718E-02

COND INC	INC NODE	INC MODE	INC CURV	EVX NO	COND VAL
296	1	1	1	70	2 1330E-03
300	1	28	0	41	2 2800E-04
299	0	72	0	0	8 1600E-02
197	0	94	0	0	2 1420E-01
198	0	95	0	0	1 3708E-01
199	0	96	0	0	7 7400E-02
200	0	96	0	0	5 1300E-02
201	0	97	0	0	8 1769E-02
202	0	97	0	0	5 2981E-02
203	0	98	0	0	5 7507E-02
204	0	98	0	0	5 8455E-02
205	0	99	0	0	6 2081E-02
206	0	99	0	0	6 3166E-02
207	0	100	0	0	6 3611E-02
208	0	100	0	0	7 7874E-02
209	0	101	0	0	7 5967E-02
210	0	101	0	0	9 1733E-02
211	0	102	0	0	8 5611E-02
212	0	102	0	0	1 0406E-01
213	0	103	0	0	9 4855E-02
214	0	103	0	0	1 0753E-01
215	0	104	0	0	9 4833E-02
216	0	104	0	0	9 9180E-02
217	0	105	0	0	8 0972E-02
218	0	105	0	0	1 0526E-01
219	0	106	0	0	5 9500E-02
220	0	106	0	0	1 2892E-01
221	0	107	0	0	1 5571E-01
223	0	108	0	0	1 3218E-01
225	0	109	0	0	1 8108E-01
227	0	110	0	0	1 1102E-01
228	0	111	0	0	1 1030E-01
229	0	112	0	0	1 1105E-01
230	0	113	0	0	1 1090E-01
231	0	114	0	0	1 1090E-01
232	0	115	0	0	1 1092E-01
233	0	116	0	0	1 1050E-01
234	0	117	0	0	1 1133E-01
235	0	118	0	0	1 1146E-01
236	0	119	0	0	1 1146E-01
237	0	120	0	0	1 1187E-01
238	0	121	0	0	1 1239E-01
239	0	122	0	0	1 2504E-01
240	0	122	0	0	1 1685E-01
241	0	9	0	0	1 1100E-01
242	0	9	0	0	1 1089E-01
243	0	12	0	0	1 1105E-01
244	0	15	0	0	1 1090E-01
245	0	13	0	0	1 1092E-01
246	0	13	0	0	1 1105E-01
247	0	24	0	0	1 1105E-01
248	0	27	0	0	1 1133E-01
249	0	30	0	0	1 1146E-01
250	0	33	0	0	1 1146E-01
251	0	36	0	0	1 1187E-01
252	0	81	0	0	1 1239E-01
253	0	124	0	0	1 2504E-01
254	0	125	0	0	8 7560E-02
255	0	126	0	0	8 7560E-02
256	0	127	0	0	8 7560E-02
257	0	128	0	0	8 7560E-02
258	0	128	0	0	7 7730E-02
259	0	130	0	0	7 7730E-02
260	0	131	0	0	9 0700E-02
261	0	132	0	0	9 0300E-02
262	0	133	0	0	9 0300E-02
263	0	134	0	0	9 0300E-02
264	0	36	0	0	8 7560E-02
265	0	39	0	0	8 7560E-02
266	0	42	0	0	8 7560E-02
267	0	43	0	0	8 7560E-02
268	0	48	0	0	8 7560E-02
269	0	51	0	0	7 9980E-02
270	0	54	0	0	7 7730E-02
271	0	57	0	0	7 6230E-02
272	0	60	0	0	9 0300E-02
273	0	63	0	0	9 0300E-02
274	0	66	0	0	9 0300E-02

RMAL TRANSIENT ANALYSER REVISION NO. 2.0
 NASA COOLED RADIAL TURBINE-HALF BLADE-HEAT TR. FER-G.AIGRET

COND	INC	MODE	INC	MODE	INC	CURV	EVX	NO.	COND.	VAL.
547	1	145	1	268	0	41	0	3	2.6667E-02	
550	1	193	1	269	0	41	0	3	1.5758E-02	
553	1	217	1	270	0	41	0	3	1.4710E-03	
556	1	220	1	271	0	41	0	3	1.4679E-02	

OTHER VALUES

LOC. INC NO. VALUE

VARIABLE LINES

ANS	INC	PRMA	INC	PRMB	INC	PRMC	INC	CODE	CURV	EVX	NO.	PARAM. A	PARAM. B	PARAM. C
20110	1	41003	0	0	0	0	0	6	0	1	13	0.0	5.8320E+00	0.0
10124	0	10123	0	0	0	0	0	6	0	1	11	0.0	1.0000E+00	0.0
20124	1	41003	0	0	0	0	0	6	0	1	11	0.0	3.4020E+00	0.0
10136	0	10110	0	0	0	0	0	6	0	1	4	0.0	1.0000E+00	0.0
20136	1	41003	0	0	0	0	0	6	0	1	4	0.0	1.4580E+00	0.0
10141	0	10123	0	0	0	0	0	6	0	1	3	0.0	1.0000E+00	0.0
20141	1	41003	0	0	0	0	0	6	0	1	3	0.0	2.4300E+00	0.0
20223	1	41003	0	0	0	0	0	6	0	1	2	0.0	1.4580E+01	0.0
20231	1	41003	0	0	0	0	0	6	0	1	2	0.0	1.9926E+00	0.0
20237	1	41003	0	0	0	0	0	6	0	1	2	0.0	1.2887E+01	0.0
20240	1	41003	0	0	0	0	0	6	0	1	3	0.0	9.1854E+00	0.0
20244	1	41003	0	0	0	0	0	6	0	1	4	0.0	7.8732E+00	0.0
20249	1	41003	0	0	0	0	0	6	0	1	3	0.0	9.1516E+00	0.0
20253	1	41003	0	0	0	0	0	6	0	1	3	0.0	5.1516E+00	0.0
20256	0	41003	0	0	0	0	0	6	0	1	3	0.0	1.3122E+00	0.0
10234	0	10230	0	0	0	0	0	6	0	1	0	0.0	1.6524E+00	0.0
10237	0	10236	0	0	0	0	0	6	0	1	0	0.0	1.0000E+00	0.0
10249	0	10243	0	0	0	0	0	6	0	1	0	0.0	1.0000E+00	0.0
10256	0	10235	0	0	0	0	0	6	0	1	0	0.0	1.0000E+00	0.0
10231	0	10230	0	0	0	0	0	6	0	1	0	0.0	1.0000E+00	0.0
10240	0	10239	0	0	0	0	0	6	0	1	0	0.0	1.0000E+00	0.0
10253	0	10239	0	0	0	0	0	6	0	1	0	0.0	1.0000E+00	0.0
40243	0	10243	0	0	0	0	0	6	0	1	0	0.0	1.0000E+00	0.0
40224	0	10224	0	0	0	0	0	6	0	1	0	0.0	7.8732E+00	0.0
40244	0	40243	0	40224	0	0	0	4	0	1	0	0.0	1.4580E+01	0.0
10244	0	40244	0	0	0	0	0	7	0	1	0	0.0	0.0	0.0
													2.2453E+01	0.0

CURVE NO. 41 IN 79? THER. CON

0.0	7	9200E+00
8.0000E+02	1	0000E+01
1.0000E+03	1	0420E+01
1.2000E+03	1	1420E+01
1.4000E+03	1	2580E+01
1.6000E+03	1	4170E+01
1.8000E+03	1	6330E+01
2.0000E+03	2	0000E+01
0.0	0	0.0

OUTPUT CODES

I.D.	INC	NO.
10001	1	271
0	0	0

P-315 THERMAL TRANSIENT ANALY: NASA COOLED PSEUDO SEQUI

P-315 THERMAL TRANSIENT ANALYSE RE NASA COOLED RADIA

P-315 THERMAL TRANSIENT ANALYSE REVISI NASA COOLED RADIAI THA

CAP. COND. NODE RCX STU DCND

1 1 2 0 0 0 0

2 1 1 1 0 0 0
 53 4
 128 67
 161 90
 219 106
 295 70

3 2 2 2 0 0 0
 55 6
 130 69
 163 90
 227 110
 240 111
 298 72

4 3 5 0 0 0
 53 1
 56 7
 131 64
 164 89
 217 105

5 3 4 0 0 0
 4 6
 54 2
 57 8
 132 65
 165 89

6 4 5 0 0 0
 55 3
 58 9
 133 66
 166 89
 228 111
 241 112

7 5 8 0 0 0
 56 4
 59 10
 134 61
 167 88
 215 104

8 6 9 0 0 0
 57 5
 60 11
 135 62
 168 88

9 6 8 0 0 0
 58 6
 61 12
 136 63
 169 88
 219 112
 241 113

CAP. COND. NODE RCX STU DCND

10 7 11 0 0 0
 59 7
 62 13
 137 58
 170 87
 213 103

11 8 12 0 0 0
 60 3
 63 14
 138 59
 171 87

12 8 11 0 0 0
 61 9
 64 15
 139 60
 172 87
 230 113
 243 114

13 9 14 0 0 0
 62 10
 65 16
 140 55
 173 86
 211 102

14 9 13 0 0 0
 10 15
 63 11
 66 17
 141 56
 174 86

15 10 14 0 0 0
 64 12
 67 18
 142 57
 175 86
 231 114
 244 115

16 11 17 0 0 0
 65 13
 68 19
 143 52
 176 85
 209 101

17 12 18 0 0 0
 66 14
 69 20
 144 53
 177 85

18 12 17 0 0 0
 67 15
 70 21
 145 54
 178 85
 232 115
 245 116

CAP. COND. NODE RCX STU DCND

20 13 19 0 0 0
 71 22
 146 49
 179 84
 207 100

21 14 20 0 0 0
 70 13
 73 24
 148 51
 181 84
 233 116
 246 117

22 15 23 0 0 0
 71 19
 74 25
 149 46
 182 83
 205 99

23 16 24 0 0 0
 72 20
 75 26
 150 47
 183 83

24 16 23 0 0 0
 73 21
 76 27
 151 48
 184 83
 234 117
 247 118

25 17 26 0 0 0
 74 22
 77 28
 152 43
 185 82
 203 98

26 17 25 0 0 0
 18 27
 75 23
 78 29
 153 44
 186 82

27 18 26 0 0 0
 76 24
 79 30
 154 45
 187 82
 235 118
 248 119

28 19 29 0 0 0
 77 25
 80 31
 155 46
 188 81
 211 119

P-315 THERMAL TRANSIENT ANALYSER REVIST
NASA COOLED RADIAL T

CAP. COND. NODE RCX STU DCND
201 97
300 82

29 19 28 0 0 0
20 30 88 36
78 26 91 42
81 32 160 33
156 41 254 125
301 82 265 126

30 20 29 0 0 0
79 27 27 41
82 33 89 37
187 42 92 43
236 119 155 28
249 120 202 97
302 82

31 21 32 0 0 0
60 28 27 40
83 34 28 42
158 37 90 38
199 96 93 44
156 29

32 21 31 0 0 0
22 33 28 41
81 29 91 39
84 35 94 45
159 38 157 30
159 38 255 126
159 38 266 127

33 22 32 0 0 0
82 30 29 44
85 36 92 40
160 39 95 46
237 120 152 25
250 121 204 98

34 23 35 0 0 0
83 31 29 43
86 37 30 45
198 95 93 41
293 79 96 47
153 26

35 23 34 0 0 0
24 36 30 44
84 32 94 42
87 38 97 48
294 80 154 27
256 127
267 128

36 24 35 0 0 0
85 33 31 47
88 39 95 43
238 121 98 49
251 122 149 22
253 124 206 99
264 125
295 81

P-315 THERMAL TRANSIENT ANALYSER REVIST
NASA COOLED RADIAL T

CAP. COND. NODE RCX STU DCND
159 32

39 26 38 0 0 0
88 36 36
91 42
160 33
254 125
265 126

40 27 41 0 0 0
89 37 27 41
92 43 89 37
155 28 92 43
202 97

41 27 40 0 0 0
28 42 27 40
90 38 28 42
93 44 90 38
156 29 93 44

42 28 41 0 0 0
91 39 28 41
94 45 91 39
157 30 94 45
255 126
266 127

43 29 44 0 0 0
92 40 29 44
95 46 92 40
152 25 95 46
204 98

44 29 43 0 0 0
30 45 29 43
93 41 30 45
96 47 93 41
153 26

45 30 44 0 0 0
31 47 30 44
94 42 31 47
97 48 94 42
154 27 97 48
256 127
267 128

46 31 47 0 0 0
32 48 31 47
95 43 32 48
96 44 95 43
99 50 96 44
150 23

P-315 THERMAL TRANSIENT ANALYSER REVIST
NASA COOLED RADIAL T

CAP. COND. NODE RCX STU DCND
98 46

50 33 49 0 0 0
34 51 33 49
99 47 34 51
102 53 99 47
147 20 102 53

51 34 50 0 0 0
100 48 34 50
103 54 100 48
148 21 103 54
258 129 148 21
269 130

52 35 53 0 0 0
101 49 35 53
104 55 101 49
143 16 104 55
210 101

53 35 52 0 0 0
36 54 35 52
102 50 36 54
105 56 102 50
144 17 105 56

54 36 53 0 0 0
103 51 36 53
106 57 103 51
145 18 106 57
255 130
270 131

55 37 56 0 0 0
104 52 37 56
107 58 104 52
140 13 107 58
212 102

56 37 55 0 0 0
38 57 37 55
105 53 38 57
108 59 105 53
141 14

57 38 56 0 0 0
106 54 38 56
109 60 106 54
142 15 109 60
260 131
271 132

P-315 THERMAL TRANSIENT ANALYSER REVIST
NASA COOLED RADIAL T

CAP. COND. NODE RCX STU DCND
39 59

58 39 59 0 0 0
107 55 39 59
110 61 107 55
137 10 110 61
214 103

59 39 58 0 0 0
40 60 39 58
108 56 40 60
111 62 108 56
138 11 111 62
215 104

ORIGINAL PAGE IS
OF POOR QUALITY

P-315	ERMAL TRANSIENT ANALYSER REVI NASA COOLED RADIAL	P-315	THERMAL 1 NASA COOLED RADIAL 1	P-315	THERMAL TRANSIEN NASA	P-315	THERMAL REVISIC JLED RADIAL TJE
CAP. COND. NODE RCX STU DCND	CAP. COND. NODE RCX STU DCND	CAP. COND. NODE RCX STU DCND	CAP. COND. NODE RCX STU DCND	CAP. COND. NODE RCX STU DCND	CAP. COND. NODE RCX STU DCND	CAP. COND. NODE RCX STU DCND	CAP. COND. NODE RCX STU DCND
60	40 59 109 57 112 63 139 12 261 132 272 133	71	122 73 185 91 221 107 296 1	81	239 122 252 123 281 141 288 142 292 80 295 36	0 0 0	0 0 0
61	41 62 110 58 113 64 134 7 216 104	72	47 70 48 72 120 68 123 74 189 91 297 2	110	227 3 299 72	1 1 1	1 1 1
62	41 61 42 63 111 59 114 65 135 8	73	48 71 121 69 124 75 190 81 276 137 280 138 298 3 299 110	111	228 6	1 1 1	1 1 1
63	42 62 112 60 115 66 136 9 262 133 273 134	74	49 74 122 70 125 76 191 92 223 108	112	229 9	1 1 1	1 1 1
64	43 65 112 61 116 67 131 14 218 105	75	49 73 50 75 123 71 126 77 192 92	113	230 12	1 1 1	1 1 1
65	43 64 44 66 114 62 117 68 132 5	76	50 74 124 72 127 78 193 92 277 138 281 139	114	231 15	1 1 1	1 1 1
66	44 65 115 63 118 69 133 6 263 134 274 135	77	51 77 125 73 194 93 225 109	115	232 18	1 1 1	1 1 1
67	45 68 116 64 119 70 128 1 220 106	78	51 76 52 78 126 74 195 93	116	233 21	1 1 1	1 1 1
68	45 67 46 69 117 65 120 71 129 2	79	52 77 127 75 196 93 278 139 282 140	117	234 24	1 1 1	1 1 1
69	46 68 118 66 121 72 130 3 275 136 279 137	80	197 94 287 143 290 144 291 80 293 34	118	235 27	1 1 1	1 1 1
70	47 71 67	81	197 94 287 143 290 144 291 80 293 34 286 142 289 143 291 79 292 81 294 35	119	236 30	1 1 1	1 1 1
				120	237 33	1 1 1	1 1 1
				121	238 36	1 1 1	1 1 1
				122	239 81	1 1 1	1 1 1
				124	253 36	1 1 1	1 1 1
				125	254 39	1 1 1	1 1 1
				126	255 42	1 1 1	1 1 1
				127	256 45	1 1 1	1 1 1
				128	257 48	1 1 1	1 1 1
				129	258 51	1 1 1	1 1 1
				130	259 54	1 1 1	1 1 1
				131	260 57	1 1 1	1 1 1
				132	261 60	1 1 1	1 1 1
				133	261 60	1 1 1	1 1 1

P-315 THERMAL TRANSIENT ANALYSER REV NASA COOLED RADIAL				P-315 THERMAL TRANSIENT ANALYSER REV NASA COOLED RADIAL				P-315 THERMAL TRANSIENT ANALYSER REV NASA COOLED RADIAL			
CAP.	COND.	MODE	RCX STU DCND	CAP.	COND.	MODE	RCX STU DCND	CAP.	COND.	MODE	RCX STU DCND
134	263	66	1 1 1	152	307	151	0 0 0	163	441	177	0 0 0
136	275	69	1 1 1	153	308	153	0 0 0		471	229	
137	276	72	1 1 1		359	149			478	228	
138	277	75	1 1 1	154	309	155	0 0 0	163	315	164	0 0 0
139	278	78	1 1 1		361	151			370	160	
141	285	81	1 1 1		364	157			373	155	
142	286	80	1 1 1		433	181			442	172	
143	287	79	1 1 1		523	261			520	258	
145	303	146	0 0 0	155	309	154	0 0 0	164	315	163	0 0 0
	355	148			310	156			316	165	
	424	190			362	152			371	161	
	526	264			365	158			374	167	
	547	268			434	182			443	173	
146	303	145	0 0 0	156	310	155	0 0 0	165	316	164	0 0 0
	304	147			363	153			372	162	
	356	149			435	193			375	168	
	425	191			469	227			444	174	
	548	268			476	226			472	230	
147	304	146	0 0 0	157	311	158	0 0 0	166	317	167	0 0 0
	357	150			364	154			373	163	
	426	192			367	160			376	169	
	466	224			436	178			519	258	
	473	223			522	261		167	317	166	0 0 0
	549	268			311	157			318	168	
148	305	149	0 0 0	158	312	159	0 0 0	168	318	167	0 0 0
	355	145			365	155			375	165	
	358	151			368	161			378	171	
	427	187			437	179			480	232	
	525	264			311	157			482	231	
	544	267			312	159		169	319	170	0 0 0
149	305	148	0 0 0	159	312	158	0 0 0		376	166	
	306	150			366	156			518	258	
	356	146			369	162		170	319	169	0 0 0
	359	152			438	180			320	171	
	428	188			477	227			377	167	
	545	267		160	313	161	0 0 0	171	320	170	0 0 0
150	306	149	0 0 0		367	157			378	168	
	357	147			370	163			481	233	
	360	153			439	175			483	232	
	429	189			521	261		172	321	173	0 0 0
	467	225		161	313	160	0 0 0		321	172	
	474	224			314	162			379	175	
	546	267			368	158			442	163	
151	307	152	0 0 0		371	164			527	259	
	358	148			440	176		173	321	172	0 0 0
	361	154		162	314	161	0 0 0		322	174	
	430	184			369	159			380	176	
	524	264			369	159			443	164	
					369	159		174	322	173	0 0 0
					369	159			381	177	
					369	159			444	165	

P-315	HERMAL TRANSIENT ANALYSER REVIS NASA COOLED RADIAL T	P-315	THERMAL NASA COOLED RADIAL T	P-315	ORMAL TRANSIENT NASA	P-315	ORMAL TRANSIENT NASA
CAP. COND. NODE RCX STU DCND	CAP. COND. NODE RCX STU DCND	CAP. COND. NODE RCX STU DCND	CAP. COND. NODE RCX STU DCND	CAP. COND. NODE RCX STU DCND	CAP. COND. NODE RCX STU DCND	CAP. COND. NODE RCX STU DCND	CAP. COND. NODE RCX STU DCND
205	408 207 453 183 512 254 514 253	215	349 214 350 216 415 212 419 218 464 194	231	482 168	231	482 168
	0 0 0		0 0 0		1 1 1		1 1 1
206	343 206 406 207 409 208 454 184 538 263	216	350 215 417 213 420 219 465 195 499 246 503 245	232	483 171	232	483 171
	0 0 0		0 0 0		1 1 1		1 1 1
207	343 205 344 207 407 203 410 209 455 185	217	351 218 418 214 421 220 542 256 553 270	233	486 174	233	486 174
	0 0 0		0 0 0		1 1 1		1 1 1
208	344 206 408 204 411 210 456 186 508 252 511 251	218	351 217 352 219 419 215 422 221 554 270	234	487 177	234	487 177
	0 0 0		0 0 0		1 1 1		1 1 1
209	345 209 409 205 412 211 457 187 539 263	219	352 218 420 216 423 222 500 247 504 246 555 270	235	487 177	235	487 177
	0 0 0		0 0 0		1 1 1		1 1 1
210	345 208 346 210 410 206 413 212 458 188	220	353 221 421 217 543 266 556 271	236	490 180	236	490 180
	0 0 0		0 0 0		1 1 1		1 1 1
211	346 209 411 207 414 213 459 189 507 251 510 250	221	353 220 354 221 422 218 557 271	237	490 180	237	490 180
	0 0 0		0 0 0		1 1 1		1 1 1
212	347 212 412 208 415 214 460 190 540 266	222	354 221 423 219 501 248 505 247 558 271	238	491 183	238	491 183
	0 0 0		0 0 0		1 1 1		1 1 1
213	347 211 348 213 413 209 416 215 461 191	223	473 147	239	495 186	239	495 186
	0 0 0		1 1 1		1 1 1		1 1 1
214	348 212 414 210 417 216 462 192 506 250 509 249	224	474 150	240	495 186	240	495 186
	0 0 0		1 1 1		1 1 1		1 1 1
	349 215 415 211 418 217 463 193 541 266	225	475 153	241	496 189	241	496 189
	0 0 0		1 1 1		1 1 1		1 1 1
		226	476 156	242	497 192	242	497 192
		227	477 159	243	502 195	243	502 195
		228	478 162	244	503 216	244	503 216
		229	479 165	245	504 219	245	504 219
				246	505 222	246	505 222
				247	509 213	247	509 213
				248	510 210	248	510 210
				249	511 207	249	511 207
				250	514 204	250	514 204
				251	515 201	251	515 201
				252	517 198	252	517 198
				253		253	
				254		254	
				255		255	
				256		256	

TEMPERATURES

1	1.7070E+03	1.5188E+03	1.2661E+03	1.6873E+03	1.5150E+03	1.3150E+03	1.6735E+03	1.5201E+03	1.3524E+03	1.6517E+03
11	1.5188E+03	1.3763E+03	1.6191E+03	1.5054E+03	1.3835E+03	1.5821E+03	1.4862E+03	1.3836E+03	1.5452E+03	1.4661E+03
21	1.3820E+03	1.5149E+03	1.4500E+03	1.3812E+03	1.5046E+03	1.4501E+03	1.3915E+03	1.5570E+03	1.5063E+03	1.4528E+03
31	1.5682E+03	1.5185E+03	1.4670E+03	1.6072E+03	1.5513E+03	1.4925E+03	1.5841E+03	1.5283E+03	1.4701E+03	1.5965E+03
41	1.5410E+03	1.4835E+03	1.6265E+03	1.5714E+03	1.5151E+03	1.6643E+03	1.6110E+03	1.5566E+03	1.7145E+03	1.6611E+03
51	1.6072E+03	1.7595E+03	1.7028E+03	1.6474E+03	1.7778E+03	1.7186E+03	1.6593E+03	1.7845E+03	1.7216E+03	1.6587E+03
61	1.7876E+03	1.7145E+03	1.6409E+03	1.7964E+03	1.7085E+03	1.6230E+03	1.7940E+03	1.6834E+03	1.5765E+03	1.7652E+03
71	1.6308E+03	1.4896E+03	1.7733E+03	1.6398E+03	1.5285E+03	1.8254E+03	1.6410E+03	1.5288E+03	1.7175E+03	1.6192E+03
81	1.5312E+03	1.4350E+03	1.4050E+03	1.3880E+03	1.4000E+03	1.4150E+03	1.4470E+03	1.4550E+03	1.4650E+03	1.4800E+03
91	1.5050E+03	1.5530E+03	1.5700E+03	2.4740E+03	2.5500E+03	2.5160E+03	2.5380E+03	2.5290E+03	2.5170E+03	2.5060E+03
101	2.4950E+03	2.4850E+03	2.4740E+03	2.4650E+03	2.4560E+03	2.4480E+03	2.4390E+03	2.4320E+03	2.4240E+03	2.4100E+03
111	1.0058E+03	1.0174E+03	1.0299E+03	1.0428E+03	1.0555E+03	1.0678E+03	1.0795E+03	1.0908E+03	1.1021E+03	1.1152E+03
121	1.1285E+03	1.1422E+03	1.1587E+03	1.1587E+03	1.1754E+03	1.1903E+03	1.2050E+03	1.2200E+03	1.2354E+03	1.2520E+03
131	1.2694E+03	1.2895E+03	1.3086E+03	1.3258E+03	1.3412E+03	1.3561E+03	1.3700E+03	1.3834E+03	1.3963E+03	1.4089E+03
141	1.1587E+03	1.1648E+03	1.1723E+03	1.1813E+03	1.1913E+03	1.2020E+03	1.2135E+03	1.2251E+03	1.2378E+03	1.2516E+03
151	1.4691E+03	1.3872E+03	1.3020E+03	1.4806E+03	1.4055E+03	1.3277E+03	1.4778E+03	1.4117E+03	1.3425E+03	1.2790E+03
161	1.4214E+03	1.3604E+03	1.5135E+03	1.4632E+03	1.4100E+03	1.5850E+03	1.5509E+03	1.5163E+03	1.4802E+03	1.4430E+03
171	1.7252E+03	1.7210E+03	1.6881E+03	1.6554E+03	1.6621E+03	1.6207E+03	1.5775E+03	1.5357E+03	1.4922E+03	1.4473E+03
181	1.6299E+03	1.5816E+03	1.5321E+03	1.6254E+03	1.5704E+03	1.5144E+03	1.6046E+03	1.5432E+03	1.4802E+03	1.4190E+03
191	1.5138E+03	1.4366E+03	1.5535E+03	1.4608E+03	1.3627E+03	1.7541E+03	1.7179E+03	1.6809E+03	1.6437E+03	1.6000E+03
201	1.6849E+03	1.7291E+03	1.6892E+03	1.6476E+03	1.7312E+03	1.6880E+03	1.6444E+03	1.7117E+03	1.6594E+03	1.6059E+03
211	1.6750E+03	1.6132E+03	1.5490E+03	1.6493E+03	1.5706E+03	1.4864E+03	1.6507E+03	1.5640E+03	1.4740E+03	1.3627E+03
221	1.5510E+03	1.4647E+03	1.6500E+03	1.6721E+03	1.6500E+03	1.6254E+03	1.6000E+03	1.5754E+03	1.5500E+03	1.5250E+03
231	1.0182E+03	1.0665E+03	1.0763E+03	1.0182E+03	1.0300E+03	1.0424E+03	1.0577E+03	1.0718E+03	1.0831E+03	1.0921E+03
241	1.0868E+03	1.1002E+03	1.1125E+03	1.0182E+03	1.0346E+03	1.0506E+03	1.0791E+03	1.0910E+03	1.1125E+03	1.1346E+03

ORIGINAL PAGE IS
 OF POOR QUALITY

231	1.0182E+03	232	1.0685E+03	233	1.0763E+03	234	1.0182E+03	235	1.0300E+03	236	1.0424E+03	237	1.0424E+03	238	1.0577E+03	239	1.0718E+03	240	1.0718E+03
241	1.0868E+03	242	1.1002E+03	243	1.1125E+03	244	1.0182E+03	245	1.0346E+03	246	1.0590E+03	247	1.0791E+03	248	1.0910E+03	249	1.1125E+03	250	1.1346E+03
251	1.1570E+03	252	1.1782E+03	253	1.0718E+03	254	1.1616E+03	255	1.2447E+03	256	1.0300E+03	257	1.1318E+03	258	1.1400E+03	259	1.2325E+03	260	1.2400E+03
261	2.0800E+03	262	2.2650E+03	263	2.3400E+03	264	2.0200E+03	265	2.2050E+03	266	2.2800E+03	267	1.2200E+03	268	1.3190E+03	269	1.4300E+03	270	1.5200E+03
271	1.5600E+03																		

CAPACITANCES

1	0.0	2	0.0	3	0.0	4	0.0	5	0.0	6	0.0	7	0.0	8	0.0	9	0.0	10	0.0
11	0.0	12	0.0	13	0.0	14	0.0	15	0.0	16	0.0	17	0.0	18	0.0	19	0.0	20	0.0
21	0.0	22	0.0	23	0.0	24	0.0	25	0.0	26	0.0	27	0.0	28	0.0	29	0.0	30	0.0
31	0.0	32	0.0	33	0.0	34	0.0	35	0.0	36	0.0	37	0.0	38	0.0	39	0.0	40	0.0
41	0.0	42	0.0	43	0.0	44	0.0	45	0.0	46	0.0	47	0.0	48	0.0	49	0.0	50	0.0
51	0.0	52	0.0	53	0.0	54	0.0	55	0.0	56	0.0	57	0.0	58	0.0	59	0.0	60	0.0
61	0.0	62	0.0	63	0.0	64	0.0	65	0.0	66	0.0	67	0.0	68	0.0	69	0.0	70	0.0
71	0.0	72	0.0	73	0.0	74	0.0	75	0.0	76	0.0	77	0.0	78	0.0	79	0.0	80	0.0
81	0.0	110	6.5610E+00	111	6.5610E+00	112	6.5610E+00	113	6.5610E+00	114	6.5610E+00	115	6.5610E+00	116	6.5610E+00	117	6.5610E+00	118	6.5610E+00
119	6.5610E+00	120	6.5610E+00	121	6.5610E+00	122	6.5610E+00	123	6.5610E+00	124	6.5610E+00	125	6.5610E+00	126	6.5610E+00	127	6.5610E+00	128	6.5610E+00
130	3.8273E+00	131	3.8273E+00	132	3.8273E+00	133	3.8273E+00	134	3.8273E+00	135	3.8273E+00	136	3.8273E+00	137	3.8273E+00	138	3.8273E+00	139	3.8273E+00
142	2.7338E+00	143	2.7338E+00	144	2.7338E+00	145	2.7338E+00	146	2.7338E+00	147	2.7338E+00	148	2.7338E+00	149	2.7338E+00	150	2.7338E+00	151	2.7338E+00
153	0.0	154	0.0	155	0.0	156	0.0	157	0.0	158	0.0	159	0.0	160	0.0	161	0.0	162	0.0
163	0.0	164	0.0	165	0.0	166	0.0	167	0.0	168	0.0	169	0.0	170	0.0	171	0.0	172	0.0
173	0.0	174	0.0	175	0.0	176	0.0	177	0.0	178	0.0	179	0.0	180	0.0	181	0.0	182	0.0
183	0.0	184	0.0	185	0.0	186	0.0	187	0.0	188	0.0	189	0.0	190	0.0	191	0.0	192	0.0
193	0.0	194	0.0	195	0.0	196	0.0	197	0.0	198	0.0	199	0.0	200	0.0	201	0.0	202	0.0
203	0.0	204	0.0	205	0.0	206	0.0	207	0.0	208	0.0	209	0.0	210	0.0	211	0.0	212	0.0
213	0.0	214	0.0	215	0.0	216	0.0	217	0.0	218	0.0	219	0.0	220	0.0	221	0.0	222	0.0
223	1.6402E+01	224	1.6402E+01	225	1.6402E+01	226	1.6402E+01	227	1.6402E+01	228	1.6402E+01	229	1.6402E+01	230	1.6402E+01	231	1.6402E+01	232	1.6402E+01
235	1.4161E+01	237	1.0334E+01	238	1.0334E+01	240	8.8574E+00	241	8.8574E+00	242	8.8574E+00	244	6.7955E+00	245	5.7955E+00	246	5.7955E+00	247	5.7955E+00

249	5.7955E+00	251	253	254	255				
1	9.9164E-02	2	2.9732E-01	4	3.3521E-01	5	5.4796E-01	6	5.9528E-01
11	7.0909E-01	12	8.2837E-01	14	9.6445E-01	15	1.1118E+00	16	1.2710E+00
21	1.5196E+00	22	2.3964E+00	24	3.3184E+00	25	4.3615E+00	26	5.5412E+00
31	1.0273E+00	32	1.1272E+00	34	1.0840E+00	35	1.2366E+00	36	1.4900E+00
41	8.9706E-01	42	7.5264E-01	44	7.0809E-01	45	6.5188E-01	46	6.2000E-01
51	2.0422E-01	52	1.8381E-01	54	1.5527E-02	55	1.4644E-02	56	1.3354E-01
61	1.0097E-01	62	8.4613E-02	64	7.8284E-02	65	6.6146E-02	66	5.8253E-02
71	3.5672E-02	72	3.2592E-02	74	2.7306E-02	75	2.6825E-02	76	2.5539E-02
81	2.3464E-02	82	2.2744E-02	84	2.2259E-02	85	2.2028E-02	86	2.1366E-02
91	1.2755E-02	92	1.5791E-02	94	1.4733E-02	95	2.2240E-02	96	2.1389E-02
101	3.2607E-02	102	3.1375E-02	104	3.3706E-02	105	4.2010E-02	106	4.0317E-02
111	5.8108E-02	112	5.5405E-02	114	6.3678E-02	115	6.0121E-02	116	5.9167E-02
121	1.0126E-01	122	1.0430E-01	124	1.0409E-01	125	1.1023E-01	126	1.1389E-01
131	2.2877E-02	132	1.9128E-02	134	1.6796E-02	135	1.5476E-02	136	1.4389E-02
141	1.1011E-02	142	1.0704E-02	144	1.0129E-02	145	9.6281E-03	146	9.3417E-03
151	8.4673E-03	152	8.1489E-03	154	7.9061E-03	155	7.0005E-03	156	6.8744E-03
161	1.2386E-01	162	1.1730E-01	164	1.0899E-01	165	1.0986E-02	166	1.0983E-02
171	3.1192E-02	172	2.9857E-02	174	2.5699E-02	175	2.4749E-02	176	2.1632E-02
181	1.7103E-02	182	1.6412E-02	184	1.5767E-02	185	1.4985E-02	186	1.4715E-02
191	1.5476E-01	192	1.4735E-01	194	1.4274E-01	195	1.3789E-01	196	1.3317E-01
201	8.1769E-02	202	5.2981E-02	204	5.8455E-02	205	6.2081E-02	206	6.5366E-02
211	8.5611E-02	212	1.0906E-01	214	9.4855E-02	215	9.4837E-02	216	8.0972E-02
221	1.5571E-01	222	1.3218E-01	224	1.1685E-01	225	1.1109E-01	226	1.0526E-01
231	1.1333E-01	232	1.1146E-01	234	1.1187E-01	235	1.1239E-01	236	1.1685E-01
241	1.1133E-01	242	1.1108E-01	243	1.1089E-01	244	1.1089E-01	245	1.1089E-01

ORIGINAL PAGE IS
 OF POOR QUALITY

516	517	518	519	520	521	522	523	524	525
1.4048E-01	1.4048E-01	9.7533E-02	1.7417E-01	2.1335E-01	2.1335E-01	2.1335E-01	2.1771E-01	2.2206E-01	1.6110E-01
526	527	528	529	530	531	532	533	534	535
6.5313E-02	2.6957E-01	2.2619E-01	2.1933E-01	2.0562E-01	1.9192E-01	1.8049E-01	1.6381E-01	1.3021E-01	2.6196E-01
536	537	538	539	540	541	542	543	544	545
1.8182E-01	1.8660E-01	1.9187E-01	1.9476E-01	1.9139E-01	1.8852E-01	1.7725E-01	1.7513E-02	1.9162E-02	3.8301E-02
546	547	548	549	550	551	552	553	554	555
3.7425E-02	3.2904E-01	3.2426E-01	3.1981E-01	2.0973E-01	2.0392E-01	1.8790E-01	2.0872E-02	2.0166E-02	1.0010E-02
556	557	558							
2.0728E-01	2.0281E-01	1.9777E-01							

MISCELLANEOUS VALUES

224	243	244	1003
1.4102E+04	8.7589E+03	2.2861E+04	1.1250E+00

TIME CONSTANTS

HEAT BALANCE

1	2	3	4	5	6	7	8	9	10
8.3542E-04	6.5613E-04	9.7370E-04	1.0529E-03	5.7793E-04	4.2725E-04	7.4768E-04	1.6812E-03	9.6130E-04	9.2656E-04
11	12	13	14	15	16	17	18	19	20
-3.1652E-03	5.1880E-04	7.9346E-04	-4.0417E-03	1.2207E-03	8.2397E-04	-3.2682E-03	2.2982E-04	2.5940E-04	2.7100E-03
21	22	23	24	25	26	27	28	29	30
-5.7983E-04	-3.9673E-03	-1.6307E-03	2.9602E-03	-3.3875E-03	-3.7851E-03	-2.8687E-03	-3.5132E-03	5.7476E-03	4.4204E-03
31	32	33	34	35	36	37	38	39	40
-5.8441E-03	3.8466E-03	-4.2114E-03	4.2706E-03	-8.3055E-03	3.5982E-03	-6.4087E-04	-3.6703E-03	9.9182E-04	-6.1035E-04
41	42	43	44	45	46	47	48	49	50
-3.3804E-03	-1.4038E-03	-2.6703E-03	-3.1139E-03	-2.2278E-03	-4.1351E-03	-5.9404E-03	-3.1586E-03	-6.4087E-03	-4.6616E-03
51	52	53	54	55	56	57	58	59	60
-5.0507E-03	-3.2501E-03	-6.0682E-03	6.4397E-03	-4.9285E-03	3.1061E-03	-6.9427E-03	-3.7384E-03	5.4140E-03	-3.1291E-03
61	62	63	64	65	66	67	68	69	70
-4.1504E-03	-2.4137E-03	-3.0365E-03	1.0834E-03	-2.8820E-03	-3.5095E-04	-4.5776E-05	-1.7843E-03	8.1923E-04	2.4033E-04
71	72	73	74	75	76	77	78	79	80
-1.3571E-03	-1.5411E-03	1.0681E-03	-1.2217E-03	8.6975E-04	6.8655E-04	9.6130E-04	5.2220E-04	1.6460E-03	3.0146E-03
81	145	146	147	148	149	150	151	152	153
-2.3012E-03	6.9613E-04	1.0185E-03	6.6948E-04	-1.8487E-03	1.2741E-03	-2.4853E-03	-5.0509E-04	4.5257E-03	1.8311E-04
154	155	156	157	158	159	160	161	162	163
-1.0376E-03	8.1415E-03	-1.2054E-03	2.3193E-03	7.7468E-03	6.5613E-04	3.0511E-03	1.1232E-02	1.5255E-05	1.5167E-02
164	165	166	167	168	169	170	171	172	173
3.0655E-02	1.7489E-02	4.5517E-02	7.2548E-02	4.4708E-02	7.9117E-02	1.6554E-01	8.1361E-02	5.2048E-02	1.0192E-01
174	175	176	177	178	179	180	181	182	183
5.5740E-02	2.4170E-02	5.5399E-02	3.2684E-02	1.3962E-02	2.8077E-02	1.9714E-02	1.3748E-02	1.9235E-02	1.5076E-02
184	185	186	187	188	189	190	191	192	193
1.0681E-04	1.5397E-02	2.8992E-04	2.9907E-03	7.1997E-03	5.7983E-04	-5.8289E-03	1.0960E-02	-3.8300E-03	3.2197E-04
194	195	196	197	198	199	200	201	202	203
9.4032E-04	7.6580E-04	7.9010E-02	1.3930E-01	8.2962E-02	3.7674E-02	6.9436E-02	3.9856E-02	1.7839E-02	4.4596E-02
204	205	206	207	208	209	210	211	212	213
2.6016E-02	1.3474E-02	2.1087E-02	1.7838E-02	2.3687E-03	1.1626E-02	4.5624E-03	-1.9226E-03	1.2502E-02	-4.5776E-05
214	215	216	217	218	219	220	221	222	
-2.5940E-04	7.2563E-03	-6.1035E-05	5.3120E-04	-5.8657E-04	2.5408E-03	-6.5804E-05	1.4351E-03	2.5040E-04	

RELATIVE HEAT BALANCE

1	2	3	4	5	6	7	8	9	10
8.5384E-06	1.2184E-05	7.6400E-06	7.8738E-06	5.1407E-06	2.9861E-06	4.7436E-06	1.2057E-05	6.2455E-06	5.9261E-06
11	12	13	14	15	16	17	18	19	20
2.0992E-03	3.3287E-06	5.0236E-06	2.7093E-05	8.1674E-06	5.59E-06	2.2806E-05	1.6009E-05	1.8696E-05	2.0071E-05

21	4.2317E-06	3.0691E-05	1.2643E-05	24	25	26	27	28	29	30
				2.2458E-05	2.7464E-05	3.0004E-05	2.1716E-05	2.1749E-05	3.6146E-05	2.8210E-05
31	3.8087E-05	2.4891E-05	2.7155E-05	34	35	36	37	38	39	40
				1.5803E-05	3.0246E-05	1.3024E-05	6.4308E-06	3.6568E-05	9.8054E-06	6.0606E-06
41	3.3555E-05	1.3919E-05	2.4912E-05	44	45	46	47	48	49	50
				2.9410E-05	2.1279E-05	3.6281E-05	5.3028E-05	2.8746E-05	5.0802E-05	3.7906E-05
51	4.2311E-05	2.3758E-05	4.6150E-05	54	55	56	57	58	59	60
				5.1328E-05	3.1786E-05	2.0709E-05	4.8223E-05	2.5143E-05	3.7480E-05	2.2607E-05
61	3.0622E-05	1.8265E-05	2.3842E-05	64	65	66	67	68	69	70
				7.8012E-06	2.1656E-05	2.7086E-07	1.1105E-05	5.7158E-06	1.0989E-06	
71	6.8962E-06	7.6131E-06	5.7545E-06	74	75	76	77	78	79	80
				1.0561E-05	9.1432E-06	3.1673E-06	1.2766E-05	9.4991E-06	5.0792E-06	1.1219E-05
81	1.0206E-05	6.9435E-06	2.0577E-05	147	148	149	150	151	152	153
				1.0027E-05	9.7582E-06	7.4731E-06	1.4659E-05	2.3902E-06	1.8074E-05	7.2977E-07
154	3.9578E-06	3.1155E-05	4.6123E-06	157	158	159	160	161	162	163
				8.9622E-06	2.9611E-05	2.4794E-06	1.1609E-05	4.1589E-05	5.5128E-08	5.4497E-05
164	1.0724E-04	4.5774E-05	2.2308E-04	167	168	169	170	171	172	173
				3.5264E-04	2.1640E-04	1.0509E-03	2.5755E-03	1.5555E-03	1.5986E-04	3.2000E-04
174	1.8077E-04	7.8639E-05	1.7812E-04	177	178	179	180	181	182	183
				1.0362E-04	4.9794E-05	9.9022E-05	6.9164E-05	5.2340E-05	7.3147E-05	5.7377E-05
184	4.3240E-07	6.2891E-05	1.1954E-06	187	188	189	190	191	192	193
				1.3534E-05	3.2477E-05	2.6283E-06	2.6437E-05	5.0806E-05	1.8192E-05	4.6076E-06
194	6.7540E-06	4.5290E-06	2.3325E-04	197	198	199	200	201	202	203
				4.1177E-04	2.4558E-04	1.6158E-04	3.0377E-04	1.7809E-04	7.7039E-05	1.9031E-04
204	1.0963E-04	5.7675E-05	9.1774E-05	207	208	209	210	211	212	213
				7.9219E-05	1.1619E-05	4.7675E-05	1.8952E-05	8.0913E-06	5.2272E-05	1.9138E-07
214	1.0684E-06	2.9179E-05	2.3827E-07	217	218	219	220	221	222	
				2.4500E-06	2.8146E-06	1.2176E-05	6.2559E-07	1.7301E-05	2.1244E-06	

33
35

ORIGINAL PAGE IS
OF POOR QUALITY

APPENDIX E

NASA AIR-COOLED RADIAL TURBINE WHEEL DRAWINGS

131100 Proposal - Engine Assembly, With High Temperature Turbine Wheel
(Full Size to Fit T-62)

131102 Layout - Turbine Wheel, Air-Cooled (Two-Piece 10X Size)

131301 Proposal - Air-Cooled Turbine Wheel Assembly (Multi-Piece
Construction 10X Size)

131454 Wheel, Turbine - Air Cooled (Cast Star Wheel)

131103 Wheel, Turbine - Air Cooled (Brazed Star Wheel)

131467 Insert, Blade - Air Cooled (Brazed Star Wheel)

131455 Exducer, Turbine - Air Cooled (Cast One-Piece)

131599 Blade, Exducer - Air Cooled (Cast and Machined)

954959C1 Hub, Exducer - Air Cooled (Machined)

954960C1 Ring, Exducer - Air Cooled (Machined)

954961C1 Retainer, Exducer Blade (Machined)

131453-100 Wheel Assembly, Turbine - Air Cooled (Cast Wheel and Exducer)
-200 Wheel Assembly (Brazed Wheel and Cast Exducer)
-300 Wheel Assembly (Cast Wheel and Multi-Piece Exducer)
(Includes assembly, balancing and spinning)

DSK 17073 Material Specification

PRECEDING PAGE BLANK NOT FILMED

DISTRIBUTION LIST
 FABRICATION OF COOLED RADIAL TURBINE ROTOR

Final Report - NAS3-22513

	<u>M.S.</u>	<u>Number of Copies</u>
1. NASA Lewis Research Center 21000 Brookpark Road Cleveland, OH 44135 Attn:		
Report Control Office	60-1	1
Technology Utilization Office	7-3	1
Library	60-3	2
Aeronautics Directorate	3-8	1
Propulsion Systems Division	86-1	1
C. L. Ball	77-6	1
R. W. Niedzwiecki	77-6	1
P. L. Meitner	77-12	1
K. C. Civinskas	5-11	1
R. J. Roelke	77-6	1
J. E. Hass	6-8	10
R. G. DeAnna	77-6	1
2. NASA Scientific and Technical Information Facility Attn: Acquisition Branch P.O. Box 8757 Baltimore/Washington International Airport, MD 21240		25
3. C. E. Bentz AFWAL/POT Wright-Patterson AFB Dayton, OH 45433		1
4. Propulsion Directorate, M.S.77-12 Attn: Director U.S. Army Aviation Research & Technology Activity-AVSCOM 21000 Brookpark Road Cleveland, OH 4 4135-3217		2
5. Director Aviation Applied Technology Directorate U.S. Army Aviation Research & Technology Activity-AVSCOM Attn: SAVRT-TY-AT Ft. Eustis, VA 23604-5577		2
6. Director U.S. Army Aviation Research & Technology Activity-AVSCOM Attn: SAVRT-AS M/S 207-5 Ames Research Center Moffett Field, CA 94035-1099		1

7. Director 1
 U.S. Army Aviation Research & Technology Activity-AVSCOM
 Attn: SAVRT-POM M/S 206-4
 Ames Research Center
 Moffett Field, CA 94035-1099
8. Director 1
 U.S. Army Aviation Systems Command
 Attn: AMSAV-N
 4300 Goodfellow Boulevard
 St. Louis, MO 53120-1798
9. Commander 1
 U.S. Army Aviation Systems Command
 Attn: AMSAV-EQP
 4300 Goodfellow Boulevard
 St. Louis, MO 3120-1798
10. Commander 4
 U.S. Army Troop Support Command
 Attn: AMSTR-DIL
 4300 Goodfellow Boulevard
 St. Louis, MO 53120-1798
11. Commander 1
 U.S. Army Mobility Equipment R&D Command
 Attn: DRDME-ZT (Mr. Dinger)
 Ft. Belvoir, VA 22060
12. Commander 1
 U.S. Army Tank-Automotive R&D Command
 Attn: DRDTA-RGE (Mr. Whitcomb)
 Warren, MI 48090
13. Dr. Donald Dix 1
 Staff Specialist for Propulsion
 OSD/OUSDR&E(ET)
 Room 1809, The Pentagon
 Washington, DC 20301
14. Commander 1
 Army Research Office
 Attn: Dr. R. Singleton
 P.O. Box 12211
 Research Triangle Park, NC 27709
15. Commandant 1
 U.S. Military Academy
 Attn: Chief, Department of Mechanics
 West Point, NY 1 0996

16. Commander 1
Southwest Research Institute
U.S. Army Fuels & Lubricants Research
P.O. Drawer 28510
San Antonio, TX 78284
17. Department of the Army 1
Aviation Systems Division
ODCSRDA (DAMA-WSA, R. Ballard)
Room B454, The Pentagon
Washington, DC 20310
18. U.S. Army Material Systems Analysis Activity 1
Attn: DRXSJ-MP (Mr. Herbert Cohen)
Aberdeen Proving Ground, MD 21005
19. Director, Turbopropulsion Laboratory 1
Code 67SF
Naval Post-Graduate School
Monterey, CA 93940
20. Mr. Richard Alpaugh 1
U.S. DOE
1000 Independence Avenue
Washington, DC 20585
21. Garrett Turbine Engine Company 1
Attn: Tom Booth (Dept. 93-53)
111 South 34th Street
P.O. Box 5217
Phoenix, AZ 85010
22. Allison Gas Turbine Operations 1
Attn: Phil Snyder
P.O. box 894
Indianapolis, IN 46206
23. AVCO Lycoming 1
Atn: Rick Bozzola
550 South Main Street
Stratford, CT 06497
24. Sundstrand Corporaiton 1
ATtn: Paul Hermann
4747 Harrison Avenue
Rockford, IL 61101
25. Williams Research Corporation 1
Attn: R. F. Honn, MS 4-8
2280 West Maple Road
Walled Lake, MI 48088

- 26. Creare, Inc. 1
Hanover, NH 03755
- 27. Cummins Engine Company 1
Attn: John Mulloy
1900 McKinley
Columbus, IN 47201
- 28. Northern Research & Engineering 1
Attn: K. Ginwala
219 Vassar Street
Cambridge, MA 02138
- 29. General Electric Company 1
Aircraft Engine Group
Attn: Bart J. Ferrari, MS 240G1
1000 Western Avenue
Lynn, MA 01910
- 30. Pratt & Whitney Aircraft 1
Government Products Division
Attn: J. Pete Mitchell, MS R16
Palm Beach Gardens Facility
P.O. Box 2691
West Palm Beach, FL 33402
- 31. Wallace Murray Corporation 1
Attn: Nicholas Kirincich
1125 Brookside Avenue
P.O. Box 80-B
Indianapolis, IN 46206
- 32. Mr. Bill Cleary 1
Associate Divison Director
ORI, Inc.
1400 Sprint Street
Silver Spring, MD 20910
- 33. General Motors Research Laboratory 1
Attn: David C. Sheridan
12 Mile and Mound Roads
Warren, MI 48090
- 34. Ford Motor Company 1
Research & Engineering Center
Attn: Robert R. Baker, Room E-3172
P.O. Box 2053
Dearborn, MI 48121